The American Mineralogist

Journal of the Mineralogical Society of America

UNIVERSITY OF ILLINOIS LIBRARY
AUG 26 1959
CHICAGO

VOL. 44 JULY–AUGUST, 1959 Nos. 7 and 8

Contents

(*Continued on Cover 2*)

MINERALOGICAL SOCIETY OF AMERICA
CRYSTALLOGRAPHY PETROGRAPHY MINERALOGY
MCMXIX

EDITOR: LEWIS S. RAMSDELL

BOARD OF ASSOCIATE EDITORS:

ROBERT GARRELS
D. JEROME FISHER
GEORGE W. BRINDLEY
JOSEPH MURDOCH (1957–59)
GEORGE T. FAUST (1958–60)
ADOLF PABST (1959–61)

Published bi-monthly by the Society

Mineralogical Society of America

ASSOCIATED WITH THE GEOLOGICAL SOCIETY OF AMERICA

President: Ralph E. Grim, University of Illinois, Urbana, Illinois.
Vice-President: Joseph Murdoch, University of California at Los Angeles, Los Angeles, California.
Secretary: C. S. Hurlbut, Jr., Harvard University, Cambridge 38, Massachusetts.
Treasurer: Marjorie Hooker, U. S. Geological Survey, Washington 25, D. C.
Editor: Lewis S. Ramsdell, University of Michigan, Ann Arbor, Michigan.
Councilors: Alfred O. Woodford, Pomona College, Claremont, California.
Samuel S. Goldich, University of Minnesota, Minneapolis 14, Minnesota.
Brian H. Mason, American Museum of Natural History, New York 24, New York.
Richard H. Jahns, California Institute of Technology, Pasadena, California.
Charles Milton, U. S. Geological Survey, Washington 25, D. C.
Wilfrid R. Foster, Ohio State University, Columbus 10, Ohio.
Edward W. Nuffield, University of Toronto, Toronto 5, Ontario, Canada.
George E. Goodspeed, University of Washington, Seattle 5, Washington.

The enlarged issues of this journal for 1959 are made possible by a grant from the Penrose Fund of the Geological Society of America.

The American Mineralogist—Journal of the Mineralogical Society of America

The journal, containing articles on mineralogy, crystallography, and allied sciences, is issued every two months. Contributions are invited.

The general conduct of the journal is in the hands of the editor, Lewis S. Ramsdell, Department of Mineralogy, University of Michigan, to whom all manuscripts should be submitted. To assist the editor, the Council of the Society has appointed the following Board of Associate Editors:

Robert M. Garrels, Harvard University, Cambridge 38, Massachusetts.
Joseph Murdoch, University of California at Los Angeles, Los Angeles, California.
D. Jerome Fisher, University of Chicago, Chicago 37, Illinois.
George T. Faust, U. S. Geological Survey, Washington 25, D. C.
George W. Brindley, Pennsylvania State University, University Park, Pennsylvania.
A. Pabst, University of California, Berkeley 4, California.

Authors are requested to submit two copies of each manuscript, typewritten on standard size paper, 8½×11 inches. Photographs submitted for cuts should be glossy prints.

Authors are entitled to 50 free reprints, without covers, of each article published.

Sent to all members and fellows of the Mineralogical Society of America. Membership dues $4.00 annually, fellowship dues $5.00 annually, which includes receipt of the American Mineralogist and GeoTimes, which is published by the American Geological Institute. Subscriptions for libraries, colleges, institutions, companies and similar organizations $6.00 annually.

Entered as second class matter at the post office at Menasha, Wis., under Act of March 3, 1879. Acceptance for mailing at the special rate of postage provided for in section 1103, Act of Oct. 3, 1917, paragraph 4 section 429 P. L. & R. authorized March 13, 1922.

Notice of change of address, orders, and remittances should be sent to Marjorie Hooker, c/o U. S. Geological Survey, Washington 25, D. C.

Printed by the George Banta Company, Inc., Menasha, Wisconsin
Printed in the United States of America

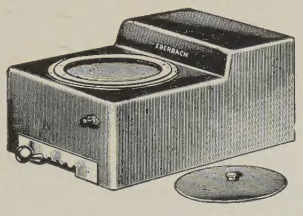

POLISHER FOR PETROGRAPHIC SPECIMENS

For preparation of fine petrographic specimens. Wheel speeds of 300, 375, 450, 525 and 600 r.p.m. are obtained by adjustment of the speed control knob. The V-belt drive is smooth and quiet; the motor and polishing wheel have ball bearings. Two 8 inch diameter aluminum polishing plates with a flexible spiral wire band to hold polishing paper or cloth are provided. Threaded hole is provided for ½ inch rod to support aspirator bottle. Outlet and rubber tubing are provided so no permanent plumbing is required. The cast aluminum case measures 16 by 22 inches; the polishing wheel is 9 inches above table surface. The aluminum bowl has a removable splash ring and cover. For 115 volt, 60 cycle A.C. Catalog number 53-431 polisher sells for $345.00. A cast iron polishing plate for lapping is available under catalog number 53-522 for $25.00.

Eberbach CORPORATION
SCIENTIFIC INSTRUMENTS & APPARATUS
ANN ARBOR, MICH. ESTABLISHED 1849

MINERAL SPECIMENS

Large variety of crystals, crystal groups, rare minerals, and ore minerals for collectors, universities and museums.

Mineral Catalog 25¢, or sent free when requested on official letterhead.

Filer's are interested in buying or exchanging for good quality minerals, especially from foreign countries. Correspondence is invited.

FILER'S
P. O. Box 372, Redlands, California

Our Specialty is
SELECTED MINERAL SPECIMENS
FROM WORLD-WIDE LOCALITIES FOR COLLECTORS AND MUSEUMS

we also carry a complete line of
MINERALIGHTS, DETECTRON GEIGER COUNTERS, ESTWING PROSPECTOR PICKS, MINERALOGICAL BOOKS, ETC.

Send for free current bulletin

SCHORTMANN'S MINERALS
6 McKinley Avenue **Easthampton, Massachusetts**

For Mineralogists:

Index of Refraction Liquids

Range: 1.35 to 2.11 index; available in sets of limited range, or in sets with various intervals, or in any selection. Note that liquids 2.01 to 2.11 are now available.

See detailed price list of index liquids in our three-page advertisement in the July-August and September-October issues of the American Mineralogist. Or, write for Price List Nd-AM

Allen Reference Sets for Microscopical Studies in Mineralogy and Petrology

Six sets of Authentic materials for use as standards for refractive index, for standard materials mounted in balsam to be compared with unknowns, and for demonstration of typical optical characteristics under microscopical study.

Write for descriptive material A-AM

Text: Practical Refractometry by Means of the Microscope

By ROY M. ALLEN, D.SC.

Describes the technique of the immersion method of microscopy, with particular reference to the identification of minerals. Written primarily for elementary instruction, but this text will be very useful also to advanced workers. Price $1.00. Copy will be sent on approval.

Heavy Liquids

Formulated especially for determination of specific gravity of minerals, but special formulations are being made to order for various procedures. If you have any special problem in this field of separation of minerals or other materials by differences in specific gravity, please write us about your problem. Or, just write for leaflet HL-AM.

Lovins Field Finder

For re-locating any point of interest on microscope slide. Same size as a 3″ x 1″ microscope slide; has 1012 1mm. squares, each square numbered and lettered, with sides graduated into tenths. A beautiful example of micro-photography.

Write for Leaflet LFF-AM

Gems, Testing For Identity and For Defects

The CARGILLE-ALLEN GEM TESTING SET is the title of our new book describing the properties of gems and also the equipment for certain identification of gems by a new simple procedure. Price $1.00; this amount applicable to purchase price of any of the items listed in the book.

R. P. Cargille Laboratories, Inc.
117 Liberty St., New York 6, N.Y.

THE AMERICAN MINERALOGIST

JOURNAL OF THE MINERALOGICAL SOCIETY OF AMERICA

Vol. 44 JULY–AUGUST, 1959 Nos. 7 and 8

THE CRYSTALLOGRAPHY OF PETZITE, Ag_3AuTe_2

ALFRED J. FRUEH, JR., *Department of Geology, University of Chicago, Chicago 37, Illinois.**

ABSTRACT

From small single crystals of petzite found intimately intergrown with hessite (Ag_2Te) from Bótes, Transylvania, the space group was determined to be cubic, $I\,4_132$ with a cell edge of 10.38 Å. There are 8(Ag_3AuTe_2) per cell and the atoms are located on the following special positions: 24 silver atoms on x, 0, $\frac{1}{4}$, etc. with $x=.365$; 8 gold atoms on $\frac{1}{8}$, $\frac{1}{8}$, $\frac{1}{8}$, etc.; 16 tellurium atoms on x, x, x, etc. with $x=.266$.

The powder diffraction record of a high temperature form of petzite was obtained, and the material was observed to return to the low form upon rapid cooling. Heating experiments indicate some hessite-petzite solid solubility above 250° C.

INTRODUCTION

While investigating the crystallography of hessite, Ag_2Te, it was discovered that the small single crystals of that mineral from Bótes, Transylvania, obtained from the Harvard University Museum (#99348) and from the U. S. National Museum (U.S.N.M. #R9556) all contained small amounts of an additional phase. The x-ray powder diffraction pattern of this phase proved to be identical with the pattern of petzite, Ag_3AuTe_2, synthesized from the elements and described by Thompson (1948, 1949). This pattern could be successfully indexed on the basis of a body-centered cubic cell of $a=10.38$ Å. Table I compares the d spacings reported by Thompson with the calculated values and with those measured from the Bótes samples.

The petzite appeared as irregular-shaped blebs within the small single crystals of hessite (Fig. 4). By fracturing the hessite at liquid nitrogen temperature, a minute, irregular-shaped fragment of petzite was obtained from which single crystal data could be gathered.

Crystal Structure

From Buerger precession data, using Mo Kα radiation, the space group was unequivocally determined as $I\,4_132$ and the edge of the body-centered cubic cell was found to be 10.38 Å as previously determined

* Present Address: Department of Geological Science, McGill University, Montreal, P.Q., Canada.

TABLE I. *X*-RAY POWDER DATA FOR PETZITE

hkl	Thompson (1949)		Calculated; $a = 10.38$ Å	Bótes, Transylvania	
	I	*d*	*d*	I	*d*
110	2	7.5	7.34	5	7.31
220	2	3.67	3.67	3	3.66
310	½	3.27	3.28	1	3.27
222	1	2.99	3.00	3	2.99
321	10	2.77	2.77	10	2.77
400	½	2.59	2.59	2	2.59
411 } 330 }	3	2.44	2.45	6	2.44
420	3	2.31	2.32	6	2.32
332	—	—	2.21	1	2.21
422	5	2.11	2.12	8	2.12
510 } 431 }	4	2.02	2.04	7	2.03
521	3	1.897	1.895	5	1.893
440	2	1.826	1.835	3	1.835
611 } 532 }	—	—	1.684	1	1.683
622	1	1.558	1.565	2	1.565
631	1	1.525	1.531	2	1.532
444	1	1.492	1.498	2	1.499
710 } 550 } 543 }	1	1.458	1.468	2	1.469
640	1	1.434	1.439	2	1.440
721 } 633 } 552 }	1	1.405	1.413	3	1.403
642	2	1.380	1.387	—	—
732 } 651 }	3	1.312	1.318	5	1.316
800	1	1.292	1.298	3	1.296
811 } 741 } 554 }	1	1.271	1.278	3	1.276
831 } 750 } 743 }	1	1.200	1.207	3	1.205
752	1	1.170	1.175	3	
910 } 833 }	½	1.142	1.146	1	1.146
842	½	1.126	1.133	2	1.132
921 } 761 } 655 }	½	1.114	1.119	2	1.119
664	½	1.101	1.106	2	1.106
930 } 851 } 754 }	½	1.089	1.094	2	1.093
844	1	1.069	1.059	3	1.070
941 } 853 } 770 }	½	1.043	1.049	2	1.048
950 } 943 } 1,031 }	½	1.004	1.008	1	1.008
952 } 765 }	1	.988	.990	4	.990

from the powder record. From the density of 8.7–9.4 the number of formula weights per cell was determined as $Z=8$. This yields a theoretical x-ray density of 8.74.

Intensity data for the a axis zero through fifth level were gathered by an equi-inclination Geiger-counter spectrometer using Cu Kα radiation. The data were corrected for Lorentz and polarization factors by the accepted method (Buerger and Klein, 1945).

The constancy of the chemical composition listed in Doelter (1926) and in the Dana system (Palache, Berman and Frondel, 1941), as well as the

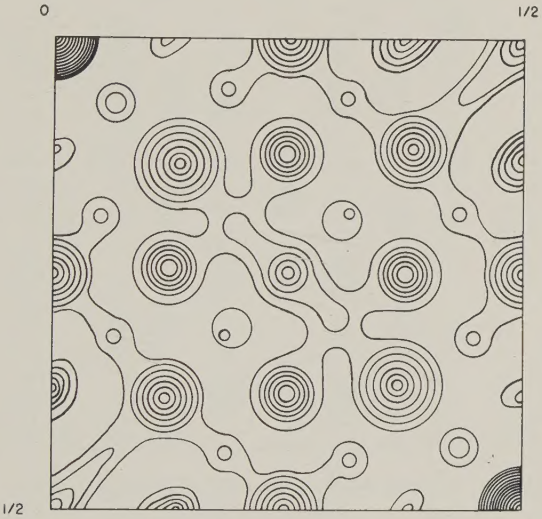

FIG. 1. Patterson projection of petzite on (001).

work of Thompson (1948, 1949) indicate that petzite is a compound with a definite silver-to-gold ratio which would suggest distinct ordered positions for the gold and silver atoms. The symmetry of the space group requires that the 8 gold atoms be located on one of the two special positions 8a or 8b (notation used is that of the International Tables for X-ray Crystallography, 1952). As the two positions are centrosymmetrically related, the position 8a, with a gold atom at $\frac{1}{8}$, $\frac{1}{8}$, $\frac{1}{8}$, etc., was arbitrarily chosen. The 16 tellurium atoms then must be located on the 16e special positions at x, x, x, etc. This means that the interatomic distance vector between gold and tellurium as seen in projection on the Patterson projection (001), must lie along the body-diagonal in vector space. Such a peak is easily discernible on this Patterson projection (Fig. 1), and an approximate parameter ($x=.275$) for tellurium was obtained.

With a knowledge of the gold and tellurium locations, the Patterson could be easily interpreted to yield a reasonable silver parameter utilizing special position 24*f* or x, 0, $\frac{1}{4}$; etc.; with $x=.375$.

An electron density projection on (001) from the observed data and from signs calculated from these assumed positions confirmed the validity of the assumptions (Fig. 2). The tellurium and silver parameters were further refined by the electron density map and by means of a $(Fo-Fc)$ synthesis. The final parameters are as follows: 8 gold atoms at $\frac{1}{8}$, $\frac{1}{8}$, $\frac{1}{8}$, etc.;

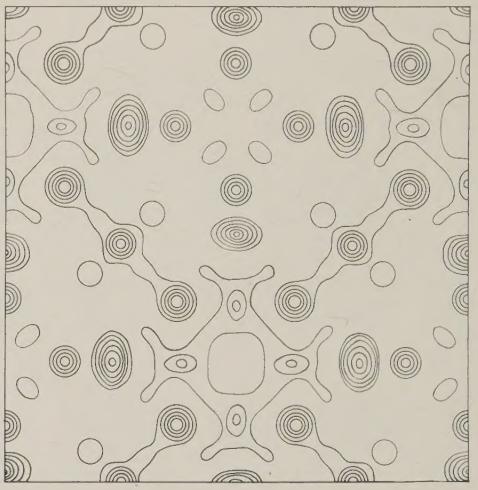

FIG. 2. Electron density projection of petzite on (001).

24 silver atoms at x, 0, $\frac{1}{4}$, etc., with $x=0.365$; 16 tellurium atoms at x, x, x, etc., with $x=0.266$.

These values yield a standard discrepancy factor $R=.14$ for the zero level reflections and an $R=.25$ for all observed reflections. The intensities for all reflections as calculated from these parameters are compared with those observed (Table II).

The structure is illustrated in Figs. 3*a* and *b*. Each gold atom has two close tellurium neighbors at a distance of 2.53 Å. The silver atoms are tetrahedrally surrounded by Te atoms, with two of the Te atoms at 2.90 Å and two at 2.95 Å. The Te-Ag-Te bond angles are 108° and 140° respectively. The tellurium atoms are each surrounded by six silver atoms, one gold atom, and one close tellurium atom in the following manner. If one considers an axis with a tellurium atom at the center and a gold atom 2.53 Å away at one pole of the axis, then at the other pole 3.91 Å away from the central tellurium another tellurium atom is located.

TABLE II. OBSERVED AND CALCULATED |F| VALUES

Index	|F| obs.	|F| cal.	α in degrees	Index	|F| obs.	|F| cal.	α in degrees
110	223	255	90	891	181	104	346
130	86	110	270	222	343	560	270
150	472	467	270	242	570	823	0
170	297	305	90	262	413	454	90
190	—	81	90	282	142	146	0
1, 11, 0	196	94	90	2, 10, 2	261	338	270
220	343	373	0	332	96	179	0
240	522	569	0	352	129	252	90
260	206	195	0	372	584	263	180
280	—	27	0	392	449	434	325
2, 10, 0	—	37	0	3, 11, 2	182	179	256
2, 12, 0	239	298	0	442	74	17	270
330	523	580	270	462	589	604	0
350	153	114	270	482	366	376	356
370	—	31	90	4, 10, 2	306	388	0
390	211	239	90	552	105	27	180
3, 11, 0	458	470	270	572	537	472	209.6
400	407	397	0	592	422	374	31.4
440	708	725	0	662	348	447	270
460	490	458	180	682	—	75	0
480	—	104	0	6, 10, 2	393	365	90
4, 10, 0	378	373	180	772	135	56	180
550	235	112	270	792	397	217	271
570	274	257	270	882	171	42	90
590	400	358	270				
5, 11, 0	303	321	90	343	—	33	90
660	155	111	0	363	170	154	180
680	98	0	0	383	363	360	270
770	340	280	270	3, 10, 3	134	33	0
800	973	1,396	0	453	348	294	284
880	1,199	1,025	0	473	431	346	276
				493	159	394	102
121	—	30	0	4, 11, 3	185	242	288
141	363	293	270	563	153	220	97
161	73	38	180	583	229	254	229
181	154	186	90	673	309	304	329
1, 10, 1	103	15	0	693	508	450	333
1, 12, 1	103	161	270	783	159	100	54
231	434	593	350	444	643	706	180
251	361	253	31	464	—	42	90
271	288	267	280	484	280	415	0
291	251	229	263	4, 10, 4	99	52	90
2, 11, 1	359	398	343	554	554	494	270
341	304	351	98	574	156	147	124
361	320	415	351	664	434	478	0
381	150	141	281	684	301	67	270
3, 10, 1	281	364	184	6, 10, 4	160	322	0
451	—	55	41	774	111	92	90
471	158	144	119	794	160	201	112
491	276	275	283	884	92	16	180
4, 11, 1	372	238	253				
561	491	509	196	565	166	110	180
581	316	317	258	585	85	32	90
5, 10, 1	89	215	0	5, 10, 5	208	159	180
671	314	220	247	675	273	371	209
691	288	213	241	695	396	467	201
781	257	109	0	785	277	266	300

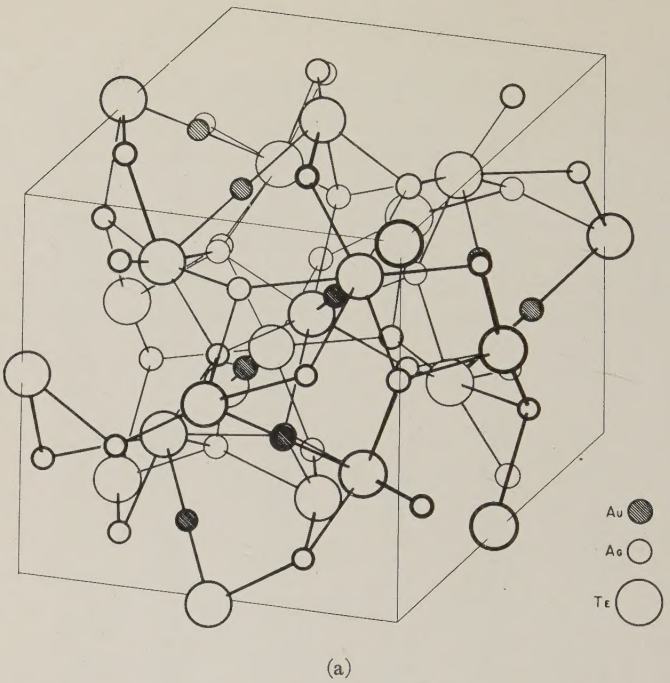

(a)

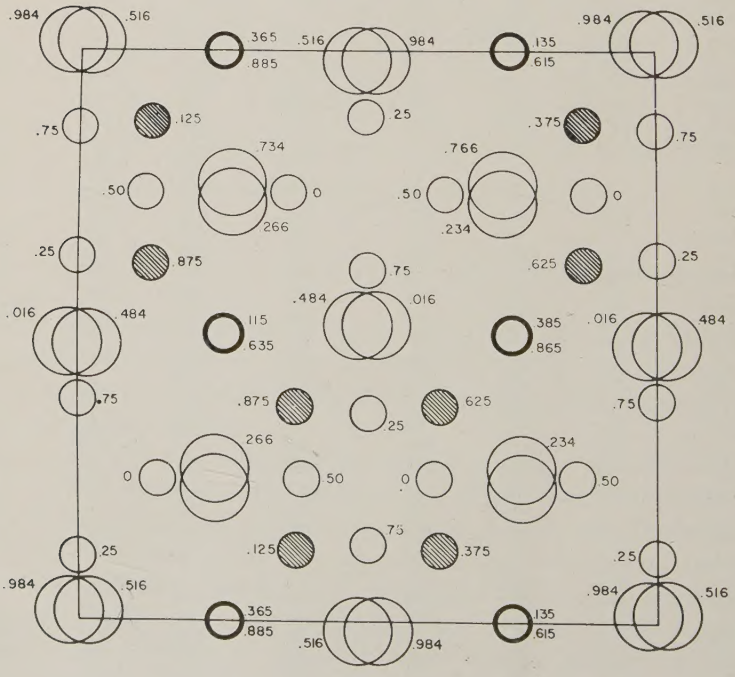

(b)

FIG. 3. (a) Oblique drawing of petzite. (b) Projection of petzite on (001).

The six silver atoms are fairly evenly distributed, three a little above and three a little below the plane which is perpendicular to this axis and passes through the central tellurium. This axis is always parallel to one of the body-diagonals of the unit cell.

The Au-Te distance of 2.53 Å is somewhat closer than that of the closest Au-Te distance (2.63 Å) found in the gold-silver ditellurides (Tunell & Pauling, 1952). At the same time the Te-Te distance of 3.91 Å is a little greater than the greatest distance (3.65 Å) found in the gold-silver ditellurides. If one adjusted the parameter (x, x, x) of tellurium to $x = .273$, one would increase the Au-Te distance to 2.66 Å while decreasing the Te-Te distance to 3.65 Å. However, where intensities are computed after any change in x is made, the R factor from the zero level is observed to increase. The minimum R value of .14 is obtained when the parameters are as originally stated above. Until better data are obtained from a crystal for which absorption and temperature corrections can be made, these parameters and interatomic distances must be accepted.

An explanation of the closer Au-Te distance may rest in the fact that in the ditellurides the gold atoms are bonded to six fairly close tellurium atoms, while in petzite the gold has only two close neighbors. A similar explanation can be offered for the larger Te-Te distance. In the ditellurides the tellurium is bonded to three gold or silver atoms and three other tellurium atoms, while in petzite the tellurium atoms are bonded to six silver, one gold, and one tellurium atom.

High Temperature Behavior

As noted above, the petzite was found intimately intergrown with hessite. Attempts were made to see if these intergrowths would form a single phase at higher temperatures. Several specimens, similar to and including that illustrated in Fig. 4*a*, of irregular-shaped pieces of petzite surrounded by hessite were heated in sealed evacuated pyrex tubes to 150° C. and held for 72 hours. This temperature is slightly above that at which hessite inverts to a high temperature phase (Rahlfs, 1936). No change was apparent in the shape or character of the inclusions after this treatment.

The same samples were then raised to 250° C. and held for 72 hours. After this treatment the surface of both the hessite and the petzite had a similar tarnished appearance and further polishing was necessary to distinguish the petzite (Fig. 4*b*). The petzite appeared to become smaller in extent and its outlines less sharp. Some of the change may be due to the fact that a slightly different cross section is viewed every time this rather soft material is given an additional polish. However, as the several

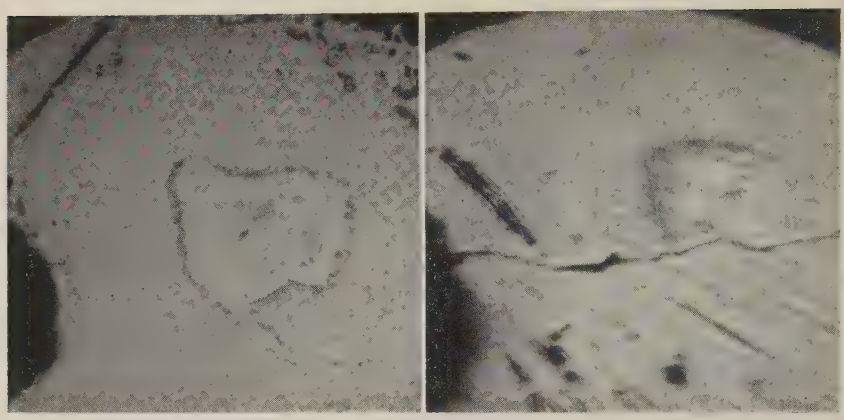

FIG. 4. (a) Polished section of petzite surrounded by hessite.
(b) Same section after heat treatment. 70×

specimens observed appeared to undergo a similar change, a slight increase in the solubility of gold in hessite with increasing temperature can be assumed. No transformation twinning such as that described by Stillwell (1931) was observed on any of the heat-treated samples.

Petzite itself undergoes a rapid and reversible transformation between

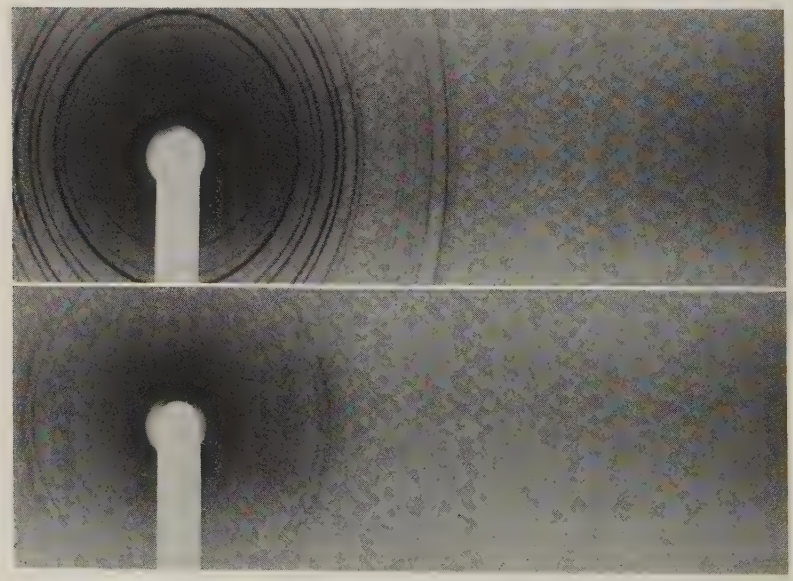

FIG. 5. (a) Powder photograph of petzite at room temperature.
(b) Powder photograph of petzite at 250° C.

TABLE III. X-RAY POWDER DATA FOR HIGH TEMPERATURE FORM

I	d	I	d	I	d
2	3.802	2	2.156	2	.943
6	3.121	5	2.071	1	.921
3	2.797	1	1.955	2	.839
9	2.392	4	1.495	5	.791
10	2.254	5	1.247		

150°–250° C.* The powder diffraction record of the high form taken with Cu Kα is illustrated in Fig. 5*b* in conjunction with the room temperature form (Fig. 5*a*). Table III lists the *d* spacings and estimated intensities of the high form. No attempt has been made to index the pattern.

ACKNOWLEDGMENTS

This work is part of a research program on the crystal chemistry of the sulfides, made possible, in part, by a grant from the National Science Foundation. The author wishes to express his appreciation to Prof. Clifford Frondel and Dr. George Switzer for supplying the crystals investigated. The technical assistance of David Northrop and George Chao is gratefully acknowledged.

REFERENCES

BUERGER, M. J., AND KLEIN, G. (1945). Correction of *x*-ray diffraction intensities for Lorentz and polarization factors. *J. Appl. Physics*, **16**, 406–418.

DOELTER, C. (1926). Handbuch der Mineral-Chemie **4**, T. Steinkopff, Dresden and Leipzig.

International tables for *x*-ray crystallography (1952), **1**, Kynock Press, Birmingham, England.

PALACHE, C., BERMAN, A., AND FRONDEL, C. (1944). Dana's System of Mineralogy, 7th ed., **1**, Wiley, New York.

RAHLFS, P. (1936). Über die kubischen hochtemperatur Modifikationen der Sulfide, Selenide und Telluride des Silbers und des einwertigen Kupfers. *Z. physik Chem.*, **B 31** 157–194.

STILLWELL, F. L. (1931). The occurrence of telluride minerals at Kalgoorlie. *Aust. Inst. of Min. and Met. Proc.*, **84**, 115–190.

THOMPSON, R. M. (1948). Pyrosyntheses of telluride minerals. *Am. Mineral.*, **33**, 209.

THOMPSON, R. M. (1949). Telluride minerals and their occurrence in Canada. *Am. Mineral.* **34**, 350–353.

TUNELL, G. AND PAULING, L. (1952). The atomic arrangement and bonds of the gold silver detellurides, *Acta Cryst.*, **5**, 357–381.

Manuscript received September 25, 1958.

* F. C. Kracek and C. J. Ksanda, by thermal analysis found a transition in petzite at 210±10° C. (private communication).

STRONTIAN META-AUTUNITE FROM THE DAYBREAK MINE, MT. SPOKANE, WASHINGTON[1]

A. VOLBORTH, *University of Nevada, Reno, Nevada.*

ABSTRACT

Chemical analysis, *x*-ray, and optical data of meta-autunite from Daybreak Mine, near Mt. Spokane, Wash., are compared with previous data on meta-autunite. It is shown that Mt. Spokane meta-autunite represents a very pure material with properties close to the theoretical with the exception of the strontium content. According to the analysis the composition of Mt. Spokane meta-autunite corresponds with the formula proposed by Beintema (1938)—$Ca(UO_2)_2(PO_4)_2 \cdot 6\frac{1}{2}H_2O$.

INTRODUCTION

In 1955 Mr. W. Oke, Curator in Mineralogy at California Institute of Technology, drew my attention to an unusually beautiful and well-crystallized sample of yellowish green and dark green meta-autunite from Mt. Spokane, Washington, that appeared very similar to torbernite. In 1957 Prof. J. Butler, Metallurgist at the Nevada Mining Analytical Laboratory, kindly supplied me with adequate amounts of the mentioned meta-autunite. This work was done on these samples which have been stored for over a year in a dry cellar room with a steady temperature of about 65° F. in the Mackay School of Mines Building. When this manuscript was completed, the author learned that Mr. G. W. Leo, U. S. Geological Survey, Menlo Park, California, was working on the same material and had already published an abstract in connection with the Fifty-Fourth Annual Meeting of the Geological Society of America, Cordilleran Section, Eugene, Oregon (1958). Before sending the manuscript, the author was able to meet Mr. Leo and to discuss both investigations. It was then discovered that the material on which both authors have worked is from the same locality. The scope of each work is different, so that they can be regarded as supplementing each other with very little overlapping information. Mr. Leo's work deals mainly with the fully hydrated autunite and with the variation in composition and physical properties of the zoned mineral; it is concerned also with considerations regarding the probable origin of the deposits. The present paper deals only with the stable, dark-green meta-autunite from Daybreak Mine. It was mutually agreed then to publish each paper separately.

According to our knowledge, combined *x*-ray, optical, and chemical data on natural meta-autunite, obtained from the same material, are not listed in the literature. Berzelius (1824) gives an analysis of Autun material that is the closest in composition to meta-autunite. Fairchild

[1] Publication authorized by the Director, Nevada Bureau of Mines.

(1929) gives an analysis of synthetic meta-autunite practically identical with the theoretical composition of meta-autunite with $6\frac{1}{2}$ H_2O. No optical data for a distinct meta-autunite species, nor a complete chemical analysis of such natural species is available. This situation and the excellent material obtained have stimulated this study.

Meta-Autunite and Autunite

The stable variety of autunite at room conditions is called meta-autunite (I) (was called first metakalkuranit by Rinne, 1901), is tetragonal, and contains, according to Beintema (1938), $6\frac{1}{2}$ to $2\frac{1}{2}H_2O$. The formula is written $Ca(UO_2)_2(PO_4)_2 \cdot 2\text{–}6H_2O$ by Donnay and Donnay (1955). Brichard and Brasseur (1958) have recently restudied the autunite problem and arrived at results very similar to those of Donnay and Donnay. They state, on the basis of dehydration experiments on autunite at temperatures up to 250° C., that the stable variety of "natural autunite" contains $6H_2O$ and is identical with Beintema's meta-autunite I. This is in slight disagreement with Beintema's dehydration studies at different vapor tensions (1938, p. 159) which show that the stable meta-autunite variety contains $6\frac{1}{2}H_2O$ at temperatures 15°, 38°, and 57° C., and vapor tensions 0.8–2, 10–20, and 30–90 mm. Hg respectively. Beintema's and Brichard's and Brasseur's (1958) experiments show that meta-autunite I is easily transformed to autunite $Ca(UO_2)_2(PO_4)_2 \cdot 10\frac{1}{2}H_2O$ when stored in humid atmosphere or treated with water at room temperature.

The fully hydrated autunite is supposed to contain theoretically $12H_2O$ (21.92% H_2O). No natural material so far analyzed has contained so much water. Work by Beintema (1938) and Nakanishi (1951) indicates that a stable variety of autunite at high humidity values and in water exists and contains $10\frac{1}{2}$ (Beintema)—10 (Nakanishi) H_2O. Analyses of natural autunite are in good agreement with these results (Church, 1875; Henrich, 1922; Hodge Smith, 1926). Frondel, Riska and Frondel (1956) write the formula with $8\text{–}12H_2O$, Fiorentini Potenza (1958) uses $12H_2O$ for the unit cell, but does not analyze the water content of the Biella autunite. Strunz (1957), based on Beintema's data (1938), writes $10(12\text{-}10)$ H_2O for autunite, emphasizing therefore $10H_2O$ for the formula. The reason for so many different data is obviously the reversible transformation meta-autunite$\rightleftharpoons$autunite and the instability of autunite under laboratory conditions.

Meta-Autunite from Mt. Spokane

The Daybreak Mine is located about 30 miles NE of Spokane in Sec. 11, R. 44 E., T. 28 N., in Spokane Co., Washington. The described

meta-autunite occurs in shear zones in the Loon Lake quartz monzonite. The sample came from the oxidized zone, about 10 feet below the surface (Donald L. Hetland, private communication). No other uranium minerals have so far been discovered here (G. W. Leo, private communication). Norman (1957) gives a short description of the mine with photographs of the shear contact, a typical meta-autunite sample, and the mine. Thurlow (1955) describes another autunite occurrence NW of Spokane on the Indian reservation at the contact of the Weaver's Deer Trail argillite and the Loon Lake granite. Here also uranophane and uraninite associated with pyrite have been found.

The sample consisted of coarse aggregates of tabular slightly deformed dark green crystals usually several mm. in diameter, standing on their edges upon compact crusts of dark green meta-autunite. Central parts of the crystals were colored dark bluish green and some edges a yellowish green with traces of canary-yellow material that under magnification appeared to represent areas crushed probably when the sample was taken. The change in color is apparently due to minor cracks and therefore presence of air along the (001) cleavage planes. The greenish yellow color on edges seemed to become more intense in a few days on disturbed edges and surfaces of the green flakes used for specific gravity determination by immersion in toluene and carbon tetrachloride with the Berman balance. The color of the fresh green meta-autunite resembles that of torbernite very closely. Specific gravity: 3.48. During specific gravity determinations with Berman balance, it was noted here that longer immersion gave higher values, e.g., 3.28 (immediate)—3.35, 3.40 (2 hrs.)—3.48 (>3 hrs.) in toluene, and 3.35, 3.40 (1 hr.)—3.48 (>2 hrs.) in carbon tetrachloride. This indicates that it takes that long for the liquids to penetrate and fill the minor cracks in the micaceous mineral. It is obvious that this is possible only to a certain extent, so that the true value must be slightly higher. Beintema (1938) gives the specific gravity for $Ca(UO_2)_2(PO_4)_2 \cdot 6\frac{1}{2}H_2O$ as 3.569 (calc.); his meta-autunite had a value >3.33. The fluorescence under short-wave ultraviolet light, of parts of the dark green material is a weak yellowish green. The yellowish green material and parts of the green material fluoresce a bright yellowish green, see Iimori and Iwase (1938). Refractive indices were determined using gelatin-coated slides on a universal stage. To obtain a correct value for the *c*-direction (ϵ) an oil immersion objective was used and no cover glass was applied, so as not to disturb the grains standing on their edges. The upper hemisphere was left off, and immersion liquids were applied directly between the objective and the slide. (Any corrosive liquids must be avoided and the objective cleaned carefully immediately after the work is completed.) Sodium light was used. The range of values

obtained for the green mineral are $(\epsilon)\pm0.003$ and $(\omega)\pm0.002$. The refractive indices of this meta-autunite are higher than previously reported for autunites, corresponding well with George's data (1949).

Refractive indices for greenish yellow material were not measured separately, but appear to be close to the lower limits of the range given in Table 1, or slightly lower for the more yellow material.

2V was measured on the universal stage on large flakes on gelatin-coated slides. Examined in polarized light the flakes appeared homogeneous. Under crossed nicols over 60 per cent of the area of the flakes appears in extinction. Very low birefringence can be detected in the

Table 1. Optical Properties of Meta-Autunite and Autunite

	Meta-autunite Mt. Spokane	Autunite Autun[1]	Autunite Maryland[2]	Meixner[3]	Autunites—Meta-autunite[4]
$\epsilon(\alpha)=c$	1.584 ± 0.003	1.553	1.555		1.585–1.600
(β)		1.575	1.575	1.58–1.59	1.595–1.610
$\omega(\gamma)$	1.607 ± 0.002	1.577	1.578	1.59–1.60	1.595–1.613
2V	0°–20° (anomalous) also uniaxial in part				
Birefringence	0.023	0.024	0.023		
Sign	—	—	—		

[1] Michel-Levy and Lacroix (1888).
[2] Shannon (1926).
[3] Meixner (1940).
[4] George, D'Arcy (1949).

other parts. These optically different areas resemble the quadrille structure of microcline. In some of these flakes straight completely isotropic lamellae occur. 2V was measured in several spots which had the highest birefringence (light gray). The highest value in about 20 measurements was 20°. Typical series of measurements were: 2V = 18°, 12°, 16°, 13°, 16°, 15°, 13°, 15°, 18°, 20°, 16°, 15°. Dichroic with $\omega>\epsilon$, ω—grayish green, ϵ—faint yellowish green.

Powder diagrams were recorded with a Norelco wide-range goniometer. A nickel filter was used (CuK—1.5418 Å). In Table 2 the *x*-ray data so obtained are compared with the data for natural meta-autunite given by Brichard and Brasseur (1958) and the data for meta-autunite from Sabugal, Portugal, by Frondel, etc. (1956). The *d*-values and intensities were obtained with the wide-range goniometer at a speed of $\frac{1}{4}°=1$ min. with coll. $1°-0.006''$. Intensity is measured by estimating the peak curve areas. Differences in intensities as compared to those given by Brichard (1958) and Frondel (1956) are due to the micaceous nature of

the mineral. The powder samples for the goniometer scanning were prepared by pressing the mineral powder slightly in the sample holder form with a glass plate and removing the excess by sliding the glass plate in a diagonal direction until a smooth surface was obtained. This way better peaks and intensities were obtained, but the preferred orienta-

TABLE 2. X-RAY DATA FOR META-AUTUNITE FROM MT. SPOKANE, WASH., COMPARED WITH DATA ON META-AUTUNITE I BY BRICHARD (1958) AND FRONDEL (1956)

Meta-Autunite, Mt. Spokane					Meta-Autunite I, Brichard				Meta-Autunite Sabugal, Portugal Frondel	
d meas.	*d* calc.	I meas.	*hkl*[1]	*HKL*[2]	Synthetic *d* meas.	I	*hkl*[3]	Natural *d* meas.	*d* meas.	I
					10.15 Aut.					
8.47	8.47	100	001	001	8.465	s	001	8.52	8.51	10
5.37	5.38	44	101	221	5.39	s	221	5.41	5.39	7
4.93	4.93	21	110	040	4.92	s	040	4.95	4.96	5
	4.26		111	041	4.42	vf	240*		4.28	6
4.23	4.24	69	002	002	4.25	m	002	4.26		
3.61	3.62	85	102	222	3.64	m	222	3.64	3.63	8
3.48	3.49	31	200	440	3.48	s	440	3.51	3.50	9
					3.30 Aut.					
3.22	3.22	23	201	441					3.24	8
	3.21		112	042	3.23	s	042	3.24		
2.93	2.93	15	211	261	2.93	m	621	2.94	2.94	4
	2.82		003	003						
	2.69		202	442	2.70	vf	213*	2.705	2.68	1
2.61	2.62	35	103	223				2.62	2.61	3
2.51	2.51	6	212	262	2.52	f	323*	2.52	2.51	2
2.47	2.47	4	220	080	2.47	w	080	2.48	2.47	2
2.45	2.45	4	113	043						
2.37	2.37	8	221	081	2.38	w	423*	2.38	2.38	3
2.24	2.24	5	301	661	2.24	w	523*	2.25	2.25	2
2.21	2.21	10	310	480	2.21	m	480	2.215	2.21	3
	2.19		203	443						
	2.13		311	481	2.14	w	613*	2.14	2.14	3
	2.13		222	082						
2.11	2.12	71	004	004						
	2.09		213	263	2.10	f	623	2.10	2.10	3
2.04	2.04	9	302	662	2.05	w	633*	2.05	2.04	3
2.02	2.03	14	104	224						
	1.956		312	482						
1.943	1.946	14	114	044					1.941	2
	1.885		321	2.10.1	1.89	f	653*	1.89	1.893	1
	1.857		223	083				1.85		
1.807b	1.810	8	204	444						
	1.794		303	663				1.795	1.802	2
1.758b	1.759	6	322	2.10.2	1.77	f	10.2.2	1.77	1.757b	3
	1.752		214	264	1.75	f	544*	1.75		
1.745	1.743	9	400	880						

vs—very strong; s—strong; m—medium; w—weak; f—faint; vf very faint; b—broad.

[1] Small cell, $a_0=6.972$, c_0 8.47.

[2] Large cell, $a_0=19.72$, c_0 8.47; by the transformation $2\bar{2}0/220/001$.

[3] Where Brichard and Brassuer's indexing does not agree with ours the *hkl* indices are marked with an asterisk.

tion of the mineral particles could not be avoided, which is clearly demonstrated by the intense 001 peak.

In Table 2 measured and calculated d values and all possible planes in the smaller cell ($a_0=6.97$ Å, $c_0=8.47$ Å), with the space group $P4/nmm$, are given for spacings greater than 1.743. Through transformation $2\bar{2}0/220/001$ corresponding indices of the larger cell are given in column HKL.

Unit cell dimensions of the Mt. Spokane meta-autunite and $c_0:a_0$

Table 3. Unit Cell Dimensions of Meta-Autunite

Meta-autunite Mt. Spokane (Volborth)	Meta-autunite I (Beintema)	Meta-autunite I (Donnay & Donnay)	"Autunite naturelle" (Brichard & Brasseur)
$a_0=6.972$ Å	6.994	7.01	6.97
($a_0'=19.72$ Å)		(19.82 Å±0.3%)	(19.72 Å±0.3%)
$c_0=8.47$ Å	8.437	8.49 Å±0.3%	8.50 Å±0.3%
$c_0/a_0=1.211$	1.206	1.211	1.211
($c_0/a_0'=0.4295$)		(0.4282)	(0.4309)
Sp.gr.$_{meas.}$ 3.48	3.33	3.48	
Sp.gr.$_{calc.}$ 3.586 ($6\frac{1}{2}H_2O$)	3.569 ($6\frac{1}{2}H_2O$)		
Sp.gr.$_{calc.}$ 3.542 ($6H_2O$)		3.50 ($6H_2O$)	
Z=1 (8)	1	(8)	

ratios, obtained from the wide-range goniometer pattern measurements, are in close agreement with those measured by Beintema (1938). If Beintema's data are converted to true Å we obtain: $a_0=6.994$, and $c_0=8.437$.

Since Brichard and Brasseur (1958) and Donnay and Donnay (1955) have recently used a larger cell, a_0 is also transformed in Table 3 according to $a_0'=a_0\cdot 2\sqrt{2}$ for comparison. The data for the larger cell are given in parentheses.

Since the meta-autunite from Daybreak Mine is zoned with colors ranging from yellow to green and dark green, nearly black, an attempt was made to distinguish between the yellow and green material. Optical properties of both mineral varieties proved to be very similar. In a mixture of grains these varieties cannot be distinguished in a satisfactorily manner. In thin flakes the green material shows only a slightly stronger dichroism and higher refractive indices.

Dr. A. Pabst kindly offered to run precession and Weissenberg patterns on small green and yellow meta-autunite crystals for comparison. His data are practically identical, indicating that both the green and the

yellow phases are the equivalent of Beintema's meta-autunite I. See Table 4.

Pabst found no evidence for the 19.76 Å a_0 since all the reflections on the *hk*0 and *hkl* precession patterns could be accounted for by taking a cell with an a_0 of 6.985.

For chemical analysis dark blue-green, thick, compact flakes were selected. The yellowish edges were avoided as much as it was possible in hand separation. The color of this selected material was practically identical with the color of the fresh meta-autunite from the same locality that was coated with plastic immediately after sampling. Since the uncoated, undisturbed material does not change its color even after being

Table 4. Unit Cell Dimensions of Green and Yellow Meta-Autunite (Pabst)

	Small green xl. Å	Small yellow xl. Å
a_0 (precession)	6.985±0.010	6.99±0.01
a_0 (Weissenberg)	6.98 ±0.02	6.96±0.02
c_0 (precession)	8.44 ±0.02	8.45±0.02
c_0 (Weissenberg)	8.45 ±0.02	8.44±0.03

stored for over a year and does not show any visible alteration which could be due to possible dehydration, it would seem probable that its composition also does not change, and it can be therefore assumed that the analyzed material represents the natural meta-autunite as found in the fault gouge at Mt. Spokane, or is very close to it in its composition and physical properties. According to Norman (p. 665–666, 1957), the primary mineral at Daybreak Mine is meta-autunite.

Results of the chemical analysis are practically identical with the theoretical data for meta-autunite with a formula $Ca(UO_2)_2(PO_4)_2 \cdot 6\frac{1}{2}H_2O$ as is shown in Table 5.

Qualitative spectrographic analysis by Mr. Harold Vincent (Bausch and Lomb quartz spectrograph) shows the following elements present in traces: Al, Fe, Mg, Pb, V. Not detected: As, Bi, Cu, Mn, Sb, Sn, Tl.

Pereira-Forjaz (1917) found traces of Cu, Al, V, Fe, Pb, Mn, As, Sn, Bi, Mg, and Tl in autunite from Nellas, Portugal.

This analysis was carried out using the method proposed by the author (1954, 1958). The water determination was done according to the Penfield method (1894). The results indicate $6\frac{1}{2}H_2O$ molecules for the stable natural meta-autunite which is in good agreement with Beintema's

data (p. 159, 1928). Unit cell dimensions and specific gravity determinations (Table 3) indicate, however, that $6H_2O$ molecules are perhaps more likely. The difficulty of the specific gravity determination (see above), and the high molecular weight of the mineral makes it difficult to determine the water content of the meta-autunite on the basis of physical data. It is possible that the original material contained a minor amount of an autunite with more water. Brichard and Brasseur (1958) conclude

TABLE 5. STRONTIAN META-AUTUNITE, MT. SPOKANE, WASHINGTON
Anal., A. Volborth

	Per cent	Atomic ratios to $18\frac{1}{2}$ oxygens	$Ca(UO_2)_2(PO_4)_2 \cdot 6\frac{1}{2}H_2O$ M = 887.27
CaO	5.16		6.32
SrO[1]	1.38		
Na_2O	0.22	1.06	
K_2O	0.33		
UO_3	63.92	1.98	64.48
P_2O_5	15.54		16.00
SiO_2	0.39	2.00	
H_2O	13.36	6.57	13.20
Rem.[2]	0.14		
	100.44		100.00
	Sp. gr. 3.48		

[1] SrO was determined by Mr. H. Vincent flame-spectrophotometrically (Beckman Model DU) using the standard addition method described by Chow and Thompson (1955). Mr. G. W. Leo drew my attention to the fact that this mineral contains Sr.

[2] $Fe_2O_3+Al_2O_3=0.03\%$; insol. $=0.11\%$; $MgO=0.00\%$; $BaO=0.00\%$; Cu—no blue coloration in NH_4OH filtrate. Values for K_2O and Na_2O have to be regarded as slightly too high because of the accumulation of traces of these elements during the analysis from the reagents and glassware used. See Volborth, 1954, 1958.

on the basis of dehydration experiments conducted up to 250° C. that meta-autunite contains only $6H_2O$ molecules. Recent experiments in this laboratory indicate that the last water in phosphates escapes at temperatures as high as 900–1000° C.

It is obvious that much of the natural autunite material as found today is actually meta-autunite. The question of whether the natural material is autunite or meta-autunite seems to be of minor importance considering the fast reversible change between these minerals. It merely depends on whether the mineral is found in humid or dry environments. Beintema's study (p. 159, 1938) on water content indicates that at higher tempera-

tures and higher humidity values, the stability of meta-autunite increases. To tell whether meta-autunite is actually the stable phase under hydrothermal conditions, a study in a pressurized bomb is needed.

Acknowledgments

The author wishes to thank Dr. A. Pabst for his suggestions and help during this work.

Mr. H. Vincent has made the spectrographic determinations, and Dr. L. S. McGirk has critically reviewed the manuscript and has made numerous valuable suggestions; for this the author wishes to express his gratitude.

References

Beintema, J. (1938) On the composition and the crystallography of autunite and the meta-autunites: *Rec. trav. chim. Pays-Bas.*, **57,** No. 2, 155.

Berzelius, J. J. (1824) Zerlegung des Uranites von Autun: *Pogg. Ann. Phys.*, **1 (77),** 379.

Brichard, H. and Brasseur, H. (1958) Sur les autunites naturelles et synthetiques: *Bull. Soc. franç. Miner. Crist.*, **81,** no. 1–3, 4.

Chow, T. J. and Thompson, T. G. (1955) Flame photometric determination of strontium in sea water: *Anal. Chem.*, **27,** 18.

Church, A. H. (1875) On the composition of autunite: *J. Chem. Soc. London*, **28,** 109.

Donnay, Gabrielle, and Donnay, J. D. H. (1955) Contribution to the crystallography of uranium minerals: *U.S.A.E.C. Tech. Inf. Serv., Oak Ridge*, **TEI-507**.

Fairchild, J. G. (1929) Base exchange in artificial autunites: *Am. Mineral.*, **14,** 265.

Fiorentini Potenza, Maria (1958) Autunite e metatorbernite nella sienite di Biella: *Rend. Soc. Min. Italiana*, Anno **XIV,** 215.

Frondel C., Riska, D., and Frondel, J. W. (1956) *X*-ray powder data for uranium and thorium minerals: *U. S. Geol. Surv. Bull.* **1036-G.**

George, D'Arcy (1949) Mineralogy of uranium and thorium bearing minerals: *U.S.A.E.C. Tech. Inf. Serv., Oak Ridge*, **RMO-563.**

Henrich, F. (1922) Beitrage zur Kenntniss der Kalk-uran-glimmer (Autunite): *Ber. Deutshe Chem. Ges.* **55,** 1212.

Hodge Smith, T. (1926) Mineralogical notes No. 2. Autunite, Mount Painter, South Australia: *Australian Mus. Records*, **15,** 74.

Iimori, S., and Iwase, E. (1938) The fluorescence spectrum of autunite: *Inst. Phys. Chem. Res., Tokyo, Sci. papers*, **34,** 372.

Leo, G. W. (1958) Autunite from Mt. Spokane, Washington: *Bull. Geol. Soc. Am.*, **69,** No. 12, part 2, 1694.

Meixner, H. (1940) Fluoreszenzanalytische, optische und chemische Beobachtungen an Uranmineralien: *Chemie der Erde* **12,** 433.

Michel-Levy, A., Lacroix, Alf. (1888) Les Mineraux des Roches: p. 157.

Nakanishi, M. (1951) Water content of autunite: *Nat. Sci. Rept., Ochanomizu Univ.* **1,** *71.*

Norman, H. W. (1957) Uranium deposits of Northeastern Washington: *Mining Engineering*, **June,** 662.

Penfield, S. L. (1894) On some methods for the determination of water: *Am. J. Sci.* (*3*), **48,** 30.

Pereira-Forjaz, A. (1917) Etudes spectrographiques des mineraux portugais d'uranium et de zirconium: *C. R., Paris*, **164,** 102.

Rinne, F. (1901) Kalkuranit und seine Entwässerungsprodukte (Metakalkuranite): *Cbl. Min.*, 709.

Shannon, E. V. (1926) Some minerals from the Kensington mica mine, Montgomery County, Maryland: *Am. Mineral.*, **11,** 35.

Strunz, H. (1957) Mineralogische Tabellen: Leipzig, p. 253.

Thurlow, E. E. (1955) Uranium deposits at the contact of metamorphosed sedimentary rocks and granitic intrusive rocks in Western United States: *G. S. Prof. Paper* **300,** 85.

Volborth, A. (1954) Eine neue, die Phosphatanalyse verkürzende Methode und ihre Anwendung in der Analyse der Beryllium-Phosphate: *Zeits. Anorg. Allg. Chemie.*, **276,** 3–4, 159.

Volborth, A. (1958) Simplified analysis of uranyl and other phosphates: *Bull. Geol. Soc. Am.*, **69,** No. 12, part 2, 1657.

Manuscript received September 24, 1958.

STUDIES OF BORATE MINERALS (V): REINVESTIGATION OF THE *X*-RAY CRYSTALLOGRAPHY OF ULEXITE AND PROBERTITE*

JOAN R. CLARK AND C. L. CHRIST, *U. S. Geological Survey, Washington 25, D. C.*

ABSTRACT

Ulexite and probertite crystals have been examined by *x*-ray precession methods and earlier findings confirmed. Revised data for the crystallographic elements are as follows: ulexite, $NaCaB_5O_9 \cdot 8H_2O$, triclinic $P\bar{1}-C_i^1$, $a=8.80_9\pm0.02$, $b=12.86\pm0.04$, $c=6.67_8\pm0.02$ Å, $\alpha=90°15'$, $\beta=109°07'$, $\gamma=105°06'$ (all $\pm05'$); probertite, $NaCaB_5O_9 \cdot 5H_2O$, monoclinic $P2_1/a-C_{2h}^5$, $a=13.43\pm0.04$, $b=12.57\pm0.04$, $c=6.58_9\pm0.02$ Å, $\beta=100°15'\pm05'$. *X*-ray powder patterns of both minerals have been indexed, and all calculated interplanar spacings are given for $d\geq2.5$ Å.

INTRODUCTION, EXPERIMENTAL TECHNIQUES, AND ACKNOWLEDGMENTS

In connection with current crystal structure studies of sodium calcium borates, the *x*-ray crystallography of ulexite and probertite have been re-examined and *x*-ray powder patterns of these minerals have been indexed.

Single crystal studies were made on a quartz-calibrated precession camera with both Mo/Zr and Cu/Ni radiations. Film measurements were corrected for horizontal and vertical film shrinkage. A 114.59 mm. diameter powder camera was used with Cu/Ni radiation for the powder films and the measurements were corrected for film shrinkage.

We are grateful to several colleagues at the U. S. Geological Survey for their collaboration during these studies: W. T. Schaller supplied crystals of ulexite and probertite, Mary E. Mrose prepared the *x*-ray powder patterns, H. T. Evans, Jr. contributed helpful discussion, and D. E. Appleman carried out the calculations for *d*-spacings.

SINGLE CRYSTAL STUDY OF ULEXITE

The crystallography of ulexite, $NaCaB_5O_9 \cdot 8H_2O$, was the subject of a comprehensive study by Murdoch (1940), who summarized earlier findings and compiled crystallographic data based on his own goniometric measurements of terminated crystals and on his measurements from *x*-ray oscillation photographs. Ulexite crystals used in the present study originated at the Baker mine, Boron, California. *X*-ray examination of these crystals shows that ulexite is triclinic and the space group is therefore either $P1$ or $P\bar{1}$. Piezoelectric tests were made of the crystals, using an apparatus of the Giebe-Scheibe type. The negative results of these

* Publication authorized by the Director, U. S. Geological Survey.

tests, considered together with the crystal morphology found by Murdoch (1940), confirm his selection of space group $P\bar{1}$ with cell contents $2[NaCaB_5O_9 \cdot 8H_2O]$. Values of the direct crystallographic elements obtained in the present study are compared in Table 1 with those found by Murdoch (1940); the agreement is excellent.

Table 2 contains a complete set of data for direct and reciprocal cell elements of ulexite, including the direct and reciprocal Cartesian matrices together with the components v_1 and v_2 of the b-axis on the x- and y-axes, respectively, of Cartesian coordinates (Evans, 1948). The six reciprocal cell elements listed in Table 2 were chosen from among all available data as the best measurements, the three reciprocal lengths being those obtained from the present precession x-ray studies and the three reciprocal angles, those found by Murdoch (1940) from goniometric measurements. The six direct cell elements in Table 2 were calculated from the given six reciprocal cell elements. The present calculated density is in much better agreement with the observed density of Murdoch (1940) than was the earlier calculated value.

Single Crystal Study of Probertite

Barnes (1949) examined probertite crystals with precession x-ray techniques using Cu/Ni radiation. He makes no statement regarding

Table 1. Comparison of Direct Cell Elements for Ulexite

Triclinic, space group $P\bar{1}-C_i^1$, $Z=2[NaCaB_5O_9 \cdot 8H_2O]$

	Present Study*	Murdoch (1940)†
a	$8.80_9 \pm 0.02$ Å	8.73 Å
b	12.86 ± 0.04	12.75
c	$6.67_8 \pm 0.02$	6.70
α	$90°15' \pm 05'$	90°16′
β	$109°10' \pm 05'$	109°08′
γ	$105°05 \pm 05'$	105°07′
$a:b:c$	$0.685_0:1:0.519_3$	0.6855:1:0.5191
Cell Volume	687.0 Å^3	676.9 Å^3
Density (calc.)	1.959 g.cm.$^{-3}$	1.988 g.cm.$^{-3}$

* Values of a, b, c, and α were calculated from the reciprocal elements given in Table 2; values for β and γ are readings obtained from the precession camera dial settings.

† Values of a, b, and c were calculated by Murdoch "from the x-ray data using the morphologic axial angles." The axial ratio $a:b:c$ is from goniometric measurements, not from the given axial lengths. Conversion from kX to Ångstrom units has been carried out by the present authors.

calibration of camera or correction for film shrinkage. The direct cell elements which he found are listed in Table 3, column 1; these elements define a direct cell corresponding to the crystal description given by Schaller (1930) as modified by Palache, Berman, and Frondel (1951). The space group assigned by Barnes (1949) is $P2_1/n-C_{2h}^5$. Standard settings for C_{2h}^5 are given in International Tables (1952) as $P2_1/c$ or $P2_1/a$. If the crystal form taken by Schaller (1930) as {101} is trans-

TABLE 2. DIRECT AND RECIPROCAL CRYSTALLOGRAPHIC DATA FOR ULEXITE

Triclinic, space group $P\bar{1}-C_i^1$, $Z=2[NaCaB_5O_9\cdot 8H_2O]$

Direct Cell Elements:†

$a = 8.80_9 \pm 0.02$ Å $\alpha = 90°15' \pm 05'$

$b = 12.86 \pm 0.04$ $\beta = 109°07' \pm 05'$

$c = 6.67_8 \pm 0.02$ $\gamma = 105°06' \pm 05'$

$a:b:c = 0.685_0:1:0.519_3$

Volume = 687.0 Å^3 Density (g.cm.$^{-3}$), calc. 1.959

obs. (Murdoch, 1940) 1.955 ± 0.001

Reciprocal Cell Elements:‡

$a^* = 0.1250_6$ Å^{-1} $\alpha^* = 84°20.5'$

$b^* = 0.0809_1$ $\beta^* = 70°05.5'$

$c^* = 0.1592_6$ $\gamma^* = 73°53.5'$

$p_0:q_0:r_0 = 0.785_3:0.508_0:1$

Projection Elements:§

$x_0' = 0.3467$ $p_0' = 0.8352$

$y_0' = 0.1049$ $q_0' = 0.5403$

$\nu = 73°53.5'$

Cartesian Matrices:§

$v_1 = -0.2774_5$ $v_2 = 0.9607_3$

Direct Matrix:

$$\begin{Vmatrix} 8.323 & -3.569 & 0 \\ 0 & 12.360 & 0 \\ -2.886 & -0.059 & 6.678 \end{Vmatrix}$$ (in Å)

Reciprocal Matrix:

$$\begin{Vmatrix} 0.12015 & 0 & 0.05192 \\ 0.03470 & 0.08091 & 0.01570 \\ 0 & 0 & 0.14974 \end{Vmatrix}$$ (in Å^{-1})

† Direct cell elements were calculated from the six reciprocal cell elements.

‡ Values for a^*, b^*, and c^* are from precession x-ray measurements; values for α^*, β^*, and γ^* are from goniometric measurements by Murdoch (1940). Reciprocal angles obtained from precession film measurements were within $\pm 2,5'$ of Murdoch's values.

§ Values calculated from direct and reciprocal cell elements using equations given by Evans (1948). Projection element values listed by Murdoch (1940) agree with these to ± 0.0001.

formed to {001}, the transformation matrix being $\bar{1}0\bar{1}/010/001$, the direct cell thus obtained is in the $P2_1/a$ orientation. In both descriptions of the cell the cleavage plane is (110). Table 3, column 2, gives the measurements of Barnes (1949) as transformed to the $P2_1/a$ setting. In the present study probertite crystals from the California mine, Boron, California, were examined and the values of the crystallographic elements found are given in Table 3, column 3, for the $P2_1/a$ setting. A slight improvement in the agreement of calculated with observed density has resulted.

TABLE 3. CRYSTALLOGRAPHIC DATA FOR PROBERTITE

Monoclinic, space group $P2_1/a-C_{2h}^5$, $Z=4[NaCaB_5O_9\cdot 5H_2O]$

	Barnes (1949)		Present Study
	(1) $P2_1/n$	(2)* $P2_1/a$	(3) $P2_1/a$
a	13.88 Å	13.44	13.43±0.04 Å
b	12.56	12.56	12.57±0.04
c	6.609	6.609	6.58_9±0.02
β	107°40′	100°17′	100°15′±05′
$a:b:c$†	1.1053:1:0.5263	1.070:1:0.526	1.068:1:0.524
Volume	1097.2 Å^3		1095 Å^3
Density (calc.)	2.126 g.cm.$^{-3}$		2.131 g.cm.$^{-3}$
(obs.)	2.141 (Schaller, 1930)		

* Transformed from original values in column (1) with the matrix $\bar{1}0\bar{1}/010/001$.

† Schaller (1930) from morphologic measurements found 1.1051:1:0.5237; for the transformed cell, using his average of 99°53′ for β, the ratio becomes 1.0683:1:0.5237.

POWDER DIFFRACTION STUDY

A pattern of ulexite was prepared from crystals originating at the Jenifer shaft, Boron, California; a probertite pattern, from type locality crystals found at the Baker mine, Boron, California. A complete set of interplanar spacings for each mineral was calculated down to values of 1.5 Å on the Datatron computer using a program developed by D. E. Appleman. For ulexite, the reciprocal matrix given in Table 2 was used for the calculations, and for probertite, a reciprocal matrix prepared from the data in Table 3, column 3, was used. Table 4 lists observed and calculated interplanar spacings for ulexite and Table 5, those for probertite. Indexing for probertite is given for both the original cell ($P2_1/n$) and the transformed cell ($P2_1/a$). Observed spacings found in the present

TABLE 4. *X*-RAY POWDER DATA FOR ULEXITE, $NaCaB_5O_9 \cdot 8H_2O$

Triclinic $P\bar{1}$: $a = 8.80_9 \pm 0.02$, $b = 12.86 \pm 0.04$, $c = 6.67_8 \pm 0.02$ Å;
$\alpha = 90°15'$, $\beta = 109°07'$, $\gamma = 105°06'$ (all $\pm 05'$)

Measured*		Calculated†		Measured*		Calculated†	
I	d_{hkl}	d_{hkl}	hkl	I	d_{hkl}	d_{hkl}	hkl
100	12.2	12.36	010	15	2.914	2.918	$0\bar{2}2$
15	8.03	8.00	100			2.915	$\bar{3}11$
80	7.75	7.77	$\bar{1}10$			2.888	$\bar{1}41$
		6.28	001			2.887	$0\bar{4}1$
		6.18	020			2.859	$\bar{2}40$
30	6.00	6.04	$\bar{1}01$			2.858	$\bar{2}12$
		6.00	110			2.851	$\bar{3}21$
7	5.83	5.835	$0\bar{1}1$	15	2.844	2.844	$\bar{2}22$
		5.717	$\bar{1}20$			2.824	$\bar{3}01$
6	5.66	5.688	$\bar{1}11$			2.809	$1\bar{4}1$
4	5.42	5.388	011	10	2.767	2.769	$\bar{3}10$
4	5.19	5.195	$\bar{1}\bar{1}1$			2.765	$\bar{2}41$
		4.639	$0\bar{2}1$			2.746	$2\bar{3}1$
7	4.60	4.590	$\bar{1}21$			2.739	$\bar{3}20$
15	4.33	4.345	$1\bar{1}1$			2.718	211
		4.341	120	15	2.692	2.694	022
		4.281	101			2.692	131
		4.202	021				
30	4.16	4.163	$\bar{1}30$			2.672	$1\bar{1}2$
		4.157	$\bar{2}10$			2.670	041
		4.129	$\bar{2}11$	15	2.661	2.665	300
		4.120	030			2.659	$\bar{3}31$
		4.090	$\bar{1}21$			2.646	140
		4.056	$\bar{2}01$			2.633	102
4	3.98	3.998	200			2.631	$\bar{1}41$
		3.939	$1\bar{2}1$			2.625	$0\bar{3}2$
3	3.89	3.884	$\bar{2}20$			2.619	$2\bar{3}1$
3	3.79	3.799	111			2.615	$3\bar{1}1$
		3.791	$\bar{2}21$	10	2.597	2.606	$\bar{1}32$
		3.627	$\bar{2}\bar{1}1$			2.597	$\bar{2}22$
7b	3.59	3.612	$0\bar{3}1$			2.590	$1\bar{2}2$
		3.601	$\bar{1}31$			2.589	$\bar{3}30$
		3.528	210			2.580	$\bar{2}32$
		3.375	$\bar{2}30$			2.578	$\bar{1}32$
		3.352	$1\bar{3}1$	10	2.572	2.572	$\bar{1}50$
		3.334	$\bar{1}02$			2.539	230
6	3.29	3.308	130			2.535	$\bar{3}12$
		3.299	$03\bar{1}$	5d	2.415		
		3.268	$\bar{2}31$	3	2.381		
		3.235	$\bar{1}\bar{3}1$	3	2.350		
		3.228	$\bar{1}12$	3	2.313		
10b	3.20	3.210	121, $\bar{1}12$	3	2.282		
		3.196	$\bar{1}40$	7	2.232		
		3.140	002	6	2.198		
		3.117	$0\bar{1}2$	6	2.173		
15b	3.10	3.096	$\bar{2}21$	3	2.129		
		3.090	040	4	2.090		
		3.045	$2\bar{1}1$	3	2.063		
15	3.01	3.019	$\bar{2}02$	4b	2.023		
		3.013	$\bar{2}12$	15	1.933		
		2.999	220				
		2.974	012	plus additional lines,			
		2.966	$2\bar{2}1$	all with I ≤ 7			
		2.948	201, $\bar{1}22$				
		2.921	$\bar{1}22$				

* Corrected for shrinkage; b = broad, d = diffuse. Radiation: Cu/Ni, $\lambda CuK\alpha = 1.5418$ Å. Lower limit of 2θ measurable: approximately 7° (13 Å).

† All calculated lines listed for $d_{hkl} \geq 2.5$ Å.

TABLE 5. *X*-RAY POWDER DATA FOR PROBERTITE, $NaCaB_5O_9 \cdot 5H_2O$

Monoclinic $P2_1/a$; $a = 13.43 \pm 0.04$, $b = 12.57 \pm 0.04$, $c = 6.58_9 \pm 0.02$ Å; $\beta = 100°15' \pm 05'$

Measured*		Calculated†		
Present Study		Present Study		For $P2_1/n$ (Barnes, 1949)
I	d_{hkl}	d_{hkl}	hkl	hkl
100	9.1_2	9.108	110	110
20	6.62	6.608	200	200
		6.484	001	$\bar{1}01$
		6.285	020	020
		5.849	210	210
10	5.74	5.762	011	$\bar{1}11$
		5.676	120	120
		5.618	$\bar{1}11$	011
		5.104	$\bar{2}01$	101
9	5.02	5.000	111	$\bar{2}11$
9	4.73	4.729	$\bar{2}11$	111
10	4.53	4.554	220	220
		4.513	021	$\bar{1}21$
10	4.44	4.442	$\bar{1}21$	021
		4.264	201	$\bar{3}01$
2	4.16	4.157	310	310
		4.118	121	$\bar{2}21$
10	4.05	4.038	211	$\bar{3}11$
10	4.00	3.994	130	130
		3.962	$\bar{2}21$	121
6	3.80	3.802	$\bar{3}11$	211
		3.607	320	320
		3.539	230	230
20	3.52	3.529	221	$\bar{3}21$
		3.519	031	$\bar{1}31$
		3.485	$\bar{1}31$	031
2	3.37	3.368	$\bar{3}21$	221
3	3.31	3.322	131	$\bar{2}31$
		3.304	400	400
		3.260	311	$\bar{4}11$
9	3.24	3.242	002	$\bar{2}02$
		3.239	231	131
		3.195	410	410
2	3.18	3.182	$\bar{4}01$	301
		3.180	$\bar{1}12$	$\bar{1}12$
		3.143	040	040
2	3.14	3.140	$\bar{2}02$	002
		3.139	012	$\bar{2}12$
		3.084	$\bar{4}11$	311
10b	3.08 to 3.04	3.057	140	140
		3.046	$\bar{2}12$	012
		3.036	330	330
		2.989	231	$\bar{3}31$
		2.974	321	$\bar{4}21$
20	2.935	2.942	112	$\bar{3}12$
		2.924	420	420
		2.913	$\bar{1}22$	$\bar{1}22$
20	2.884	2.889	$\bar{3}31$	231
		2.881	022	$\bar{2}22$
		2.839	$\bar{4}21$	321
4	2.837	2.838	240	240
		2.828	041	$\bar{1}41$
		2.810	$\bar{1}41$	041
35	2.807	2.809	$\bar{2}22$	022
		2.794	$\bar{3}12$	112

(*continued on next page*)

TABLE 5.—(*continued*)

Measured*		Calculated†		
Present Study		Present Study		For $P2_1/n$ (Barnes, 1949)
I	d_{hkl}	d_{hkl}	hkl	hkl
		2.752	401	$\bar{5}01$
		2.727	122	$\bar{3}22$
6	2.731	2.725	202	$\bar{4}02$
		2.722	141	$\bar{2}41$
2	2.697	2.689	411	$\bar{5}11$
2	2.666	2.676	$\bar{2}41$	141
		2.663	212	$\bar{4}12$
		2.628	331	$\bar{4}31$
		2.608	$\bar{3}22$	122
9	2.591	2.594	430	430
		2.586	$\bar{1}32$, 510	$\bar{1}32$, 510
		2.564	032	$\bar{2}32$
6	2.558	2.561	$\bar{5}11$	411
		2.558	340	340
		2.552	$\bar{4}02$	202
		2.534	$\bar{4}31$	331
		2.530	241	$\bar{3}41$
		2.521	421	$\bar{5}21$
		2.513	$\bar{2}32$	032
		2.501	$\bar{4}12$	212
		2.500	222	$\bar{4}22$
4	2.473			
7b	2.378 to 2.327			
1	2.241			
1	2.217			
20	2.172			
6	2.138			
6	2.120			
9	2.080			
9	2.020			
20	1.993			
1	1.938			
6	1.860			
6	1.824			
10	1.805			
6	1.777			
plus additional lines, all with $I \leq 4$				

* Corrected for shrinkage; b=broad. Radiation: Cu/Ni, $\lambda CuK\alpha = 1.5418$ Å. Lower limit of 2θ measurable: approximately 7° (13 Å).

† All calculated lines listed for $d_{hkl} \geq 2.5$ Å.

study are in good agreement with those given in previously published powder data. Observed spacings for ulexite are given on ASTM card 2-0914 and in a paper by Baur and Sand (1957). Powder data for probertite are listed on ASTM card 4-0107. No indexed patterns for these minerals have previously been available.

REFERENCES

BARNES, WILLIAM H. (1949), The unit cell and space group of probertite: *Am. Mineral.* **34**, 19–25.

Baur, Gretta S., and Sand, L. B. (1957), *X*-ray powder data for ulexite and halotrichite: *Am. Mineral.*, **42,** 676–678.

Evans, Howard T., Jr. (1948), Relations among crystallographic elements: *Am. Mineral.*, **33,** 60–63.

International Tables for X-Ray Crystallography, Vol. I (1952): Birmingham, The Kynoch Press.

Murdoch, Joseph (1940), Crystallography of ulexite: *Am. Mineral.*, **25,** 754–762.

Palache, C., Berman, H., and Frondel, C. (1951), *The System of Mineralogy*, 7th ed., vol. 2: New York, John Wiley and Sons, Inc.

Schaller, Waldemar T. (1930), Borate minerals from the Kramer district, Mohave Desert, California: *U. S. Geol. Survey Prof. Paper* **158-I,** 137–173.

Manuscript received October 16, 1958.

RELATION BETWEEN CHEMICAL COMPOSITION AND LATTICE CONSTANTS OF EPIDOTE

YÔTARÔ SEKI, *Department of Earth Sciences, Saitama University, Urawa, Japan.*

ABSTRACT

Chemical, optical and x-ray data on five members of the clinozoisite-pistacite series are presented. The unit cell becomes larger with increasing ferric iron content. It is shown that the members of the clinozoisite-pistacite series can be readily distinguished from zoisite by the x-ray powder method.

INTRODUCTION

The x-ray study of epidote was attempted by Gossner and Mussgnug (1930), Bujor (1931), Strunz (1935), Ito (1950), Ito, Morimoto and Sadanaga (1954) and Lapham (1957). The most elaborate analysis of the crystal structure was given by Ito, Morimoto and Sadanaga (1954).

The writer was greatly interested in the epidote minerals (clinozoisite, pistacite, piemontite and zoisite) during his study of regional metamorphism in the Kanto Mountains, central Japan (Seki, 1958). The behavior of epidote in this progressive metamorphic terrain has been described and discussed by Miyashiro and Seki (1958).

In the present paper, some relations between the chemical composition and lattice constants for the members of the clino-zoisite-pistacite series and the distinction of the members of this series from zoisite by the x-ray powder method will be described in some detail. The nomenclature of the members of the epidote group adopted in this paper are the same as that adopted by Miyashiro and Seki (1958).

CHEMICAL COMPOSITIONS AND OPTICAL PROPERTIES OF CLINOZOISITES AND PISTACITES

The localities and modes of occurrence of the five epidotes used in this paper are shown in Table 1.

The samples were purified by means of the isodynamic separator and Clerici solution.

Among them, the chemical composition and optical properties of the Hawleyville pistacite were already given by Lapham (1957). The chemical analysis and optical measurements on the other four minerals were newly carried out by the present writer and Miss Chigusa Kato of the Saitama University. These data are summarized in Table 2.

In the table, the analyses are arranged in the order of increasing $Fe^{+3}/(Al+Fe^{+3})$ ratio. The atomic ratios were calculated on the anhydrous basis of $O=25$, because the water contents shown in Table 2 are somewhat unreliable.

The indices of refraction, double refraction and the intensities of

TABLE 1. LOCALITIES AND MODES OF OCCURRENCE OF THE CLINOZOISITES AND PISTACITES USED

No.	Name	Locality	Mode of occurrence
1	Sasaguri clinozoisite	Nakakoti, Sasaguri, Hukuoka Prefecture, Japan (YS-C1–3)	Occurs in leucocratic veins and nodules in serpentinites. Minerals associated with the clinozoisite are sericite, quartz and albite. The serpentinites are intruded into low grade crystalline schists including crossite-bearing green schists
2	Kanto clinozoisite	Huppu, Yorii-mati, Saitama Prefecture (Kanto Mts.), Japan (TT57032206)	Occurs as fine grained crystals in chlorite-clinozoisite-albite-titanite schist derived from mafic pyroclastic materials. This metamorphic rock with conspicuous albite porphyroblasts represents the highest grade of metamorphism in the Kanto Mountains (Miyashiro and Seki, 1958; Seki, 1958)
3	Hawleyville pistacite	East of Danbury, Connecticut, U.S.A.	Occurs in single crystals or parallel groups in the pink feldspar-epidote-chlorite pegmatites intrusive into medium to coarse grained diorite. Minerals associated with this pistacite are apatite, quartz, prochlorite, muscovite and orthoclase (Lapham, 1957)
4	Kanto pistacite	Northwestern side of Mt. Hoto, Minano-mati, Saitama Prefecture (Kanto Mts.), Japan (YS57062609)	This pistacite is associated with chlorite, actinolite, quartz, albite and titanite in a low-grade green schist derived from mafic pyroclastic rock. This green schist without any conspicuous porphyroblast of albite belongs to the writer's non-spotted schist formation (Miyashiro and Seki, 1958; Seki, 1958)
5	Dauphine pistacite	Dauphine, Bourg d'Oisans, Swiss	Unknown to the writer. It is composed of an aggregate of dark green crystals in parallel growth, up to several cm. in length

pleochroism of these minerals generally increase with the ferric iron content.

Optically, clinozoisites (with 0–10 per cent Fe^{+3} end-member) are positive, while pistacites (with more than 10 per cent Fe^{+3}) are negative.

X-RAY POWDER DATA AND LATTICE CONSTANTS OF CLINOZOISITES AND PISTACITES

X-ray powder diffraction data of the above five epidotes were obtained by means of the Philips Geiger counter *x*-ray diffractometer using CuKα-radiation. Silicon powder or Brazilian quartz was used as the internal standard. The data are listed in Table 3, where about fifty peaks between 10 and 60 degrees in angle 2θ were indexed.* The results

* Lapham (1957) stated that the Hawleyville pistacite is characterized by the presence of the 7.02 Å and 1.590 Å lines. However, no reflections with these d values were found in the writer's *x*-ray powder data of epidotes including the Hawleyville pistacite. It is probable that these reflections in the Lapham's data are due to admixed chlorite and/or other minerals. Lapham also said that the 6.60 Å and 3.325 Å lines are characteristic reflections of his Timmins clinozoisite. However, these lines were not found in any of the clinozoisites treated here.

There are minor differences between this indexing and that of Fisher (*Am. Mineral.*, **43**, 588–589) obtained on single crystal precession photographs.

Table 2. Chemical Compositions and Optical Properties* of Clinozoisites and Pistacites

	1† Clinozoisite (Sasaguri)	2† Clinozoisite (Kanto)	3 Pistacite (Hawleyville)	4† Pistacite (Kanto)	5† Pistacite (Dauphine)
SiO_2	37.35	37.41	37.96	37.69	36.88
Al_2O_3	29.53	29.88	27.34	20.73	18.61
Fe_2O_3	4.03	4.09	8.88	14.03	17.93
FeO	0.29	0.58	0.97	1.17	0.37
MnO	0.60	0.14	0.16	0.27	0.48
MgO	0.02	tr.	0.34	0.22	tr.
CaO	23.65	23.92	22.07	22.72	23.06
Na_2O	—	0.11	—	0.09	—
K_2O	—	—	—	—	—
H_2O+	3.21	3.12	2.14	2.77	2.30
H_2O-	0.62	0.34	0.08	0.35	0.02
Total	99.30	99.59	99.94	100.04	99.65
Si	6.01	5.90	5.96	6.12	6.06
		0.10 } 6.00	0.04 } 6.00		
Al	5.46	5.45	5.02	3.97	3.60
Fe'''	0.47	0.48	1.05	1.72	2.21
Fe''	0.04 } 6.05	0.08 } 6.03	0.13 } 6.28	0.16 } 5.94	0.05 } 5.93
Mn	0.08	0.02	0.02	0.04	0.07
Mg	0.00	—	0.08	0.05	—
Ca	3.97	4.03	3.71	3.96	4.06
Na	— } 3.97	0.03 } 4.06	— } 3.71	0.03 } 3.99	— } 4.06
K	—	—	—	—	—
O	25.00	25.00	25.00	25.00	25.00
H_2O+ / Fe'''	1.67	1.66	1.11	1.50	1.26
Al+Fe'''	0.08	0.08	0.20	0.30	0.38
α	1.710	1.710	1.726	1.729	1.740
β	1.713	1.714	1.735	1.754	1.768
γ	1.719	1.719	1.741	1.776	1.787
$\gamma-\alpha$	0.009	0.009	0.015	0.047	0.047
2V	(+)65°	(+)74°–78°	(−)>50°	(−)73°–74°	(−)74°
X	Colorless	Colorless	Colorless	Pale yellow	Pale yellow
Y	Colorless	Pale yellow	Pale pink	Pale greenish yellow	Greenish yellow
Z	Colorless	Colorless	Colorless	Pale greenish yellow	Pale yellow
c∧X	<2°	2°	7°	8°	13°
Color to the unaided eye	Pale pink	Pale grey	Straw brown	Yellowish green	Dark green

* The maximum possible error for α, β and γ is ± 0.003. 2V was determined by means of the universal stage, using Na-light.

† Analyzed by Y. Seki and Chigusa Kato. No. 3 was quoted from Lapham (1957).

TABLE 3. X-RAY POWDER DATA AND LATTICE CONSTANTS OF CLINOZOISITES AND PISTACITES

hkl	1 Clinozoisite (Sasaguri)		2 Clinozoisite (Kanto)		3 Pistacite (Hawleyville)		4 Pistacite (Kanto)		5 Pistacite (Dauphine)	
	d(Å)	I	*d*(Å)	I	*d*(Å)	I	*d*(Å)	I	*d*(Å)	I
100	8.04	6	8.04	10	8.04	10	8.04	10	8.04	10
101 10$\bar{2}$	5.01	30	5.04	30	5.01	25	5.04	35	5.05	25
011	4.72	25	—	—	—	—	—	—	4.79	10
002	—	—	—	—	4.59	5	—	—	4.59	15
200	4.003	25	4.006	45	4.010	25	4.011	45	4.019	50
20$\bar{2}$	—	—	3.974	10	3.980	25	3.990	20	3.992	10
111	3.748	10	3.749	15	3.754	10	—	—	3.767	20
21$\bar{1}$	3.477	15	3.478	40	3.483	35	3.490	35	3.490	30
102	3.396	15	3.398	20	3.398	20	3.407	35	3.401	40
201	3.197	20	3.201	50	3.206	25	3.209	30	3.209	20
003	3.052	10	3.058	15	3.061	10	3.059	30	3.062	20
30$\bar{1}$	2.913	30	2.914	10	2.917	15	2.925	20	2.930	10
112	2.901	30	2.901	35	—	—	2.920	20	2.920	25
11$\bar{3}$	2.889	100	2.891	100	2.895	100	2.902	100	2.900	100
020	2.796	50	2.794	30	2.803	45	2.815	30	2.817	40
211	2.778	15	2.778	25	2.783	10	—	—	2.786	15
021	2.680	50	2.679	60	2.682	50	2.686	50	2.688	70
300	2.671	50	2.673	30	2.677	50	2.678	40	2.679	100
120	2.642	20	2.640	30	2.650	25	2.656	30	2.656	30
31$\bar{1}$	2.590	40	2.593	50	2.596	45	2.597	40	2.599	50
103 202	2.525	30	2.526	40	2.529	25	2.530	30	2.531	40
121	2.451	15	2.453	20	2.452	25	2.460	20	2.460	50
31$\bar{3}$	2.399	20	2.396	40	2.399	30	2.406	30	2.409	40
022	2.389	30	2.389	30	2.394	40	2.400	30	2.401	40
220 004	2.290	30	2.290	10	2.296	15	2.301	10	2.301	10
22$\bar{2}$	2.287	30	2.287	20	2.289	15	2.295	20	2.294	30
122	2.161	30	2.161	20	2.163	25	2.165	10	2.166	30
12$\bar{3}$	2.151	15	2.154	20	2.157	20	2.160	30	2.163	30
014	2.121	10	2.121	20	2.125	10	2.131	20	2.131	10
221	2.106	30	2.107	30	2.115	25	2.116	30	2.117	25
22$\bar{3}$	2.099	30	2.098	30	2.104	25	2.108	40	2.109	25
41$\bar{2}$ 023	2.062	10	2.062	30	2.068	25	2.072	40	2.072	15
203	2.040	10	2.040	15	2.047	10	2.047	20	2.048	20
41$\bar{3}$	2.021	10	—	—	—	—	—	—	2.026	10
400	2.001	25	2.000	10	2.006	10	2.010	10	2.010	15
30$\bar{5}$	1.951	10	1.952	10	—	—	—	—	—	—
213	1.919	10	1.919	30	1.922	5	1.928	30	—	—

(*continued on next page*)

TABLE 3.—(*continued*)

hkl	1 Clinozoisite (Sasaguri)		2 Clinozoisite (Kanto)		3 Pistacite (Hawleyville)		4 Pistacite (Kanto)		5 Pistacite (Dauphine)	
	d(Å)	I	*d*(Å)	I	*d*(Å)	I	*d*(Å)	I	*d*(Å)	I
$12\bar{3}$ 114 222	1.873	15	1.873	30	1.879	15	1.884	30	—	—
$11\bar{5}$ $12\bar{4}$ $22\bar{4}$	1.866	20	1.867	30	1.870	30	1.876	20	1.876	20
312	1.856	5	1.857	5	1.860	10	1.864	5	1.866	5
$32\bar{4}$	1.772	5	—	—	—	—	—	—	—	—
$50\bar{2}$	1.765	10	—	—	—	—	—	—	—	—
015	1.759	10	—	—	—	—	—	—	1.748	10
132	1.637	30	1.637	30	1.637	35	1.642	20	1.642	30
420	1.628	20	1.633	20	1.634	20	1.634	20	1.639	30
124	1.621	10	1.621	10	1.625	10	1.627	10	1.628	10
$12\bar{5}$	—	—	1.616	10	1.618	5	—	—	—	—
115	1.574	10	1.574	10	1.578	5	1.578	10	1.579	10
$33\bar{2}$ $11\bar{6}$	1.569	10	1.571	5	1.573	10	—	—	1.574	10
a_0	8.87 Å		8.87 Å		8.88 Å		8.89 Å		8.90 Å	
b_0	5.59 Å		5.59 Å		5.61 Å		5.63 Å		5.63 Å	
c_0	10.15 Å		10.15 Å		10.17 Å		10.19 Å		10.20 Å	
β	115°27′		115°27′		115°25′		115°24′		115°24′	

Note: The *d* values are for CuKα_1, so far as the peak for CuKα_1 can be distinguished from that of CuKα_2.

are in harmony with the symmetry of $C_{2h}{}^2-P_{2_1/m}$. The unit-cell dimensions obtained are in good accord with those given by Gossner and Mussgnug (1930), Bujor (1931), Strunz (1935), and Ito, Morimoto and Sadanaga (1954).

From the data in Table 2 and 3, it is clear that a_0, b_0, and c_0 generally increase with the $Fe^{+3}/(Al+Fe^{+3})$ ratio of the mineral.

Table 4 shows the variations of the unit cell volume and the "packing index" (Fairbairn, 1943) of the clinozoisite-pistacite series calculated from the data given in Tables 2 and 3. The unit cell volume gradually increases with increasing iron content. On the other hand, the packing index generally decreases with increasing iron content.

These data suggest that the variation of the lattice constants may

Table 4. Unit-Cell Volumes and Packing Indices of Clinozoisites and Pistacites. The Packing Indices Were Calculated on the Assumption that One Molecule of Water Is in a Unit-Cell

	Clinozoisite (Sasaguri)	Clinozoisite (Kanto)	Pistacite (Hawleyville)	Pistacite (Kanto)	Pistacite (Dauphine)
Unit-cell volume	454.5 Å^3	454.5 Å^3	457.6 Å^3	460.7 Å^3	461.7 Å^3
Packing index	6.14	6.16	6.08	6.06	6.06
	6.15 (average)				

Note: Packing index = ionic volume × 10/unit-cell volume.

show a break at the composition of about 30 per cent Fe^{+3} end-member.* The possible break may be related to that the epidote structure is probably most "stable" or unstrained when the mineral has compositions near 33 per cent Fe^{+3} end-member, as was discussed by Miyashiro and Seki (1958).

Discrimination of Clinozoisite from Zoisite by *X*-Ray Powder Data

As is well known, clinozoisite and zoisite are very similar to each other in their optical properties, crystal form and other appearances. Especially, so-called β-zoisite, the optical plane of which is parallel to 001 (normal to the cleavage plane), can hardly be distinguished from clinozoisite by optical examination in thin sections. However, zoisite and clinozoisite show distinctive x-ray powder patterns.

The present writer obtained, by means of the Philips Geiger counter x-ray diffractometer using CuKα-radiation, the x-ray powder data of two zoisites. One of them is α-zoisite (optical plane is parallel to 010) from Cummington, Mass., U.S.A., and the other is β-zoisite from Nagatoro, Saitama Prefecture, central Japan. The data thus obtained are shown in Table 5.† About eighty peaks between 10° and 70° in angle 2θ were indexed on the basis of orthorhombic unit cell with the dimensions

* Such a break was noticed in the unit cell dimensions of nepheline (Smith and Sahama, 1954).

† No reflections with d-spacings of 4.245 Å, 2.459 Å, 2.238 Å, 1.666 Å, 1.544 Å and 1.453 Å were found in these zoisites, though Lapahm (1957) presented these reflections for his Ducktown zoisite. These reflections are probably due to quartz impurities included in the Ducktown zoisite.

TABLE 5. *X*-RAY POWDER DIFFRACTION DATA OF α- AND β-ZOISITES

Indices	α-zoisite from Cummington, Mass., U.S.A.		β-zoisite from Nagatoro, Saitama Pref., Japan	
	d(Å)	Intensity	d(Å)	Intensity
200	8.12	20	8.12	25
002	5.018	17	5.023	20
111	4.662	7	4.657	5
400	4.070	36	4.070	58
401	3.757	5	3.755	19
302	3.678	10	3.681	12
311	3.619	15	3.616	18
402	3.151	17	3.155	9
411	3.108	9	3.112	7
501	3.083	23	3.087	24
013	2.864	51	2.868	40
113	2.824	8	2.824	10
020	2.779	23	2.777	22
502	2.722	30	2.722	40
600	2.699	100	2.698	100
220	2.628	10	2.626	13
313	2.533	12	2.531	13
104	2.481	5	2.481	7
122	2.404	12	2.401	14
204	2.398	8	2.397	7
611	2.358	5	2.354	3
413	2.341	7	2.340	8
222	2.331	11	2.327	15
420	2.289	4	2.289	4
304	2.276	7	2.276	6
701	2.255	7	2.255	7
421	2.236	12	2.235	10
404	2.135	4	2.134	7
702 603	2.102	16	2.103	18
521	2.066	20	2.064	18
800	2.026	26	2.025	46
323	1.990	5	1.990	5
504	1.982	17	1.982	18
205	1.975	6	1.975	8
613	1.967	4	1.967	5
522	1.947	10	1.944	8
703	1.905	4	1.903	5
810 621	1.900	3	1.899	3
801	1.878	6	1.879	7
514	1.870	4	1.870	3
124	1.851	10	1.850	11
604	1.838	5	1.839	4
424	1.693	4	1.695	7

TABLE 5.—(*continued*)

Indices	α-zoisite from Cummington, Mass., U.S.A.		β-zoisite from Nagatoro, Saitama Pref., Japan	
	d(Å)	Intensity	*d*(Å)	Intensity
911 430	1.687	7	1.689	6
722 623	1.676	6	1.677	7
006	1.674	9	1.674	8
812	1.654	4	1.654	3
820	1.637	4	—	—
515	1.633	6	1.633	5
714	1.627	4	1.628	5
033 912	1.622	10	1.622	7
10.0.0	1.620	15	1.621	17
524	1.615	16	1.615	18
10.0.1 306 432	1.599	8	1.599	11
116	1.595	5	—	—
531	1.588	6	1.587	7
821 10.1.0.	1.556	10	1.556	10
333	1.552	8	1.552	5
615	1.548	7	1.548	7
10.1.1.	1.537	12	1.537	10
624	1.534	4	1.533	6
715	1.464	6	1.464	7
10.0.3.	1.459	6	1.459	6
107 126	1.429	4	1.429	4
040 732 633	1.390	10	1.390	5
10.2.1.	1.387	8	1.386	7
240	1.371	6	—	—
10.2.2.	1.349	10	1.349	10
141 317	1.345	7	1.345	5
a_0	16.20 Å		16.20 Å	
b_0	5.56 Å		5.56 Å	
c_0	10.04 Å		10.04 Å	

Note: The values of *d* are for CuKα_1 so far as the peak for CuKα_1 can be distinguished from that for CuKα_2. The reflections due to hematite inclusions in the Cummington zoisite were excluded.

shown in the same table. Brazilian quartz was used as the internal standard. These x-ray diffraction data of α- and β-zoisites are very similar to each other and are in harmony with the symmetry of V_h^{16}-*Pnma*. These unit cell dimensions are close to those given by Gossner and Mussgnug (1930), Gossner and Reichel (1932), Waldbauer and McCann (1935) and Ito (1950).

The chemical compositions of these zoisites are shown in Table 6. The writer attempted to purify these zoisites by means of the isodynamic separator and Clerici solution, but a small amount of hematite impurity included in the Cummington zoisite could not be removed. Accordingly, the chemical analysis of the Cummington zoisite shows an unusually large content of ferric iron.

Table 6. Chemical Composition and Optical Properties† of α- and β-Zoisite

α-zoisite from Cummington, Mass.					β-zoisite from Nagatoro, Saitama Pref., Japan*				
Analysis		Atomic ratio			Analysis		Atomic ratio		
SiO_2	38.97	Si	6.04		SiO_2	37.47	Si	5.78	6.00
Al_2O_3	29.13				Al_2O_3	33.44	Al	0.22	
Fe_2O_3	5.11	Al	5.32		Fe_2O_3	1.33		5.86	
FeO	0.37	Fe‴	0.60		FeO	0.00	Fe‴	0.15	
MnO	0.10	Fe″	0.05	5.98	MnO	0.04	Fe″	—	6.02
MgO	tr.	Mn	0.01		MgO	0.00	Mn	0.01	
CaO	24.01	Mg	—		CaO	24.52	Mg	—	
Na_2O	0.00	Ca	3.97		Na_2O	0.00	Ca	4.04	
K_2O	n.d.	Na	—	3.97	K_2O	n.d.	Na	—	4.04
H_2O+	2.26	K	—		H_2O+	2.73	K	—	
H_2O-	0.12	O	25.00		H_2O-	0.05	O	25.00	
Total	100.07	H_2O+	1.14		Total	99.58	H_2O+	1.40	
α		1.702					1.694		
β		1.707					1.698		
γ		1.714					1.707		
$\gamma-\alpha$		0.012					0.013		
(+)2V		72°–87°					39°–49°		
Color in thin section		Colorless					Colorless		
Color to the unaided eye		Pale grey					Colorless		

† The maximum possible error for α, β and γ is ± 0.003; 2V was determined by means of the universal stage, using Na-light.

* Analyzed by Y. Seki and Chigusa Kato. The high Fe_2O_3 content of the Cummington zoisite is due to hematite inclusions.

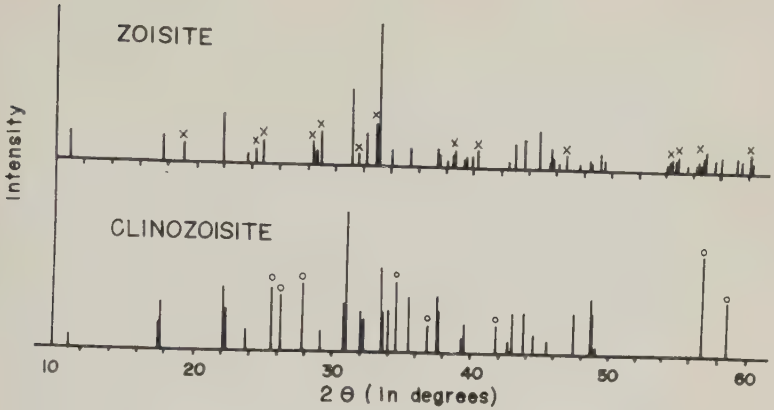

FIG. 1. Comparison of the x-ray powder patterns of zoisite and clinozoisite (see Tables 3 and 4).

x = Peaks characteristic of zoisite.

o = Peaks characteristic of clinozoisite.

The x-ray powder patterns of clinozoisite and zoisite are diagrammatically compared in Fig. 1. The difference between them is very clear.

ACKNOWLEDGMENTS

The present writer is greatly indebted to Dr. A. Miyashiro of the Tokyo University for his valuable suggestions during the study of epidote and for his critical reading of the manuscript. In the x-ray work much help and advice were given by Dr. Fumiko Shidô and Mr. Akira Kato of Tokyo University to whom the writer's thanks are also due.

The writer also wishes to express his sincere thanks to Miss Chigusa Kato for her help in chemical analysis, and to Dr. Kinichi Sakurai for his cordial giving a sample of zoisite from Nagatoro. Dr. D. M. Lapham of Department of Internal Affairs, Commonwealth of Pennyslvania and Professor P. F. Kerr of Columbia University kindly sent to the writer samples of the Hawleyville pistacite and Timmins clinozoisite respectively.

REFERENCES

BUJOR, D. J., 1931, Über die Kristallstruktur des Epidots. I: *Zeits. Krist.*, **78,** 386–411.

FAIRBAIRN, H. W., 1943, Packing in ionic minerals: *Bull. Geol. Soc. Amer.*, **54,** 1305–1374.

GOSSNER, B. UND F. MUSSGNUG, 1930, Über kristallographische Beziehungen zwischen Epidot und Zoisit: *Centr. Min. Abt. A*, 369–371.

GOSSNER, B. UND CH. REICHEL, 1932, Über das Kristallgitter einige sog. Orthosilikate: *Centr. Min. Abt. A*, 225–229.

ITO, T., 1950, *X*-ray studies on polymorphism: Maruzen Co., Ltd., Tokyo.

ITO, T., MORIMOTO, N., AND R. SADANAGA, 1954, On the structure of epidote: *Acta Cryst.* **7,** 53–59.

Lapham, D. M., 1957, Epidote from Hawleyville, Connecticut: *Am. Mineral.*, **42,** 62–72.

Miyashiro, A. and Y. Seki, 1958, Enlargement of the composition field of epidote and piemontite with rising temperature: *Amer. Jour. Sci.*, **256,** 423–430.

Seki, Y., 1958, Glaucophanitic regional metamorphism in the Kanto Mountains, central Japan: *Japanese Jour. Geol. Geograph.*, (in press).

Smith, J. V., and Th. G. Sahama, 1954, Determination of the composition of natural nephelines by an *x*-ray method: *Mineralog Mag.*, **30,** 439–449.

Strunz, H., 1935, Strukturelle und morphologische Beziehungen zwischen Epidot und Zoisit und zwischen Epidot und Ardennit: *Zeits. Krist.*, **92,** 402–407.

Waldbauer, L. and D. C. McCann, 1935, Crystal structure of common zoisite: *Am. Mineral.*, **20,** 106–111.

Manuscript received September 15, 1958.

THE AMERICAN MINERALOGIST, VOL. 44, JULY-AUGUST, 1959

A CONTINUOUS *X*-RAY INVESTIGATION USING AN AUTOCLAVE OF THE CONVERSION OF GYPSUM TO HEMIHYDRATE

JOHN B. DROSTE* AND RALPH E. GRIM, *University of Illinois, Urbana, Illinois.*

ABSTRACT

An autoclave fitting into an *x*-ray spectrometer diffraction unit permitting continuous *x*-ray diffraction studies at moderately elevated temperatures and steam pressures is described. The instrument is used for the study of the conversion of gypsum to hemihydrate. Temperature and steam pressure conditions necessary and favorable for the conversion are given, and it is suggested that there is no intermediate step in the transition.

INTRODUCTION

For years mineralogists have been interested in the range of stability of many minerals and a vast literature exists describing the stability range and new phase formation on heating for many crystalline and amorphous compounds. Until recently all the available data were obtained on samples that had been cooled to ordinary temperature and atmospheric pressure following subjection to elevated temperature and pressure. It has been assumed that the phases identified are those which existed when the sample was actually at the elevated conditions. It is obviously more desirable to identify the phases present at a given temperature, pressure, and atmosphere while the material is subjected to these conditions. Recently results have been published (Rowland, Weiss and Bradley, 1956, Weiss and Rowland, 1956, and Grim and Kulbicki, 1957) of studies of the changes taking place in the clay minerals while they are being heated by means of continuous *x*-rays using a small furnace mounted in the *x*-ray spectrometer diffraction unit. The use of the spectrometer, rather than the camera, makes it possible to literally watch one phase change to another as the sample is raised in temperature or held at a given elevated temperature.

Phase changes of minerals on heating may be related to the pressure and atmosphere as well as to the temperature. To study the effect of pressure and atmosphere as well as temperature, a small autoclave was constructed that would fit into a General Electric spectrometer diffraction unit through which *x*-rays could be transmitted. Results are presented herein using the apparatus for the study of the dehydration of gypsum.

DESCRIPTION OF AUTOCLAVE

The autoclave used in this study, Fig. 1, has six essential parts: heating element, the entrance and exit ports for the *x*-ray beam, a sample

* Now assistant Professor of Geology, University of Indiana, Bloomington, Indiana.

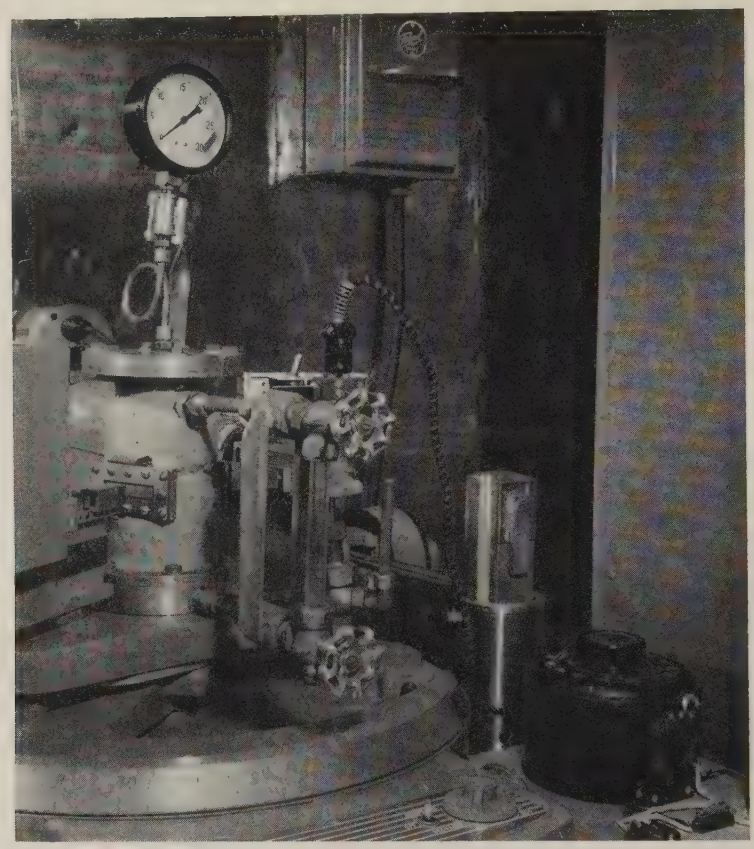

FIG. 1. Autoclave mounted in diffraction unit.

holder and sample holder stand, steam gauge, water gauge, and the container itself which consists of a stainless steel cylinder flanged at both ends to which base plates are bolted.

The autoclave has two heating elements each consisting of 12 feet of chromel (A) wire of 18 gauge wrapped around the stainless steel cylinder which is 3 inches in outside diameter with a wall thickness of $\frac{3}{8}$ inch. One coil of wire is placed below and one above the windows. A toggle switch is included in the system which makes possible the use of one or both heating elements at once. After water is placed in the cylinder, both elements were used to raise the temperature to 100° C. After all the air is evacuated and a few pounds of steam pressure is generated, only the lower element is used so that the upper element will not superheat the steam. Current is fed to the heating elements through a variable transformer.

The windows of the autoclave are 1/16 inch sheets of beryllium which are secured to the cylinder by a double gasket arrangement. The 1/16 inch window allows a wide margin of safety for operations up to 25 pounds steam pressure. The pressure necessary to cause failure of the windows is not known, but it is above 30 pounds of air pressure at room temperature.

The sample stand and sample holder used are shown in Fig. 2. With the vertical sample arrangement used in the General Electric *x*-ray diffraction equipment, the sample holder presents a design problem. Since steam must completely saturate the sample, the cavity holding the sample is open at the top for the full length of the holder. Several lines of holes were drilled from the back of the sample holder into the sample cavity on a slight angle (about 10°) so that the powder saturated with steam will not seep out of the sample cavity. A 1/10,000 inch sheet of mylar plastic is secured to the front of the sample holder after the

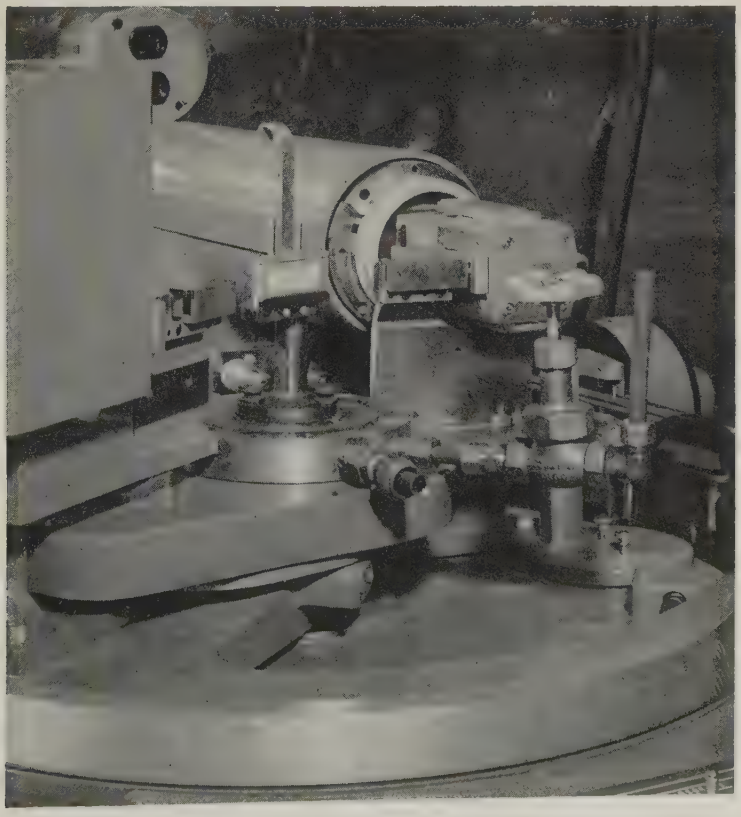

FIG. 2. Sample stand and sample holder for autoclave unit.

sample has been loaded to prevent the powder from falling out of the sample holder during the run.

The use of the steam gauge is self evident and the temperature within the autoclave is determined by consulting steam tables. A thermocouple may be inserted in the autoclave and attached to the sample, if it appears desirable. The water valve is not only very convenient, but a necessary safety device.

Experimental Results

In this study gypsum ($CaSO_4 \cdot 2H_2O$) is treated in the autoclave with sufficient temperature and steam pressure to change it to the hemihydrate ($CaSO_4 \cdot \frac{1}{2}H_2O$), and the transformation is observed by watching continuously the (020) peak for gypsum and for hemihydrate. As the water begins to leave the gypsum structure the (020) of gypsum decreases and an (020) of hemihydrate appears. By varying the steam pressure the rate of transformation of gypsum to hemihydrate can be changed. The gypsum used was from Southard, Oklahoma, and was finer than 100 mesh.

Four runs are described herein to demonstrate the kind of data obtained using the apparatus. These data are from a few of the many such runs and are typical for the gypsum-hemihydrate transformation. The per cent of the maximum (020) reflection intensity is plotted vertically and time in minutes is plotted horizontally in Figs. 3, 4, 5, and 6.

Figure 3 shows the change during a slow run. The steam pressure was elevated very slowly so that 14 pounds pressure (120° C.) was reached in 30 minutes and 20 pounds was reached 18 minutes later. The pressure was maintained at 20 pounds (126° C.) for the remainder of the run. The hemihydrate appeared when 14 pounds pressure was reached and the gypsum simultaneously began to disappear. The (020) of hemihydrate reached maximum intensity 18 minutes after it first appeared and just after the 20 pounds pressure was reached. The (020) of gypsum did not completely disappear until 7 minutes after the (020) of the hemihydrate reached its maximum intensity.

Figure 4 shows the results when the steam pressure is elevated rapidly to a high level. In 17 minutes steam pressure was raised to 23 pounds and 5 minutes later it was 25 pounds (130.4° C.). A very sharp drop of gypsum (020) intensity is accompanied by a very sharp increase (almost straight line in both cases) of the hemihydrate (020) indicating that the transformation is very rapid. In 12 minutes after the reaction started all the gypsum was converted to hemihydrate. The (020) of gypsum did not begin decreasing and the (020) of hemihydrate did not appear until 23 pounds of steam pressure was obtained. Apparently the heating rate was

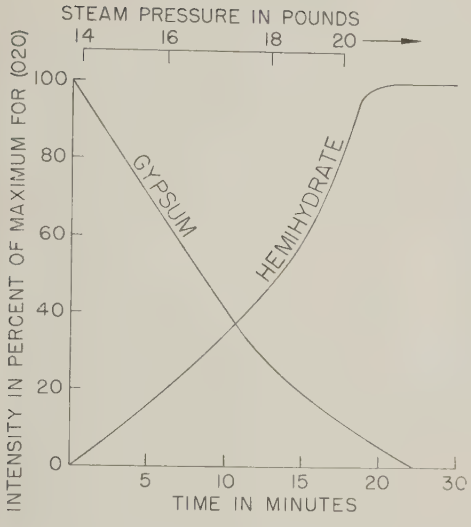

FIG. 3. Gypsum-hemihydrate transition during slow increase of temperature and steam pressure.

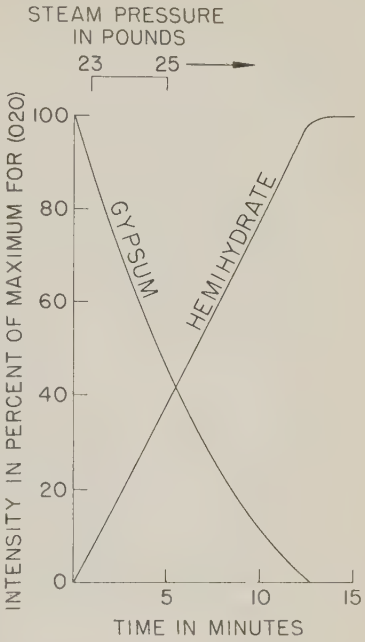

FIG. 4. Gypsum-hemihydrate transition during rapid increase in steam pressure.

so rapid that the gypsum remained even though for a time it was unstable in the environment.

Figure 5 shows a reaction similar in part to that shown in Fig. 3 in that steam pressure was never over 20 pounds. This run also has features of the run shown in Fig. 4 in that steam pressure was built up very rapidly so that 13 pounds was reached in 12 minutes, and 20 pounds 8 minutes later. The gypsum disappears and the hemihydrate appears very rapdily under these conditions.

Figure 6 shows the results of a run in which the pressure was elevated slowly at the start, and held at only 20 pounds for one hour. Under these conditions the (020) of the hemihydrate appeared 10 minutes after 15 pounds of steam pressure was reached and showed a very small gradual increase during the next 50 minutes. After one hour at 15 pounds, the pressure was rapidly raised to 20 pounds. The sample was continuously *x*-rayed for one hour at 20 pounds pressure and the intensity of (020) of hemihydrate showed only a very small increase. Similarly thoughout the

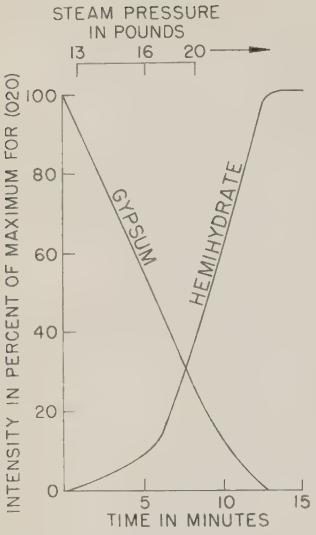

FIG. 5. Gypsum-hemihydrate transition during rapid increase in steam pressure to 20 pounds gauge.

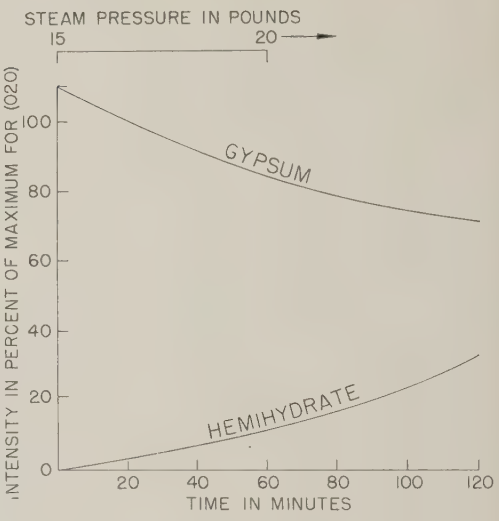

FIG. 6. Gypsum-hemihydrate transition during slow increase in steam pressure to 20 pounds gauge.

run there was only a small gradual and partial loss of the intensity of the gypsum reflection. The data suggests that complete conversion is favored by a rapid increase in pressure to something in excess of 15 pounds. Further if the pressure is initially held at a low value, later raising it to a high value does not attain the rapid conversion rate that develops with a rapid increase in pressure directly to the higher values.

DISCUSSION AND CONCLUSIONS

The dehydration of gypsum to hemihydrate can be "watched" continuously by the use of an autoclave built to fit in an x-ray spectrometer diffraction unit. The phase changes of any similar material could be followed in the same way.

The gypsum changes directly to the hemihydrate. There is no evidence of an intermediate phase. Also there is no evidence of any intermediate liquid step, even a momentary one, in the transition. In fact the data strongly suggest that such a liquid step is not present and that the transition is a direct solid state reaction. In every case the loss of gypsum and the appearance of the hemihydrate are comparable. Further, the character of the sample in the holder before and after the run does not suggest any intermediate liquid step.

Steam pressures in excess of 15 pounds are required for rapid conversion, and at 20 pounds the conversion is very rapid. If coarser material were used, it is probable that more time would be required for the conversion. It is also possible that if the rock gypsum had undergone a different geologic history than the Southard, Oklahoma area, the factors governing its dehydration might not be the same. Thus if a rock gypsum had undergone several natural gypsum-hemihydrate-anhydrite cycles, it is entirely possible that somewhat different temperatures and pressures would be necessary to cause the change from gypsum to hemihydrate in the laboratory or in industry. Further, if the gypsum contained traces of certain impurities, the conditions of conversion would probably be somewhat different.

References

Rowland, R. A., Weiss, E. J., and Bradley, W. F. (1956) Dehydration of monoionic montmorillonites: Pub. 456, Nat. Res. Council, 85–95.

Weiss, E. J., and Rowland, R. A. (1956) Effect of heat on vermiculite and mixed-layered vermiculite-chlorite: *Am. Mineral.*, **41**, 899–914.

Grim, R. E., and Kulbicki, G. (1957) Etude aux Rayons X des Reactions des Mineraux Argileux a Haute Temperature: *Bull. Soc. franc. Ceramique*, **36**, 21–27.

Manuscript received October 27, 1958.

THE MAGNETIC SEPARATION OF SOME ALLUVIAL MINERALS IN MALAYA*

B. H. Flinter, *Minerals Examination Division, Geological Survey Department, Federation of Malaya.*

Abstract

This paper presents the results of a series of magnetic separations which have been investigated for a number of minerals occurring in Malayan alluvial concentrates. The purpose of the investigations was to establish, by the isolation of individual mineral species, a reproducible and reliable method for the identification and quantitative estimation of minerals in alluvial concentrates examined by the Geological Survey in Malaya. In particular was sought the isolation of columbite from ubiquitous ilmenite. All the separations were made on the small, highly sensitive Frantz Isodynamic Model L-1 laboratory separator. The minerals which have been successfully separated include allanite, anatase, andalusite (and chiastolite), arsenopyrite, brookite, cassiterite, columbite, epidote, gahnite, garnet (pink), ilmenite, manganese oxide (51.6% Mn), monazite, pyrite, rutile, scheelite, siderite, staurolite, thorite, topaz, tourmaline, uranoan monazite, wolframite, xenotime, and zircon.

Procedure

When using an inclined feed, the Frantz Isodynamic separator (see Figs. 1(A) & (B)) has three inherent variables. These are the field strength (current used), the side slope, and the forward slope.

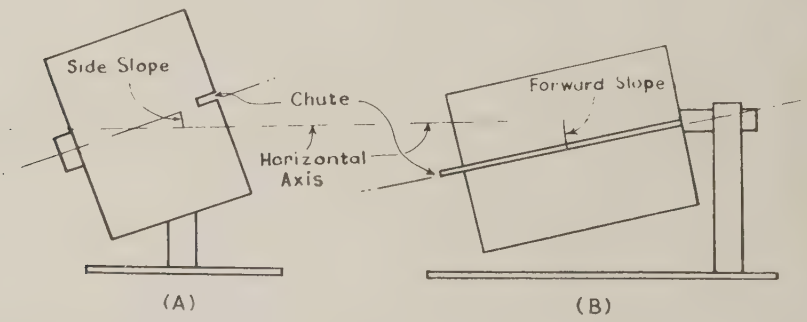

Fig. 1. Diagrammatic representation of side slope and forward slope.

The field strength is increased by means of a rheostat which raises the current from zero in stages of 0.05 amps. to 1.4 amps. Early in the investigations it was decided that steps of 0.1 amp. would be sufficiently gradual.

The side slope can be varied continuously from 0 to 90° and can also be given a reverse slope, as much as 90°, for the diamagnetic separation of minerals such as zircon. Results of a few separations made by my

* Published by permission of the Director, Geological Survey, with the authority of the Minister of Natural Resources. Government copyright is reserved.

colleagues when the separator was first installed showed that, for the purpose of these investigations, side slopes varying by less than 5° would produce no significant differentials, and further, that side slopes greater than 15° showed more promise, as regards the separation of columbite from ilmenite, than did slopes of less than 15°. Accordingly a series of tests was carried out at side slopes of 15°, 20°, 25°, and 30°.

The forward slope and a fourth, independent, variable, the rate of feed, control the rate of flow of the sample. The steeper the slope, the faster is the flow. The rate of flow of a sample is not critical provided that it is slow enough to allow the mineral to remain long enough in the magnetic field for the magnetic pull exerted by the separator to be fully effective. A forward slope of 15° was chosen for, and maintained throughout, the investigation.

Much more critical is the uniformity of grain size of the sample, as the larger grains tend to "suppress" the finer material. For the purpose of simple identification and the estimation of mineral percentages in an alluvial concentrate a grain size of 0.4 mm. or 0.0166 inch (36 mesh B.S.S.) is considered a satisfactory upper limit. With larger grains difficulty is experienced in distinguishing amongst the opaque minerals and between the opaque minerals and the translucent minerals such as gahnite, cassiterite and rutile. The grain size of 0.2 mm. or 0.0083 inch (72 mesh B.S.S.) was selected as a suitable lower limit. This gave uniformity to the sample and provided finer material for a parallel series of tests to be conducted, thereby ascertaining whether a difference in grain size gives rise to any significant difference in results.

For each mineral the same sample was used for all the separations, thus eliminating variations independent of the change in side slope. Each sample, averaging 2 to 3 gms., was dried before being passed through the separator. After separation the fractions were examined under the microscope and the weight percentages recalculated to allow for any impurities, which were estimated visually.

Assessment of Results

On the basis of the separations carried out the minerals tested can be divided into two groups, the "magnetic" and the "non-magnetic." The "non-magnetic" minerals are those that are not attracted at a value of 1.4 amps. giving the maximum field strength of the separator. They are anatase, andalusite (and chiastolite), arsenopyrite, brookite, cassiterite, pyrite, rutile, scheelite, topaz, and zircon. The "magnetic" minerals are given in Tables 1 to 8.

A study of these tables shows that, for the purpose for which the investigations were effected, side slopes of 20° (Tables 3 and 4) and 30°

TABLE 1. WEIGHT PERCENTAGES SEPARATED BY INDICATED CURRENT STRENGTHS USING 15° SIDE SLOPE, 15° FORWARD SLOPE ON −36+72 MESH BSS MATERIAL

Current (Amps.) Strength	0.1	0.2	0.3	0.4	0.5	0.6	0.7	0.8	0.9	1.0	1.1	1.2	1.3	1.4	Non
Allanite	1.8	6.4	14.4	74.7	2.7	Tr.									
Columbite		Tr.	0.2	99.1	0.7	Tr.									
Epidote			Tr.	7.3	78.1	14.6	Tr.								
Gahnite					10.4	69.5	16.9	2.2	1.0	Tr.					
Garnet (pink)		5.4	94.6												
Ilmenite		Tr.	90.0	10.0	Tr.										
Mn. oxide		Tr.	13.5	54.1	32.4	Tr.									
Monazite					Tr.	5.1	92.8	2.1	Tr.						
Siderite		89.2	10.8	Tr.											
Staurolite				Tr.	42.7	57.3									
Thorite						0.3	3.0	24.5	43.4	23.8	4.4	0.3	0.3		
Tourmaline			Tr.	Tr.	21.8	75.7	2.5								
Uran. Monazite				Tr.	Tr.	91.3	8.7								
Wolframite			0.3	97.4	2.3										
Xenotime			2.5	83.0	12.5	2.0	Tr.								

TABLE 2. WEIGHT PERCENTAGES SEPARATED BY INDICATED CURRENT STRENGTHS USING 15° SIDE SLOPE, 15° FORWARD SLOPE ON −72 MESH BSS MATERIAL

Current (Amps.) Strength	0.1	0.2	0.3	0.4	0.5	0.6	0.7	0.8	0.9	1.0	1.1	1.2	1.3	1.4	Non
Allanite	3.1	5.7	10.7	57.6	22.9	Tr.									
Columbite			Tr.	99.2	0.8										
Epidote				Tr.	85.7	14.3	Tr.								
Gahnite					Tr.	42.3	53.9	3.8	Tr.						
Garnet (pink)			100.0	Tr.											
Ilmenite		1.0	93.8	4.7	0.5										
Mn. oxide		Tr.	7.7	61.5	30.8	Tr.									
Monazite						13.7	85.6	0.7	Tr.						
Siderite		58.8	41.2												
Staurolite		1.0	1.4	6.9	83.1	7.6	Tr.								
Thorite							Tr.	5.7	40.5	43.0	7.2	3.6			
Tourmaline			0.3	3.1	87.0	8.5	1.1	Tr.							
Uran. Monazite				Tr.	Tr.	97.8	2.2								
Wolframite			2.5	96.0	1.5										
Xenotime				88.3	11.7	Tr.									

TABLE 3. WEIGHT PERCENTAGES SEPARATED BY INDICATED CURRENT STRENGTHS USING 20° SIDE SLOPE, 15° FORWARD SLOPE ON −36+72 MESH BSS MATERIAL

Current (Amps.) Strength	0.1	0.2	0.3	0.4	0.5	0.6	0.7	0.8	0.9	1.0	1.1	1.2	1.3	1.4	Non
Allanite	Tr.	3.0	8.8	19.0	19.0	50.0	0.2								
Columbite		Tr.	Tr.	63.8	36.0	0.2									
Epidote				2.6	52.7	44.7	Tr.								
Gahnite					3.5	22.1	49.4	22.5	1.8	0.7					
Garnet (pink)			88.1	11.9											
Ilmenite		Tr.	75.1	24.6	0.3										
Mn. Oxide			8.3	38.9	52.8	Tr.									
Monazite						Tr.	42.7	56.5	0.8	Tr.					
Siderite		10.3	89.7	Tr.											
Staurolite						99.4	0.3	0.3							
Thorite							0.3	3.5	4.6	46.0	33.3	10.2	1.5	0.6	
Tourmaline			0.9	0.9	1.8	16.5	79.0	0.9							
Uran. Monazite				Tr.	Tr.	7.1	55.8	36.4	0.7						
Wolframite			0.3	78.1	21.6										
Xenotime			Tr.	5.3	94.7	Tr.	Tr.								

TABLE 4. WEIGHT PERCENTAGES SEPARATED BY INDICATED CURRENT STRENGTHS USING 20° SIDE SLOPE, 15° FORWARD SLOPE ON −72 MESH BSS MATERIAL

Current (Amps.) Strength	0.1	0.2	0.3	0.4	0.5	0.6	0.7	0.8	0.9	1.0	1.1	1.2	1.3	1.4	Non
Allanite	1.3	2.4	5.4	10.8	80.0	0.1									
Columbite			Tr.	38.9	60.6	0.5									
Epidote				Tr.	14.3	85.7	Tr.								
Gahnite						12.5	75.0	6.3	6.2	Tr.					
Garnet (pink)			16.7	83.3											
Ilmenite		0.8	92.0	5.7	1.5	Tr.									
Mn. Oxide			9.0	27.3	45.5	18.2									
Monazite						0.3	27.5	64.2	8.0	Tr.					
Siderite		15.3	84.7												
Staurolite		Tr.	1.2	1.8	8.9	82.4	5.7	Tr.							
Thorite								Tr.	5.8	34.3	36.5	18.3	3.6	0.8	0.7
Tourmaline			Tr.	Tr.	65.5	28.9	3.1	2.5	Tr.						
Uran. Monazite						1.2	98.8	Tr.							
Wolframite				98.3	1.5	0.2									
Xenotime				2.5	97.3	0.2									

TABLE 5. WEIGHT PERCENTAGES SEPARATED BY INDICATED CURRENT STRENGTHS USING 25° SIDE SLOPE, 15° FORWARD SLOPE ON −36+72 MESH BSS MATERIAL

Current (Amps.) Strength	0.1	0.2	0.3	0.4	0.5	0.6	0.7	0.8	0.9	1.0	1.1	1.2	1.3	1.4	Non
Allanite		3.0	7.5	17.2	20.5	51.4	0.4								
Columbite			Tr.	0.5	97.7	1.4	0.4								
Epidote					7.1	64.3	26.2	2.4							
Gahnite						Tr.	42.9	51.2	3.5	1.7	0.7				
Garnet (pink)			65.4	34.6											
Ilmenite		Tr.	67.4	25.9	6.7	Tr.									
Mn. oxide			Tr.	14.3	38.1	42.9	4.7								
Monazite							Tr.	49.6	48.9	1.5					
Siderite			100.0	Tr.											
Staurolite						30.2	58.0	11.8							
Thorite								Tr.	1.9	6.0	47.4	19.3	16.3	4.7	4.4
Tourmaline					1.4	6.0	43.4	45.4	2.7	1.1	Tr.				
Uran. Monazite					Tr.	Tr.	Tr.	96.4	3.6	Tr.					
Wolframite			0.4	0.9	90.6	8.1									
Xenotime				1.3	53.7	43.7	1.3								

TABLE 6. WEIGHT PERCENTAGES SEPARATED BY INDICATED CURRENT STRENGTHS USING 25° SIDE SLOPE, 15° FORWARD SLOPE ON −72 MESH BSS MATERIAL

Current (Amps.) Strength	0.1	0.2	0.3	0.4	0.5	0.6	0.7	0.8	0.9	1.0	1.1	1.2	1.3	1.4	Non
Allanite	1.4	1.4	3.5	6.1	13.5	73.7	0.4								
Columbite			Tr.	Tr.	72.7	27.3	Tr.								
Epidote					7.0	67.6	25.4	Tr.							
Gahnite							18.7	31.3	43.8	6.2					
Garnet (pink)			40.0	60.0											
Ilmenite		0.4	77.5	19.8	2.3	Tr.									
Mn. oxide			Tr.	30.0	30.0	40.0									
Monazite							0.3	44.3	54.8	0.6	Tr.	Tr.			
Siderite		0.7	89.5	9.8											
Staurolite		Tr.	0.3	1.0	3.9	34.8	56.8	3.2							
Thorite									Tr.	5.7	18.6	37.9	22.7	14.1	1.0
Tourmaline			Tr.	Tr.	Tr.	95.5	2.4	2.1	Tr.	Tr.					
Uran. Monazite							3.7	94.4	1.9						
Wolframite				2.1	96.7	1.2									
Xenotime					38.7	60.1	1.2								

TABLE 7. WEIGHT PERCENTAGES SEPARATED BY INDICATED CURRENT STRENGTHS USING 30° SIDE SLOPE, 15° FORWARD SLOPE ON −36+72 MESH BSS MATERIAL

Current (Amps.) Strength	0.1	0.2	0.3	0.4	0.5	0.6	0.7	0.8	0.9	1.0	1.1	1.2	1.3	1.4	Non
Allanite		2.2	4.5	9.3	24.5	58.6	0.9								
Columbite			Tr.	Tr.	62.7	32.4	4.9	Tr.							
Epidote					2.5	22.5	72.5	2.5	Tr.						
Gahnite						2.0	20.5	30.7	40.0	5.8	1.0				
Garnet (pink)			Tr.	53.2	31.5	15.3									
Ilmenite		Tr.	17.9	37.5	23.2	19.4	2.0	Tr.							
Mn. oxide				13.2	31.6	50.0	5.2	Tr.							
Monazite								15.5	43.0	20.8	20.7				
Siderite			38.9	61.1											
Staurolite							51.5	37.1	11.4						
Thorite								Tr.	0.6	7.9	8.4	28.1	15.4	14.6	25.0
Tourmaline						4.2	27.2	38.1	26.3	4.2	Tr.				
Uran. Monazite						Tr.	Tr.	33.8	64.7	1.5					
Wolframite			Tr.	0.6	76.0	20.5	2.9								
Xenotime					26.6	59.6	12.9	0.9	Tr.						

TABLE 8. WEIGHT PERCENTAGES SEPARATED BY INDICATED CURRENT STRENGTHS USING 30° SIDE SLOPE, 15° FORWARD SLOPE ON −72 MESH BSS MATERIAL

Current (Amps.) Strength	0.1	0.2	0.3	0.4	0.5	0.6	0.7	0.8	0.9	1.0	1.1	1.2	1.3	1.4	Non
Allanite	Tr.	2.0	2.9	5.7	12.4	47.0	30.0								
Columbite				Tr.	98.0	2.0	Tr.								
Epidote					11.1	55.6	33.3	Tr.							
Gahnite							Tr.	40.0	40.0	20.0	Tr.				
Garnet (pink)				100.0	Tr.	Tr.									
Ilmenite		0.5	6.8	58.4	29.0	5.3	Tr.								
Mn. oxide				Tr.	11.1	88.9	Tr.								
Monazite								9.3	46.2	23.0	14.5	7.0	Tr.	Tr.	Tr.
Siderite			64.7	35.3											
Staurolite		Tr.	0.8	1.0	2.3	10.2	66.7	19.0	Tr.						
Thorite										Tr.	6.3	15.0	31.5	19.6	27.6
Tourmaline				Tr.	Tr.	68.6	26.5	3.5	1.1	0.3	Tr.				
Uran. Monazite								96.8	3.2						
Wolframite				0.6	99.1	0.3									
Xenotime					33.5	49.0	17.5								

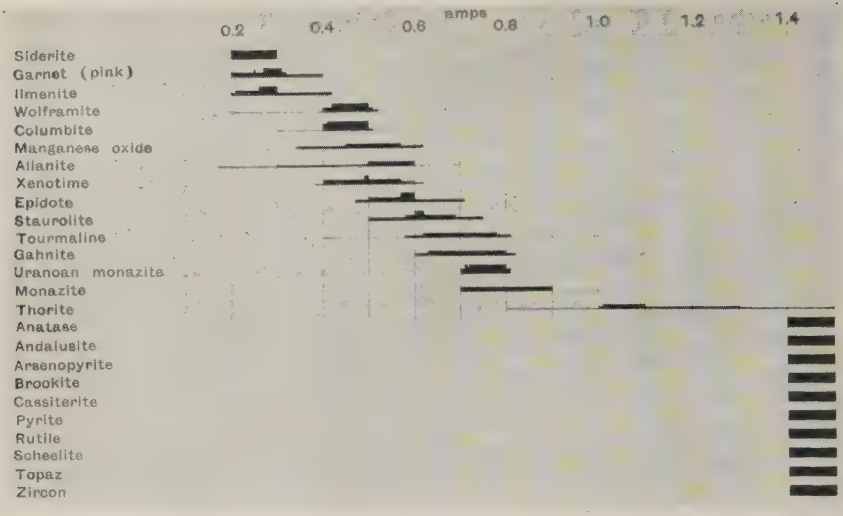

FIG. 2. A plot of data from Table 5. Side slope 25°, forward slope 15°; grain size −36+72 mesh B.S.S.

(Tables 7 and 8) can be disregarded, because there is too much overlapping of the mineral species, particularly columbite and ilmenite, and that at a side slope of 30° (and therefore above) effective separation cannot be achieved because the magnetic attraction at the lower amperages is not strong enough to overcome the effect of gravity.

However, side slopes of 15° (Tables 1 and 2) and 25° (Tables 5 and 6) give convenient breaks at amperages of 0.3, 0.5 and 0.8 and 0.4, 0.7 and 1.0 respectively, and these separations are summarized in Fig. 2.

Although most of the minerals tested give rise to some variation due to grain size, in nearly all cases these variations become negligible over a suitable range of amperages. For a side slope of 15° and amperages of 0.3, 0.5 and 0.8, only four minerals (gahnite, staurolite, thorite and tourmaline) show a marked variation, and for a side-slope of 25° and amperages of 0.4 , 0.7 and 1.0, the only two minerals showing a marked variation are gahnite and tourmaline. For this reason, and because of the better separation of columbite from ilmenite and monazite from xenotime, a side slope of 25° is preferable to one of 15°.

EXCEPTIONS

Occasionally an anomalous result is encountered. The most common cause is the presence of a partial coating of iron oxide, which can be removed by treating the mineral with hydrochloric acid, when it will behave normally. A less frequent cause is the presence of very fine in-

clusions of a more magnetic mineral. Notable examples of this are zircon and monazite and, in columbite areas, cassiterite (due to inclusions of the columbite). Both these causes result in the mineral becoming more magnetic.

It is known that, from certain localities in Malaya, cassiterite and ilmenite will give anomalous results. Cassiterite from these localities is attracted at all fractions, from 1.4 amps. to 0.1 amps. and is also attracted by a horse-shoe magnet. This magnetic cassiterite is found in areas of major iron-ore development. No inclusions are discernible at high power in transmitted light, but it is thought that this apparently inherent magnetism, which can be destroyed by heating to a temperature of a few hundred degrees Centigrade, is due to micro-fine exsolution lamellae of magnetite.

Ilmenite, on the other hand, becomes less magnetic. This is due to its alteration to "arizonite." The greater the degree of alteration, the less magnetic is the ilmenite. The maximum current so far required to attract Malayan material (at a side slope of 25°) is 0.7 amps.

Rutile is often quoted as being magnetic. Magnetic rutile is commonly encountered in Malaya. Exhaustive tests have shown that the magnetism is due to the ionic substitution of Ta/Nb (and therefore Fe). These Ta/Nb-rutiles range, in Malaya, from non-magnetic material to material attracted at a current strength of 0.7 amps. depending on the amount of substitution present. The increase in magnetism is accompanied by an increase in opacity. Pure rutile is non-magnetic.

The Estimation of Magnetic Behavior from Known Results

The results given in Tables 1 to 8 represent the mass magnetic susceptibilities of the minerals tested. The mass magnetic susceptibility (K_M) of a mineral is given as (1):

$$\frac{\text{magnetic susceptibility}}{\text{density}}$$

An approximate value for K_M can be obtained from the equation

$$K_M = \frac{20 \sin a}{I^2} \times 10^{-6} \text{ c.g.s.}$$

where

a = the angle of slide-slope

and

I = the current in amperes, provided that K_M is much less than 1 and that determinations are made at amperages lower than 1.3, as saturation sets in above this value.

An important application of this rule is that, once the K_M value for

Table 9. Mass Magnetic Susceptibility (K_M) in 10^{-6} C.G.S.

a / I Amps.	Side Slope			
	15°	20°	25°	30°
0.1	517.64	684.04	845.24	1000.00
0.2	129.41	171.01	211.31	250.00
0.3	57.52	76.00	93.92	111.11
0.4	32.35	42.75	52.83	62.50
0.5	20.71	27.36	33.81	40.00
0.6	14.38	19.00	23.48	27.78
0.7	10.56	13.96	17.25	20.41
0.8	8.09	10.69	13.21	15.63
0.9	6.39	8.44	10.44	12.35
1.0	5.18	6.84	8.45	10.00
1.1	4.28	5.65	6.99	8.26
1.2	3.59	4.75	5.87	6.94
1.3	3.06	4.05	5.00	5.92
1.4	2.64	3.49	4.31	5.10

any mineral is known, the current at which it is attracted can be calculated for any other side slope or because of any compositional variation affecting the specific gravity. In order that the information contained in this paper can be so used, the K_M values for the various amperages, at side slopes of 15°, 20°, 25° and 30°, are given in Table 9.

The application of this relationship to the results given in the tables shows that the most significant factor influencing the magnetic susceptibility of a mineral is the percentage of ferrous iron (Fe^{2+}) present in its composition. Thus ilmenite and siderite, both with a high percentage of Fe^{2+} (and a fairly low density) have similar high values of K_M. The pink garnet, with its high mass magnetic susceptibility, is a highly ferroan variety (almandite). The increased amperage needed to attract ilmenite when it is altering to "arizonite" can be foreseen because of the decreased value for K_M resulting from a loss in Fe^{2+} content whereas the specific gravity remains similar.

The columbite/tantalite mineral series is very interesting. Although no tantalite has been separated it would presumably be attracted at higher amperages than columbite because of its much higher specific gravity, and it should be possible to obtain, from the current used, the tantalum/niobium ratio of the mineral. Research in hand on the Ta/Nb-rutile minerals indicates that a relationship exists between the ferrous iron content, the ratio of tantalum to niobium and the specific gravity. With the Ta/Nb-rutile minerals, however, a variable amount of substi-

tution is possible, with correspondingly variable amounts of ferrous iron, which give rise to an added complication which must be taken into account.

Conclusion

The effective separation of minerals according to their mass magnetic susceptibility depends principally upon a fine balance between gravity (controlled by variation in the side slope), and field strength (controlled by the current used). Other factors such as forward slope, rate of feed, and grain size, are subsidiary provided they fall within certain fairly broad limits.

For the routine examination and estimation of the approximate percentages of minerals in Malayan concentrates it has been shown that electromagnetic separation is effective and that the best separation is achieved by using a side slope of 25° and current strength of 0.4, 0.7 and 1.0 amps. on material less than 36 mesh B.S.S.

In order of decreasing mass magnetic susceptibility the minerals separated are siderite, garnet (pink), ilmenite, wolframite, columbite, manganese oxide (51.6% Mn), allanite, xenotime, epidote, staurolite, tourmaline, gahnite, uranoan monazite, monazite and thorite, with anatase, andalusite (and chiastolite), arsenopyrite, brookite, cassiterite, pyrite, rutile, scheelite, topaz, and zircon being non-magnetic.

Reference

(1) H. H. Hess, 1956 "Notes on operation of Frantz Isodynamic Magnetic Separator." Pamphlet published by S. G. Frantz Co., Inc., p. 8.

Manuscript received October 15, 1958.

HIGH TEMPERATURE PHASES IN SEPIOLITE, ATTAPULGITE AND SAPONITE

GEORGES KULBICKI,* *Department of Geology, University of Illinois, Urbana, Illinois.*

ABSTRACT

The high temperature reactions of sepiolite, attapulgite and saponite were studied by continuous high temperature x-ray diffraction techniques.

The easy formation of enstatite from the fibrous minerals is explained by structural analogy. The reactions of the well crystallized specimens of sepiolite and attapulgite differ somewhat from those of their massive sedimentary varieties. The differences cannot be explained with the chemical and structural data, suggesting possible variations in some intimate details of the framework of these two varieties.

INTRODUCTION

The nature of the crystalline phases formed by firing the magnesian clay minerals has been described (2, 3, 7, 10, 12, 15, 16), but only for the well crystallized chlorites (3) have the precise conditions of formation of these phases as well as their structural relationships with the starting material been clearly determined.

The three minerals chosen for this investigation provide different structural arrangements of the same type of lattice in a series of Al-Mg hydrous silicates. Saponite and sepiolite have the same bulk composition but they differ in the mode of assemblage, i.e. layers or ribbons, of their structural units. Attapulgite has the same kind of framework as sepiolite, but a large proportion of magnesium has been replaced by aluminum or iron. It was thought that, by taking advantage of these features and by using a method of continuous high-temperature x-ray diffraction analysis, a new contribution to the problem would be possible.

Details of the procedure were described previously (8, 9). Differential thermal curves with a heating range extended to 1400° C. were also obtained.

SAMPLES INVESTIGATED

Sepiolite

Sepiolite may occur either in large fibrous crystals associated with hydrothermal deposits, or in cryptocrystalline masses of sedimentary origin. Specimens of both types were included in this investigation. Many samples, from various localities were examined and their purity checked by x-ray diffraction. Two apparently homogeneous specimens were retained for high temperature study: an excellent fibrous sepiolite from Ampandandrava (Madagascar) and a fine grained sedimentary one

* Present address: Centre de Recherches S.N.P.A., Pau (B-P), France.

from Vallejas (Spain). The former contains some free cristobalite which could not be separated but did not affect the high temperature reactions (Fig. 1).

Attapulgite

Attapulgite also occurs in sedimentary as well as in probable hydrothermal deposits (mountain leather). A sample of mountain leather from the Aleutian Islands* appeared to be a very well crystallized and seemingly pure attapulgite (Fig. 1), but it was impossible to find a sedimentary attapulgite free of other clay minerals. For example, in the course of an extensive study of every clay horizon of the Hawthorne formation, in the Attapulgus, Georgia, area (more than 500 samples have been so far examined and determined), attapulgite was always found with variable amounts of other clay minerals: sepiolite, montmorillonite, illite, or kaolinite. The selected sample contained an estimated 5 to 10% montmorillonite which was removed by centrifugation (Fig. 1).

No chemical analysis of the mountain leather was available, but data published for specimens of similar origin suggest a relatively high aluminum content (Table 1). The Attapulgus sample is rich in magnesium and iron.

Saponite

The selected sample comes from the bentonite deposits of Ksabi (Morocco). It is apparently free of impurities, but its very poor diffrac-

Table 1. Chemical Data of Raw Samples (Recomputed Without the Water)

	1	2	3	4	5	6
SiO_2	66.82	70.57	63.07	66.67	67.28	69.68
MgO	27.12	21.82	34.12	13.86	8.42	6.93
Al_2O_3	.76	2.79	1.02	10.72	18.05	17.17
Fe_2O_3	3.81	2.20	1.19	3.78	2.04	2.67
FeO	.89				.41	
CaO	.60	2.62	.01	1.92	3.80	3.55
TiO_2				.61		
Na_2O				.52		
K_2O			.60	.43		
P_2O_5				1.61		

1. Sepiolite from Ampandandrava (after Caillere) (5).
2. Sepiolite from Vallejas (after Vivaldi, Cano Ruiz) (11).
3. Saponite from Ksabi (after Millot) (13).
4. Attapulgite from Attapulgus (courtesy of Minerals and Chemical Corp. of America).
5. Palygorskite from Nijni-Novgorod (after Caillere) (5).
6. Palygorskite from Taodeni (after Caillere) (5).

* Courtesy of Dr. W. F. Bradley.

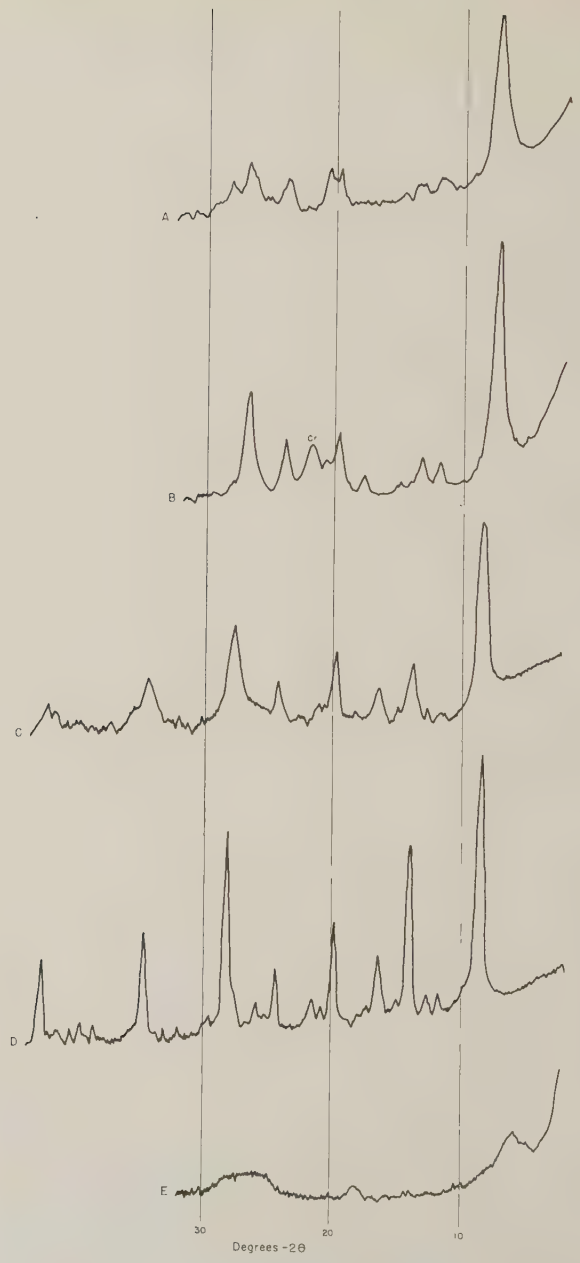

FIG. 1. *X*-ray spectrometer traces: A. Sepiolite (Vallejas). B. Sepiolite (Ampandandrava). C. Attapulgite (Georgia). D. Attapulgite (Aleutian Islands). E. Saponite (Ksabi). Unoriented aggregate. CuKα. 2°/1 minute.

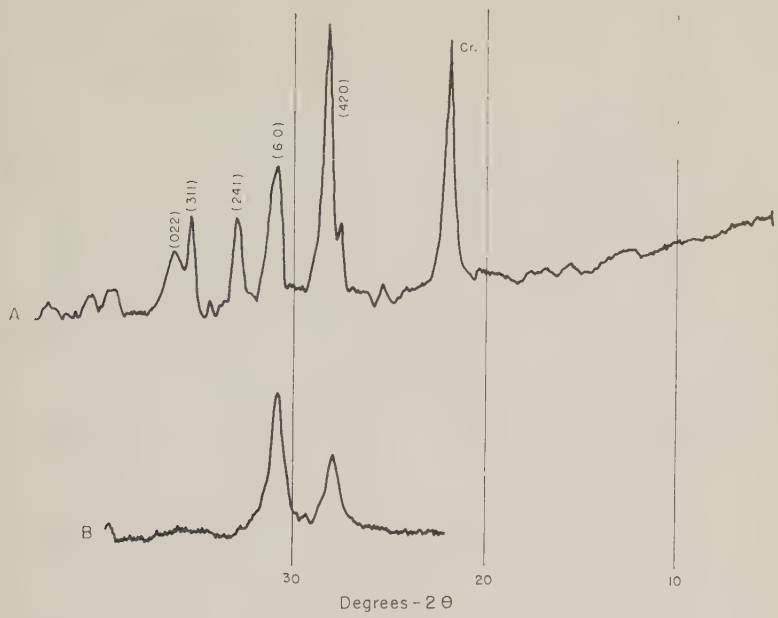

FIG. 2. *X*-ray spectrometer traces: A. Sepiolite (Vallejas) heated at 1400° C. B. Sepiolite (Ampandandrava) heated at 850° C. Enstatite lines are indexed. Cr: cristobalite.

tion diagram (Fig. 1) suggests many dislocations and lattice irregularities. It is believed to have the same composition as the specimen described by G. Millot from the same deposit (13) which has but little substitutions for magnesium (Table 1).

The influence of exchanged or adsorbed cations on the nature and the conditions of formation of high temperature phases in clay minerals was shown previously (9). Most of these cations can be eliminated by two 15 minute soakings in HCl N/10, followed by a filtration. Except when otherwise indicated, the specimens of this study received this treatment.

RESULTS

Sedimentary sepiolite

The diffraction pattern of the mineral disappears around 800° C. (Fig. 3-A). Simultaneously, two broad lines at 3.20 Å (27.8°, 2θ) and 2.90 Å (30.8°, 2θ) are recorded. These lines grow slowly between 1100° C. and 1350° C., and at that temperature they increase substantially and sharpen, while others appear, completing a pattern of enstatite (Fig. 2-A). Some β-cristobalite is formed at the same time (1350° C). When the firing is stopped, at 1500° C., the sample is sintered but not melted, and enstatite and β-cristobalite are still present. Below 1400° C. the two

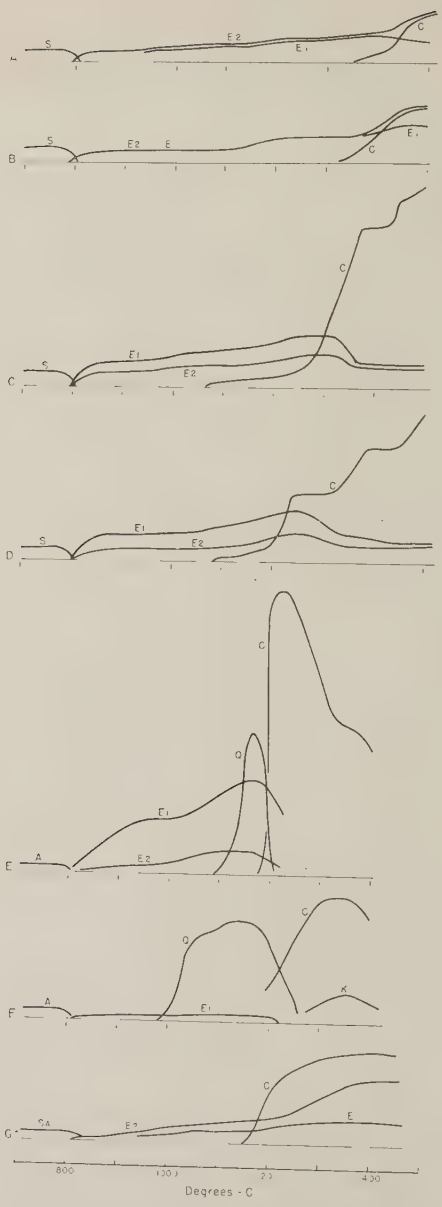

FIG. 3. Intensity of diffraction by high temperature phases in heated specimens of: A. Sepiolite (Vallejas). Treated with HCl. B. Sepiolite (Vallejas). No treatment. C. Sepiolite (Ampandandrava). Treated with HCl. D. Sepiolite (Ampandandrava). No treatment. E. Attapulgite (Georgia). Treated with HCl. F. Attapulgite (Aleutian Island). Treated with HCl. G. Saponite (Ksabi). Treated with HCl. E_1 and E_2: (610) and (420) of enstatite.

main reflections of enstatite (610) and (420) have approximately the same intensity; between 1400° C. and 1500° C. the pattern becomes normal and (420) is twice as intense as (610).

The differential thermal analysis curve shows an endothermic peak at 800° C. followed immediately by an exothermic reaction (Fig. 4-A). The endothermal figure can be related to the departure of water shown on the dehydration curves (10, 11, 12). The exothermal branch is very sudden and sharp, suggesting, according to Bradley and Grim (2), "the incorporation into new phases of large articulate units from reactant structures, without catastrophic rearrangements within the units." There is no other peak on the curve but, above 1200° C., the shrinkage of the sample due to sintering and, possibly, the slow crystallization of β-cristobalite, cause the curve to rise gradually.

Since there is no difference in the high temperature reactions before

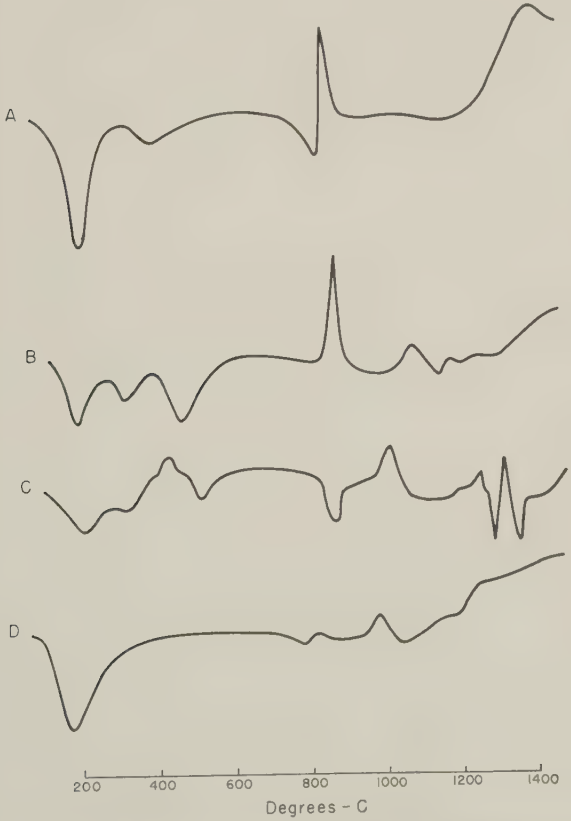

FIG. 4. D.T.A. curves. Specimens treated with HCl. A. Sepiolite (Vallejas). B. Attapulgite (Georgia). C. Attapulgite (Aleutian Islands). D. Saponite (Ksabi).

and after HCl treatment, it can be concluded that exchangeable Mg and extraneous Ca cations have no appreciable influence on these reactions (Fig. 3-A, B).

Hydrothermal sepiolite

Enstatite begins to form at 800° C. (Fig. 3-C). Unlike the sedimentary sepiolite, the (610) reflection is more intense than (420). β-cristobalite appears at 1075° C., developing stepwise at 1300° C. and 1450° C. with corresponding decrease of enstatite. It is noteworthy that a sample heated at 1400° C. keeps the needle shape of its particles, as revealed by microscopic observation.

The removal of exchangeable or extraneous cations by HCl treatment does not notably affect the high temperature phases (Fig. 3-C,D).

The high temperature diagrams of the two sepiolite specimens (Fig. 3-A, C) show notable differences in the growing of enstatite, the temperature of initiation and the amount of β-cristobalite. These differences cannot be accounted for by the size of the crystals in the two specimens nor by the slight differences in bulk composition since the sepiolite which contains less silica grows more β-cristobalite and at a lower temperature. No explanation can be proposed at this time.

Sedimentary attapulgite

Like the sepiolite specimens, enstatite is formed when the clay structure is destroyed, at 800° C. (Fig. 3-E). The formation of β-quartz at 1100° C. seems to accentuate the enstatite reflections. Both minerals disappear at 1200° C. with the formation of β-cristobalite. The (420) reflection of enstatite is here 4 times smaller than (610), indicating the preferential growth of the crystals in the *a* direction.

The D.T.A. curve (Fig. 4-B) shows a single sharp exothermal peak at 800° C. marking the formation of enstatite. A second exothermal peak around 1100° C. can be correlated with the crystallization of β-quartz. The other features are faint and cannot be interpreted.

Various cations (NH_4, K, Cs, Al, Ba, Ni . . .) were fixed on the lattice by base exchange. They did not affect visibly the formation of enstatite, but they acted on the silica phases. The effects were similar to those observed with montmorillonites (9). The most notable was the absence of β-quartz and β-cristobalite in the specimens containing K or Cs.

Mountain leather

Enstatite is formed at the same temperature as for sepiolite but only in a small quantity (Fig. 3-F). It is not affected by the production of

β-quartz at 1100° C. At 1200° C. β-quartz inverts to β-cristobalite. Another magnesian phase, cordierite, appears at 1200° C. It must be noted here that, except for the formation of enstatite between 800° C. and 1200° C., this specimen behaves like a Mg-rich montmorillonite. Thus, a high temperature diagram like Fig. 3-F, including β-quartz, β-cristobalite and cordierite, is typical of a dioctahedral montmorillonite containing a considerable amount of Mg (4–5%) replacing Al (8, 9). Base exchange treatments were also made with various cations, but, unlike sedimentary attapulgite or montmorillonite, no appreciable change in the high temperature phases was recorded. Possibly this indicates only the difficulty of introducing significant amounts of cations inside the framework of this largely crystallized specimen.

At 1200° C. the material is well agglomerated and the needle shape of the starting product is no longer recognizable under the microscope.

Above 800° C., the D.T.A. curve differs completely from that of the Attapulgus sample (Fig. 4-C). Indeed, it is identical with a curve of Mg-rich dioctahedral montmorillonite (8, 9). The collapse of the structure seems to cause the endothermal peak at 805° C. and the crystallization of β-quartz correlates with the exothermic peak at 100° C.

Saponite

The reactions of saponite are very similar to those of the well crystallized sepiolite, but there is very little enstatite at the beginning and its growth is very slow (Fig. 3-G). The relative intensities of (420) and (610) are those of a normal pattern, indicating no preferential growing of the crystals. β-cristobalite appears in appreciable amount at 1200° C. and is accompanied by a substantial increase of enstatite. The reactions cannot be closely correlated with the thermal curves, probably because they are not sufficiently abrupt.

After heating at 1500° C. the specimen is not fused and the two phases are still present.

The high temperature diagrams of the specimens investigated show some significant differences between the well crystallized sepiolite and attapulgite and their sedimentary massive varieties. It has been noted for example that the former have many similarities with the layer minerals of the montmorillonite group. This is not expected from the composition nor the existing structural data. It is suggested that some intimate structural features may be responsible and that the distinction between the two varieties of sepiolite or attapulgite is more than an accidental difference in crystal size due to different growing environments. More studies are needed on this point.

Remarks on the Formation of Enstatite

The enstatite nucleation around 800° C. is a common feature of all specimens, which seems at first to indicate that the reaction is primarily due to the magnesium content, regardless of the structure of the starting material. However, it occurs more rapidly and with more intensity in most specimens of the fibrous type minerals, sepiolite and attapulgite, suggesting in turn a favorable effect of this kind of assemblage. This point seems to be supported by the examination of the different structures.

The various structures encountered in this study have been schematically represented in Figs. 5, 6, 7, 8 and 9. These stylized drawings are projections onto the *bc* plane for saponite, and *ab* for the others. It should

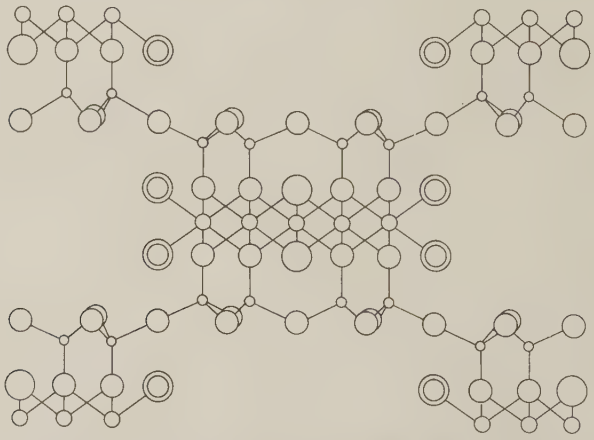

Fig. 5. Idealized structure for attapulgite projected onto 001 (after Bradley).

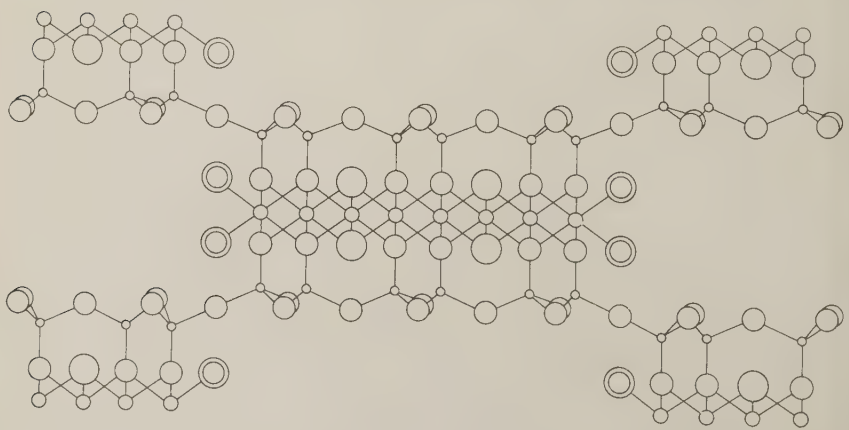

Fig. 6. Idealized structure for sepiolite projected onto 001 (after Brauner-Preisinger).

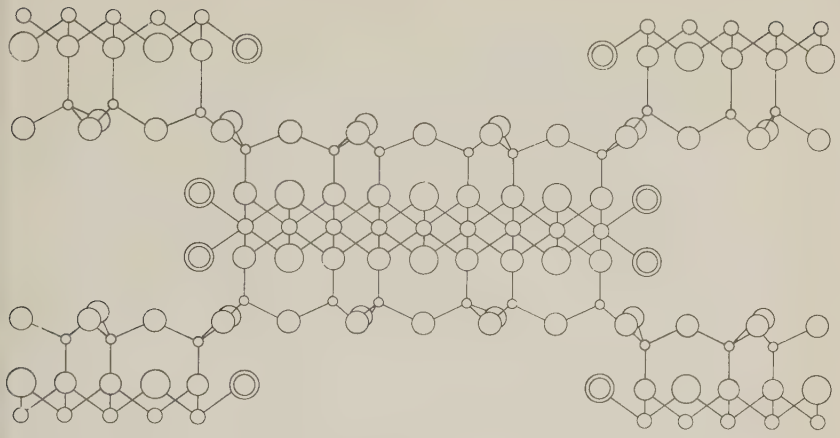

FIG. 7. Idealized structure for sepiolite projected onto 001 (after Bradley).

be remembered that these planes are structurally identical, since the usage has been to call the 5.2 Å period of these silicates, *a* in the layer structures and *c* in the fibrous structures.

For the purpose of the discussion, the hexagonal net of tetrahedra making up the silica layers of all these minerals can be seen as groupings of silica chains ($Si_2 \cdot O_6$) extending in a direction normal to the drawing. In fact, if we disregard isomorphous replacements, these structures are identically made of groups of "basic units" which are formed of two such silica chains linked by octahedral cations. The relative disposition of these units in the various structures is shown in Fig. 9.

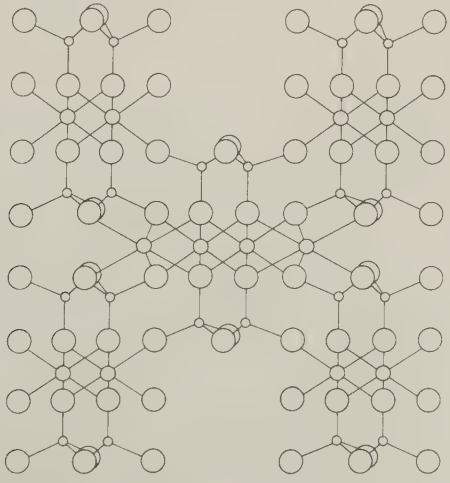

FIG. 8. Idealized structure for enstatite projected onto 001.

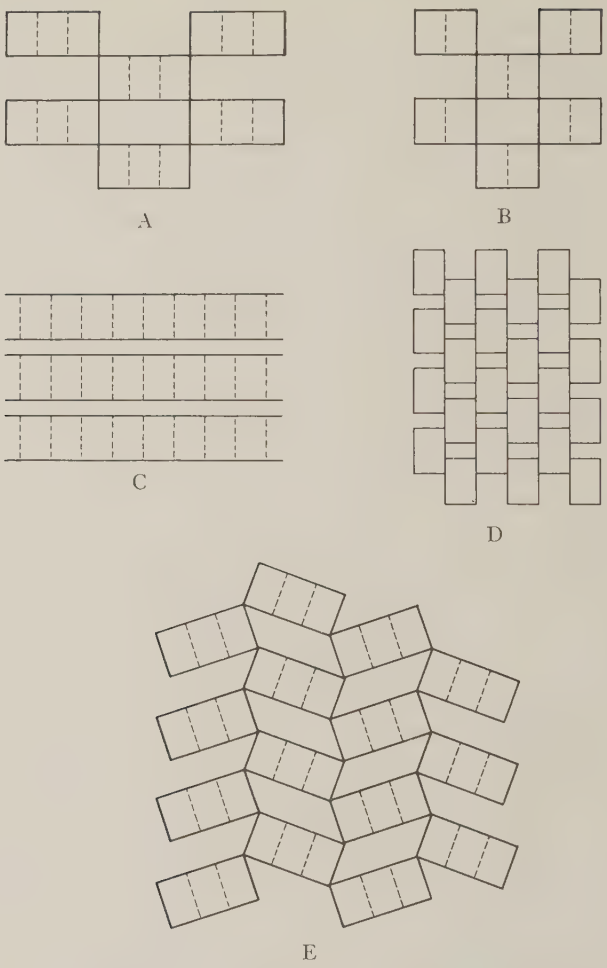

FIG. 9. Schematic structures for the investigated minerals showing the mode of association of the "basic-chain-units" (dotted lines). A. Sepiolite projected onto 001 (Brauner-Preisinger proposed structure). B. Attapulgite projected onto 001 (Bradley proposed structure). C. Saponite projected onto 100. D. Enstatite projected onto 001. E. Dehydrated sepiolite projected onto 001 (after Preisinger). The angle of tilting is arbitrary.

The close relationships between the enstatite structure and the structures of sepiolite and attapulgite appear clearly. They explain the ease of formation of the pyroxene from the latter minerals: the generation of enstatite can be achieved through the rearrangement of whole "basic units" reacting edgewise and remaining parallel to their primitive elongation, without any major disturbance within these units. Thus enstatite nuclei will be generated upon breaking of the oxygen-ribbon-

edge bonds of the sepiolite assemblage and their linking to the Mg of the octahedral level (Fig. 6, 8 and 9). These nuclei extend mainly in the *a* and *c* directions, resulting in only two diffraction lines (610) and (420) with the predominance of (610). In another step, the 3 "basic units" making up a sepiolite ribbon will be separated and then complete the enstatite framework.

These views are based on one of the two alternative sepiolite structures (4, 14, 15) (Fig. 6). In the other one, where the ribbons are linked by double oxygen bonds (Fig. 7), the formation of enstatite as described does not appear immediately possible since it necessitates a more complete reorganization of the atoms. It is suggested that the differences in the production of enstatite in various sepiolite specimens might be due to the coexistence of both structures in a given specimen.

Preisinger (15) has shown that below 800° C. the ribbons of sepiolite take a tilted position as indicated in Fig. 9. The same thing has since been observed for attapulgite by W. F. Bradley and the author* who show that large exchangeable cations like potassium may prevent this tilting to a certain extent. However, in the experiments reported here the amount of tilting of the ribbons does not seem to affect the formation of enstatite.

In the case of attapulgite, the reaction could be theoritically seen in the same way, the variations in the production of enstatite indicating the existence of two alternative linkages of the ribbons (1, 14). However, the different composition of the octahedral layer may, in addition, cause some notable differences. In this mineral, chemical analyses indicate that, in general, only $\frac{1}{3}$ to $\frac{1}{2}$ of the octahedral cations are Mg. If the formation of enstatite necessitates Mg ions along the edges of the ribbons, it will vary with the proportion and with the position of this cation; but in every case it should be less intense than in a sepiolite specimen. On the contrary, high temperature diagrams indicate that, in some instances, enstatite forms more easily than from sepiolite (Fig. 3). It is suggested that the separation of the "basic units," which is necessary for the building of enstatite, is controlled by the disposition of the cations within the octahedral sheet. Unfortunately, nothing is known of the pattern versus composition of the octahedral level to predict the behavior of a specimen.

In saponite, the slowness of the enstatite crystallization may be attributed to the layer structure of the mineral. Some nuclei are first realized along the edge-contacts provided by latice irregularities and dislocations within the crystals. Although these are not negligible, the reaction remains limited to a relatively small number of positions. Upon

* Report in preparation.

increased heating, the "basic units" are progressively separated and they contribute to the gradual growing of the pyroxene structure.

Acknowledgments

The author wishes to express his gratitude to Dr. R. E. Grim for his guidance and aid throughout the course of this investigation. He is also deeply grateful to Dr. W. F. Bradley who contributed valuable criticisms and suggestions in the structural aspects of the problem.

References

1. Bradley, W. F. The structural scheme of attapulgite: *Am. Mineral.*, **25,** 405–510, 1940.
2. Bradley, W. F. and Grim, R. E. Thermal effects of clay and related sediments: *Am. Mineral.*, **36,** 182–201, 1951.
3. Brindley, G. W. and Ali, S. Z. Thermal transformations in magnesian chlorite: *Acta Crist.*, **3,** 25–30, 1950.
4. Brauner, K. and Preisinger, A. Struktur und Entstehung dex Sepioliths: *Tschermaks Min. Pet Mit.*, **1–2,** 120–140, 1956.
5. Caillere, S. Chap. VIII in *X*-ray identification and structure of clay minerals: Monograph of Min. Soc. London 1951.
6. Caillere, S. and Henin, S. Chap. IX in "*X*-ray identification and structure of clay minerals": Monograph of Min. Soc. London 1951.
7. Caillere, S. and Henin, S. Chap. IX in "The differential thermal investigation of clays": Monograph of Min. Soc. London 1957.
8. Grim, R. E. and Kulbicki, G. Etude aux rayons X des reactions des mineraux argileux a haute temperature: *Bull. Soc. Fr. Ceram.*, **36,** 21–28, 1957.
9. Kulbicki, G. High temperature phases in montmorillonites: 5th Nat. Clay Conf., Urbana, 1956. Nat. Research Coun. 1958.
10. Longchambon, H. Sur certaines caracteristiques de la sepiolite d'Anpandandrava (Madagascar) et la formule des sepiolites: *Bull. Soc. Min. Fr.*, **60,** 232–276. 1937.
11. Martin, Vivaldi J. L. and Cano, Ruiz J. Contribucion al estudio de la sepiolita. I. Caracterizacion y propiedades de sepiolites espanolas: *Anal. Edafol. Madrid*, **12,** 827–855, 1953. II. "Some considerations regarding the mineralogical formula": Proceedings IV Nat. Clay Conf. Nat. Research Council, 1956.
12. Migeon, G. Sepiolites: *Bull. Soc. Fr. Min.*, **59,** 6–134, 1936.
13. Millot, G. *C.R.Ac.Sc.* #2, 11 Jan. 257–259, 1954.
14. Nagy, B. and Bradley, W. F. The structural scheme of sepiolite: *Am. Mineral.*, **40,** 885–892, 1955.
15. Preisinger, A. "An *X*-ray study of the structure of sepiolite": VI Nat. Clay Conf., Berkeley 1957.
16. Thilo, E. and Rogge, G. *Strukturbericht*, **7,** 164, 1939.

Manuscript received November 8, 1958.

THE AMERICAN MINERALOGIST, VOL. 44, JULY–AUGUST, 1959

GEOMETRY, ALIGNMENT AND ANGULAR CALIBRATION OF *X*-RAY DIFFRACTOMETERS

W. Parrish and K. Lowitzsch, *Philips Laboratories, Irvington-on-Hudson, New York.*

Abstract

The counter tube *x*-ray diffractometer is widely used both for routine and complicated mineralogical analyses. Very little has been published on the principles and techniques of diffractometry, and consequently many of the instrumental factors which have a profound effect on the data are often overlooked. This paper describes a rapid, precise and reproducible method for the alignment and angular calibration of the goniometer. Simple mechanical devices are employed. The alignment, the zero angle determination to a precision of approximately $\pm 0.001°$ 2θ, the precise setting of the 2:1 angular relationship between the receiving slit and the specimen surface and the adjustment of anti-scatter slits can be completed in about one hour. The method makes it possible to achieve optimum performance and to compare data with other diffractometers aligned in the same manner. The geometry, the effects of the more important instrumental and specimen factors, and some performance tests are outlined.

Introduction

The increased use of counter tube diffractometers in mineralogical problems has made possible various types of *x*-ray analyses which were difficult or impossible with powder cameras. Although some spectacular results have been achieved with the diffractometer, its full potential has not often been realized. Many factors contribute to the performance, reproducibility and precision of the results. One of these factors is the alignment and angular calibration of the goniometer. In this paper a method that employs simple mechanical devices for rapid and precise alignment and calibration will be described. The instrument and specimen geometrical factors which have a dominant effect on the results obtained with the diffractometer will be outlined.

The diffractometer is obviously a much more complicated instrument than the powder camera and the alignment is therefore correspondingly more difficult. Optimum performance can be achieved only when the goniometer is correctly aligned. Improper alignment may cause a loss of intensity and resolution, distortion of line profiles, increase in background, decrease in peak-to-background ratio and incorrect angle and intensity measurements. The lack of a standard procedure for alignment and calibration causes uncertainty in the results and makes it difficult to compare data with other laboratories or even in the same laboratory.

A few examples will show the difficulties which may be caused by improper alignment. In quantitative analyses of powder mixtures the peak intensities of several lines of the unknown and of a standard substance are measured. If the 2:1 setting is incorrect or different for the

standard and unknown, the peak intensities will be decreased by an amount dependent upon the 2:1 missetting, the absorption and the reflection angle. Since the effect decreases with increasing Bragg angle, the relative intensities will be in error regardless of the statistical accuracy of the counter tube measurements. Good precision in trace analyses requires a minimum background and maximum peak-to-background ratio which can be achieved only with correct alignment. In the study of clay minerals the disorder stacking of the silica sheets and the particle size may be obtained from Fourier analysis of the line profiles. If the line profiles are distorted because of incorrect alignment as well as from the diffraction effects, the separation of the two is practically impossible. In precision measurements of lattice parameters and interplanar spacings for indexing low symmetry substances, accurate angular calibration is essential to achieve the required precision. In qualitative analyses of mixtures and low symmetry substances, good resolution is required to minimize overlapping. There are many more examples that could be cited.

Of course there are other factors in addition to alignment that must be considered to achieve optimum performance, but these will not be described here. The reader may consult the literature on the use of counter tube methods (Parrish and Kohler, 1956); intensity measurement techniques and counting statistics (Parrish, 1956; Mack and Spielberg, 1958); specimen crystallite size statistics (Klug and Alexander, 1954; de Wolff, Taylor and Parrish, 1959), and instrumental aberrations (Parrish and Wilson, 1959; Parrish, 1959b).

X-ray Protection

It is essential in making the alignment to be particularly careful to avoid exposure to the x-ray beam. Since the procedure involves some manipulation of devices without the benefit of all the radiation protective features, caution should be exercised and temporary radiation shields should be used as required. The diffractometer counter tube may be used to survey the set-up (Kohler and Parrish, 1956).

Goniometer Alignment

The conditions that must be realized for correct alignment can be obtained from a study of Fig. 1. The axis of rotation of the goniometer should lie midway between the line focus of the x-ray tube, which is used as the geometrical source, and the receiving slit. The long axes (Z-direction) of the x-ray tube line focus, divergence, receiving and anti-scatter slits must have a common median line, be parallel to each other and to the goniometer axis of rotation O, and lie in the YZ-plane when the detector is at 0°. The metal foils of the parallel or Soller slits must lie in planes normal to the Z-axis.

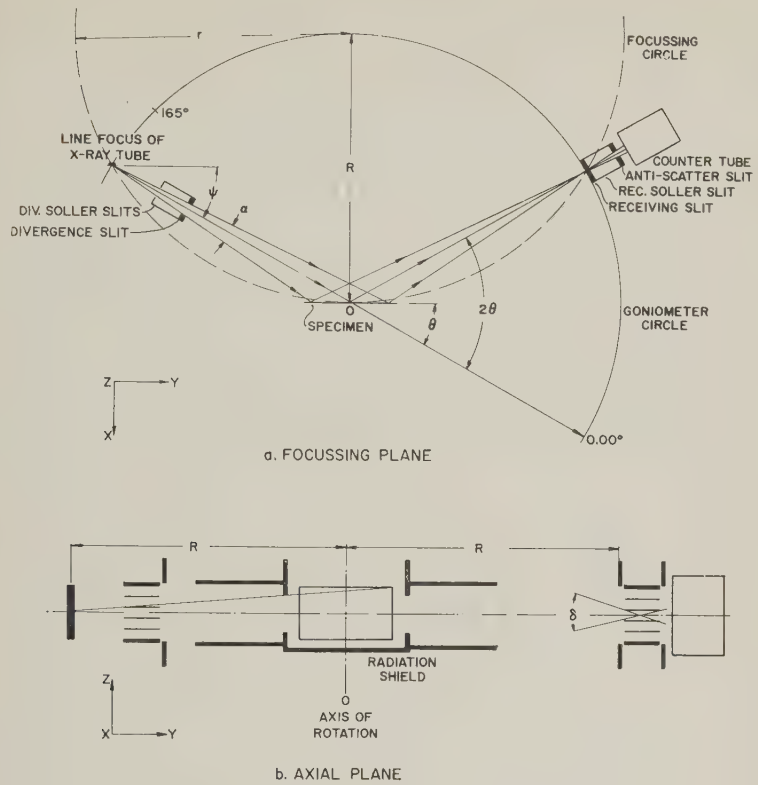

FIG. 1. Geometry of the diffractometer in the focussing plane (above) and axial plane (below). R radius of goniometer, r radius of focussing circle, O goniometer axis of rotation, ψ angle of view of target, α full angular aperture in focussing plane, δ angle aperture limited by Soller slits. The orthogonal coordinate system XYZ is used to facilitate descriptions.

The angle-of-view of the x-ray tube target surface, ψ, is defined with respect to the ray that passes through O. A divergent beam is used and the zero angle of the goniometer scale is defined with respect to the ψ-angle. The 2:1 (receiving slit: specimen surface scanning relationship) setting is made with respect to the zero angle.

The distance between the target and mounting surfaces may vary slightly from one tube to another, and if this occurs ψ will also vary slightly. Although small changes in ψ do not change the resolution, they do require a recalibration of the zero angle and consequently the 2:1 setting. The procedure described below makes it easy to allow for such variations. Care must be taken to avoid tilting the axis of the x-ray tube with respect to the mounting surface of the tube shield.

If the focal spot of the x-ray tube is rotated with respect to the window,

or the plane of the target surface is not perpendicular to the long axis of the tube, the projected size of the line focus accordingly will be increased or decreased. This alignment and projected size can be checked by establishing a reference line from pinhole images of both spot focus windows and then making a pinhole image of the line focus at a known magnification. Normally this is not done unless the construction of the tube is believed to be faulty.

Drawings of the alignment and calibration devices are shown in Fig. 2. Although these devices have been designed for the Norelco goniometer (Parrish, Hamacher and Lowitzsch, 1954), the same principles are applicable to other goniometers. The dimensions of the devices permit direct alignment of the goniometer simply by matching one surface against another. The only critical dimension is the height of D in the X-direction, which must be the same as the height of the slit and horizontal line on the

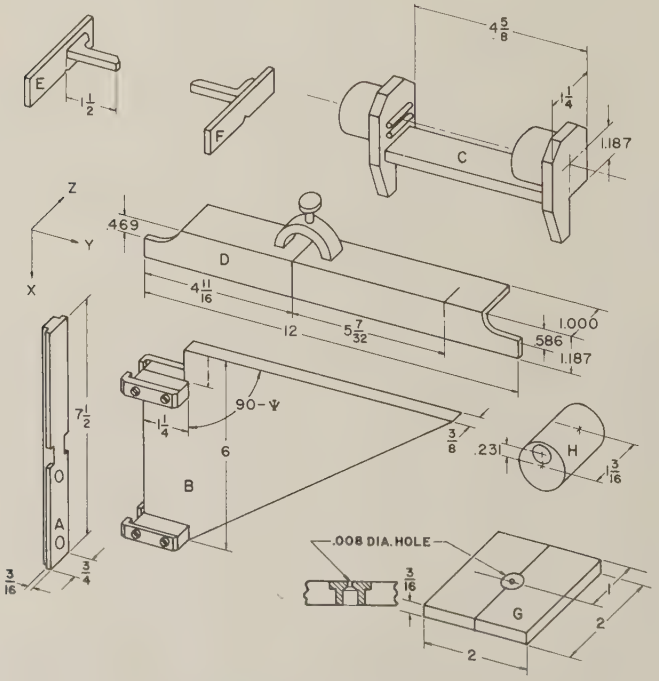

FIG. 2. Mechanical devices designed for alignment and calibration of Norelco goniometer. A bar mounted on x-ray tube tower, B machined ψ-angle surface, C slit and fluorescent screen which clips on B to set ψ, D alignment device which sets in specimen holder, E and F fixtures set in divergence and receiving slit positions, G pinhole and flat plate for zero angle calibration and 2:1 setting, H bushing with off-center hole for elevating divergence Soller slit assembly for $\psi = 6°$.

fluorescent screen above the mounting surface of C. These devices can be easily duplicated with ordinary machine shop facilities.

Preliminary Alignments

Several preliminary steps are required before proceeding to the final alignment. Normally these are done only when making an installation for the first time, or when major modifications are made. It is good practice to adjust the x-ray unit so that the table is horizontal.

Bar A is permanently screwed to the middle of the face of the x-ray tube tower with its long axis perpendicular to the top surface as shown in Fig. 3. This mounting may be facilitated by removing the x-ray tube and using a machinist's square on the top surface of the tower.

The alignment of the elements of the goniometer itself (slit assemblies and goniometer axis) is accomplished with devices D, E, and F. Device D should be mounted on the specimen post with its reference line coinciding with the reference line of the specimen post (Fig. 3b). D must rest straight against the back surface of the post to avoid a rotation in the YZ-plane. The clamp holding the specimen post is loosened so that the post can be rotated freely (but not translated in the Z-direction); the counter tube arm is set at approximately 0° and D is rotated until its left side strikes the bottom of the divergence slit assembly. E and F are inserted and this may require a small angular movement of the counter tube arm. The divergence and receiving slit posts are then rotated until the arms of E and F lie evenly on the top surface of D (YZ-plane).

The position of the receiving Soller slit assembly in the direction parallel to Z is fixed with respect to the counter tube arm and should not be changed. Furthermore, the goniometer is constructed so that the long axes of the divergence and receiving slit assemblies (Z-direction) are parallel to each other and to the goniometer axis of rotation. The specimen post and divergence Soller slit assembly should be translated along Z until the front surfaces of arms E and F are flush with the front surface of D in the XY-plane. When the arms of E and F are flush with the top and front surfaces of D, the divergence, receiving, and antiscatter slits have a common median line which intersects and is normal to the goniometer axis of rotation. If the tip of arm F does not coincide with the reference mark on D, the receiving Soller slit assembly should be translated along Y to set $R = 17$ cm. The Soller slit assemblies should then be locked, E and F removed, and the specimen post with D still mounted on it should be slipped out of the goniometer.

Setting Angle-of-View

The triangular device B is placed on A as shown in Fig. 3(a). B has been machined so that the top surface is inclined by the desired ψ-angle. C consists of a narrow horizontal slit in the front (left) and a flat plastic fluorescent screen in the back (right). C is clipped on B, which is moved vertically on bar A by means of a thumb screw until the image of the x-ray tube focal spot appears centered on the horizontal line in the middle of the fluorescent screen.* B is then locked in position with the other thumb screw and C is removed. The top surface of B is now at the correct height for device D.

Goniometer Position

The goniometer must now be aligned with respect to the x-ray tube. The screws on the under side of the x-ray table that hold the goniometer locating plate should be loosened to allow free movement of the goniometer. The front two levelling screws are set in the locat

* An alternative procedure is to remove the fluorescent screen, use the second slit (right side of C) and a stationary counter tube.

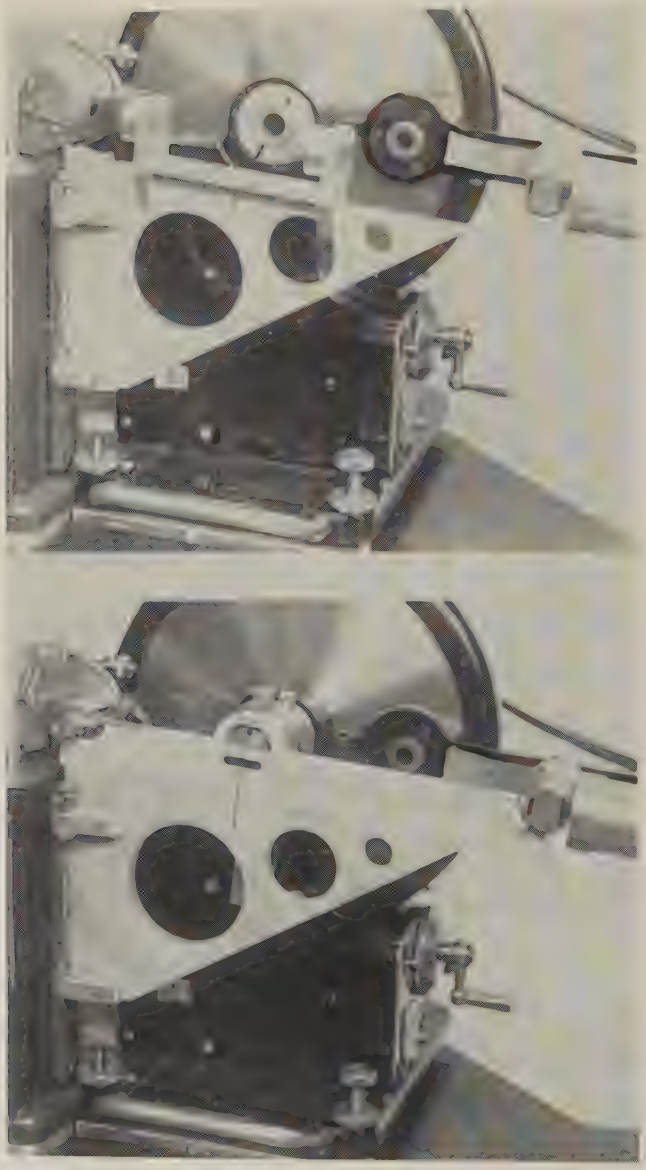

FIG. 3. (*a*) The ψ-angle is obtained by clipping C on B and moving B vertically on A until the image of line focus of the x-ray tube appears centered on the fluorescent screen on C. (*b*) The goniometer alignment is made by moving the goniometer to match B and D (See Fig. 2.)

ing plate. The distance of O above the table top must be made large enough (by rotating the levelling screws) to allow the reinsertion of D and the specimen post as shown in Fig. 3(b). Three adjustments of the goniometer position must then be made: (1) The goniometer (and locating plate) are moved on the x-ray table until the reference line on D matches that on B; this sets O to the correct distance in front of the focal line of the x-ray tube so that the focal line lies on the goniometer circle. (2) The levelling screws are adjusted so that the bottom surface of D touches the top surface of B; this sets O at the correct height for the selected ψ-angle. (3) The levelling screws are readjusted until the front surfaces of D and B are flush in the XY-plane (check with a straight-edge); this aligns the position and direction of the median line of the goniometer with respect to the focal line of the x-ray tube.

In practice it is usually necessary to repeat these three steps a few times because step 3 may alter the settings of the levelling screws made in step 2. There should be no appreciable contact pressure between D and B. E and F may be reinserted to make certain the front surfaces of their arms are flush with the front surface of D in the XY-plane. The levelling screws and locating plate are then tightened. D, E and F are removed, but B is left in place for the angular calibration. The goniometer alignment can usually be completed in less than one-half hour.

Centering the Primary Beam

If in the construction of the divergence slit, the opening was not accurately centered, the procedure described above may not give a precise centering of the primary beam on the specimen. The centering of the beam may be checked with the x-ray tube operating at full power and a *flat* ruled fluorescent screen in the specimen post. Since a divergent beam and extended flat specimen are used, the primary beam can be centered exactly only at some chosen angle. In scanning to other angles the geometrical center of the beam will gradually change with respect to O. For example, if the 1° divergence slit is rotated to center the beam on the fluorescent screen which has been set normal to the incident beam, the latter will appear off-center by about 1 mm. when the screen is set for $2\theta = 20°$.

It is generally desirable in routine work to center the beam with the screen set at the lowest scanning angle to be used, particularly when working at small angles, say $\theta < 10°$, because here the length of specimen illuminated increases rapidly with a small decrease in θ. This procedure eliminates scatter which may occur from the primary beam striking the ends of the specimen holder. It should also be noted that the centering of the primary beam may vary among several divergence slits if the distances between the middle of the opening and the reference edge are different.

The distribution of intensity across the specimen in the Z-direction may be observed by looking down on a fluorescent screen mounted in the specimen holder with the specimen radiation shield in place. The angle at which this is done is not important, but the primary x-ray beam intensity should be sufficiently small (say 25 kV, 10 ma) that variations of the fluorescent intensity are discernible. The front and back edges of the screen in the Z-direction will appear to be slightly less strongly illuminated because of the way the divergent rays overlap in passing through the divergence Soller slit. The brighter strip of illumination should appear centered on the screen. If it is to one side, the focal spot of the x-ray tube may be improperly oriented or mis-centered, there may be a cutoff at the window of the x-ray tube housing, or the divergence Soller slit assembly may be inclined from its proper position normal to the Z-direction.

Angular Calibration

Several methods have been used for calibrating the angular scale of the goniometer. The most common method has been to use a "standard"

substance whose lattice parameter has been accurately determined by some other x-ray instrument, usually a powder camera, to construct a calibration curve. The limitations of this method will be described below. In the mechanical method the 0° angle is accurately measured and it is assumed that the gear system accurately moves the receiving slit-counter tube arm to the angle indicated on the scale. If desired, the angular precision of the gear train can be checked to about one second of arc by use of precision polygons (Taylerson, 1947; Haven and Strang, 1953). The equipment required for this purpose is expensive and specialized techniques are used for the calibration.

Mechanical Method

This method is based upon determining the 0° angle with respect to the ray that makes the desired ψ-angle with the target surface and passes through the goniometer axis of rotation and center of the receiving slit. The procedure is done with x-rays, but it does not require reflection from a specimen and hence is not subject to systematic errors. It may be applied with a fine slit, pinhole (Parrish, Hamacher and Lowitzsch, 1954), or a knife edge (Tournarie, 1954), and is far more accurate than the other methods described below. The principle is illustrated in the ray diagram and observed intensity distributions in Fig. 4. The anti-scatter slit should be removed and the x-ray machine and circuits operated for about an hour with full power on the x-ray tube to make certain that equilibrium conditions have been reached before making the calibration.

The $\frac{5}{8}$ in. diameter rod of the specimen post must fit snugly into the goniometer because loose fitting will cause an error in the calibration by approximately twice the amount of clearance (measured on an angular scale). The use of the calibrating slit requires the removal of the specimen post, but use of the flat plate with fine pin-hole (≈ 0.008 in. diameter) or knife edge does not. The three calibration devices should give the same results, but there are some advantages in the use of the pinhole. The intensities are considerably lower (and hence less filtering is required) than for the slit or knife edge. In addition, the pinhole device is also used to make the 2:1 setting, whereas the other devices cannot be used for this purpose. There may be some confusion in the use of the knife edge. In Fig. 4, all rays up to the dotted line will pass through the upper half of the divergence slit, but beyond the dotted line the intensity falls off giving a sloping line similar in appearance to the calibration line. The angle at which this occurs depends upon the angular aperture α. For example, with $\alpha = 1°$ it occurs at approximately 0.5° 2θ from the 0° position.

The pinhole plate is set in the specimen holder with the pinhole ap-

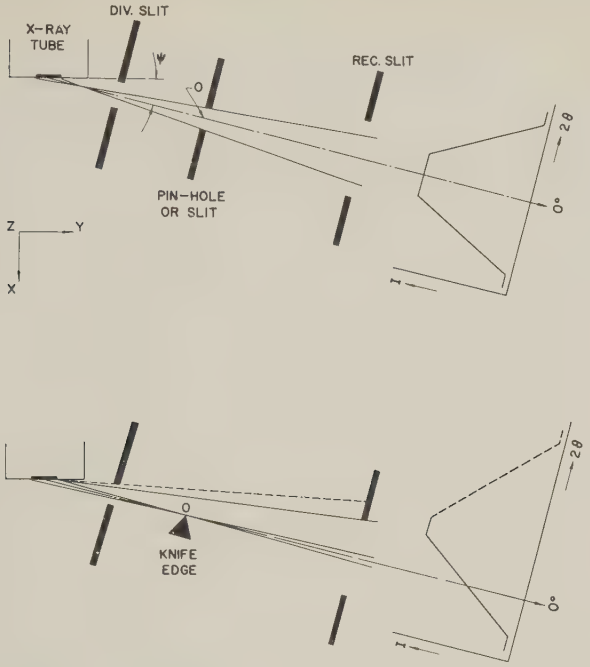

FIG. 4. Schematic ray diagram of 0° calibration using pinhole or slit (above) and knife edge (below). The intensity distributions are on the right.

proximately aligned on the axis of rotation (middle of the specimen post) and the large surface of the plate normal to the selected central ray as shown in Fig. 4. A small machinist's square set on top of *B* may be used to make the setting, which, although not critical, should be approximately correct in order to obtain the same intensities for the following two series of measurements. One series is made with the plate in this position and another series is made after the specimen holder (with pinhole plate) is rotated 180°. The pinhole plate must not be moved with respect to the specimen holder from its original clamped position.

The intensity distributions are measured by step-scanning in 0.01° steps using either manual settings or step gears (Parrish, Hamacher and Lowitzsch, 1954; Parrish, 1956; Hamacher and Lowitzsch, 1956). To avoid backlash errors, the distribution should always be scanned in the same direction; the counter tube arm should be moved manually in this direction for a few tenths of a degree before beginning the recording at the base of the peak. The intensities must be measured with good statistical accuracy. A simple method is to continuously drive the step gears and record with the ratemeter using a 2 sec. time constant. It takes

30 secs. for the drive gears on the goniometer to make one revolution so that about 28 secs. is spent at each step.

The counting rates should be kept low enough to avoid the necessity of non-linearity corrections for counter or circuit resolving time. In the case of full-wave rectified operation of a copper target tube operated at about 15 kVp, 7 ma, $\psi = 6°$, 0.0025 in. nickel filter, 1° divergence slit and 0.006 in. receiving slit, the observed peak intensity is about 4×10^3 counts per sec. with a scintillation counter without pulse amplitude discrimination. If a Geiger counter is used the filtering should be increased to reduce the peak counting rate to about 500 counts per sec. By using a low voltage on the *x*-ray tube nearly all the radiation measured has about the same wavelength as CuKα. If higher voltages were used, greater filtering would be required and the radiation measured would consist largely of considerably shorter wavelengths.

The data from the recordings may be plotted as shown in Fig. 5. The median line (dashed) of each set of readings is constructed and the line (dot-dash) lying midway between the two median lines is the 0.00° position. Since both distributions are symmetrical, the median lines are vertical. The angular separation of the two sets of readings will depend on how closely the pinhole was aligned with the axis of rotation; the separation should not exceed about 0.2°. The 0.01° dial may be set to the measured zero angle or a correction may be applied to all future readings.

The 0° angle can also be derived from the knife edge data as shown in Fig. 5 (right). The two sets of data for the 180° rotation are symmetrical, and the vertical median line is easily constructed from the midpoints.

Using the procedure outlined above, it is possible to determine the zero angle position to a precision of about $\pm 0.001°$ in about one-half hour. By manual setting on the peaks of the pinhole curves, a precision of $\pm 0.01°$ may be obtained in a few minutes.

Effect of Receiving Slit on Calibration

The greater the height of the receiving slit (in the *X*-direction), the broader the curves obtained with the pinhole and the less steep the knife edge curves. Both methods give the same answer when the *same* receiving slit is used. However, if the *X*-distance between the central longitudinal line of the receiving slit and the reference edge (Fig. 5 insert) varies from one slit to another, the derived zero angle will also vary. For example, two different 0.006 in. receiving slits were used to determine the data used in Fig. 5 and gave zero angles, 0.003° apart, because *X* was not the same in both slits. Furthermore, if the *X*-distance of the 0.018 in. receiving slit had been the same as that of the 0.006 in. slit, the zero angles derived from both also would have been the same. Since it is difficult to achieve the mechanical tolerances required to obtain exactly the same zero angle calibration with different receiving slits, a separate calibration should be made for each receiving slit.

It should be noted that the receiving slit height has a major role in determining the resolution, intensity and peak-to-background ratio (Parrish, 1956). The narrower the slit,

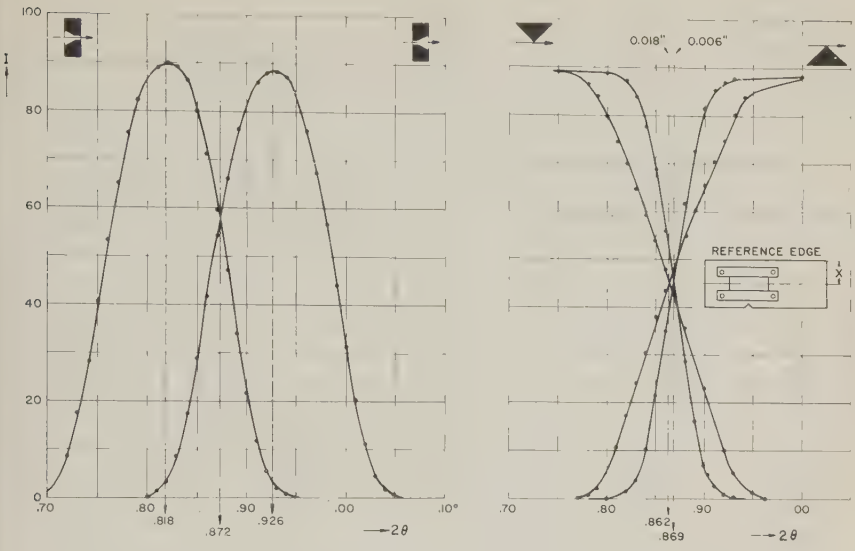

FIG. 5. Plot of data to determine 0° angle using pinhole (left) and knife edge (right).

down to about 0.003 in., the greater the resolution and the lower the intensity. However, aside from its effect on the observed Kα-doublet overlap, the receiving slit height causes only symmetrical broadening, whereas other instrumental aberrations cause asymmetric broadening and shifts in the line positions.

4θ-Method

Another method for determining the zero angle is to measure the 2θ-angles of a number of reflections on both side of the 0° position. This method is equivalent to measuring 4θ in powder camera calibrations; it has been used for a long time and has recently been described as the Cornu method (Neff, 1956). It requires setting the 2:1 relationship (see below) *before* making the calibration. It also requires the specimen holder be temporarily disengaged from the goniometer, rotated exactly 180°, and then reengaged before scanning to obtain the reflection below 0°. Any error in the 180° rotation causes an incorrect 2:1 setting which broadens the line, shifts the peak and thereby introduces a random error. The angular positions of a number of reflections must be measured above and below 0° and averaged. The precision of the determination is limited by the random errors in the individual measurements and it also requires much longer time than the mechanical method.

Use of Standards

Frequently a specimen of a "standard" substance whose lattice parameter has been established by other methods is used for angular calibration. The reflection angles $2\theta_{cal}$ are calculated and a graph is drawn relating the observed angles of the standard, $2\theta_{obs}$ or $2\theta_{obs} - 2\theta_{cal}$ to the calculated values. The unknown substance is then measured under the

same experimental conditions, and its $2\theta_{obs}$ values are corrected by means of the calibration curve.

Assumptions which are implicit in this procedure are that the random errors in the measurement of the standard are negligible and that the systematic errors (Parrish and Wilson, 1959; Parrish, 1956b) will be the same for both the standard and unknown. Thus it must be assumed that the standard and unknown are both perfect specimens, that the specimen surface displacement error is the same for both, and that both have the same absorption. It is also clear that the precision of the method cannot exceed the precision with which the lattice parameter of the standard has been determined. In fact, good practice in physical measurements requires that the reflection angles of the calibration substance be known with considerably better precision than is required in the measurement of the unknown. Unfortunately, there is now considerable doubt that the accuracy attainable in precision lattice parameter measurements exceeds about 0.013% (Parrish, 1959a). Nevertheless, standards are useful in assessing the performance of the equipment. Reflection angles and recordings for diamond, silicon and tungsten and other substances for several x-ray wave lengths are given elsewhere (Parrish and Mack, 1959). The line profiles of well-crystallized standards are required to check the resolution, peak-to-background ratio, intensity, and similar factors as described at the end of this paper.

Some of the uncertainties that arise from the use of standards may be circumvented by using an internal standard (Chayes and MacKenzie, 1957; Swanson, Gilfrich and Cook, 1957). A small amount of the standard substance is intimately blended with the unknown, and the measurements of $2\theta_{obs}$ of the standard and $2\theta_{obs}$ of the unknown are then made on the same specimen. This procedure may reduce the errors from differences in specimen surface displacement, but most of the difficulties remain. In addition, the standard adds more, although known, lines to the pattern.

It should be clear that when the zero angle calibration is made by the mechanical method, the peak positions of the lines of a standard substance show deviations from the calculated values by amounts dependent upon the systematic and random errors in the measurements.

Specimen Surface Displacement and Transparency

Displacement of the specimen surface from the goniometer axis of rotation is the common source of many relatively large systematic errors in angular measurements. If the specimen surface is displaced a distance $x_{s.d.}$ from O, the observed reflection angle is shifted (Wilson, 1950) by an amount

$$\Delta(^\circ 2\theta)_{s.d.} = 114.5916\, x_{s.d.} \cos\theta/R.$$

A plot of this expression for various values of $x_{s.d.}$ is shown in Fig. 6. The shift is toward higher angles if the specimen surface is inside the focussing circle or toward lower angles if it is outside. The entire line profile is shifted, and thus the formula applies to the peak, median, center-of-gravity* or other measures of the line position.

This displacement error may be caused by non-coincidence of the reference surface of the goniometer specimen holder with 0, and in this

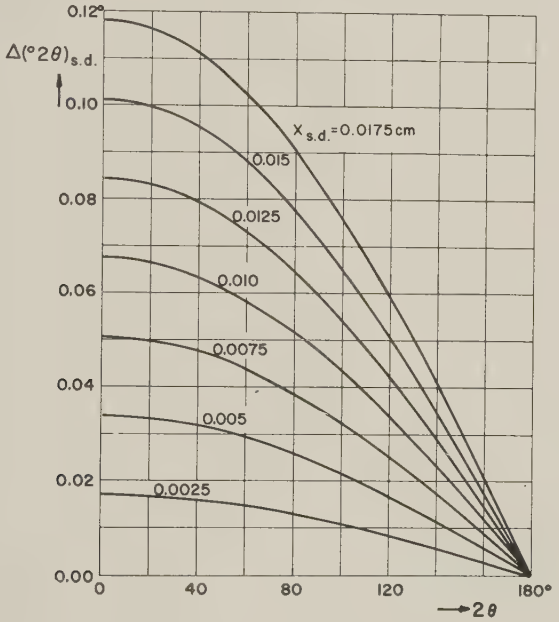

Fig. 6. Angular error caused by specimen surface displacement.

case readings on all specimens will be in error by a constant amount at a given angle. The surface of the holder should be checked with respect to the $\frac{5}{8}$ in. diameter rod with a precision dial indicator gauge, surface plate and gauge blocks. If the errors are caused by poor specimen preparation, or failure to shim the mounting surface when using slide smear preparations, the errors will vary from one specimen to another. The calibration procedures described above do not take these types of errors into account and they must be treated separately. (See also Parrish, 1959b.)

Unless the shift is extremely large, the shape of the line profile and the intensity are unchanged.

* The center-of-gravity $\tilde{\theta}$ is defined as $\tilde{\theta} = \int\theta f\theta d\theta / \int f(\theta) d\theta$; see Ladell, Parrish and Taylor (1957, 1959).

A somewhat similar error will arise if the specimen has a low linear absorption coefficient μ, because some of the diffraction will take place below the specimen surface. This transparency error always shifts the lines to smaller angles and causes asymmetric broadening of the lines. The shift of the center-of-gravity of a line $\Delta(2\theta)_{tr}$ (expressed in radians) is

$$\Delta(2\theta)_{tr} = \frac{\sin 2\theta}{2\mu R} - \frac{2x_t \cos\theta}{R\,[\exp(2\mu\, x_t \csc\theta) - 1]}$$

where x_t is the specimen thickness. If the beam is completely absorbed in a thick absorbing specimen, $\mu\, x_t \csc\theta$ is large and the second term may be dropped. The shift thus increases with decreasing μ, is maximum at 90° (2θ) and zero at 0° and 180°. Some typical values of $\Delta(2\theta)_{tr}$ at 90°(2θ) for $R = 17$ cm. expressed in degrees are: 0.067° for $\mu = 25$ cm^{-1}, 0.017° for $\mu = 100$ cm^{-1}, 0.002° for $\mu = 1000$ cm^{-1}. In the case of negligible absorption of the beam in a thin transparent specimen, the expression becomes

$$\Delta(2\theta)_{tr} = x_t \cos\theta / R$$

(expressed in radians).

2:1 Setting

To obtain proper focussing conditions, the counter tube must be set at twice the angle of the specimen with respect to the 0° ray, and this 2:1 relationship must be maintained at all reflection angles by an accurate tracking arrangement. Deviations from the correct 2:1 setting cause line broadening and a decrease of peak intensity. Also, if other misalignments are present they may combine with 2:1 missetting to cause a shift of the line. The magnitude of these effects increases with decreasing 2θ, which causes further errors in the relative peak intensities and line-breadths. In measurements of line profiles and peak intensities and small Bragg angles, such as are required in clay mineral studies, an incorrect 2:1 setting will have a profound effect on the results (Parrish, 1959b).

A powder specimen in the reflecting position is frequently used to set the 2:1. This method has the disadvantage of being relatively insensitive to small missettings. A single crystal plate might be used to make this setting, but this requires that the atomic reflecting plane be exactly parallel to the surface of the crystal and that a very narrow incident ray be accurately centered on the axis of rotation.

A mechanical method of precisely setting the 2:1 at 0° is recommended. It is assumed that the goniometer gears will maintain this relationship at all angles. A long slit, a double knife edge or a flat plate* may be used, as illustrated in Fig. 7. The x-ray intensity should be some-

* To avoid total reflection at grazing incidence, the surface should not be highly polished.

what reduced from that used for the 0° calibration by the addition of more filters. The 2:1 setting must be made with the goniometer locked in the previously determined 0.00° position. One of the three devices is placed in the specimen holder and the latter is rotated until maximum intensity is obtained. The correct 2:1 position is sharply defined because even a slight rotation of the order of 0.01° will cause a large decrease of intensity. The specimen holder is locked in this position while the count-

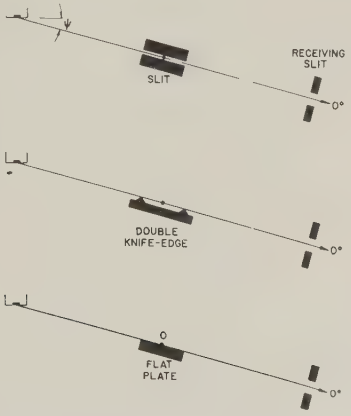

Fig. 7. Methods for 2:1 setting at 0°.

ing rate is observed on the rate-meter to make certain that the locking has not changed the 2:1 setting.

A new device, shown in Fig. 8, facilitates the accurate setting of the 2:1 position. It consists of two arms operated in scissor fashion by a micrometer screw about 4 in. from the axis of rotation, and it is spring loaded to give a positive action and to allow adjustments from either direction. One full turn of the micrometer screw rotates the specimen post 0.03°. The device may be mounted on the specimen post or on the rear of the goniometer. The later placement is desirable when temperature chambers, helium path, etc., are to be used.

When the rotating specimen holder (Parrish, 1956) is employed, the devices described above are not used and the 2:1 setting is made by use of a slot about $\frac{1}{4}$ in. wide and 0.001 in. deep milled across the median line on top of the holder. With the counter tube at 0.00°, the holder is rotated to the position of maximum intensity and locked in the same manner as described above.

Anti-Scatter Slits

A low, nearly uniform background can be obtained by the proper use of anti-scatter slits. The receiving slit and the anti-scatter slit in front

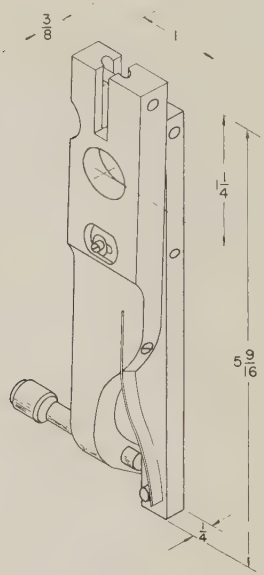

FIG. 8. Precision 2:1 adjustment device. The dimensions are in inches.

of the counter tube together limit the radiation which enters the counter tube to only that radiation scattered from the length of the specimen illuminated in the Y-direction. The air scatter is thereby also reduced to a minimum. The X-dimension of the anti-scatter slit opening is made slightly larger than the X-dimension of the beam at this position. This may be calculated from the angular aperture α and the X-dimension of the receiving slit. The anti-scatter slit is aligned by slowly rotating it around the Z-direction until the peak intensity of a strong reflection from a good specimen is observed to be maximum. The peak intensity should remain nearly the same when the slit is removed. If the intensity increases markedly (say $>2\%$) when the slit is removed, the alignment is incorrect or the slit height is too small.

The slot in the internal cylinder of the specimen radiation shield also reduces extraneous scatter by preventing primary x-rays from striking beyond the 1 cm. width (Z-direction) of the specimen as shown in the lower left side of Fig. 1. For specimens 1 cm. wide, Soller slits with full aperture $\delta = 4.5°$, and $R = 17$ cm., the slot should be 0.85 cm. wide. It is essential that the median line of the slot coincide with the median line of the specimen.

The front of the specimen radiation shield facing the x-ray tube may scatter x-rays into the counter tube at high reflection angles. The internal

cylindrical shield which contains the slot is $2\frac{1}{8}$ in. diameter, and above about 140° 2θ the background begins to rise slightly because of scatter from the metal. If the diameter of the cylinder with the slot is increased to 5 in., the increase of background from metal scattering will be apparent only above about 170° 2θ. If the larger diameter is used the slot must be made narrower or a wider specimen used to avoid scatter from the specimen holder in the Z-direction as explained above.

Angle-of-View of Target

Normally a small angle-of-view ($\psi = 3°$) of the target surface has been used to obtain a small projected height of the x-ray tube line focus (Parrish and Hamacher, 1952). It has recently been found that the projected height can be increased by a factor of two without decreasing the resolution (Parrish, 1958). Since the intensity is zero at grazing incidence and increases with increasing ψ at a rate dependent upon the voltage, atomic member of the target element and smoothness of the target surface, the intensity may be increased about 25% by increasing ψ from 3° to 6° for a given set of experimental conditions. For a given aperture α, the primary intensity along the Y-dimension of the specimen also becomes more uniform at larger ψ.

In high precision diffractometry it is preferable to set the center-of-gravity of the primary x-ray beam intensity distribution rather than the geometrical center on the axis of rotation (Wilson, 1954). The center-of-gravity remains fixed at all angles and the effects of certain instrumental misalignments are minimized. The geometrical center and center-of-gravity differ by an amount dependent upon the distribution of intensity in the primary beam. With a copper target x-ray tube operated at 40 kVp, $\alpha = 4°$ and $\psi = 3.0°$, the center-of-gravity is at 3.3°. For the same conditions except that $\psi = 6.0°$, the center-of-gravity is at 6.06° which is so close to the geometrical center that the latter may be used.

In the case of the Norelco goniometer, increasing ψ from 3° to 6° decreases the upper limit of the scanning range from 165° to 162° 2θ, and several minor modifications are required. A collar $\frac{1}{2}$ in. high should be inserted at the base of the x-ray tube tower to raise the x-ray tube tower window. The lower part of the window opening in the tower may also have to be enlarged. The divergence Soller slit assembly must be raised, and an easy way of doing this is to make a bushing (Fig. 2H) which fits into the boss that holds the assembly. The right side of the Soller slit assembly is also turned down to fit into the $\frac{3}{8}$ in. hole of the bushing. Another bushing with a centered hole can be used with the same assembly at $\psi = 3°$. The alignment procedure is exactly the same as for $\psi = 3°$, but the top surface of the triangular fixture B must be machined at 6°.

Alignment for Single Crystals

When either large flat single crystal plates or small crystals for structure work are to be studied, certain modifications in the procedure are required. The goniometer alignment and zero angle setting are made with a 1° divergence slit and 0.006 in. receiving slit according to the procedure described above. With the counter tube locked in the zero angle position, the pinhole is manually translated small distances in the specimen holder (*keeping fingers out of the beam*) until successive 180° rotations cause no variation of intensity, which indicates that the hole is centered on the goniometer axis of rotation. A smaller divergence slit, say $\alpha = 1/12°$, is then centered by noting the maximum intensity transmitted by the centered pinhole. The smaller divergence slit is required to reduce the intensity to measurable limits, to illuminate only the narrow region around the axis of rotation, and to prevent

"walking" of the reflected beam from a large plate during rotation (the latter would cause errors in the relative intensities at different angles if the reflecting power varied along the crystal surface.) The 2:1 setting is made with the crystal by adjusting the precision 2:1 device to obtain maximum intensity while the goniometer is slowly scanning in the region of the wide peak of the continuous radiation (around 8°–10°2θ at 40 kVp). This technique avoids possible small changes in the 2:1 setting which might occur when the clutch is engaged. Finally, the narrow receiving slit is replaced by a wide receiving slit of the order of 1 mm. in the X-direction to make the recording less sensitive to slightly erratic movements of the gear train, which would cause large intensity variations in single crystal measurements. The total intensity may be greatly reduced by the insertion of pinholes or lead stops on the divergence and receiving slits to limit their lengths in the Z-direction.

Mechanical Tests

It is assumed that the divisions on the dial which read to 0.01° are accurately engraved. For precision work the divisions should be checked against an accurately engraved scale by standard precision machine ship procedures.

The uniformity of movements of the counter tube, the 2:1 gear tracking, and the backlash may be checked as follows: A large range dial indicator gauge which is sensitive to 0.0001 in. is mounted on the base of the goniometer and its contact point placed against the bottom of the receiving slit assembly when the gauge is in about the middle of its range. When the goniometer arm is driven at a slow speed ($\frac{1}{8}$° per min.) the motion of the arm can be seen on the gauge and erratic movements readily observed. The goniometer arm is driven down scale to any selected gauge reading and the corresponding 0.01° dial reading noted. Scanning should be continued about 0.1° beyond this point, the scanning direction reversed and the goniometer driven to the same gauge reading where another reading of the 0.01° dial is made. The difference between the two dial readings is a measure of the backlash. To check the uniformity and backlash of the 2:1 tracking, the contact point of the dial indicator gauge is placed against a rigid bar about 6 in. long mounted on the specimen post. These checks should be repeated at several positions in the scanning range of the goniometer.

To obtain reproducible readings it is essential that the reference edge of the slits (top) be flat and parallel to the median line of the slit opening. If the two sides of the slit opening are not parallel, various aberrations may be introduced. If two slits have the same nominal height in the X-direction but do not in fact have *exactly* the same opening, the intensity and resolution will vary accordingly. It is usually satisfactory to measure the effects of the differences for some standard conditions so that the proper corrections can be made if required. Other consequences of imperfect slit construction were pointed out in the section on angular calibration.

There are several points to check in the recorder system. The angle-marking pen records 0.5°(2θ) increments on the chart. If necessary the microswitch on the 0.01° dial must be adjusted so that it operates exactly at the 0.00° and 0.50° positions. The chart pen on the recorder must ink a line parallel to the chart grid when the chart is not in motion. This can be checked by turning the chart drive motor off and manually moving the pen by means of the knurled drive inside the recorder. The directions for calibrating and checking the electronic circuits and detector are beyond the scope of this paper.

X-ray Results

The recordings in Fig. 9 show the type of results that may be obtained with a properly aligned diffractometer. Quartz was used as an example

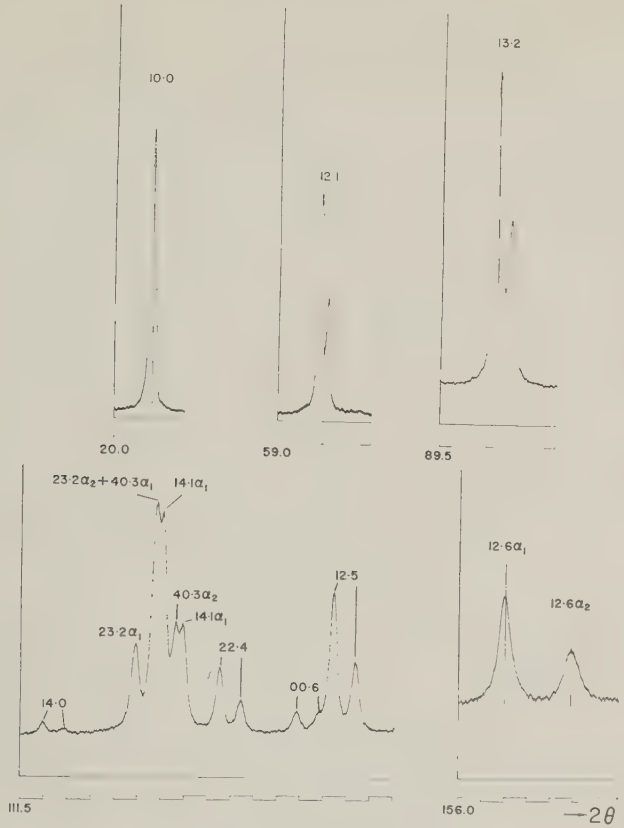

FIG. 9. Recordings of portion of quartz powder pattern. Rotating specimen, $<20\mu$ crystallites, CuK, 40 kVp, 20 ma, 0.0007 in. Ni filter, $\psi=6°$, scintillation counter with pulse amplitude discrimination, 2 sets of Soller slits each with $\delta=4.5°$, scanning speed $1/8°(2\theta)$ per min., scale factor 32 (full scale = 1600 counts per sec.) for all recordings except $12\cdot1$ where scale factor was 16

$hk\cdot l$	10·0	12·1	13·2	12·5	12·6
Ang. Ap. α (deg.)	1	1	4	4	4
Rec. Slit (in.)	0.003	0.003	0.012	0.012	0.012
Time Constant (sec.)	4	4	8	8	8
P-B (counts/sec.)	1022	389	1116	483	360
(P-B)/B	45	35	8	3	1
Backg. meas. at (°2θ)	19.0	58.5	92.0	119.5	156.0
Width (°2θ, (P-B)/2)	0.18	0.12	0.20	0.20	0.31_5

because it is ideally suited for such tests and is widely available. A powder with crystallites $<20\mu$ was prepared from a large Brazilian crystal of oscillator-plate quality. The powder was mixed with a small

amount of binder (1 vol. collodion diluted with 10 vol. amyl acetate), packed in a flat holder for a rotating specimen, and after drying, the top surface was scraped flush with the reference rim. The experimental conditions are described in the caption of Fig. 9.

The x-ray tube had been used about 5000 hours, and it is likely that somewhat higher intensities would have been obtained with a newer tube. The intensity data were obtained from manual settings on the $K\alpha_1$ peaks and the backgrounds were read at the angles indicated. The intensities with Geiger counters or proportional counters would be about one-half the values obtained with the scintillation counter because of their lower quantum counting efficiencies (Taylor and Parrish, 1955). The backgrounds would be higher if pulse-amplitude discrimination had not been used (Parrish and Kohler, 1956). In the present case the window of the pulse-height analyzer was set symmetrically around the average pulse amplitude for CuKα to detect about 93% of CuKα.

In the description of the results given below, it should be noted that if a recording which matches only one of those shown in Fig. 9 is obtained, this is not sufficient evidence that the instrument is properly aligned. Similar results must be obtained for several reflections over the entire scanning range to be certain the alignment is correct. The complex of lines appearing in the region 111° to 119° (2θ) serve as a good measure of the overall performance. The small intensity of the $14\cdot0\alpha_1$ line is clearly visible above background although the peak-to-background ratio is only 0.3. The three lines $23\cdot2$, $14\cdot1$ and $40\cdot3$ each with $K\alpha_1$–$K\alpha_2$ components are resolved except for $23\cdot2\alpha_2$ and $40\cdot3\alpha_1$ where the separation is only 0.034° (2θ). The $00\cdot6\alpha_2$ line is partially resolved from the base of $12\cdot5\alpha_1$.

The line profiles of well-crystallized specimens obtained with even a properly aligned diffractometer are not symmetrical. They are asymmetrically broadened and shifted by various aberrations inherent in the geometry of the instrument. Some of these, such as specimen surface displacement, specimen transparency, receiving slit height, and 2:1 missetting have been mentioned above. The effects of a few of the other aberrations will be briefly described so that the nature of the profiles may be better understood. Practically all the aberrations have been analyzed and experimentally confirmed (Wilson, 1950; Parrish and Wilson, 1959; Parrish, 1959b).

The flat specimen aberration is caused by the use of a flat specimen rather than one whose curvature varies continuously during scanning to match the focussing circle. It causes a shift in the center-of-gravity of the reflection to smaller angles (the peak also shifts by an amount which is smaller but much more difficult to calculate) by an amount

$$\Delta(^\circ 2\theta)_{f.s.} = (\alpha^2 \cot \theta)/343.7748.$$

This error is zero at 180° 2θ and increases with decreasing 2θ-angle. Some typical values of the shift are 0.008° ($\alpha = 4°$, $2\theta = 160°$), 0.046° ($\alpha = 4°$, $2\theta = 90°$), 0.003° ($\alpha = 1°$, $2\theta = 90°$), 0.016° ($\alpha = 1°$, $2\theta = 20°$). The reason for the asymmetric broadening and the greater shift of the center-of-gravity than of the peak is that the high-2θ side of the reflection remains nearly fixed but the low 2θ-side, particularly the lower part, is stretched toward smaller 2θ-angles.

The axial ("vertical") divergence (Pike, 1957) also asymmetrically broadens and shifts the line, toward lower angles below 100°2θ and toward higher angles above 100°2θ. The shift of the center-of-gravity is given by the expression

$$\Delta(^\circ 2\theta)_{a.d.} = 0.01125 \cot 2\theta + 0.00188 \csc 2\theta$$

for two sets of Soller slits and the instrumental parameters of the Norelco goniometer. Some typical values of the shift are: −0.074° (10°2θ), −0.012° (45°2θ), +0.011° (140°2θ), and +0.035° (165°2θ).

The asymmetry and shift may be reduced by decreasing the apertures α and δ but only at the expense of a large loss of intensity. All the aberrations "fold" (convolute) with each other and require rather elaborate mathematical unfolding procedures to determine each of the separate effects. However, the centers-of-gravity of the aberrations are additive. For example, the shift of the center-of-gravity of the 10·0 line is: flat specimen (−0.016°) + transparency (−0.008°) + axial divergence (−0.036°) = 0.060°2θ. The asymmetry of this line is evident particularly in the lower portion of the low-2θ side of the profile. This additive property and the fact that the aberrations are not known in terms of the shift of the peak are the principle reasons for using the center-of-gravity rather than the peak angle in high precision measurements (Ladell, Parrish and Taylor, 1957, 1959).

The width of the partially resolved CuKα_1 lines in the front-reflection region using an aperture $\alpha = 1°$ and 0.003 in. receiving slit varies from 0.10° to 0.12° (2θ) measured at one-half peak height above background. The width depends on the degree of overlapping of the Kα-doublet lines and the instrumental aberrations, and is smaller at the larger reflection angles. When the aperture α is increased from 1° to 4° and the receiving slit from 0.003 in. to 0.012 in. to obtain greater intensity in the back-reflection region, the line breadth of the 13·2 reflection is doubled, the peak intensity increased by a factor of 12, and the peak-to-background ratio decreased from 9·5 to 7·8. Although the axial divergence effect is small in this region, the flat specimen aberration is large and the line is asymmetrically broadened. The line symmetry may be restored by

using a smaller aperture α, but this would cause a reduction in the intensity.

In the far back-reflection region (above about 140°), the contributions to the line breadth and position of all the aberrations except axial divergence becomes less important. However, the dispersion increases rapidly in this region and the lines become broader because the primary x-rays are not strictly monochromatic. In fact, the intensity distributions of the x-ray spectral lines are generally asymmetric, and the degree of asymmetry and the breadth vary among the lines from the same target as well as from one target element to another (Bearden and Shaw, 1935). The Lorentz and polarization factors and the dispersion increase so rapidly in this region that they cause a distortion of the line profile and contribute significantly to the breadth and asymmetry. These effects can be seen in Fig. 9 in which the 12·6 CuKα_1 line is $0.31_5°$ wide and the 12·6 CuKα_2 line is $0.36_2°$ wide (Ladell *et al.*, 1959).

References

Bearden, J. A. and Shaw, C. H. (1935), Shapes and wavelengths of K series lines of elements Ti 22 to Ge 32: *Phys. Rev.*, **48,** 18–30.

Chayes, F. and Mackenzie, W. S. (1957), Experimental error in determining certain peak locations and distances between peaks in x-ray diffractometer patterns: *Am. Mineral.*, **42,** 534–547.

de Wolff, P. M., Taylor, J. M. and Parrish, W. (1959), Experimental study of effect of crystallite size statistics on x-ray diffractometer intensities: *J. Appl. Phys.*, **30,** 63–69.

Hamacher, E. A. and Lowitzsch, K. (1956), The "Norelco" counting-rate computer: *Philips Tech. Rev.*, **17,** 249–254.

Haven, C. E. and Strang, A. G. (1953), Assembled polygon for the calibration of angle blocks: *J. Research Natl. Bur. Standards*, **50,** 45–50.

Klug, H. P. and Alexander, L. E. (1954), X-ray Diffraction Procedures: John Wiley & Sons, Inc., New York.

Kohler, T. R. and Parrish, W. (1956), Conversion of quantum counting rate to Roentgens: *Rev. Sci. Instr.*, **27,** 705–706.

Ladell, J., Parrish, W. and Taylor, J. (1957), Measurement and use of the center-of-gravity of line profiles in x-ray powder diffractometry: *Am. Cryst. Assoc.*, Pittsburgh meeting, Nov. 8, 1957, Paper No. 46; Parrish, W. and Taylor, J. (1957), The precision diffractometer measurement of lattice parameters: *Acta Cryst.*, **10,** 741.

Ladell, J , Parrish, W. and Taylor, J. (1959), Center-of-gravity method of precision lattice parameter determination: *Acta Cryst.*, **12,** 253–254; Interpretation of diffractometer line profiles: *ibid.*, **12** (in press); Dispersion, Lorentz and polarization effects in the centroid method of precision lattice parameter determination: *ibid.*, **12,** (in press).

Mack, M. and Spielberg, N. (1958), Statistical factors in x-ray intensity measurements: *Spectrochim. Acta*, **12,** 169–178.

Neff, Hans (1956), Über die präzisionsbestimmung von gitterkonstanten mit dem zählrohr-interferenz-goniometer: *Zeit. f. ang. Phys.*, **10,** 505–507.

Parrish, W. (1956), X-ray intensity measurements with counter tubes: *Philips Tech. Rev.*, **17,** 206–221.

PARRISH, W. (1958), Optimum *x*-ray tube focal spot geometry for powder diffractometry: *Am. Cryst. Assoc.*, Milwaukee meeting, June 24, Paper No. G-8, p. 35.

PARRISH, W. (1959a), Precision measurement of lattice parameters of polycrystalline specimens: (I.U.Cr. Apparatus Commission Report) *Acta Cryst.* (in preparation).

PARRISH, W. (1959b), Advances in *x*-ray diffractometry of clay minerals: *Proc. Seventh Natl. Conf. Clays and Clay Minerals*, Washington, 1958, Pergamon Press, Inc., New York. In press.

PARRISH, W. AND HAMACHER, E. A. (1952), Geiger counter *x*-ray spectrometer: instrumentation and techniques: *Trans. Inst. and Meas. Conf., Stockholm*, 95–105.

PARRISH, W., HAMACHER, E. A. AND LOWITZSCH, K. (1954), The "Norelco" diffractometer: *Philips Tech. Rev.*, **16,** 123–133.

PARRISH, W. AND KOHLER, T. R. (1956), Use of counter tubes in *x*-ray analysis: *Rev. Sci. Instr.*, **27,** 795–808.

PARRISH, W. AND MACK, M. (1959), *X*-ray reflection angle tables: (In preparation.)

PARRISH, W. AND WILSON, A. J. C. (1959), Precision measurement of lattice parameters of polycrystalline specimens, Int. Tables for *X*-Ray Cryst.: vol. 2 (216–234).

PIKE, E. R. (1957), Counter diffractometer—The effect of vertical divergence on the displacement and breadth of power diffraction lines: *J. Sci. Instr.*, **34,** 355–363; *ibid.*, **36,** 52–53.

SWANSON, H. E., GILFRICH, N. T. AND COOK, M. I. (1957), Standard *x*-ray diffraction powder patterns: Natl. Bur. Standards Circular 539.

TAYLERSON, C. O. (1947), Testing circular division by means of precision polygons: *The Machinist* (London), **71,** 1821–1824.

TAYLOR, J. AND PARRISH, W. (1955), Absorption and counting efficiency data for *x*-ray detectors: *Rev. Sci. Instr.*, **26,** 367–373, *ibid.*, **27,** 108.

TOURNARIE, M. (1954), Reglage absolu d'un goniometre a compteur de Geiger-Müller: *J. Phys. et Radium*, **15,** Supp. No. 1, 11A–15A.

WILSON, A. J. C. (1950), Geiger counter *x*-ray spectrometer-influence of size and absorption coefficient of specimen on position and shape of powder diffraction maxima: *J. Sci. Instr.*, **27,** 321–325.

WILSON, A. J. C. (1954), A theoretical re-investigation of geometrical factors affecting line profiles in counter diffractometry, distributed at 3rd I.U.Cr., Paris; abstract: PARRISH, W. AND WILSON, A. J. C. (1954), *Acta Cryst.*, **7,** 622.

Manuscript received November 11, 1958.

SYNTHETIC MONTMORILLONOIDS WITH VARIABLE EXCHANGE CAPACITY*

MITSUE KOIZUMI AND RUSTUM ROY, *The Pennsylvania State University, University Park, Pennsylvania.*

ABSTRACT

An attempt has been made to resolve the questions: 1) Do montmorillonoids exist with widely varying exchange capacities: 2) Which of these phases are stable under given conditions of pressure and temperature?

Two series of gels have been prepared in the saponite and beidellite regions respectively, and reacted in sealed inert systems over the range 200°–850° C. at 1000 atmospheres water pressure. The effects of temperature, time, open or closed systems, etc. have geen evaluated. In a time period which is demonstrated to be considerably longer than necessary for the completion of crystallization (as shown by a time-crystallinity study) beidellites can be synthesized with exchange capacities varying from 1/2N to over 2N (where N represents the "ideal" exchange capacity of about 90 m.eq. of the formula $Na_{.33}Al_2Al_{.33}Si_{3.67}O_{10}OH)_2$. These phases are homogeneous and all expand to 17 Å with glycol, the 2N exchange capacity members being the best crystallized. At 300° C. these phases persist for weeks at 1000 atm. and are probably stable. With increasing temperatures only the "N" composition remains single phase up to 425° C.

The range of saponites that can be formed is much narrower. Only the N and 2N members can be prepared as single phases with a stability maximum of about 550° C. Above this temperature a new montmorillonoid (probably a Na-hectorite) is formed and this phase is stable up to 850° C. at 1000 atmospheres.

Cation exchange capacity measurements made by *x*-ray fluorescence on these Mn-saturated clays shows good correlation with expected values on a relative scale. A wide latitude in compositions for *stable* montmorillonoid formation is thus established especially in the beidellite family. The properties of both low c.e.c. and high c.e.c. members should be of interest.

Two other new phases corresponding to a pure magnesian stilpnomelane and a 14 Å "aluminum chlorite" are encountered in this study.

INTRODUCTION

A matter of considerable interest to clay mineralogists can be stated in the questions: Do montmorillonites have a fixed or ideal cation exchange capacity? If so, are the reported variations due to admixture with impurities or faulty measurements? If a real latitude exists in the cation exchange capacity, what are the maximum and minimum limits to the c.e.c. value? Under what conditions do these different montmorillonites form and are they stable?

An analysis of the literature values for cation exchange capacity will show a rather definite peak for values near 90 and a high fraction of values in the range 110–140 m.eq./100 gm. Other values reported range from 40 to over 150 m.eq./100 gm. and it is extremely difficult to obtain

* Contribution No. 58–73, College of Mineral Industries, The Pennsylvania State University, University Park, Pennsylvania.

an answer to the questions listed above by a study of whatever sample one obtains from nature. In fact it might be thought, that one of the best ways to solve this problem would be to synthesize various montmorillonites and measure their exchange capacity. The obvious difficulty here as in the natural samples of course is the problem of how to be certain of mineral homogeneity. If the value is low perhaps some low-exchange material is admixed, if high perhaps some high-capacity material, such as an amorphous gel, is included in the sample. Indeed this latter problem is virtually insuperable since the proof of the absence of "gel" in a natural montmorillonite sample is essentially impossible.

It may be argued that, if most montmorillonites showed the same fixed value for the c.e.c., this may be considered an "ideal" composition. This is partly true for the 90 c.e.c. value but definite exceptions are common.

The synthetic approach on a systematic basis was tried by Roy and Roy (1952, 1955) in the system MgO-Al_2O_3-SiO_2-H_2O. The range of composition which could be prepared as single phase montmorillonoids was determined. While this did not give unequivocal evidence of the variability of c.e.c., it did, in effect, show that since montmorillonoids could be prepared over such a wide range of composition it was to be expected that both very low and very high exchange capacities should be possible. In Sand, Roy and Osborn's study (1953, 1957) likewise, an unexpectedly wide range of compositions appeared to crystallize in a single montmorillonoid structure. More specific efforts to check this question included Roy and Sand's (1956) measurement of the c.e.c. value of an ideal beidellite; the fact that the c.e.c. was close to that calculated from the total composition lent additional weight to the idea that variability was real. Mumpton and Roy (1956) studied the differences in thermal stability of the compositionally different montmorillonites and showed a continuous variation. The most direct attack on this very problem was that of Karsulin and Stubican (1954) who in their work claimed to show that they had synthesized montmorillonoids with varying compositions and they measured their exchange capacities and showed them to vary also. In their comprehensive study many other measurements, such as the ratio of octahedral to tetrahedral aluminum, were also made to confirm the variation. However, it appeared to us that insufficient emphasis had been placed on verifying the central argument that the phases were both homogeneous and completely crystalline. Moreover, the variations did not follow a simple crystal chemical substitutional scheme.

The work undertaken in the present study was an attempt to demonstrate unequivocally that single phase beidellites and saponites can be prepared with variable exchange capacities, to measure the properties

of these phases including the dehydration-rehydration phenomena, exchange capacities, thermal stability and x-ray properties, and to attempt thereby to derive the limits of solid solution in the montmorillonoid structure. The beidellite family was chosen since in this only tetrahedral substitution of Al for Si is involved and only this changes as one changes the exchange capacity. In the saponite family the desired substitution is likewise the introduction of tetrahedral aluminum, although here one cannot be certain that some alumina does not reside in the octahedral layer.

Experimental

Starting Materials

Mixtures to be used as starting materials in this investigation were prepared as gels. The mixtures were made by mixing calculated amounts of "Ludox" silica sol,* a solution of the nitrates of Al and Mg as required, a NaOH solution of known strength, adjusting the pH to slightly acidic with HNO_3, and evaporating to dryness. They were then fired to about 500° C. until the nitrates were completely decomposed. The products were ground to fine powders.

Techniques of Hydrothermal Synthesis

In every run, the materials were contained in small sealed gold tubes to prevent selective leaching. A small amount of distilled water was added before the tube was sealed. The weight of each sealed tube containing the specimen and water was measured before and after the run to detect any leakage. "Large" batches (0.5 gm.) were made using wider gold tubing in order to prepare enough material for the base exchange capacity measurements. Typical examples of actual weights of the above materials including gold tubing, specimen and water are shown below, especially to convey an idea of the ratio of sample to excess water:

	Small Tubes	*Large Tubes*
Tubing	226.7 mg.	3899.1 mg.
Tubing plus sample	233.9	4419.7
Tubing plus sample and water	247.3	4549.9
Total weight after sealing, before run	236.0	4286.4
Total weight after sealing, after run	236.2	4286.9

The usual hydrothermal equipment was used throughout the investigation. The type of pressure vessel used was the test-tube or cold seal bomb,

* "Ludox" silica sol is an ammonium-stabilized sol with particles of about 150 Å in size. Analysis shows 0.262% NH_3 and 0.35% Na_2O. This material was generously supplied to us by R. K. Iler of the E. I. duPont de Nemours and Company.

(Roy and Tuttle, 1956) made of Stellite-25 alloy. The pump used for high pressure was an air-operated multiplying-piston type pump.

Up to four gold tubes were placed side by side in the pressure vessel. Temperatures were automatically regulated and measured with chromel-alumel thermocouples. The charge was quenched by removing the furnace from the bomb and immediately placing the bomb in cold water. Upon removal from the pressure vessels, the samples were dried at room temperature in air, and were then powdered, mounted on glass slides with water, and kept at room temperature in air over night.

The products were identified in every case by x-ray diffraction techniques with a wide-range Norelco diffractometer.

The limits of accuracy of the data were as follows: Temperature: $\pm 5°$ C. Pressure: $\pm 5\%$. Spacing: 0.05° 2θ fast scan, 0.01° 2θ slow scan.

Cation Exchange Capacity Measurements

A rapid instrumental method for determining the cation exchange capacity of small quantities of synthetic clays was developed. A procedure similar to that of Bower and Truog (1940) was used to saturate a clay with Mn^{2+} ions. The manganese content was then measured directly by x-ray fluorescence methods.

A one-half gram specimen of each synthetic montmorillonoid was placed in a 15-ml. centrifuge tube, ten milliliters of a 1N $MnCl_2$ solution, acidified to pH = 4–5 with HCl, were added, and then the material was shaken vigorously for a few minutes to obtain a good dispersion. After being shaken automatically for 30 minutes, the material was centrifuged and the supernatant liquid was discarded. This treatment was repeated five times. The residue was washed with water using the shaking and centrifuging procedure four times. In order to remove the excess of $MnCl_2$ completely, the specimen was then washed with water by a dialysis method until the washings no longer gave a test for chloride. One week of washing was usually sufficient. The samples were dried at 110° C.

Manganese is a particularly good element for use in fluorescent x-ray spectroscopy, with LiF as the analyzing crystal, since manganese can be detected in very low concentrations.

A G.E. XRD-5 instrument was used in this x-ray fluorescence work. The intensity of the MnKα peak at 62.95° 2θ was measured. The background count was found to be negligible, compared to the intensity of the MnKα peaks for the exchange clays.

Standard samples were made by adding weighed amounts of C.P. grade $MnCO_3$ to clay blanks with the same absorption as the clays to be studied. This was followed by thorough mechanical mixing. The five

standard mixtures of clay samples with 160, 120, 80, 40 and 20 m.eq./100 gms. were prepared in this way. A calibration curve, which was quite close to a straight line, was obtained and extrapolated to 0 c.p.s. at 0% Mn. For each set of measurements made at intervals of several weeks it was found best to re-run the calibration curve and thus to allow for changes in instrumental settings.

The base exchange capacity determination using the *x*-ray fluorescence method was made on several natural standard clay minerals, the exchange capacity values of which were "known." The three specimens included a purified hectorite from National Lead Company, kaolinite (Lustra clay, RS-286) and montmorillonite clay (FCB) from Filtrol Corporation. They were treated in an indentical manner.

The cation exchange capacity values for those specimens involving the "known" values and the values determined from *x*-ray fluorescence method are listed below:

Specimen	*Base-Exchange Capacity*	
	"Known" Value	*Value Determined*
Purified Hectorite	82.7 m.eq./100 gm. (105° C.)	75 m.eq. Mn^{2+}/100 gm.
Kaolinite (Lustra clay, RS-286)	—	2
Montmorillonite clay (FCB)	133 m.eq./100 gm.	116

These results show that the method used gave slightly lower values of base exchange capacity than those obtained by others. One of the possible reasons for these smaller values may be the week-long washing with dialysis. Some leaching of Mn^{2+} may occur.

However, since the relative values appeared to agree within 2% the method used appears quite satisfactory. Increasing our figures by 10% brings them into line with the numerical values obtained by other methods.

Results

Composition of Starting Materials

Eight gels were prepared as starting materials in this investigation. The compositions and the theoretical formulae of the expected types of montmorillonoids are listed in Table I.

Check on Crystallization Rate

Experiments to prove whether or not the entire sample was crystalline were carried out by determining the length of time it takes to achieve crystallinity in the gels used in this investigation.

Several runs were made on three of the beidellite compositions (0.5N,

TABLE I. SYNTHETIC STARTING MIXTURES

Mixture No.	Composition (Mole ratios)				Calculated theoretical formulae
			Beidellite Compositions		
		Al_2O_3 :	SiO_2 :	Na_2O	
B-0.5N		1.09	3.83	0.09	$Al_2(Al_{0.17}Si_{3.83})O_{10}(OH)_2Na_{0.17}$
B-1N		1.17	3.67	0.17	$Al_2(Al_{0.33}Si_{3.67})O_{10}(OH)_2Na_{0.33}$
B-2N		1.34	3.33	0.34	$Al_2(Al_{0.67}Si_{3.33})O_{10}(OH)_2Na_{0.67}$
B-4N		1.67	2.67	0.67	$Al_2(Al_{1.33}Si_{2.67})O_{10}(OH)_2Na_{1.33}$
			Saponite Compositions		
	MgO :	Al_2O_3 :	SiO_2 :	Na_2O	
S-0.5N	3	0.09	3.83	0.09	$Mg_3(Al_{0.17}Si_{3.83})O_{10}(OH)_2Na_{0.17}$
S-1N	3	0.17	3.67	0.17	$Mg_3(Al_{0.33}Si_{3.67})O_{10}(OH)_2Na_{0.33}$
S-2N	3	0.34	3.33	0.34	$Mg_3(Al_{0.67}Si_{3.33})O_{10}(OH)_2Na_{0.67}$
S-4N	3	0.67	2.67	0.67	$Mg_3(Al_{1.33}Si_{2.67})O_{10}(OH)_2Na_{1.33}$

N and 2N) for various run durations, up to 14 days, at 300° C. and 15,000 psi to determine the effects of run duration on the formation of crystalline phases.

In the one-day run, the 0.5N gel did not crystallize and the other two gels yielded a single phase of very poorly crystallized montmorillonoid. The three-day run gave a single phase montmorillonoid from all three gels, although the phase obtained from the 0.5N gel was still poorly crystallized. After 7 days, a well crystallized montmorillonoid, expanding with glycol to 17–18 Å, was formed from all the compositions. Longer runs of up to two weeks seem to have no further effect.

These results, which are illustrated in Fig. 1, show that in 5- to 7-day runs complete crystallization of such gels to a montmorillonoid phase is achieved. There is considerable crystallization even in a short run of 1–3 days but at this time level it is possible to assume that some material may still be left amorphous. What has been established is the fact that it is not possible to assume that any amorphous phase (with composition near those used) will remain amorphous under the conditions generally used in this investigation.

BEIDELLITE COMPOSITION MONTMORILLONOIDS

Phase equilibrium studies

About 40 runs have been made on the four beidellite composition gels in the temperature range of 260-770° C. at 15,000 psi. Critical runs are summarized in Table II and the results shown in the *t-x* diagram of Fig. 2.

From the three beidellite gels including the 0.5N, N, and 2N composi-

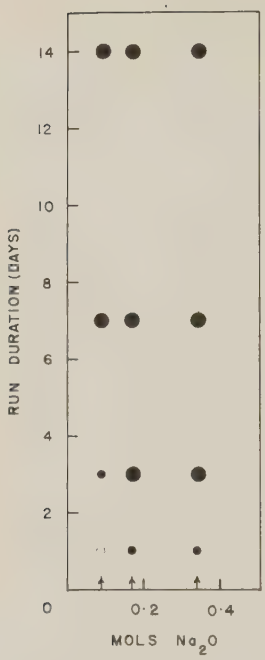

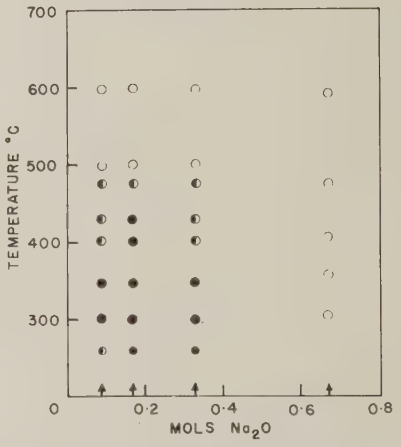

FIG. 1 (*left*). Crystallization rate of gels of beidellite composition at 300° C., 15,000 psi. Open circle: no crystallization, small solid circle: poorly crystallized montmorillonoid, large solid circle: well crystallized montmorillonoid.

FIG. 2 (*right*). t-x diagram at 15,000 psi for gels of beidellite compositions. Solid circle: montmorillonoid, open circle: other phases (see Table II), small circle: very poorly crystallized phase.

tions, in the temperature range of 300–350° C. (one-week runs), a single well crystallized montmorillonoid phase was formed. The (001) spacings of the products were 11–13 Å and they expanded with glycol to 17–18 Å. The 4N composition gel did not yield any expanding phase but paragonite alone or paragonite plus analcite was formed. The most favorable conditions for the growth of well crystallized beidellites with variable charge have been therefore fixed as at 300–350° C. and 15,000 psi for 7 days.

At 260° C., single phase montmorillonoids were obtained only from the two gels of N and 2N composition, for the 0.5N beidellite composition gel yielded a kaolinite (or dickite) phase plus a montmorillonoid phase. These expanding phases were not well crystallized.

In the higher temperature range near 400° C. pyrophyllite, mica, or a complex mixed-layer phase of montmorillonoid and mica appeared in

TABLE II. REPRESENTATIVE RUNS FOR THE BEIDELLITE COMPOSITION GELS AT 15,000 PSI

Run No.	Temp. (° C.)	Duration (days)	Products*
			Composition $1.09Al_2O_3:3.83SiO_2:0.09Na_2O$
1,241	262	11	Poorly crystallized mont+kaol (or dickite)
1,341	302	7	Mont (12.2–18.0)
1,351	346	6	Mont (11.1–17.7)+1 pyr (?)
1,301	401	5	Mont+pyr
1,421	430	5	ML (mont, mica)+pyr
1,491	474	4	Al-chlor.+hyd+ML (mont, mica)
1,391	498	5	Al-chor+hyd+pyr+qtz
1,291	598	3	Al-chlor+hyd+qtz
1,331	770	3	Qtz+Ab+mull
			Composition $1.17Al_2O_3:3.67SiO_2:0.17Na_2O$
1,242	262	11	Poorly crystallized mont (12.8–18.0)
1,342	302	7	Mont (12.8–17.7)
1,352	346	6	Mont (12.3–17.3)
1,301	401	5	Mont (12.6–17.7)
1,421	430	5	Mont (12.7–17.7)
1,491	474	4	ML (mont, mica)+hyd
1,391	498	5	Al-chlor+hyd+qtz
1,331	770	3	Atz+Ab+mull
			Composition $1.34Al_2O_3:3.33SiO_2:0.34Na_2O$
1,243	262	11	Mont (12.8–18.0)
1,343	302	7	Mont (12.6–17.6)
1,353	346	6	Mont (12.6–17.3)
1,303	401	5	ML (mont, mica)+mica
1,423	430	5	ML (mont, mica)+mica
1,493	474	4	Hyd+ML (mont, mica)
1,393	498	5	Al-chlor+hyd+mica
1,293	598	3	Al-chlor+hyd+qtz
1,333	770	3	Ab+mull
			Composition $1.67Al_2O_3:2.67SiO_2:0.67Na_2O$
1,514	303	7	Mica+anal
1,484	357	6	Mica
1,524	406	5	Mica
1,494	474	4	Mica+anal+1 cor
1,504	593	3	Ab+cor+neph

* Abbreviations used: mont = montmorillonoid, kaol = kaolinite, pyr = pyrophyllite, ML = mixed layer, Al-chlor = aluminum-chlorite, hyd = hydralsite, qtz = quartz, Ab = albite, mull = mullite, cor = corundum, anal = analcite, neph = nepheline, Mont (12.2–18.0) = (001) spacing of montmorillonoid expands from 12.1 Å to 18.0 Å with glycol, l = a little, minor.

addition to a montmorillonoid phase. However, the ideal beidellite composition gel (N) still gave a single phase montmorillonoid up to 430° C. At 475° C. only a small amount of the expanding phase persisted. The sodium-poor (0.5N) gel yielded an unexpected chlorite-like phase, with a 14 Å (001) spacing, plus hydralsite besides the mixed-layer phase. Hydralsite is a clay phase found in the study of the system Al_2O-SiO_2-H_2O by Roy and Osborn (1954). The chlorite-like phase will be described later in more detail. The phase assemblage in the products from the N and 2N gels was a mixed-layer phase plus hydralsite. In the above temperature range (400°–500° C.), the sodium-rich gel (4N) gave paragonite plus analcite. The assemblage shown by Sand, Roy and Osborn (1957) consists of these two phases plus alumina; however, no boehmite was found at low temperatures but corundum was found at 500° C.

At 500° C. no expanding phases persisted. The chlorite-like mineral and hydralsite were dominant in all the compositions except the sodium-richest one.

The phase assemblage of chlorite-like mineral and hydralsite was obtained even at 600° C., with quartz appearing as an additional phase at this temperature. From the 4N gel, nepheline plus albite and corundum were obtained.

The runs at 770° C. were made to check the chemical composition of the four beidellite gels. Both the sodium poor gel ($0.09Na_2O$) and the ideal beidellite composition gel ($0.17Na_2O$) gave the three phase assemblage of quartz, albite and mullite, while the gel with the $0.34Na_2O$ yielded albite plus mullite, and the sodium-richest gel gave nepheline, albite plus corundum.

The above phase equilibrium studies suggest that well crystallized montmorillonoids with variable charge, corresponding to $0.09Na_2O$ to $0.33Na_2O$, can be made from the beidellite composition gels and that the optimum condition for obtaining them are the combination of 300° C., 15,000 psi and one week. They also show unequivocally that there is a maximum of stability in the "N" member and in this sense it is an "ideal" composition.

Cation exchange capacity

The cation exchange determinations made on the synthetic montmorillonoids of beidellite compositions with variable charge and with Na_2O from 0.09 to 0.34 are listed in Table III and shown graphically in Fig. 3.

A linear relation with somewhat higher values say 45, 90 and 135 m.eq. would have presented the idealized picture of inter-layer composition

TABLE III. BASE-EXCHANGE CAPACITIES OF THE SYNTHETIC BEIDELLITE COMPOSITION MONTMORILLONOIDS

Composition (Na_2O Mol)	0.5N 0.09	1N 0.17	2N 0.34
Base-exchange capacity	33	76	110
(m.eq. Mn^{2+}/100 gm. of clay)	33	76	106
average	33	76	108
+10% (see p. 792)	36	84	119

varying with total charge. There are several possible reasons for the deviation of the curve in Fig. 3 from the ideal.

1. Since the values are all low and that for the 2N composition the lowest, it would suggest that not all the Na^+ is entering the inter-layer position. We know only that the total composition within a sealed tube is fixed. It is more than possible that:
   a. Some Na^+ is entering the octahedral sites. (It will be seen that this is probably true in the saponite case.)
   b. Some Na^+ remains in the "solution" or vapor phase.
2. The low values may also be due to admixture of the montmorillonoid with some material such as pyrophyllite, kaolinite or paragonite which has little or no exchange capacity and which escaped *x*-ray detection though specifically sought.

The most serious source of error is, in our view, that of Fig. 1*b* the

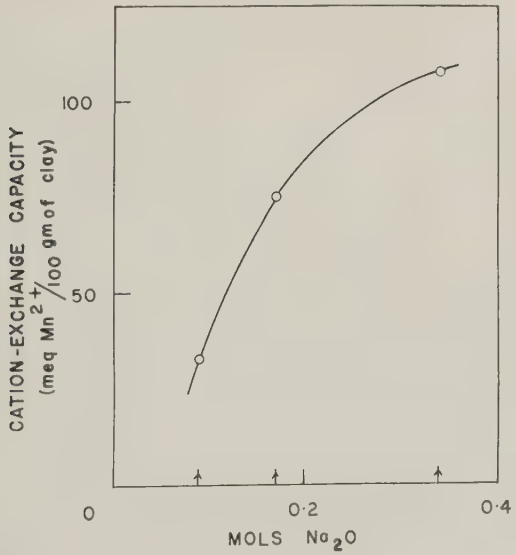

FIG. 3. Variation of cation-exchange capacity with composition in the beidellite series of montmorilllonoids.

amount of Na^+ dissolved in the liquid or vapor phase. The problem is an extremely difficult one from the experimental point of view. When a phase such as a montmorillonoid is synthesized under "H_2O" pressure at say 300 or 400° C., the composition of the fluid phase can only be assumed to be that of pure water as a very rough approximation. In fact there is at every temperature and pressure a conode joining the composition of the solid phase and the fluid phase passing through the total composition of solid+water in the system. It is clear therefore that the ratio of solid:water is a critical one in evaluating the change of composition caused by "trading." In Morey-type vessels or in an unsealed envelope in a test-tube bomb the ratio of water:solid (by weight) is frequently of the order of 10:1 or 100:1. Our main direction of effort in keeping the final composition close to the original was by reducing the volume of the water in relation to the solid. Runs were made with low water:solid ratios of 2:1 and much of the actual large sample work was done with a ratio near 1:4 (see page 790). There was a very practical reason why the ratio could not be lowered much further—the gels simply do not crystallize under such conditions, or require prohibitively long times to give decent crystallinity. This small amount of water could, however, alter the composition measurably if the solubility under these conditions were appreciable.

If the "solubility" of the gel were 10%, 0.025 gm. of a 1-gm. sample would be in solution. Of course the composition of the sample would only be altered by the difference in the Na:Al:Si ratio in the fluid and solid phases$\times$0.025. There is at present no way whatsoever to estimate either the total solubility or the real composition of the solution in equilibrium with the solid. We do know that it is certain that the solution will be rich in soda compared to our composition, but not extremely so, since in this case the alumina and silica will both enter the solution in very large amounts. It is also known that the composition of the fluid phase will vary markedly not only with pressure and temperature but with the solid phase assemblage with which it is in equilibrium. This entire area of the composition of the fluid phase in an alkali-containing system is a major gap in hydrothermal experimentation but one that will only be filled by some years of laborious analytical work. In this study the effort to minimize the extent of solution was considered a satisfactory limitation of the error introduced.

In an attempt to check the influence on hydration characteristics of direct synthesis of a Ca^{2+} beidellite as compared to a synthesized Na^+ beidellite in which Na^+ has been replaced by Ca^{2+} by washing with $CaCl_2$, a "N" Ca-beidellite was synthesized directly from the gels. The effect on hydration characteristics is reported by Gillery (1958). Its

c.e.c. value when measured was found to be only 52 m.eq./100 gm. This low value we ascribe to superior crystallinity and the inability to remove all Ca^{2+} by Mn^{2+} washing.

Saponite Composition Montmorillonoids

Phase equilibrium studies

Runs have been made on the four saponite composition gels in the temperature range of 260–800° C. at 15,000 psi. Representative runs are listed in Table IV, and the results are illustrated in the *t-x* diagrams of Fig. 4.

From the saponite composition gels, a single phase montmorillonoid expanding to 17–18 Å with glycol was obtained only from the ideal saponite composition gel and the gel with 0.33 Na_2O in the temperature range between 260 and 450° C. In this temperature range, the sodium-rich gel (0.67 Na_2O) yielded a complex mixed-layer including an ex-

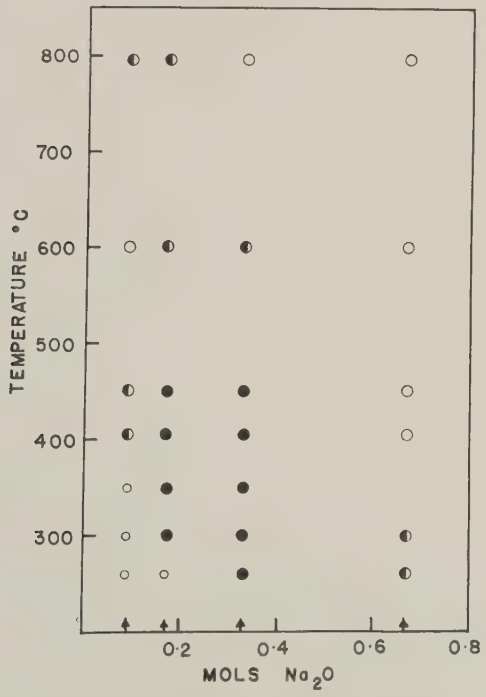

Fig. 4. t-x diagram at 15,000 psi for gels of saponite composition. Solid circle: montmorillonoid, open circle: other phases (see Table IV), small circle: very poorly crystallized and unidentified phase.

TABLE IV. REPRESENTATIVE RUNS FOR THE SAPONITE COMPOSITION GELS AT 15,000 PSI

Run No.	Temp. (° C.)	Duration (days)	Products*
	Composition: $3MgO:0.09Al_2O_3:3.83SiO_2:0.09Na_2O$		
1,261	260	12	Very poor crystallization, unidentified
1,201	300	7	Very poor crystallization, unidentified
1,271	350	6	Very poor crystallization, unidentified
1,121	404	7	Mont+talc
1,281	448	5	Mont+talc
1,321	600	3	Talc+1 mica
1,381	796	3	Mont+talc
	Composition: $3MgO:0.17Al_2O_3:3.67SiO_2:0.17Na_2O$		
1,262	260	12	Very poor crystallization, unidentified
1,202	300	7	Mont (12.6–17.7)
1,272	350	6	Mont (12.3–17.7)
1,122	404	7	Mont (12.6–17.7)
1,282	448	5	Mont (12.6–17.0)
1,322	600	3	Mont+1 talc
1,382	796	3	Mont+mica+stilp
	Composition: $3MgO:0.34Al_2O_3:3.33SiO_2:0.34Na_2O$		
1,263	260	12	Mont (12.6–17.7)
1,203	300	7	Mont (12.6–17.7)
1,273	350	6	Mont (12.6–17.7)
1,123	404	7	Mont (12.6–17.0)
1,283	448	5	Mont (12.6–17.0)
1,323	600	3	Mont+1 talc+1 mica
1,383	796	3	Stilp+mica
	Composition: $3MgO:0.67Al_2O_3:2.67SiO_2:0.67Na_2O$		
1,264	260	12	ML (mont, some other phase)
1,204	300	7	ML (mont, some other phase)
1,274	350	6	Stilp
1,124	404	7	Stilp+1 mica
1,284	448	5	Stilp+mica+chlor
1,324	600	3	Stilp+mica+1 chlor
1,384	796	3	Stilp+mica

* Abbreviations used: Mont = montmorillonoid, stilp = stilpnomelane, chlor = chlorite, ML = mixed layer, Mont (12.6–17.7) = (001) spacing of montmorillonoid, expands from 12.6 Å to 17.7 Å with glycol treatment, l = a little, minor.

panding phase at 260–300° C., but above 350° C. gave a "regular mixed-layer" phase with the (001) spacing of 12 Å. This phase was formed not only from the sodium-rich gel for the wide temperature range (350°–800° C.), but also from both the gels of N and 2N compositions at the

TABLE V. BASE-EXCHANGE CAPACITIES OF THE SYNTHETIC SAPONITE COMPOSITION MONTMORILLONOIDS

Composition (Na_2O Mol)	0.5N 0.09	1N 0.17	2N 0.34
Base-exchange capacity	33	80	126
(m.eq. Mn^{2+}/100 gm. of clay)	33	80	127
Average	33	80	127
+10% (see p. 792)	36	88	140

higher temperatures (750–800° C.). The (001) spacing of these phases obtained from the various conditions is nearly constant at 12 Å. From the constancy of these results, this phase may be considered to be a reproducible single phase, and, as discussed later, this phase may be identified as stilpnomelane.

The sodium-poor gel (0.09 Na_2O) yielded a very poorly crystallized montmorillonoid phase below 350° C., and a montmorillonoid phase plus talc at 400–450° C.

At 600° C., talc and/or mica plus montmorillonoid were formed. This phase combination was found to be stable for the two gels including the sodium-poor one and the one with the ideal saponite composition even at the unexpectedly high temperature of 800° C. The reason for the marked stability of this phase is discussed below and probably bears on the entry of Na^+ into the octahedral layers.

From these results, it was determined that saponites with variable charge cannot be prepared for the whole range corresponding to 0.09Na_2O to 0.67Na_2O, the variability in layer charge, exchange capacity, and Na_2O content extending only from about 0.13 to about 0.5Na_2O.

Cation exchange capacity

Base exchange capacity values obtained for the synthetic saponites with variable charge and with Na_2O from 0.09 to 0.33 are tabulated in Table V. A large batch of each of the specimens was synthesized at 400° C. and 15,000 psi.

Figure 5 shows a nearly linear relationship in base exchange vs. composition for these materials.

NEW PHASES: SYNTHETIC "ALUMINUM-CHLORITE," "SODIUM-HECTORITE" AND STILPNOMELANE

Three interesting new phases were encountered in this study. In the temperature range of 475–600° C., a chlorite-like phase with a basal spacing of 14.0 14.2 Å was developed from the 0.5 N, N and 2N beidel-

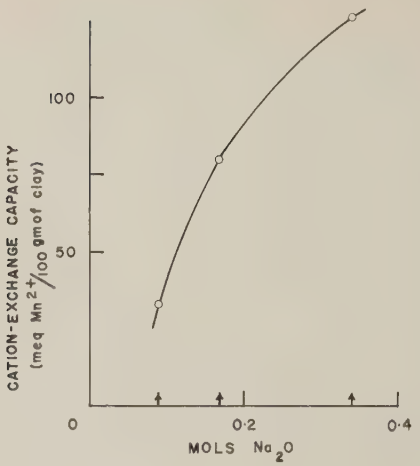

FIG. 5. Variation of cation-exchange capacity with composition in the saponite series of montmorillonoids.

lite composition gels. This phase appears quite consistently. The x-ray pattern of this phase is shown in Table VI. In a parallel concurrent study, C. M. Warshaw (1958) has consistently encountered the same phase in the K-deficient muscovite compositions. Unfortunately, as yet we have not succeeded in obtaining it pure. A reasonable hypothesis is that this phase represents a dioctahedral-chlorite with a gibbsite layer between the dioctahedral mica sheets. However, it should be noted that it has never been observed in the pure Al_2O_3-SiO_2-H_2O system (Roy and Osborn, 1954) and that some K^+ or Na^+ seem to be essential for its formation. Further studies are in progress on this phase.

Sand et al. (Sand, 1955; Sand and Ames, 1957; Ames and Sand, 1958) have commented on the "stability" of hectorite to very high temperatures of about 750° C. at 1000 atm. This is very much (200° C.) higher

TABLE VI. X-RAY DIFFRACTION PATTERNS OF NEW PHASES

"Al-chlorite"			Stilpnomelane		
hkl	*d*(Å)	I/I_0	*hkl*	*d*(Å)	I/I_0
001	14.2	100	001	11.9	100
003	4.647	30			
004	3.480	40	002	5.906	4
	2.344	10	004	2.979	40
	1.828	10	006	1.971	20
009 (?)	1.549	7	008	1.683	2

than the stability of any other montmorillonoid (Mumpton and Roy, 1956). When the "expanding" phase persisted in this work even beyond 800° C., it was obvious that again we were dealing with an exceptional montmorillonoid. It seems possible that we are dealing with a true sodium hectorite of the type $(Mg_{3-n}Na_n)(Si_{4-y}Al_y)O_{20}(OH)_2\ Na_{n+y}$. The saponite composition used obviously contains too little Na^+ and too much Mg^{++}, hence other phases appear constantly with the Na-hectorite. Apparently the monovalent ion in the octahedral layer leads to a particularly stable configuration; it may be possible that if the seat of charge could be restricted wholly to the octahedral layer in other montmorillonoids a similar stability would result. Further experimental work on this phase is in progress.

The possible "stilpnomelane" identification arose out of sheer coincidence. During the final weeks of work on this problem we were honored by a visit by Prof. J. W. Gruner of the University of Minnesota, who mentioned his recent re-newed interest in stilpnomelane. This led us to investigate the possibility that the phase obtained from the Na-rich saponite is a magnesium end member of the stilpnomelane family rather than a regular mixed-layer of chlorite and mica. The *x*-ray pattern of this phase is given in Table VI. It is fairly similar to the *x*-ray pattern of natural stilpnomelane which was given by Gruner (1937).

Morphology of the Synthetic Montmorillonoids

A series of electron micrographs (Fig. 6, *a*, *b*, *c*,) of various samples of these synthetic phases was prepared. Two observations are pertinent. The synthetic saponites appeared always to be better crystallized—showing thicker pseudohexagonal discrete crystals (Fig. 6*a*). In the beidellites of high exchange capacity, there was a definite, elongated, lath-like habit with sharp edges. The crystals were all very thin and in some specimens rolled in from both sides to give a double-barrelled gun effect (Fig. 6*c*). In most cases the habit and the maximum size appeared to be very similar to those of the natural phases.

Dehydration Properties of These Phases

These have been examined in detail by our colleague F. H. Gillery and are reported in this issue on pages 806–818.

Acknowledgments

This work is a contribution from Research Project 55 of the American Petroleum Institute at The Pennsylvania State University. We are indebted to F. H. Gillery for the Mn-saturation of the clays, and to Dr. C. M. Warshaw for several helpful suggestions with the manuscript.

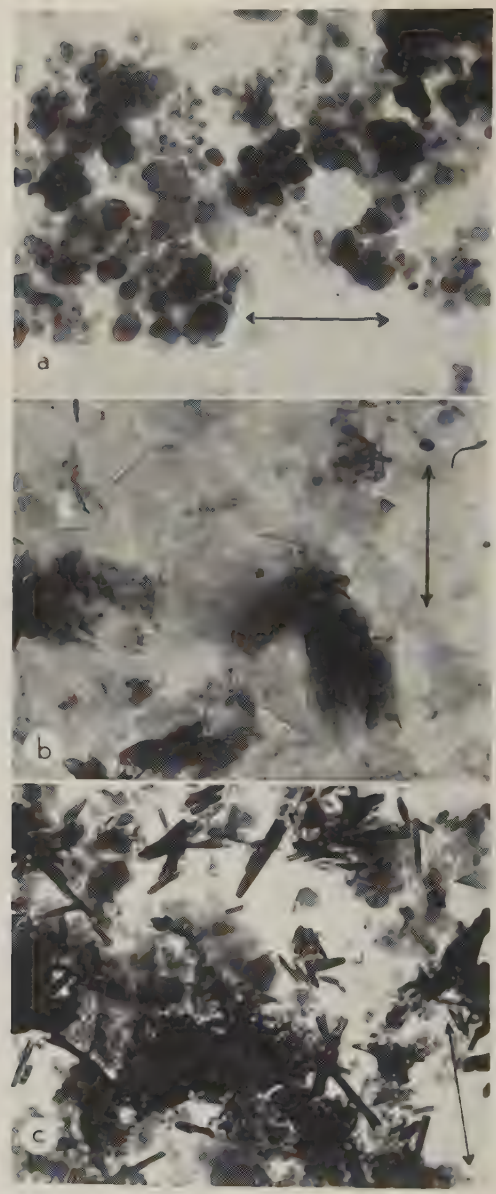

FIG. 6. Electron micrographs of Synthetic Montmorillonoids. (*a*) Saponite (2N) showing thick relatively euhedral hexagonal crystals. (*b*) Synthetic beidellite (N) showing fairly typical habit of better formed crystals which generally show a lath-like habit and are not as poorly formed as natural montmorillonites. (*c*) Synthetic beidellite (2N) showing double tube effect as though the flat rectangular laths of (*b*) above had been rolled inwards from both edges.

References

Ames, L. L., and L. B. Sand (1958), Factors effecting the maximum hydrothermal stability in montmorillonites: *Am. Mineral.*, **43,** 641–648.

Bower, C. A., and E. Truog (1940), Base exchange capacity determination of soils and other materials using colorimetric manganese method: *Ind. Eng. Chem., Anal. Ed.*, **12,** 411–413.

Gillery, F. H. (1958), Adsorption-desorption characteristics of synthetic montmorillonites: *Am. Mineral.*, this issue, pages 806–818.

Gruner, J. W. (1937), Composition and structure of stilpnomelane: *Am. Mineral*, **22,** 912–925.

Karsulin, M., and Vl. Stubican (1954), Ueber die Struktur und die Eigenschaften synthetischer Montmorillonite: *Monats. Chem.*, **85,** 806–818.

Mumpton, F. A., and R. Roy (1956), The influence of ionic substitution on the hydrothermal stability of montmorillonoids: Proceedings of Fourth National Conference on Clays and Clay Minerals, National Academy of Sciences—National Research Council, Publication **456,** 337–339.

Roy, D. M., and R. Roy (1952), Studies in the system MgO-Al_2 O_3-SiO_2-H_2O: *Bull. Geol. Soc. Am.*, **63,** 1293 (Abst.).

Roy, D. M., and R. Roy (1955), Synthesis and stability of minerals in the system MgO-Al_2O_3-SiO_2-H_2O: *Am. Mineral.*, **40,** 147–178.

Roy, R., and E. F. Osborn (1954), The system Al_2O_3-SiO_2-H_2O: *Am. Mineral.*, **39,** 853–885.

Roy, R., and L. B. Sand (1956), A note on some properties of synthetic montmorillonites: *Am. Mineral.*, **41,** 505–509.

Roy, R., and O. F. Tuttle (1956), Investigations under hydrothermal conditions: Ch. VI in Physics and Chemistry of the Earth, Pergamon Press, London.

Sand, L. B. (1955), "Montmorillonites stable at high temperatures: *Bull. Geol. Soc. Am.*, **66,** 1610–1611, (Abst.).

Sand, L. B., and L. L. Ames (1957), Stability and decomposition products of hectorite: Proceedings of Sixth National Conference on Clays and Clay Minerals, in press.

Sand, L. B., R. Roy, and E. F. Osborn (1953), Stability relations of some minerals in the system Na_2O-Al_2O_3-SiO_2-H_2O: *Bull. Geol. Soc. Am.*, **64,** 1469–1470, (Abst.).

Sand, L. B., R. Roy, and E. F. Osborn (1957), Stability relations of some minerals in the Na_2O-Al_2O_3-SiO_2-H_2O system: *Econ. Geol.*, **52,** 169–179.

Warshaw, C. M. (1958), Experimental studies of illite: Proceedings of Seventh National Conference on Clays and Clay Minerals.

Manuscript received Jan. 26, 1959.

ADSORPTION-DESORPTION CHARACTERISTICS OF SYNTHETIC MONTMORILLONOIDS IN HUMID ATMOSPHERES*

F. H. Gillery, *The Pennsylvania State University, University Park, Pennsylvania.*

Abstract

A systematic study of the desorption characteristics of synthetic Na and Ca-beidellites and saponites with various exchange capacities has been made. The results show that well defined hydrates exist over certain ranges of water vapor pressure and that between these ranges mixed layers of the hydrates predominate. The valence of the interlayer cation has a greater effect on the desorption characteristics than the exchange capacity or the type of montmorillonoid examined.

Introduction

Many papers have been published on the subject of the expansion of montmorillonoids in contact with water vapor. The specimens investigated have been of natural origin and therefore of random composition. The use of synthetic specimens in the present investigation has eliminated some of the difficulties which arise in the study of natural specimens and has made possible a systematic study of the effects produced by varying the exchange capacities and lattice composition. The specimens examined have included natural and synthetic montmorillonites, beidellites and saponites saturated with the cations Na and Ca.

Preparation of Specimens

The specimens were prepared hydrothermally from "gels" by M. Koizumi in sealed gold tubes (Koizumi and Roy, 1959). The conditions for optimum crystallinity were, for the beidellites 300° C., 15,000 psi and 7 days, and for the saponites, 400° C., 15,000 psi and 7 days. They were prepared in a Na saturated form and after the expansion characteristics of this form had been examined they were re-saturated with Ca and finally with Mn.

The re-saturations were carried out by shaking about 0.2 gm. of the clay with 10 ml. of 1M. $CaCl_2$ or 1M. $MnCl_2$ for 30 min., centrifuging, and decanting. This procedure was repeated five times. The washing was carried out in precisely the same way using deionized water in place of the 1M. solutions, until the specimens became deflocculated to such an extent that it was difficult to separate them from the water by centrifugation. At this stage washing was continued by sealing the specimen, suspended in water, in dialysis tubing and passing a slow, continuous

* Contribution No. 58-14 from the College of Mineral Industries. The Pennsylvania State University.

stream of distilled water around the tubing for about 5 days, until the evaporated washings showed no chloride ion with the $AgNO_3$ test.

For x-ray examination a dilute suspension of the specimen in water was allowed to dry out on a glass slide under room conditions, resulting in a well oriented layer suitable for the examination of the basal reflections.

Table I gives a complete list and details of the specimens examined.

Table I. Details of Specimens Examined

No.	Ex Cap	Sat Cation	Name	Formula
a	½N	Na	Beidellite	$0.17Na(Al_2)(Si_{3.83}Al_{0.17})O_{10}(OH)_2$
b	½N	Na	Saponite	$0.17Na(Mg_3)(Si_{3.83}Al_{0.17})O_{10}(OH)_2$
c	N	Na	Beidellite	$0.33Na(Al_2)(Si_{3.66}Al_{0.33})O_{10}(OH)_2$
d	N	Na	Saponite	$0.33Na(Mg_3)(Si_{3.66}Al_{0.33})O_{10}(OH)_2$
e	85†	Na	Montmorillonite	—
f	2N	Na	Beidellite	$0.66Na(Al_2)(Si_{3.33}Al_{0.66})O_{10}(OH)_2$
g	2N	Na	Saponite	$0.66Na(Mg_3)(Si_{3.33}Al_{0.66})O_{10}(OH)_2$
h	2.5N	Na	Beidellite	$0.83Na(Al_2)(Si_{3.17}Al_{0.83})O_{10}(OH)_2$
i	N	Ca	Beidellite	$0.17Ca(Al_2)(Si_{3.66}Al_{0.33})O_{10}(OH)_2$
j	N	Ca	Saponite	$0.17Ca(Mg_3)(Si_{3.66}Al_{0.33})O_{10}(OH)_2$
k	109*	Ca	Saponite	$0.25Ca(Mg_{2.92})(Si_{3.5}Al_{0.5})O_{10}(OH)_2$
l	85†	Ca	Montmorillonite	—
m	2N	Ca	Beidellite	$0.33Ca(Al_2)(Si_{3.33}Al_{0.66})O_{10}(OH)_2$
n	2N	Ca	Saponite	$0.33Ca(Mg_3)(Si_{3.33}Al_{0.66})O_{10}(OH)_2$
o	N	Mg	Beidellite	$0.17Mg(Al_2)(Si_{3.66}Al_{0.33})O_{10}(OH)_2$
p	109*	Na/Ca	Saponite	—

* Natural specimen from Allt Ribhein, Fiskavaig Bay, Skye, Scotland. Mackenzie (1957) Ex. Cap. in meq/100 gms., originally Ca saturated.

† Natural specimen of purified Wyoming Bentonite supplied by the National Lead Company, Houston, Texas. Ex Cap. in meq/100 gms. measured by Dr. M. Rustom.

Apparatus

A North American Philips Wide Range X-ray diffractometer was used to examine the specimens. The radiation shield covering the specimen was modified to contain a variable humidity atmosphere by lining the slot through which the x-ray beam passes with aluminum foil. The end of the shield was provided with tapped holes and tubes for the entrance and exit of the humid air.

The humidity of the air was controlled by splitting the incoming air from the compressed air line into two streams, one of which was dried by passage through "Drierite" and "Anhydrone" columns, and the other was completely saturated by passing it through four vessels containing

distilled water. The two streams were then remixed in proportions giving the approximate relative humidity required and passed through a saturated salt solution. The salt solution modified the humidity to correspond to that of its water vapor pressure, which was accurately known (O'Brien, 1948). Details of the solutions used are given in Table II.

The relative humidity was measured by means of wet and dry thermocouples connected differentially so that the difference in e.m.f. caused by the difference in temperature between them was measured directly with a potentiometer. The thermocouples were made from 32 B.S.

Table II. Relative Humidities Given by the Saturated Salt Solutions*

	R.H. at 20° C. (%)	R.H. at 25° C. (%)	R.H. at 30° C. (%)
Distilled Water	100	100	100
NH_4Cl	80	79	78
$NaNO_2$	—	66	—
$Ca(NO_3)_2.4H_2O$	56	51	46
$K_2CO_3.2H_2O$	44	43	—
$MgCl_2.6H_2O$	33	33	32
K. Acetate	20	19	—
H_2SO_4 (Sp. Gr. 1.570 gms/cc)	—	11	—
Anhydrone	0	0	0

* O'Brien (1948).

gauge nichrome and constantan wires giving an e.m.f. of 1mV/22.4° C. The wet junction was wound with thin cotton thread kept wet by immersing a part of its length in distilled water. The two thermocouples were mounted in a 4 mm. I.D. glass tube through which the humid air flowed. In this manner a high air velocity at the thermocouple junctions was maintained and the correct differential temperature produced.

The weight loss against humidity relations were obtained by means of a fused silica spring balance enclosed in a glass tube through which the humid air was passed. The extension of the spiral was measured with a cathetometer. No means of heating the tube was provided so that the specimen had to be removed and heated in a furnace to obtain the weight loss between 0% R.H. and heating to 350° C. This method was not satisfactory since it was suspected that the specimens absorb water very quickly from the atmosphere and also the chances of losing small portions of the sample during transference between the spiral and the furnace and back again were quite high.

Specimens Examined and Nomenclature

The general formula for the beidellites is:

$$(Al_2)(Si_{4-x}Al_x)O_{10}(OH)_2$$
$$\downarrow$$
$$M_y$$

for the saponites:

$$(Mg_3)(Si_{4-x}Al_x)O_{10}(OH)_2$$
$$\downarrow$$
$$M_y$$

and for the montmorillonites:

$$(Al_{2-x}Mg_x)(Si_4)O_{10}(OH)_2$$
$$\downarrow$$
$$M_y$$

Here M is the exchangeable cation, and $y=x$ if M is monovalent and $y=x/2$ if M is divalent. For most natural montmorillonoids $x \doteq 0.33$ and in this paper, synthetic specimens with this amount of substitution are designated N (normal) montmorillonoids. Similarly specimens with $x=0.17$ and $x=0.67$ are designated N/2 and 2N respectively.

Results

The results are summarized in graphical form in Fig. 1. In Figs. 1*a*–1*p* a full line represents a hydrate, which gives sharp *x*-ray reflections and integral orders of reflection. The full lines are drawn through points representing an average lattice spacing derived from all the integral basal reflections. Where two full lines cover the same range of relative humidity at different spacings the two hydrates exist at the same humidity as mixed crystals with little or no mixed layering. The broken lines indicate mixed layer formation of the two hydrates on either side of the broken lines. The broken lines are drawn through points representing the positions of the 001 reflections. The mixed-layer regions do not appear to be pure mixed-layers but in most cases show some mixed crystal nature as indicated by the partial resolution of the diffuse mixed-layer peaks.

Specimens *a*–*p* are represented in Figs. 1*a*–1*p* respectively.

Specimen *b*, Fig. 1*b*, was very poorly crystallized and only the 001 reflection could be detected. The results from this specimen were neglected in arriving at the final conclusions.

Figure 1*c* represents a mean of three samples, the results agreeing with each other. Two of the samples were made in different hydrothermal syntheses and since they are identical in characteristics the syntheses can be considered consistent. The third specimen was produced by re-

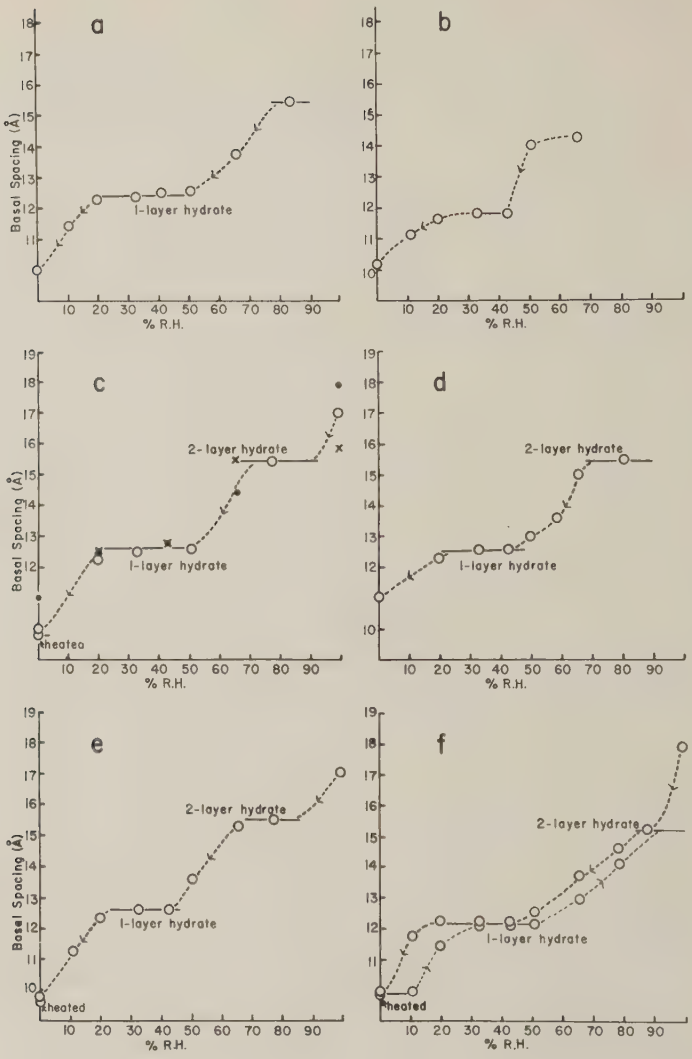

FIG. 1. 1*a*–1*p* Basal spacing—Relative humidity relations (R.H.). *a*) N/2 Beidellite. *b*) N/2 Na Saponite. *c*) N Na Beidellite. *d*) N Na Saponite. *e*) Nat. Na Montmorillonite. *f*) 2N Na Beidellite. *g*) 2N Na Saponite. *h*) 2.5N Na Beidellite. *i*) N Ca Beidellite. *j*) N Ca Saponite. *k*) Nat. Ca Saponite. *l*) Nat. Ca Montmorillonite. *m*) 2N Ca Beidellite. *n*) 2N Ca Saponite. *o*) N Mg Beidellite. *p*) Mixed Na-Ca Saponite. 1*q*–1*r* Weight loss—relative humidity relations. *q*) 2N Na Saponite. *r*) 2N Ca Saponite.

Figure continued on pages 811–812

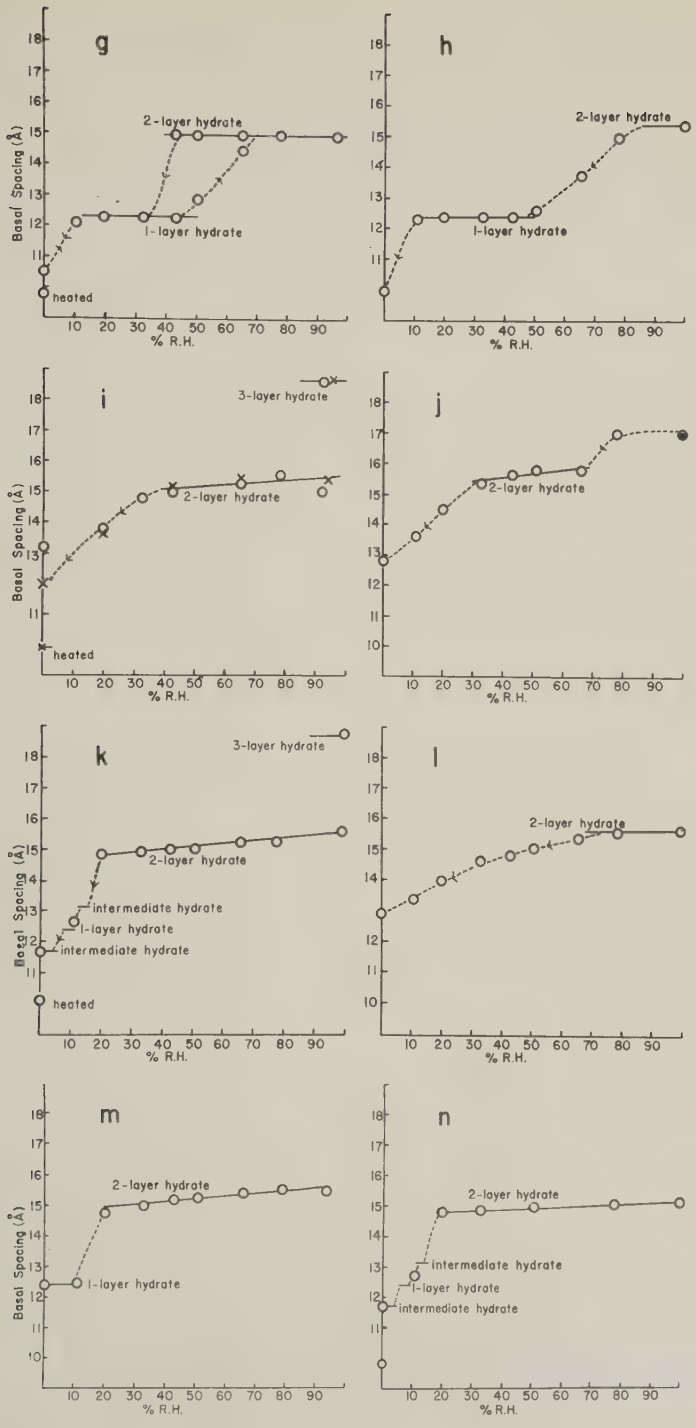
g
2-layer hydrate
1-layer hydrate
heated
Basal Spacing (Å)
% R.H.
h
2-layer hydrate
1-layer hydrate
% R.H.
i
3-layer hydrate
2-layer hydrate
heated
Basal Spacing (Å)
% R.H.
j
2-layer hydrate
% R.H.
k
3-layer hydrate
2-layer hydrate
intermediate hydrate
1-layer hydrate
intermediate hydrate
heated
Basal Spacing (Å)
% R.H.
l
2-layer hydrate
% R.H.
m
2-layer hydrate
1-layer hydrate
Basal Spacing (Å)
% R.H.
n
2-layer hydrate
intermediate hydrate
1-layer hydrate
intermediate hydrate
% R.H.

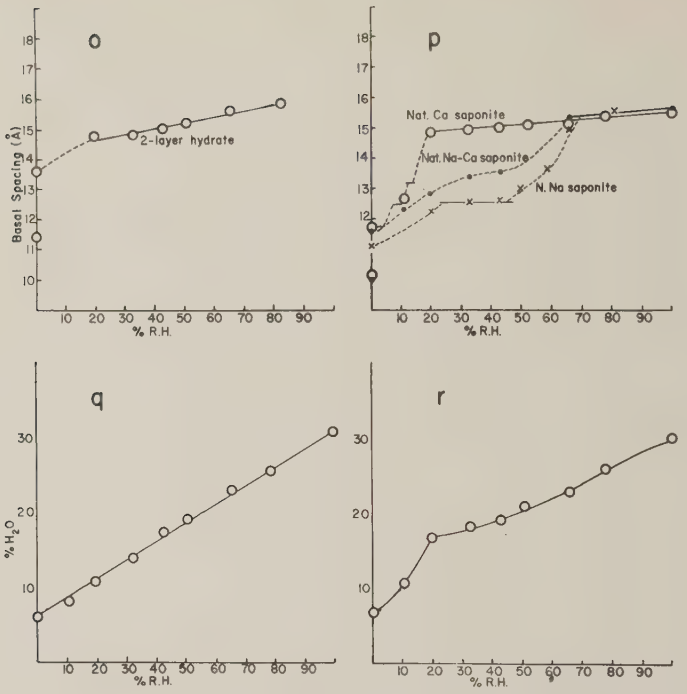

saturation of one of these samples with Na. This specimen is identical with the others and therefore it can be stated that the hydrothermal specimens as produced are fully saturated with sodium ions.

Specimen *g* (Fig. 1*g*) appears to be anomalous. It is extremely well crystallized compared with the other synthetic specimens, the hydration and dehydration curves are very sharp, yet the stability ranges of the hydrates do not agree well with those of the other Na saturated samples

Figure 1*i* shows a curve derived from a mean of two samples. One was a N.Ca beidellite synthesized as such and the other was a N.Ca beidellite prepared as a N.Na beidellite and resaturated by treatment with 1M. $CaCl_2$. The two curves are identical except for the region below 20% R.H. Here the re-saturated sample will not collapse to a basal spacing below about 13 Å, even after heating to 350° C. The N.Mg beidellite sample, *o* (Fig. 1*o*), shows a similar effect. These two were treated with 1M. $CaCl_2$ and 1M. $MgCl_2$ solutions of unadjusted pH. The rest of the samples were treated with solutions of pH 4.5–5.0. It is conceivable that under higher pH conditions, some precipitation of $CaCl^+$, $Ca(OH)^+$, $MgCl^+$, or $Mg(OH)^+$, occurred between the montmorillonite layers which prevented the collapse of the structure.

Figure 1*l* (specimen *l*) is labelled Natural Ca montmorillonite, but

the appearance of the diagram suggests a mixture of cations rather than pure Ca. A similar effect is illustrated in Fig. 1*p*. The central curve on the diagram is given by a sample in which an attempt was made to replace Ca with Na as the interlayer cation. The upper curve is that given by the original Ca saponite, while the lower curve is typical of a specimen completely saturated with Na. It is obvious that the center curve is a combination of the other two and that the substitution of Na for Ca is incomplete.

Considered generally, the *x*-ray diagrams show a trend for the degree of crystallinity to increase with an increasing amount of lattice substitution (x); this is shown by the intensity and sharpness of the reflections in the *x*-ray patterns. Another general feature of the patterns is a fairly diffuse region of scattering occurring at a spacing corresponding to $2\,d_{001}$. This is an effect produced by the specimens and not by the equipment since it moves as the 001 reflection moves, always obeying the above condition.

All the specimens were examined under conditions of decreasing humidity; some were also examined under increasing humidity conditions. These few specimens showed varying degrees of "hysteresis" in the mixed-layer portions of the curves, but this does not affect the spacing of the hydrates.

None of the specimens examined will dehydrate completely in dry air but require to be heated to 350° C. Even at this temperature some of the specimens do not collapse completely (to below 10 Å). All the specimens can be rehydrated after heating to this temperature.

On further comparing the results it can be seen immediately that the factor producing the greatest change in the hydration characteristics is the valence of the interlayer (exchangeable) cation. The amount of lattice substitution (x) and the composition (whether the specimen is saponite, beidellite or montmorillonite) have relatively minor effects.

The main features of the diagrams given by the Na saturated specimens are the two hydrates of basal spacings about 12.3 Å and 15.5 Å. The former is stable between relative humidities of about 15 and 50% and the latter stable between about 70 and 95%. The Ca specimens show hydrates with the same spacings but the first hydrate of 12.3 Å has a very small stability range at about 5% relative humidity, while the second hydrate of spacing 15.5 Å has a wide stability range extending from about 35% R.H. to about 100% R.H. In both the Na and Ca specimens there is evidence to show that a further hydrate exists at about 18 Å, but 100% R.H. is not sufficient water vapor pressure to produce this hydrate in a pure form but only in a mixed-layer or mixed crystal form with the 15.5 Å hydrate.

A closer examination of the finer details of the diagrams given by the

Na saturated samples reveals a possible significant trend in the spacing of the first hydrate (12.3 Å). The N/2 and 2N beidellites and saponites give spacings of 12.3 Å for this hydrate whilst the N. synthetic and the natural specimens give spacings of 12.6 Å indicating that a maximum occurs in the lattice spacing–exchange capacity relation at the exchange capacity usually associated with natural specimens. Another trend, less clearly defined, exists in regard to the range and position of the second hydrate of the Na beidellites, as shown in Table III.

The second hydrate of the Ca saturated specimens shows clearly in most cases a continuous decrease in spacing from about 15.5 Å to 15.0 Å

Table III. A Possibly Significant Trend in the Range and Position of the Second Hydrate of the Sodium Beidellite in Regard to Humidity

Amount of substitution	Lower humidity limit	Higher humidity limit
½N	80	90
N	80	95
2 N	90	92
2½N	100	—

with decrease in relative humidity. The decrease takes place without any observable amount of mixed layering. This effect is easily seen in this case because this particular hydrate has a wide range of stability. It may exist for the other hydrates, but if so it cannot be observed since their range of stability is too small. There is a tendency for the second hydrate (15.5 Å) of the Ca specimens to produce a two phase mixture with the third hydrate (18.0 Å) and not mixed layers. This is noticeable in all the Ca saturated specimens except those where the third hydrate does not appear. The same effect does not occur with the Na saturated specimens.

Specimens *k* and *p* show the normal Ca-saturated specimen *x*-ray diagrams, but careful analysis of the diagrams shows that in addition to the two usual hydrates there are another two occurring at about 0 and 15% R.H. with very small ranges of stability. These have spacings of 11.7 Å and 13.1 Å respectively. It is possible that these two hydrates occur in some other specimens but are difficult to recognize because of their extremely small stability range and the poorer crystallinity of most of the other samples.

The exchange capacity of most of the synthetic samples has been measured (Koizumi and Roy, 1959) using *x*-ray fluorescence to determine the amount of Mn absorbed into the exchange positions. The results were checked by using the same method on three specimens of previously

determined exchange capacity. The results determined by these methods are always lower than the values given by other methods (Table IV) but this does not detract from the results reported herein.

The weight loss curves shown in Figs. 1*q* and 1*r* are not completely satisfactory from a quantitative aspect due to the impossibility of heating the specimen in the present apparatus to determine the amount of water still present in the specimen at 0% R.H. Qualitatively, however, the break in the curve given by the Ca specimen (Fig. 1*r*) at 20% R. H. indicates a discontinuity in the rate of water desorption when the

Table IV. Exchange Capacities of the Specimens Examined

No.	Theoretical* meq/100 gms.	Measured, meq/100 gms.	Measured by other methods, meq/100 gms.
a	45	33	—
b	45	33	—
c and *i*	90	75	—
d and *j*	90	80	—
k	—	—	109
e and *l*	—	—	85
f and *m*	179	107	—
g and *n*	179	127	—
h	225	—	—
Calibration			
Kaolinite (Lustra Clay) RS-286		2	—
Hectorite (National Lead Co.)		75	83
Montmorillonite Clay (F.C.B.)		116	133

* Calculated from the formulae.

lower stability limit of a hydrate is reached. The Na curve (Fig. 1*q*) may show a similar effect, less pronounced, since the stability range of the hydrates is smaller.

Discussion

Of the specimens examined it can be seen that the saturating cation has the predominant effect in determining the dehydration characteristics. The montmorillonoid layer composition and amount of substitution (x) have comparatively small effects.

The composition of the 2N synthetic saponite is approaching that of a natural vermiculite and it is instructive to compare this specimen with vermiculite studied by Walker (1955). The hydrates described by Walker for vermiculite are given in Table V. The third column indicates the difference between the first two and is about +0.7 Å. Walker describes

Table V. The Hydrates of Mg-Vermiculite (Walker, 1955) Compared with Those of N and Natural Ca Saponites

Mg-Vermiculite hydrates (Å)	Ca-Saponite hydrates (Å)	Difference
14.81	15.5	+0.7
14.36	15.0	+0.6
13.82	13.1	−0.7
11.59	12.4	+0.8
20.6	11.7	—
9.02	9.8	+0.8

the decrease between 14.81 and 14.36 Å as being continuous and this also is observed in the saponite which decreases from 15.5 to 15.0 Å in a continuous manner. The 15.5 Å spacing of the saponite is thought to be the 2-layer hydrate corresponding to the formula

$$(Mg_3)(Si_{3.66}Al_{0.33})O_{10}(OH_2)\cdot 6H_2O \cdot \underset{\downarrow}{Na_{0.33}}$$

and the 15.0 Å spacing would correspond to the same formula containing $4H_2O$. The spacings 13.82 Å and 13.1 Å do not correspond but this may be because a *Mg* vermiculite is being compared with a *Ca* saponite, and according to Walker the transition between the 14.36 Å and 13.82 Å hydrate involves a movement of the cation from a position midway between the layers to a position adjacent to the layers. The 12.4 Å saponite hydrate corresponds closely in spacing to the 11.59 Å vermiculite hydrate and probably is the 1 water-layer hydrate ($3H_2O$) in the saponite as well as in the vermiculite. The 20.6 Å sequence in vermiculite is caused by regular mixed layering of the 11.59 and 9.02 Å hydrates, which is not the case with the saponite which gives a 11.7 Å spacing. Rowlands, Weiss and Bradley (1955) have also observed this hydrate in Ca montmorillonite and one of their explanations for it is that it corresponds to the same water content and structure as the 1 water-layer hydrate of vermiculite which is already accounted for herein. The other is that "inverted" Si-O tetrahedra eixist as in the Edelman-Favejee (1940) type montmorillonite structure. Insufficient work has been done in the present investigation either to confirm or to deny this supposition.

The variation of the 12.4 Å hydrate spacing of the sodium saturated specimens with the amount of substitution (x) is interesting. Since the N-synthetic and natural specimens appear to have the maximum spacing, this variation may be connected with the usual occurrence of natural montmorillonoids with near "normal" amounts of substitution. This

implies that a montmorillonoid with this amount of substitution is slightly more stable than montmorillonoids with either less or more substitution, that is, one with a lower free energy. Koizumi and Roy (1959) also indicated that the N specimens are more thermally stable than the N/2 and 2N specimens. If this is the case, then the maximum in the basal-spacing composition curve will correspond to a minimum in the free energy-composition curve. If we consider the number of interlayer cations increasing from zero, as in a pyrophyllite or talc type structure, the first few cations will probably expand the structure very little from the pyrophyllite or talc spacing, the layers being distorted around the cation positions. As more cations are introduced, more and more distortions will occur giving rise to poor crystallinity as is observed in the N/2 specimens examined. As the composition approaches "normal" a sufficient number of cations ($\frac{1}{3}$ of the number in a mica) and associated water molecules are present to extend the layers completely without appreciable distortion. This type of structure will presumably have a lower free energy than the distorted type of structure.

The addition of further cations causes an increase in the bonding between the layers and they are drawn closer together so decreasing the spacing. The increase in bonding will increase the difficulty of water penetrating between the layers and also increase the work necessary to produce hydration. This tendency can be seen in the higher humidity necessary to produce the second hydrate of the Na beidellites as the amount of substitution increases (Table III). The increase in the work required to obtain hydration would cause another increase in free energy of the specimens. Thus we have the minimum between this increase, and the increase due to the distortions introduced by too few interlayer cations which could account for the "normal" nature of natural montmorillonoids.

The spacing-humidity curves given by the Na-saturated and by the Ca-saturated specimens agree qualitatively with the % water absorbed-humidity curves. Due to the uncertainty of the absolute scale of the % water absorbed it is uncertain how much water is present in the different hydrates. It is possible however to state that the amount of water present (30% water corresponds to $9H_2O$/formula unit) in the 2-layer hydrates ($6H_2O$) of the Ca-saturated specimens at the higher humidities at which it is stable is more than can be accommodated between the layers having regard to the basal spacing. This gives rise to a consideration of the surface of the specimens. By measuring the *x*-ray reflection broadening of the montmorillonoid basal peaks an approximate crystal thickness can be obtained, assuming no other source of broadening. For the best crystallized specimens this is of the order of 100–200 Å or about 10 unit cell

heights. In such a crystal there will be 9 interlayers containing 2-water layers each and 2 outer surfaces with an unspecified number of absorbed water layers. This unspecified number would not have to become larger than about 3 or 4 before the adsorbed surface water becomes a very appreciable part of the total water measured by weight loss determinations. This effect could account for the surplus water apparently associated with the 2-layer Ca hydrate. It would also complicate any more accurate % water absorbed-humidity data.

The diffuse scattering band noticeable in most of the specimens, and corresponding to $2d_{001}$ can be explained only by supposing that there is some 2-layer nature in the stacking of the layers. This could be due either to a tendency to form two types of montmorillonite layers which then alternate, or (what is more likely) to hydration tending to take place in alternate layers.

Acknowledgment

This investigation forms part of A.P.I. Project 55 sponsored by the American Petroleum Institute.

References

Edelman, C. H., and Favejee, J. Ch. L., (1940), *Z. Krist.*, (A), **102,** 417–431.

Koizumi, M., and Roy, R., (1959), Geochimica et Cosmochimica Acta, in print.

MacKenzie, R. C., (1957), *Min. Mag.*, **31,** 672–680.

O'Brien, F. E. M., (1948), *Jour. Sci. Inst.*, **25,** 73–76.

Rowland, R. A., Weiss, E. J., and Bradley, W. F., (1955), in Clays and Clay Minerals: *Nat. Acad. Sci.*, Nat. Res. Council Pub. 327, 85–95.

Walker, G. F., (1955) in Clays and Clay Minerals: *Nat. Acad. Sci.*, Nat. Res. Council Pub. 327, 101–115.

Manuscript received August 26, 1959.

STABILITY AND INTERCONVERTIBILITY OF PHASES IN THE SYSTEM Mn-O-OH*

CYRUS KLINGSBERG† AND RUSTUM ROY, *The Pennsylvania State University, University Park, Pennsylvania*

ABSTRACT

Equilibrium and non-equilibrium reactions in the system Mn-O-OH have been studied under high water pressures and with varying oxygen pressures. Reproducible syntheses of well crystallized pyrochroite ($Mn(OH)_2$) and manganite ($MnO(OH)$) are described. The univariant p-t curves for the reactions $Mn(OH)_2 \rightleftarrows MnO + H_2O$ and $2MnOOH = Mn_2O_3 + H_2O$ have been determined. At 15,000 psi they pass through points at 392° C. and 272° C. respectively and are very steep in the range 3000 to 25,000 psi H_2O pressure. The isomorphous minerals, groutite and ramsdellite, have been shown to be interconvertible by low temperature oxidation or reduction. A phase intermediate in composition between these two and presumably of the same structure has been synthesized. Hydrohausmannite is shown to be unstable above 100° C. No evidence was obtained for partial entry of protons into either pyrolusite or ramsdellite to give solid solutions towards the MnOOH composition.

INTRODUCTION

Much descriptive work on the oxides and hydrous oxides of manganese may be found in the literature. However, fewer equilibrium data exist for these oxides, hydroxides, and oxyhydroxides than for many less common minerals. The main reason for this is the fact that in many of the important dehydration reactions, the manganese minerals would not only lose water but would also lose or gain oxygen.

Thus, to study a pure dehydration reaction it is necessary to be able to control the partial pressure of oxygen so that the manganese does not change valence during the reaction. To be able to do this, however, one has to be able to maintain a wide range of pressures of oxygen, hydrogen, and water vapor at high temperatures. Since it has recently become possible to do this an attempt was made to study such reactions. There are four main hydrated oxides of manganese: pyrochroite $Mn(OH)_2$, manganite and groutite MnOOH, and hydrohausmannite $Mn_3O_4 \cdot H_2O$. In addition, there is the possibility that the poorly formed manganese dioxides of considerable importance in the battery industry may contain essential hydroxyl in a solid solution of the type $Mn_{(1-n)}^{4+}Mn_n^{3+}O_{2-n}(OH)_n$.

As a preliminary study for this work it was necessary to know the equilibrium pO_2-T curves for the interconversions of the anhydrous oxides of manganese. The literature data for the equilibrium reactions of the

* Contribution No. 58–46, The Pennsylvania State University, Department of Geophysics and Geochemistry, University Park, Pennsylvania.

† Present address: Office of Naval Research, Washington, D. C.

lower valence oxides is thought to be good but the data for the $MnO_2 = Mn_2O_3 + \frac{1}{2}O_2$ and $Mn_2O_3 = Mn_3O_4 + \frac{1}{2}O_2$ curves left much to be desired. These reactions have been re-studied and our results on the anhydrous system are reported elsewhere (Klingsberg and Roy, 1959).

It is not possible to review the literature on the manganese oxides adequately in a short space. Hence for definitions of terms, methods of preparation etc. the reader is referred to excellent reviews by Cole, Wadsley and Walkley (1947), Wadsley and Walkley (1951), and McMurdie and Golovato (1948).

Apparatus

Familiar hydrothermal techniques were used throughout this investigation. Morey bombs were used only when large amounts of material (i.e., about 5–10 grams) had to be synthesized. For example, MnO and $Mn(OH)_2$ for use as starting materials were prepared in this way. The primary high pressure vessel, however, was the test tube bomb of eight inches in length, one inch outside diameter, one-fourth inch inside diameter, with an internal volume of about seven milliliters. Gold or platinum foil was folded into tiny envelopes to serve as sample holders. "Deionized" water was supplied to these bombs through stainless steel tubing by means of an air-operated pump.

Temperatures were maintained in base metal resistance wound furnaces by various commercial electronic controllers and were measured by chromel-alumel thermocouples placed in wells in the bombs.

What is believed to be an innovation in hydrothermal research is the introduction of oxygen under controlled pressures to a bomb for the purpose of influencing the oxidation state of the cation under examination. For this purpose, commercially purchased tank oxygen was delivered to the vessels by a separate line and kept separate from the water line by means of appropriate valves.

Calibrated gauges, designed to operate between 0–80 psi, 0–500 psi, 0–3000 psi, 0–30,000 psi, and 0–80,000 psi of total pressure, were used interchangeably so that whatever the pressure in a particular run might be, a gauge could be used that would operate at optimum accuracy for that pressure.

Starting Materials

In the course of this investigation 15 different starting materials were used. Before its use, each was ground to a fine powder. Some were naturally occurring crystalline minerals but most were synthetically prepared compounds, crystalline or sub-crystalline. The purity of the synthetic starting materials was examined by x-ray fluorescence analysis. All had much less than 0.1% iron.

Naturally occurring minerals:

1. Hydrohausmannite	Langban, Sweden (kindly supplied by Professor C. Frondel of Harvard University)
2. Manganite	Ilfeld, Harz, Germany (No. 258 Genth Collection of the Pennsylvania State University)
3. Groutite	1. Sagamore Mine, Minnesota (kindly supplied by Professor J. W. Gruner of the University of Minnesota) 2.* Marquette, Mich. (Genth Collection, Pennsylvania State University)
4. Ramsdellite	Chisholm, Minnesota (obtained from Dr. R. I. Harker)

Synthetic crystalline compounds:

1. Manganese metal	Fisher Scientific Co. analyzed for Fe content 0.1%
2. MnO	Prepared hydrothermally in a silver lined Morey bomb from manganese metal (480° C. and 15,000 psi water pressure for two days)
3. $Mn(OH)_2$	Prepared hydrothermally in a silver lined Morey bomb (350° C. and 15,000 psi water pressure for two days)
4. Mn_2O_3	$Mn(HO_3)_2 \cdot 6H_2O$ heated in air for eight hours at 700° C.
5. β-MnO_2	Baker Chemical Co.

Synthetic sub-crystalline compounds:

1. MnO_2	Will Corporation
2. Delta-MnO_2	Reduction of boiling $KMnO_4$ solution with HCl (McMurdie, 1944)
3. Gamma-MnO_2	Kindly supplied by Dr. S. B. Levin of the U. S. Army Signal Corps Engineering Laboratories
4. Rho-MnO_2	Same as above
5. MnOOH	Precipitated from a solution of $MnSO_4$ and NaOH (Partington, 1949)

Identification of the Phases

Phases were identified almost entirely by use of a Phillips Norelco Hi-Angle diffractometer employing CuKα radiation with a nickel filter, Most phases could be positively identified from their x-ray patterns in the region 17° to 44° 2θ.

Use of the petrographic microscope was restricted to the less common occasions when crystal size of the specimen was sufficient to permit identification of the phase. Another limitation of the microscope is the fact that manganese in its higher oxidation states forms opaque compounds.

Experimental Procedure

A. General Statement

By now a general familiarity with the techniques of hydrothermal synthesis is probably widespread, but some description of the slightly more complicated technique of adding

* This sample was labelled manganite and represents an addition to the relatively few localities recorded for groutite.

oxygen gas to water vapor, as a means of further controlling the environment of a sample seems to be in order. When water or oxygen is used individually, it is pumped into a bomb through suitable valves before a run begins. Sealing the bomb is effected by closing these same valves. The bomb is then placed in a furnace and when after about thirty minutes it reaches its desired temperature an adjustment is usually necessary to raise or lower the pressure to its proper value. For this operation the valve need be opened only momentarily.

B. Runs Using One Gas

Certain data were obtained by the introduction of water alone. For example, the reaction manganosite-pyrochroite was studied as a function of water pressure and temperature.

Other data were obtained by the use of oxygen alone as the gaseous phase. The reaction pyrolusite-bixbyite was thus studied as a function of oxygen pressure and temperature. The data determined through the heating of various materials in air are similarly examples of runs using just one gas.

C. Runs Using Two Gases

In this case both water vapor and oxygen are used. Either may be present as a trace or in an appreciable amount as long as the gas of lower pressure is introduced to the bomb first. Where oxygen was admitted first, there was no experimental difficulty. Introducing a trace of water vapor was not possible since it was "liquid" water that was pumped through the tubing connected to the bomb. For those runs described as having a trace of water present, the procedure involved putting three drops of water in a bomb just after the samples were put in (if this order is reversed, the sample envelopes may stick to the wet walls of the bomb at varying heights). The bomb was then sealed to the system and oxygen admitted. This amount of water was experimentally found to influence the total pressure in a run by only a fraction of an atmosphere after the bomb had been raised above 100° C.

D. An Important Experimental Difficulty: Failure of Gases to Mix

In the early part of this work it was hoped that it would be possible to study the reactions of interest under any chosen condition of the partial pO_2 and total pressure. Thus, one could hope to study the influence of *total* pressures on a particular pO_2-T point on a curve. It was gradually realized that some factor was complicating the work with two gases present.

Early work in this laboratory indicated strongly that under moderate pressure and even at temperatures of 500°–1000° C., two gases such as O_2 and H_2O or CO_2 and N_2, do not mix effectively in the test tube bombs which have been described. Harker (1958) has recently established this observation with detailed work.

For very low pressures (*i.e.*, those that are described as containing a "trace" of water), the chance for mixing is much greater, whereas when both gases are at pressures of even a few hundred atmospheres, the mean free path of the molecules is so reduced that mixing by diffusion is a very slow process. This result, which was intuitively quite unexpected, had far reaching results:

1. It made it impossible to work quantitatively with two gases. This does not detract from the work done, *e.g.*, on the manganite-bixbyite univariant curve in which, by trial and error, a proper ratio of oxygen pressure and water pressure was found to hold all solid phases in the desired oxidation state.

2. It made it necessary to be quite circumspect with regard to the types of starting materials run together in a bomb. Thus the combined use of hydrous and anhydrous starting materials might result in the liberation of water vapor in the immediate area. Even in a run of high pO_2, if the liberated water vapor stays exclusively at the bottom of

the bomb, the actual pO_2 *around the samples* would be quite different from the gauge reading.

E. The Importance of Heating and Quenching Procedures

A run is said to begin when the bomb, and therefore the sample within it, reaches the desired pressure and temperature for that run. It takes as long as 30 minutes in some cases to reach this point and during this time some or all of the starting materials may convert to another form. If this happens, the sample under study when the run "begins" is not the same as the sample that was originally put into the bomb. A change of this sort, if undetected by the investigator can lead to serious errors in interpretation of the run. Thus, A is put into a bomb. While the bomb is heating to its terminal temperature, A converts to B. The run lasts two days at a given pressure and temperature during which time B converts to C. An unwary investigator will report that for the given pressure and temperature, A→C. Or, if B persists for two days, the result might be given as A→B whereas this reaction may have taken place at a lower pressure and at hundreds of degrees lower temperature, with subsequent persistence of B.

For much of hydrothermal work (or dry synthesis, for that matter), the heating and quenching paths used are of little consequence. However, this is not always the case, and it was found during the course of this work that caution on this account was needed particularly in two cases:

First, it was found that in attempting to study one equilibrium curve it was sometimes necessary to cross another curve that was not under study. In such cases, a starting material might change before the run actually "began." This problem was examined by taking several starting materials up to the P-T condition of a run by different paths and immediately quenching the samples. In most cases, the starting materials had begun to alter before the run "began."

Second, there is the possibility of altering a product during the quenching of a run. This can only be a problem if the product can react with great speed. Considerations of this nature were important during the development of the equilibrium curve for the reaction: $Mn(OH)_2 = MnO + H_2O$. The speed of this reaction in either direction (at elevated pressures and temperatures) is such that the results of a run are completely unintelligible unless the quenching procedure employed is known for that run.

F. The Control of the Oxidation State of Manganese

Oxygen was admitted to a bomb under known and reproducible pressures for one of two reasons:

1. For reactions such as $4MnOOH + O_2 = 4MnO_2 + 2H_2O$, oxygen was used to make it possible to study the reaction as a function of oxygen pressure and temperature.

2. For the reaction $Mn_2O_3 \cdot H_2O = Mn_2O_3 + H_2O$, there is no change of oxidation number for the manganese, and a necessary pressure of oxygen was admitted to the bomb to maintain the trivalent state during the course of the run.

Manganese metal was used as a starting material to create reducing conditions by reacting with the water in a bomb. For the pyrochroite-manganosite curve, starting materials as well as products would have oxidized to Mn_3O_4 but for the presence of the hydrogen released from the reduction of water by the manganese metal. Also, there is the advantage that the use of manganese metal introduces no cation foreign to the Mn-O-OH system.

G. Accuracy of the Data

Temperatures were measured to an accuracy of ±1° C. but since the furnaces were controlled only to ±5° C. over long periods this figure more properly reflects the accuracy

of the data. However, in determining an equilibrium curve, the accuracy may be increased somewhat by the multiplicity of points measured along the curve.

Uncalibrated chromel-alumel thermocouples were used throughout this investigation but they were replaced frequently. Due to frequent changing of gauges, pressures are taken as accurate to $\pm 5\%$ of the gauge reading, although the gauges are in general more accurate than this.

In a future section it will be seen that the tables of data list pressures of oxygen and pressures of water vapor. Unfortunately, for simplicity, accuracy is sacrified in that these pressures refer to different measurements. No problem arises if only one gas is present in a run, or when water if present only in trace amount. In a run involving the use of two gases, oxygen is admitted to a bomb first since it is always of lower pressure than the water. The oxygen pressure that is recorded is the pressure of the admitted gas at room temperature. This pressure increases during the course of the run as the bomb rises in temperature, but this higher oxygen pressure can no longer be measured accurately since it is now part of the total pressure of which the water vapor has the far greater share. This increase in oxygen pressure has been examined experimentally, and it is a very small fraction of the introduced pressure due to the fact that only a portion of the gas in the system is heated. The gas in the gauge and tubing remains at room temperature during the course of a run, and it is only that portion of oxygen that is in the bomb that is heated.

H. Interpretation of the Data

Equilibrium is time-independent but the criteria by which it is determined are very much dependent upon the rates of the reactions being studied. The following classification will illustrate this point for the reaction, $X \rightleftharpoons Y$:

1. Both the forward and the reverse rates are such as to permit study of the reaction in each direction. This provides the most rigorous data and is used whenever possible. The manganosite-pyrochroite reaction was studied in this way.

2. At a given pressure and temperature the X structure persists for long periods of time, and at the same pressure but at a few degrees higher temperature, X rapidly inverts to Y, and it is everywhere impossible to make Y go to X. A curve determined according to this principle may or may not reflect stable equilibrium. More than likely it will indicate a series of temperatures that are higher than the equilibrium temperatures by an amount sufficient to overcome any activation energy barrier that may exist for the given reaction. The Manganite-bixyite reaction was examined partly according to this rule and partly according to the next one.

3. Neither the forward nor the reverse reaction proceed with sufficient speed to be studied in the laboratory. A third compound, Z, must be found which because of its more active state, amorphous structure, hydrous nature, etc., will rapidly form either X or Y. While a reaction of this nature was not encountered in this work, amorphous MnOOH played a comparable role in readily forming either manganite or bixbyite when it was found impossible to hydrate bixbyite.

I. The Synthesis and Properties of Phases*

During the course of this work it became possible for the first time, to synthesize reproducibly certain phases. Other naturally occurring

* Since it is reasoned that the diagrams summarize the authors' interpretation of the data and since most journals find it increasingly difficult to publish long tables of data, the data on the runs are omitted. A complete record of the runs may be obtained in the original dissertation by C. Klingsberg (Ph.D. Geochemistry, 1958) from the Library of the Penna. State University or from University Microfilms, Ann Arbor, Mich.

Mn-O-OH minerals still elude synthesis. For some of the hydrous minerals the hydrothermal method offers not only an alternative method of preparation, but a far better way of preparing compounds of unmatched purity and crystallinity. This is particularly true for pyrochroite and manganite.

A. Pyrochroite

A simple, effective preparation was found. This material can be synthesized hydrothermally, for example, from powdered manganese metal at 360° C. and 2000 psi. of water pressure. In quenching, the temperature must be lowered while the pressure is maintained. The hydrogen generated keeps all the manganese divalent.

The compound prepared in this way appears as a white powder consisting of microscopic hexagonal euhedral crystals and gives a very sharp *x*-ray pattern. Upon standing in air for a few days it turns dark brown but shows no change in *x*-ray pattern. This change in color is supposedly due to the partial oxidation of divalent to trivalent manganese with a concomitant substitution of oxygen ions for hydroxyls to preserve electrical neutrality. The *x*-ray pattern for this material is given in Table 1.

The air oxidation of $Mn(OH)_2$ is a reaction well known to chemists. In contact with aqueous solution it is a reaction that is difficult to prevent (Partington, 1949). If special precautions are observed it is possible to keep ($Mn(OH)_2$) reduced and white indefinitely. One of the samples of $Mn(OH)_2$ that resulted from the examination of the pyrochroite-manganosite reaction was washed with a copious amount of alcohol and dried rapidly. This prevented it from turning brown on standing. The sample was divided into two parts, one of which was left in air, while the other was placed in a desiccator. The sample exposed to air was dark brown in two weeks. The portion in the desiccator is still white after a year.

B. Manganite

While there are reports in the literature about the synthesis of manganite (Feitknecht and Marti, 1945, Moore et al. 1950), they all involve some measure of doubt as to the identification of the actual product. Hydrothermally, manganite is easily and reproducibly synthesized, for example, from $Mn(OH)_2$ or MnOOH at 225° C. under 10 psi. O_2 and 15,000 psi H_2O pressures.

C. Attempted Synthesis of Groutite and Ramsdellite

The attempted syntheses of groutite has been unsuccessful. This

Table 1. *X*-Ray Diffraction Data

Pyrochroite (synthetic)		Hausmannite (synthetic)	
d	I/I.	*d*	I/I.
4.726	100	3.087	45
		2.879	19
2.870	18	2.768	73
2.453	40	2.486	100
2.361	6	2.366	27
1.825	26	2.037	38
1.658	6	1.797	19
1.567	4	1.706	12
1.381	8	1.575	38
		1.544	38
1.346	3	1.441	24
1.180	3		

"Groutellite" (Synthetic—this work)

d	I/I.	*hkl*
4.219	100	110
2.633	60	130
2.380	40	040

means that groutite and ramsdellite are the only phases in the Mn-O-OH system for which no synthesis has been reported.

Since groutite is not common in nature, the ability to synthesize it would provide mineralogists with an abundant supply so that its characterization might be more easily pursued. Also, if it could be synthesized hydrothermally, some indication of natural origin might result. This is equally true for ramsdellite, and since the reversibility of the groutite-ramsdellite reaction has been demonstrated, the synthesis of either mineral would in effect involve the synthesis of both.

Unfortunately, the above mentioned advantages were not realized, despite repeated efforts to determine the necessary conditions of synthesis. It is likely that these phases are everywhere metastable in which case a systematic attempt at synthesis might fail where an "accidental" preparation might succeed.

Since γ-MnO_2 has been described as a poorly crystalline ramsdellite it was a likely starting material for the synthesis of ramsdellite (many other compounds were used as well). However, under a wide variety of temperature and pressures of water and oxygen, γ-MnO_2 either remained unchanged or converted to pyrolusite.

D. Ramsdellite-Groutellite-Groutite

The reduction of ramsdellite to groutite involves no change in structure types since these minerals both have the diaspore structure. What is involved is merely the addition of a proton to an $O^{=}$ and an electron to a Mn^{4+}. It has been pointed out (H. Kedesdy, personal communication) that what is required structurally is merely a slight angular twist between the oxygen octahedra. The absence of solid solution between these phases is demonstrated by the absence of variations in *d* interplanar spacings. This means that there is no gradual rotation but rather a "displacive" change of a fixed amount in the oxygen positions when the protons are added. However, the change does not take place in one step. An intermediate compound was found to form (tentatively named groutellite*) whose unit cell is undoubtedly related to those of ramsdellite and groutite:

	a	*b*	*c*
Ramsdellite	4.52 Å	9.27 Å	2.87 Å
Groutellite	4.71	9.52	—
Groutite	4.56	10.00	3.03

It is very likely that groutellite represents an ordered structure as the hydroxyls only partly replace oxygen ions in some statistical manner during the reduction of ramsdellite to groutite. Its powder pattern is given in Table 1. Groutellite was not observed to form during the reverse reaction, *i.e.*, oxidation of groutite to ramsdellite.

E. Table of X-Ray Data

Since *x*-ray diffraction was used as the primary tool for identification it was essential to have accurate powder data for all the phases in the system. A complete list of powder data for these phases is in the original publication (Klingsberg, 1958). In most cases† the diffractometer data for the minerals agree with one or another of the many sources of such data. However, revised data are necessary for the following synthetic phases: pyrochroite, hausmannite, and two new phases. These data are given in Table 1.

* While this phase is strictly not a mineral, there seems to be no advantage in representing it by a chemical formula which would not indicate its genetic relationship to groutite, rather than a name.

† Pyrochroite natural, manganosite synthetic, bixbyite synthetic and natural, manganite synthetic and natural, groutite natural, pyrolusite synthetic and natural, ramsdellite natural.

The following compounds were either not examined at all or not in sufficient detail to report on:

Manganosite natural, hausmannite natural, pyrochroite natural, α-MnOOH, β-MnOOH, manganous manganite, cryptomelane, δ-MnO_2, γ-MnO_2, ρ-MnO_2.

II. Equilibrium Reactions

A. The Pyrochroite-Manganosite Reaction

It was discovered in the course of studying the reaction, $Mn(OH)_2 = MnO + H_2O$, that either phase is so readily convertible to the other that a partial conversion will take place if the equilibrium curve is crossed during the quenching of a run. A point on the $Mn(OH)_2$ side of the curve can best be determined by a P-T heat (pressure is applied before heating) and a T-P quench (*i.e.*, temperature is quenched first and then the pressure is released). In this way the starting materials never enter the field of MnO and should therefore show no trace of manganosite after the run. Figure 1 is drawn from these data.

On the MnO side of the curve a point is best determined by P-T quench (pressure is reduced to 1 atm. after which the temperature is quickly quenched). The heating curve was not important in this case since the equilibrium curve had to be crossed to get to the MnO field, and it did not matter when or how it was crossed. These runs should show no trace of pyrochroite.

Before the runs can be interpreted in this way, it must first be determined how much time is required for the starting materials to react completely, *i.e.*, to achieve equilibrium at the given pressure and temperature of the point under study.

B. The Manganite-Bixbyite Reaction

For the reaction, $2MnOOH = Mn_2O_3 + H_2O$, no oxidation or reduction is desired during the course of a run. Therefore just enough oxygen was admitted to each run (about 15 psi) to keep the manganese in the trivalent state. Frequently there were inadvertent changes in oxidation state.

It was found that manganite could be dehydrated but that bixbyite could not be hydrated. Their structures are completely different, and the reaction involves a major crystalline rearrangement rather than the removal of a loosely held water molecule. Some care had to be exercised that manganite was not dehydrated during the quenching of a run. The starting material of greatest use was amorphous MnOOH which crystallized either as manganite or bixbyite with great ease. Figure 2 is drawn on the basis of the data obtained and tabulated in the original publication.

C. The Hydrohausmannite-Hausmannite Reaction

An attempt to study the reaction,

$$Mn_3O_4 \cdot H_2O = Mn_3O_4 + H_2O$$

under equilibrium conditions was unsuccessful due to the fact that only the dehydration reaction could be made to take place. Repeated attempts to synthesize hydrohausmannite hydrothermally were not successful. This

result was not expected in light of the fact that its synthesis has already been reported by wet-chemical techniques at room temperature (Feitknecht, and Marti, 1945).

Since this is known to be a low temperature mineral, only temperatures up to 400° C. were tried under varying conditions of low and high water pressures and low and high oxygen pressures. The starting materials used

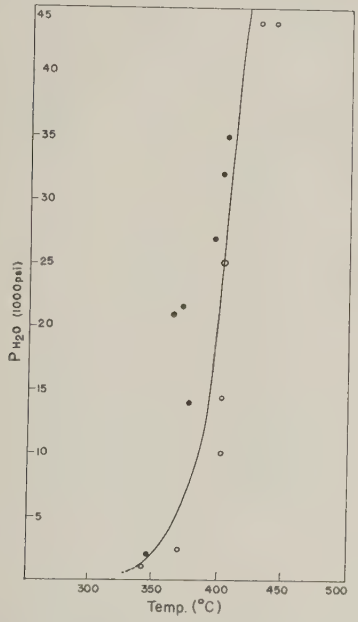

FIG. 1. The pyrochroite-manganosite reaction.

$Mn(OH)_2$ ●; MnO ○

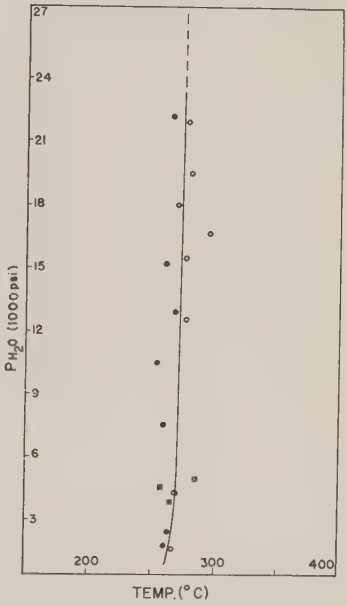

FIG. 2. The manganite-bixbyite reaction.

$Mn_2O_3 \cdot H_2O$: ●; Mn_2O_3 ○

were MnO, $Mn(OH)_2$, and MnOOH. Hausmannite, manganite, and pyrolusite were produced depending upon the conditions of the run.

Apparently the hydrohausmannite structure is not stable even at the lowest hydrothermal temperatures, and its maximum stability would appear to be near the boiling point of water. Under 3000 psi of water pressure it will persist at least one day at 78° C. but will convert to hausmannite (and manganite) at 132° C.

III. Non-Equilibrium Reactions

A. Manganite-Pyrolusite Interconvertibility

The manganite-pyrolusite reaction was not studied under conditions of equilibrium. However, interconvertibility between these two minerals was realized.

The existence of at least partial solid solution between these compounds was considered a distinct possibility, since pyrolusite often occurs in nature as a pseudomorph after manganite. Samples of manganite partly oxidized to pyrolusite, as well as partly reduced pyrolusite, were examined by x-radiation for a shift in d spacing for either the manganite or the pyrolusite. No evidence of a shift was found, and on this basis the "complete" absence of solid solution is reported. Unlike groutite-ramsdellite, there is no intermediate compound between manganite and pyrolusite.

In air, manganite converts to pyrolusite at about 130° C. The following abbreviated table shows the redox conditions under which the manganite-pyrolusite interconvertibility can be observed.

Table 2. Data on Manganite-Pyrolusite Interconvertibility

Temp. (° C.)	Press. (psi)H_2O	Press. (psi)O_2	Time (days)	Initial Condition	Result
252	2,300	30	1	Manganite	Mang. and β-MnO_2
				MnOOH	Mang. and tr. β-MnO_2
				$Mn(OH)_2$	Mang. and tr. β-MnO_2
172	14,000	0	2	β-MnO_2	Mang. and β-MnO_2
				Mn metal	$Mn(OH)_2$

B. Groutite-Ramsdellite Interconvertibility

The isostructural relationship between groutite (Mn-OHO) and ramsdellite (orthorhombic MnO_2) was known in 1949 when Collin and Lipscomb (7) and Bystrom (5) determined their structures and showed them to be members of the diaspore-goethite family.

The relationship is perhaps best seen by a comparison of unit cell parameters:

		a	b	c
groutite	Mn O OH	4.56	10.70	2.85
ramsdellite	Mn O O	4.52	9.27	2.87
diaspore	Al O OH	4.40	9.39	2.84
goethite	Fe O OH	4.64	10.00	3.03
montroseite	(V, Fe)O(OH)	4.54	9.97	3.03
paramontroseite	V O O	4.89	9.39	2.93

Hydrothermal reductions were controlled by changes in the duration of runs and by variations in the amount of manganese metal used as a

starting material. The first two following runs differ in that a slightly greater amount of manganese metal was used in the second run:

Table 3. Data on Groutite-Ramsdellite Interconvertibility

Temp. (° C.)	Press. (psi)H_2O	Added O_2 (psi)O	Time (days)	Initial Condition	Result
173	13,500	0	2	Ramsdellite Mn Metal	Ramsdellite and Groutellite $Mn(OH)_2$
172	15,000	0	2	Ramsdellite Mn metal	Groutellite+Groutite $Mn(OH)_2$
235	0	1,650	2	Groutite	Ramsdellite

In air, groutite was found to persist indefinitely below 130° C. At about 130° C, it oxidizes partly to ramsdellite in fourteen days; at 300° C. it oxidizes in a few hours. Above 300° C. it goes directly to pyrolusite.

C. Reactions in Air

Maximum temperatures of stability for a variety of manganese compounds heated in air are given in this section. They do not represent equilibrium temperatures, for in no case can the reverse reaction take place at the same temperature. The results obtained are summarized in Fig. 3.

Since these temperatures do not represent points of reversibility, the time parameter becomes significant. In this sense these are the lowest temperatures at which a reaction takes place at such a rate as to be easily observed in the laboratory. No doubt many of these reactions could be made to take place in air at even lower temperature if a substantially longer period of time were allowed to elapse.

These data, even though they do not reflect equilibrium conditions, can still serve to define limits for the reactions involved. For example, the following statement has been observed in a number of chemistry texts, "Mn_2O_3 can be prepared by heating pyrolusite at 600° C." As recently as 1956 (Kissinger et al., 1956), 550° C. was reported as the temperature of conversion as determined by differential thermal analysis.

While these statements are both valid, it is still useful to report that this same reaction was made to take place at a temperature as low as about 510° C. although the reaction is considerably slower at this temperature.

The temperature, 510° C., must provide enough energy not only to reach the equilibrium dissociation temperature at 0.21 atmospheres of

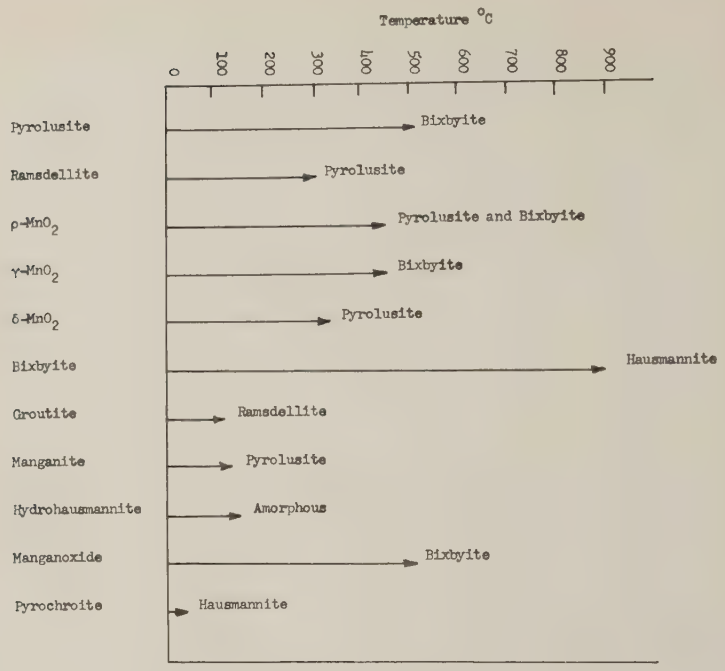

FIG. 3. Reactions in air.

O_2, but also enough to overcome the considerable activation energy required, and must therefore be substantially higher than the equilibrium value.

TEMPERATURES OF REACTIONS AS VIEWED FROM CRYSTAL CHEMISTRY

Before considering the crystal chemical generalizations which derive from the present data, there are summarized below many of the pertinent data on the oxides and hydroxides of related systems. The first table (Table 4) summarizes the structural relations among some of the variable valence elements in relation to the size of the cation. The second table (Table 5) of trivalent hydroxide and oxide structures relationship shows the temperatures at which corresponding reactions take place.

A. Dehydration of the Brucite-type Lattice

It is one of the goals of crystal chemistry to predict thermochemical reactions. It cannot be claimed that this state of development has been achieved for this relatively new field, but the continued accumulation of thermal data of solid-solid and solid-vapor reactions should hasten the development of a more quantitative treatment of this field.

TABLE 4. STRUCTURAL RELATIONS AMONG SOME OXIDES OF VARIABLE VALENCE ELEMENTS

Element	Structure Type of Oxide			
	MO_2	M_2O_3	M_3O_4	MO
Fe	(Rutile*)	Corundum	Spinel	Halite ($a_0=4.29$)
V	Rutile	Corundum	None	Halite ($a_0=4.08$)
	Diaspore (Paramontroseite)			
Ti	Rutile	Corundum	None	Halite ($a_0=4.24$)
Mn	Rutile (Pyrolusite)	C-Type Rare Earth	Distorted Spinel	Halite ($a_0=4.44$)
	Diaspore (Ramsdellite)			
U	Fluorite	None	None	Halite ($a_0=4.92$)

Increasing Cation Size†

* Compounds of tetravalent iron, such as $BaFeO_3$, are analogous to TiO_2.

† This order is not correct for all oxidation states and is given here for the trivalent ions.

Generally, the deformation of an anion is described as being related to the polarizing power of a cation. The polarizing power of a cation, in turn, is a function of its field strength (ratio of charge to size) and its electron configuration (noble-gas ions are less polarizing than non-noble-

TABLE 5. EQUILIBRIUM DECOMPOSITION TEMPERATURES OF MOOH TO M_2O_3

Element	Diaspore Structure	Decomposition Temperature*	Boehmite Structure	Oxide Structure
Al	Diaspore	390° C.	Boehmite	Corundum
Ga	Ga-diaspore	300° C.	—	Corundum
Fe	Goethite	150° C.	Lepidocrocite	Corundum
V	Montroseite	—	—	Corundum
Mn	Groutite	270° C.	(Manganite)†	C-Type Rare Earth
Sc	Sc-diaspore	410° C.	—	C-Type Rare Earth

Increasing Cation Size

* At 15,000 psi of water pressure.

† Not rigorously true. Manganite is more like lepidocrocite chemically than structurally.

Table 6. Data on Reactions in Air

Temp. (° C.)	Pressure (atmosphere) *air*	Time (days)	Initial Condition	Result
507	1	8	β-MnO_2	amorphous
515	1	4	MnO_2	β-MnO_2 and Mn_2O_3
316	1	4	Ramsdellite	Ramsdellite
313	1	14	Ramsdellite	Ramsdellite and tr. β-MnO_2
465	1	4	γ-MnO_2	β-MnO_2 and Mn_2O_3
430	1	5	γ-MnO_2	amorphous
452	1	1	γ-MnO_2	amorphous
465	1	4	γ-MnO_2	Mn_2O_3
343	1	4	γ-MnO_2	β-MnO_2
885	1	1	MnOOH	Mn_2O_3
892	1	1	MnOOH	Mn_3O_4
110	1	14	Groutite	Groutite
131	1	14	Groutite	Groutite and ramsdellite
117	1	3	Manganite	Manganite
132	1	6	Manganite	Manganite and β-MnO_2
145	1	8	Hydrohausmannite	Hydrohausmannite (very poor)
32	1	2	$Mn(OH)_2$	Mn_3O_4

gas ions). Anions exert a similar, but in most cases, a weaker influence upon the cation.

It is frequently difficult to find a case which permits direct comparison of the influence of these various qualitative concepts. (This point will be illustrated in the next section.) However, in the case of the equilibrium dehydration of the brucite-type lattice there now exists an opportunity to examine a problem in crystal chemistry for which the data are good.

Consider the following equilibrium temperatures of dehydration at 15,000 psi of water pressure:

$Ni(OH)_2$:300° C. (unpublished, this laboratory)
$Mg(OH)_2$:650° C. (Roy and Roy, 1957)
$Mn(OH)_2$:380° C. (Figure 2)
$Ca(OH)_2$:740° C. (Majumdar and Roy, 1956)

Comparisons of these hydroxides fall into the following categories:

1. Where both cations are noble-gas ions (Ca^{++} and Mg^{++}), the O-H bond strength is apparently greater for the larger cation, as evidenced by the fact that $Ca(OH)_2$ is slightly more stable (90° C. higher dissociation). This is to be expected from the weakening of the metal-oxygen bond with increasing size and the resulting increased ionic nature of the compound. The pair $Mn(OH)_2$ and $Ni(OH)_2$ appear to bear this out.

2. With cationic sizes held constant, the "fit" in a crystal of $Ni(OH)_2$

TABLE 7. DATA ON REACTION, MANGANITE⇌BIXBYITE AND WATER

Temp. (° C.)	Press. (psi)H_2O	Press. (psi)O_2	Time (days)	Initial Condition	Result
268	21,500	0	2	Mang.	Mang.
				MnOOH	Mn_3O_4
				$Mn(OH)_2$	Mn_3O_4
271	17,300	50	2	Mang.	β-MnO_2
				MnOOH	Mang. and β-MnO_2
				$Mn(OH)_2$	β-MnO_2
				MnO	β-MnO_2 and Manox.
259	14,500	0	3	Mn_2O_3	Mn_2O_3
				Mang.	Mang.
254	10,000	10	2	Mang.	Mang.
				MnOOH	Mn_3O_4
				$Mn(OH)_2$	Mn_3O_4
256	7,000	20	5	Mang.	Mang. and β-MnO_2
				MnOOH	Mang. and tr. β-MnO_2
				$Mn(OH)_2$	β-MnO_2 and Manox.
271	12,500	10	2	Mang.	Mang.
				MnOOH	Mn_3O_4
				$Mn(OH)_2$	Mn_3O_4
265	4,000	20	2	Mang.	Mang. and β-MnO_2
				MnOOH	Mang. and β-MnO_2
				$Mn(OH)_2$	β-MnO_2
257	4,000	25	1	Mang.	Mang. and tr. β-MnO_2
				MnOOH	Mang. and tr. β-MnO_2
				$Mn(OH)_2$	Mang. and tr. β-MnO_2 and Manox.
265	2,100	30	1	Mang.	Mang. and tr. β-MnO_2
				MnOOH	Mang.
				$Mn(OH)_2$	Mang. and tr. β-MnO_2 and Manox.
257	1,250	20	1	Mang.	Mang. and β-MnO_2
				MnOOH	Mang.
				$Mn(OH)_2$	Mang.
274	21,500	10	5	Mang.	Mn_2O_3 and β-MnO_2
				MnOOH	β-MnO_2 and Mn_2O_3 and tr. $Mn(OH)_2$
				$Mn(OH)_2$	

Abbreviations: Manox. = manganoxide, a new synthetic phase, Mang. = manganite, Mn_2O_3 = bixybyite, Mn_3O_4 = hausmannite, MnOOH = amorphous, β-MnO_2 = pyrolusite.

TABLE 7—(*Continued*)

Temp. (° C.)	Press. (psi) H_2O	Press. (psi) O_2	Time (days)	Initial Condition	Result
282	19,000	0	2	Mang.	Mn_2O_3
				MnOOH	Mn_3O_4
				$Mn(OH)_2$	Mn_3O_4
275	12,300	15	2	Mang.	β-MnO_2
				MnOOH	β-MnO_2 and Mn_2O_3
				$Mn(OH)_2$	β-MnO_2
279	9,000	10	3	Mang.	Mang. and Mn_2O_3
				MnOOH	Mang., Mn_3O_4, tr. Mn_2O_3
				$Mn(OH)_2$	Mang., Mn_3O_4, Mn_2O_3
260	4,600	300	2	Mang.	Mang. and Mn_2O_3
				MnOOH	Mn_3O_4
				$Mn(OH)_2$	Mn_3O_4
267	3,800	20	2	Mang.	Mn_2O_3 and β-MnO_2
				MnOOH	β-MnO_2 and Mn_2O_3
				$Mn(OH)_2$	β-MnO_2 and Manox.
265	1,100	20	2	Mang.	Mn_2O_3 and β-MnO_2
				MnOOH	β-MnO_2 and Mn_2O_3
				$Mn(OH)_2$	β-MnO_2 and Manox.

must be the same as that of $Mg(OH)_2$. However, Ni^{++} is not a noble-gas ion, and as a result is expected to have a greater polarizing power than the Mg^{++} ion. With an increase in covalency in the metal-oxygen bond, the thermal stability of $Ni(OH)_2$ is markedly reduced (by 350° C.) below that of $Mg(OH)_2$, likewise $Mn(OH)_2$ and $Ca(OH)_2$.

B. Dehydration of the Diaspore-type Lattice

In the last section it was indicated that it frequently is difficult to find examples within the framework of crystal chemistry that permit clear comparisons to be made that reflect the influence of only one characteristic of bond type. Unfortunately, the dehydration of groutite is an example of this, and therefore, can not be treated in the same manner as the dehydration of pyrochroite.

Groutite has a diaspore-like structure, and the desire is strong to compare its thermal stability with that of the Al, Ga, Sc or Fe diaspore structures. However, while the above diaspore structures convert to a corundum structure, groutite converts to a C-type rare earth structure.

TABLE 8. DATA ON REACTION: $Mn(OH)_2 \rightleftharpoons MnO + H_2O$

Temp. (° C.)	Press. (psi)H_2O	Press. (psi)O_2	Time (days)	Initial Condition	Result
344	1,950	0	1	$Mn(OH)_2$ MnO Mn	$Mn(OH)_2$ $Mn(OH)_2$ and tr. MnO β-MnO_2
375	14,000	0	2	Mn MnOOH	$Mn(OH)_2$ Mn_3O_4 (very poor)
369	21,600	0	2	Mn MnO $Mn(OH)_2$	$Mn(OH)_2$ $Mn(OH)_2$ $Mn(OH)_2$
363	21,000	0	1	Mn $Mn(OH)_2$	$Mn(OH)_2$ $Mn(OH)_2$ and tr. Mn_3O_4
395	27,000	0	1	Mn MnO $Mn(OH)_2$	$Mn(OH)_2$ MnO and $Mn(OH)_2$ Mn_3O_4
404	32,000	0	2	Mn MnO (Mn(OH)	$Mn(OH)_2$ $Mn(OH)_2$ and tr. MnO Mn_2O_3
405	35,000	0	1	Mn $Mn(OH)_2$ MnO	$Mn(OH)_2$ $Mn(OH)_2$ Mn_3O_4
417	51,000	0	$\frac{1}{6}$	Mn MnO $Mn(OH)_2$	$Mn(OH)_2$ $Mn(OH)_2$ $Mn(OH)_2$ and Mn_3O_4
428	44,000	0	1	Mn MnO $Mn(OH)_2$	MnO MnO and tr. $Mn(OH)_2$ MnO and tr. $Mn(OH)_2$
438	44,000	0	1	Mn MnO $Mn(OH)_2$	MnO MnO and tr. $Mn(OH)_2$ MnO and tr. $Mn(OH)_2$
400	25,000	0	1	Mn MnO $Mn(OH)_2$	MnO MnO and $Mn(OH)_2$ Mn_2O_3
400	14,500	0	2	Mn	MnO
400	10,000	0	2	Mn MnO	MnO MnO
368	2,600	0	1	Mn MnO $Mn(OH)_2$	MnO MnO and $Mn(OH)_2$ Mn_3O_4
338	1,200	0	2	Mn MnO $Mn(OH)_2$	MnO and Mn_3O_4 MnO and $Mn(OH)_2$ Mn_3O_4

Abbreviation: β-MnO_2=pyrolusite.

The dissimilarity of structural products could undoubtedly account for a greater difference in the energetics involved in such a transformation than could be attributed to differences in cation size or type.

However, where the breakdown involves largely the formation of water from (OH) groups the comparison may still show useful results. Thus, the Al-diaspore to corundum transformation is again at a much higher temperature than the corresponding iron one, and above the Ga one, reflecting the influence of polarizability. The stronger the metal-oxygen bond, the weaker the O-H bond and lower the decomposition temperature. The Sc^{3+} and Mn^{3+} phases should have somewhat higher decomposition temperatures than the Ga^{3+} and Fe^{3+} analogues reflecting the weakening of the metal-oxygen bond due to increased size of the cation. This is borne out experimentally.

Acknowledgments

This research was supported by the Chemical Physics Branch of the Signal Corps Engineering Laboratories. We have also had the benefit of the extensive research on the manganese oxides at these laboratories under Dr. S. B. Levin, H. Kedesdy and W. Nye.

References

1. Bystrom, Ann Marie (1949), The Crystal Structure of Ramsdellite, an Orthorhombic Modification of MnO_2: *Acta Chemica Scand.*, **3,** 163–173.
2. Collin, R. J., and Lipscomb, W. N. (1949), The Crystal Structure of Groutite, $HMnO_2$: *Acta Cryst.*, **2,** 104–106.
3. Feitknecht, W. and Marti, W. (1945), Über die Oxydation von Mangan (II) Hydroxyd mit molecularem Sauerstoff: *Helv. Chim. Acta*, **28,** 129–148.
4. Feitknecht, W. and Marti, W. (1945), Über Manganite und Kunstlicken Braunstein: *Helv. Chim. Acta*, **28,** 149–156.
5. Harker, R. I. (1958), The System MgO-CO_2-A and the Effect of Inert Pressure on Certain Types of Hydrothermal Reaction: *Am. J. Sc.*, **256,** No. 2, 128–138.
6. Kissinger, H. E., McMurdie, H. F. and Simpson, B. S. (1956), Thermal Decomposition of Manganous and Ferrous Carbonates: *J. A. Cer. Soc.*, **39,** 168–172.
7. Majumdar, A. J. and Roy, R. (1956), The System CaO-Al_2O_3-H_2O: *J. Am. Cer. Soc.*, **39,** 434–442.
8. Moore, T. E., Ellis, M. and Selwood, P. W. (1950), Solid Oxides and Hydroxides of Manganese: *J. A. Chem. Soc.*, **72,** 856–866.
9. Klingsberg, C., The System Mn-O-OH: Ph.D. Dissertation, The Pennsylvania State University, Jan. 1958.
10. Partington, J. R., General and Inorganic Chemistry: Macmillan and Co. Ltd. (1949).
11. Roy, R. and Osborn, E. F. (1952), Some Simple Aids in Hydrothermal Investigation of Mineral Systems: *Ec. Geol.*, **47,** 712–721.
12. Roy, D. M. and Roy, R. (1957), A Re-determination of Equilibrium in the System MgO-H_2O and Comments on Earlier Work: *Am. J. Sc.*, **255,** 573–582.
13. Roy, R. and Tuttle, O. F., "Investigations under Hydrothermal Conditions," a chapter from Physics and Chemistry of the Earth: vol. I, 138–180, Pergammon Press, (1956).

Manuscript received November 13, 1959.

HAIWEEITE, A NEW URANIUM MINERAL FROM CALIFORNIA

T. C. McBURNEY,* *Los Angeles, California,* AND JOSEPH MURDOCH,
University of California, Los Angeles, California.

ABSTRACT

A hydrous calcium uranium silicate, found near the Haiwee Reservoir in the Coso Mountains, California, has been determined as a new mineral and named haiweeite, from the locality.

It occurs as spherulitic aggregates, or single flake-like grains, on fracture surfaces in granite and in voids of the adjacent lake bed deposits. It is pale yellow to greenish yellow in color; hardness 3.5; specific gravity 3.35; luster pearly. A chemical analysis gives it the the following formula: $CaO \cdot 2UO_3 \cdot 6SiO_2 \cdot 5H_2O$. Optically it is biaxial negative, with 2V about 15°; the acute bisectrix is nearly normal to the broad surface of the blade-like grains {100}. Dispersion is strong, with $r \rightarrow v$. The spherules from the granite are in general made up of two components, of which the inner has higher indices of refraction, and may be considered to be meta-haiweeite. The outer shell is made up of haiweeite, with indices α 1.571, β 1.575, γ 1.578.

X-ray study of minute flakes shows that the mineral is monoclinic(?) with the following (approximate) cell-dimensions:

$$a_0 = 15.4 \text{ Å} \qquad b_0 = 7.05 \text{ Å} \qquad c_0 = 7.10 \text{ Å} \qquad \beta = 107°52'$$

Space is probably $P2/c$—C_{2h}^4.

Haiweeite was found in the Coso Mountains, California, just above the Haiwee Reservoir, for which it has been named. It occurs as a sparse coating of spherulites either on fracture surfaces of granite, or in voids of the neighboring loosely consolidated lake bed deposits. In the granite occurrence there is locally an additional coating, associated with the spherulites, of minute crystalline flakes. The spherulites show the usual radial structure, made up of minute, blade-like grains, with pearly luster on the broad surfaces. In color haiweeite is pale yellow to greenish yellow, fluorescing weakly to dull green. Hardness 3.5; specific gravity, determined in Clerici solution, close to 3.35; cleavage good on {100}.

Optically, haiweeite is biaxial negative, a nearly centered acute bisectrix figure on {100} (the broad faces) showing a 2V of about 15°; dispersion is strong, with $r > v$; not visibly pleochroic; extinction appears to be essentially parallel to elongation (c), on the {100} face.

Examination shows that the spherulites from the granite are made up of two minerals, one composing the center, the other the outer border. The inner has considerably higher indices than the outer. The two are too intimately intergrown for any separation to be made, but on igniting the mineral from the lake beds at a low red heat, its indices are raised to the value of the inner mineral, whereas they were originally identical

* Spectro-chemist, Smith-Emery Co.

Table 1. Refractive Indices of Haiweeite and "Meta-Haiweeite"

From granite		From lake beds	
Inside of spherule (meta-haiweeite)	Outside of spherule	Fresh	Ignited
α 1.611	1.571	1.571	1.611
β 1.620	1.575	1.575	1.620
γ 1.645	1.578	1.578	1.645

with those of the outer portion. The respective indices of refraction for the two minerals, and for the ignited part, are given in Table 1.

This change in index values for the ignited material, to agreement with the inner mineral, would indicate a difference in water content, and suggest a relationship between the two like that between torbernite and metatorbernite, for instance. This inner mineral may thus be tentatively considered to be meta-haiweeite.

The chemical analysis is the average of four determinations, adjusted to 100% after deduction of insolubles, mainly quartz. The formula, as calculated from this analysis, as nearly as may be comes out as follows:

$$CaO \cdot 2UO_3 \cdot 6SiO_2 \cdot 5H_2O$$

In Table 2 are shown the average analysis, and the percentages as calculated from the proposed formula. Spectroscopic analysis was used to check the details of the chemical analysis. Spectroscopic traces of Na, K, Al, Fe, Ti, Mg, and Ba, were noted, but none in sufficient amount to require consideration in the calculation of the analysis.

X-ray Study

X-ray powder photographs have been taken of both occurrences of

Table 2. Chemical Analysis of Haiweeite

	I	II
CaO	5.4	5.2
UO_3	52.8	53.0
SiO_3	33.1	33.4
H_2O	8.7	8.4

I. Average of four analyses, adjusted to 100% after deduction of insoluble, mainly quartz. T. C. McBurney, analyst.

II. $CaO.2UO_3.6SiO_2.5H_2O$.

haiweeite, and of the ignited mineral from the lake beds, with the following results:

Patterns of the two types of occurrence, not ignited, show essentially identical spacings and intensities, indicating that the core mineral with higher indices, was not present, at least in the sample selected, in amount enough to produce a visible overlay of another pattern. The ignited material, however, with identical indices to those of the core, produced a definitely different pattern. The three patterns are shown in the accompanying Table 3. The ignited pattern shows essentially the same type of differences from the others as those between torbernite and metatorbernite.

A small sliver from one of the spherulites was carefully selected and mounted with its elongation, taken as the c direction, as the axis of rotation. About this axis were taken a rotation photograph and Weissenberg photographs of the equator and first layer. The rotation photographs showed a fair alignment, but with indication of multiple crystals, even in the small flake selected, though with essentially parallel orientations in the c direction. The spacing in this direction has an average value of 7.1 Å for c_0, with very good agreement between values for three layer lines.

Weissenberg photographs, equator and first layer, involved very long exposures and were, even so, much less satisfactory, though showing a fair grouping of orientation of the multiple crystals about b. The spots on the film were elongated streaks fading in intensity in either direction. By taking readings on the points of greatest intensity in these streaks, it was possible to make a construction showing a fairly consistent pattern, rectangular or nearly so, with a measurable offset on the first layer. The symmetry is probably monoclinic, but may be triclinic. The value of b_0 was calculated from several orders of $\{0k0\}$, and a_0 was estimated by scaling off the position of $\{h00\}$. Beta was calculated from the offset of the pattern on the first layer. The cell dimensions thus calculated, and beta are as follows:

$$a_0 = 15.44 \text{ Å} \qquad b_0 = 7.05 \text{ Å} \qquad c_0 = 7.10 \text{ Å} \qquad \beta = 107°52'$$

The value of c_0 may be considered as fairly good, but b_0 is an approximation and a_0 even less reliable. Beta should be reasonably good. Observed extinction is $h0l$ with l odd, so that the space group is probably $P2/c$ (C_{2h}^4). Other possibilities are $P2/m$, $P2_1/m$, $P2$.

No crystals were developed enough to show even observable faces, except that the broad faces are apparently $\{100\}$.

Acknowledgments

For some of the optical determinations the writers are indebted to W. Harold Tomlinson, Petrographic Laboratory, Springfield, Pa.,

TABLE 3. *X*-RAY POWER PATTERNS OF HAIWEEITE AND "META-HAIWEEITE"
Copper radiation, Ni filter, CuK_α 1.5418 Å

Haiweeite				Lake bed mineral ignited (meta-haiweeite)	
from granite		from lake bed			
d	I	*d*	I	*d*	I
9.14	10	9.26	10	8.81	5
8.05	2	7.97	2	7.97	½
7.05	4	7.09	3	7.31	½
5.53	2	5.54	2	6.98	10
5.06	1	5.06	1	5.85	5
4.90	½	—		4.54	4
4.556	6	4.53	8	3.81	2
4.42	6	4.41	5	3.52	5
3.82	2	3.80	1	3.28	4
—		3.64	½	3.16	5
3.54	4	3.54	3	3.00	3
3.30	3	3.30	3	2.90	5
3.19	5	3.18	4	2.78	½
3.106	5	3.00	3	2.38	2
2.905	3	2.904	2	2.36	2
2.81	1	2.808	½	2.268	1
2.62	2	2.616	3	2.22	½
2.506	½	2.503	½	2.18	½
2.393	2	2.386	2	2.11	½
2.28	2	2.28	2	2.08	½
2.21	1	2.22	2	1.982	½
—		2.188	2	1.963	½
2.11	1	2.12	½	1.892	½
		2.096	1	1.772	1
—		2.07	½	1.721	1
1.979	1	2.01	1	1.680	½
1.923	1	1.923	1	1.648	½
1.898	1	1.892	1	1.585	½
1.854	½	1.852	1	1.546	1
1.829	1	1.825	1		
1.781	1	1.781	1		
1.732	1	1.736	1		
1.686	1	1.679	1		
1.659	½	1.650	1		
1.628	½	1.626	½		
1.598	1	1.592	1		
1.559	1	1.558	1		
—		1.526	½		
1.492	½	1.493	½		
1.454	½	1.454	½		

and for suggestions as to the adjustment of the formula to Dr. Michael Fleischer, U. S. Geological Survey, Washington, D. C. Elimination of the chance that this mineral might be an earlier known one was made by comparison with the manuscript of a publication by Clifford Frondel and others: "X-ray powder pattern data of uranium and thorium minerals."

Manuscript received November 15, 1958.

THE OPTICAL MINERALOGY, CHEMISTRY, AND *X*-RAY CRYSTALLOGRAPHY OF TEN CLINOPYROXENES FROM THE PENNSYLVANIA AND DELAWARE PIEDMONT PROVINCE

DORITA A. NORTON,* *Department of Geology, Bryn Mawr College*

AND

WALTER S. CLAVAN, *Whitemarsh Research Laboratories, Pennsalt Chemicals Corp., Philadelphia 18, Pa.*

ABSTRACT

Chemical, *x*-ray crystallographic, and optical properties of ten clinopyroxenes from rocks characteristic of the Pennsylvania and Delaware Piedmond Province have been determined and are reported in tabular form. Theoretical considerations and the presence of persistent unidentified reflections on diffractometer curves suggest that chemically complex clinopyroxenes are substructurally different from diopside. Differences between observed optical properties and properties predicted from chemical composition are due to differences between assumed and actual amounts of minor oxides present.

Geochemical relationships between clinopyroxenes and their coexisting orthopyroxene indicate that the samples studied here are of igneous origin. Subsequent metamorphism may have resulted in the introduction of Mg, the modification of pyroxene properties, and the establishment of equilibrium between pyroxene pairs.

INTRODUCTION

A study of the complex silicate minerals of the rocks of the Piedmont Province in Pennsylvania and Delaware was initiated by Rosenzweig's (1954) paper on hornblendes and Clavan's (1954) paper on hypersthenes. It was the purpose of these detailed mineralogical studies to compile for the complex silicates mentioned above optical, chemical and *x*-ray diffraction data, which at a later date could be coordinated with petrologic, structural and geochemical information, in the hope of throwing some light on the genesis and evolution of the metamorphic rocks which contained them.

This paper is a presentation of similar data for ten clinopyroxenes from the same metamorphic rocks. Optical, chemical and *x*-ray crystallographic properties have been determined and are tabulated. In addition to the presentation of detailed mineralogical information, geochemical ideas are advanced which, it is hoped, will contribute to a better understanding of the metamorphic rocks of the Piedmont Province.

GENERAL DESCRIPTION OF CLINOPYROXENE-BEARING ROCKS

The clinopyroxenes of this paper come from rock types which are typical of the Pennsylvania and Delaware Piedmont Province. In these

* Present address: Materials Analysis Dept., The National Cash Register Co., Dayton 9, Ohio.

metamorphic gabbros, norites, diorites and granites, it is rare that all three complex silicates, clinopyroxene, orthopyroxene, and hornblende, are present in quantities large enough for separation. Whenever possible, however, specimens which contained at least two of these were selected for study. A description of the samples chosen is given below. Table 1 gives volumetric analyses.

35-1N —Chester 16612.* Fine-grained massive gabbro xenolith in granite gneiss. Found as boulders in creek just north of Upper Bridge, Crum Creek Reservoir.

35-5N —West Chester 92755. Medium fine-grained hornblende norite showing faint foliation. Found as boulders in a field 300 yards west of road, 0.1 mile north of cross-

Table 1. Volumetric Analyses

%	35-1N	35-5N	35-6N	35-8N	35-9N	35-13N	35-19N	35-24N	35-25N	35-32N
Clinopyroxene	21	9	7	9	23	16	23	3	18	16
Hypersthene	15	10	10	5	9	29	17	—	—	49
Hornblende	—	21	3	—	—	—	13	4	—	5
Plagioclase	An 52	An 55	An 56	An 45	An 55	An 44	An 75	An 25	An 26	An 80
	60	55	64	56	64	44	46	11	4	28
Potash Feld.	—	—	—	—	—	—	—	Microcline 13	—	—
Quartz	—	—	10	26	—	—	—	66	26	—
Biotite	—	—	—	—	—	1	—	—	49	—
Garnet		—	—	—	—	6	—	—	—	—
Magnetite (plus Ilmenite)	4	5	5	3	4	4	<1	1	—	2
Serpentine	—	—	—	—	—	—	—	—	—	<1
Chlorite	—	<1	—	—	—	<1	—	—	—	
Sphene	—	—	—	—	—	—	—	2	1	—
Apatite	<1	<1	<1	<1	<1	<1	—	—	1	—
Zircon	—	—	—	—	—	—	—	—	<1	—

roads at Tallyville (Route 202). A part of the variable metagabbro body called the Wilmington gabbro.

35-6N —Wilmington 31268. Medium-grained massive quartz norite. Found in an outcrop in the park at Franklin and Sycamore Streets, Wilmington, Delaware. A part of the Wilmington gabbroic mass.

35-8N —Wilmington 32237. Fine-grained quartz-diorite. Found as the predominant rock type in the Alapocas Quarry on the east bank of Brandywine Creek in Wilmington, Delaware. A part of the Wilmington gabbroic mass.

35-9N —Wilmington 32237. Fine-grained massive gabbro. Found in the same quarry as 35-8N as dikes intrusive into quartz-diorite.

35-13N —Norristown 85826. Medium-grained hypersthene diorite. Found in the lower quarry wall on the west side of Radnor Quarry. A part of the Baltimore gneiss.

35-19N—West Chester 96413. Coarse-grained hornblende-eucrite. Found in boulders on the south side of Faulk Road, 1.5 miles northeast of the intersection of U. S. Route 202.

* The numbers represent a grid index on the 15 minute quadrangle maps for the area.

35-24N –Chester 43216. Medium-grained granite gneiss. Found as the predominant rock type in the Lima Quarry. A part of the Lima granite gneiss.

35-25N—Chester 43216. Fine-grained quartz-diorite showing faint gneissic banding. Occurs as a xenolith in the Lima granite gneiss.

35-32N – Chester 22476. Coarse-grained eucritic norite. Found as boulders in a field 800 feet south of West Chester Pike at the Dinwoody Home. Part of an ultrabasic intrusion into the Wissahickon formation.

Sample Preparation

Most of the pyroxenes used in this study had already been separated by Rosenzweig (1954) and Clavan (1954) in their studies of hornblendes and hypersthenes from southeastern Pennsylvania and Delaware, and details of separation have been given by Rosenzweig (1954). In cases where more clinopyroxene-separate was needed, or other clinopyroxene-bearing rocks were studied, Rosenzweig's separation scheme was followed.

In general, the rocks were crushed, using a small jaw crusher, a roller mill, and a ball mill, until they were fine enough to pass through a 100 mesh sieve. The 100 to 150 mesh portion was used for separation, particles of this size being for the most part monomineralic. Before separation was begun, however, this portion was wet screened on a 200 mesh sieve to remove dust and then rinsed with acetone and rapidly dried to avoid oxidation. Strongly magnetic particles were next removed with a hand magnet.

Because of the relatively large volumes of rock needed to obtain a sufficient amount of clinopyroxene-separate for chemical, optical, and x-ray determinations, the initial separation was accomplished using the Frantz isodynamic separator. In this way concentrates containing clinopyroxene, hornblende, and biotite were obtained and the final separation and purification was made using heavy liquids.

The purity of the clinopyroxene-separates obtained was tested by making grain counts on two balsam grain mounts of each sample. The samples range from 96.6% to 99.8% pure.

Principles of the Chemical Analysis

Most of the elements were determined by the methods outlined in the previous paper (Clavan, 1954) and are not repeated here. These include: water, silica, ferrous oxide, chromic oxide, ferric oxide, aluminum oxide, titanium dioxide, manganous oxide and nickel oxide. In addition, the determination of specific gravity and the decomposition of the sample for determining many of the elements were carried out in the same way.

However, since these minerals are high in calcium and lower in magnesium and iron, the methods for calcium and magnesium had to be changed.

Also, since the time of the previous analyses, a new method was brought forth for the determination of potassium, which made the analyses for both potassium and sodium simpler and shorter.

The methods for calcium, magnesium, sodium, and potassium are outlined below.

Procedure for the Chemical Analysis

1. *Decomposition of the sample for the determination of sodium and potassium*

Weigh a 1 gram sample into a platinum dish and treat with 5 ml. of nitric acid, 10 ml. of perchloric acid and 10 ml. of hydrofluoric acid. Evaporate the solution to half the volume and add 10 ml. of hydrofluoric acid. Evaporate to fumes of perchloric acid and continue heating for 15 minutes. Cool the solution, transfer with water to a Pyrex beaker and evaporate to dryness. Bake the residue on a hot plate until no more fumes of perchloric acid are noted. Heat the sides of the beaker with a Bunsen burner to remove the last traces of perchloric acid.

Cool, add 50 ml. of a 10 per cent ammonium hydroxide solution and boil for 10 minutes. Filter and wash with 10 per cent ammonium hydroxide. Make the filtrate just acid with hydrochloric acid, cool, transfer to a 250 ml. volumetric flask and dilute to the mark.

2. *Sodium*

Pipet 100 ml. of the solution into a beaker, evaporate to dryness on the steam bath, add one ml. of water and 10 ml. of zinc uranyl acetate solution and stir well. Allow to stand one hour and filter on a weighed sintered glass crucible. Wash with small portions of the precipitating agent, five 2 ml. portions of ethyl alcohol saturated with the precipitate and finally with a small amount of acetone. Place the crucible in the balance case for 15 minutes and reweigh. The increase in weight is sodium zinc uranyl acetate with six molecules of water of crystallization and is calculated as sodium oxide.

3. *Potassium*

Pipet 100 ml. of the solution into a beaker and evaporate to dryness. Add 20 ml. of aqua regia and evaporate to dryness. Repeat with another 20 ml. of aqua regia. Dilute to 50 ml., add 2 ml. of hydrochloric acid and cool in ice. Add 25 ml. of a 1 per cent aqueous solution of sodium tetraphenyl boron which had been cooled to 0° C. Stir occasionally for 5 to 10 minutes while in the ice bath. Filter through a weighed sintered glass crucible and wash with 3–10 ml. portions of a freshly prepared saturated solution of potassium tetraphenyl boron. Dry at 100° C. for one hour and reweigh. Calculate as potassium oxide

4. *Calcium*

Pipet a 100 ml. aliquot from the 500 ml. volumetric flask (which contains 2 grams of sample decomposed by hydrofluoric and perchloric acids) into a beaker and dilute to 250 ml. Add 2 grams of ammonium chloride, heat the solution almost to boiling and add ammonium hydroxide until it is just alkaline to litmus. Add 5 ml. of saturated bromine water, test the solution to make sure it is still ammoniacal and boil for 15 minutes. Filter the precipitate while the solution is still hot, wash well with a 3 per cent ammonium chloride solution, dissolve the precipitate off the paper with hot dilute hydrochloric acid and reprecipitate as above. Discard the precipitate and combine the filtrates. Reduce the volume of the filtrates to 250 ml., add 2 grams of ammonium oxalate and then add hydrochloric acid until the precipitate dissolves. Heat the solution almost to boiling, add 2 drops of methyl red indicator and ammonium hydroxide until the solution is just alkaline. Place on the steam bath overnight.

Cool, filter and wash with a 3 per cent ammonium oxalate solution. Save the filtrate. Dissolve the precipitate off the paper with hot dilute hydrochloric acid and reprecipitate as above. Combine the filtrates and save for the determination of magnesium. Place the precipitate in a weighed platinum crucible, dry, ignite over 950° C., cool and reweigh. The increase in weight is calcium oxide.

5. *Magnesium*

Reduce the volume of the combined filtrates from the determination of calcium to 250 ml. Make just acid with hydrochloric acid and add 0.5 grams of diammonium hydrogen phosphate. Cool to below room temperature, add ammonium hydroxide dropwise until the solution is just basic, allow the magnesium to precipitate and then add an excess of 30 ml. of ammonium hydroxide. Stir the solution occasionally during the next 30 minutes and allow to stand overnight. Filter the precipitate through paper, wash with 1:20 ammonium hydroxide, dissolve off the paper with 1:10 hydrochloric acid and reprecipitate as above. Filter this precipitate through a weighed porcelain filtering crucible, wash with 1:20 ammonium hydroxide, dry and ignite for one hour. Cool and reweigh as magnesium pyrophosphate. Calculate as magnesium oxide.

Chemical Data

The chemical compositions and specific gravities of the clinopyroxenes studied here are reported in Table 2. SiO_2 is high and fairly constant. Other major constituents, CaO, MgO, FeO, are variable. Variability is also shown by the minor constituents, especially Al_2O_3, Fe_2O_3, Na_2O, TiO_2, and MnO. Specific gravities range from 3.303 to 3.420 and are roughly related to mole per cent ferrous silicate (Fig. 1). In order to facilitate chemical and petrological calculations, weight per cents were converted to atomic ratios in Tables 5–14.

The theoretical formula for clinopyroxene (Berman, 1937) is W (X, Y) Z_2O_6, four such units belonging to a unit cell. In all cases the major W,

Table 2. Chemical Analyses and Specific Gravities

	35-1N	35-5N	35-6N	35-8N	35-9N	35-13N	35-19N	35-24N	35-25N	35-32N
SiO_2	52.67	51.03	51.00	50.17	51.55	50.95	51.43	50.77	52.37	50.00
Al_2O_3	1.42	2.40	2.49	2.38	2.44	3.49	2.63	1.65	1.38	3.05
Fe_2O_3	1.23	1.88	2.03	3.39	2.03	1.40	1.70	4.46	3.32	1.50
FeO	4.34	8.97	9.31	8.05	7.28	9.52	5.92	8.69	7.02	5.87
MgO	15.59	13.11	12.53	13.22	13.65	12.22	14.83	10.14	12.59	15.60
CaO	23.81	21.75	21.08	21.10	21.73	20.55	22.18	20.70	21.46	22.42
Na_2O	0.45	0.43	0.47	0.49	0.52	0.70	0.44	1.41	1.19	0.18
K_2O	0.00	0.00	0.00	0.00	0.00	0.24	0.00	0.14	0.24	0.00
H_2O	0.20	0.24	0.37	0.18	0.26	0.24	0.31	0.22	0.18	0.27
TiO_2	0.14	0.28	0.27	0.28	0.31	0.36	0.28	0.28	0.19	0.40
Cr_2O_3	0.00	0.00	0.00	0.00	0.01	0.06	0.04	0.01	0.05	0.07
NiO	0.00	0.01	0.01	0.01	0.01	0.01	0.01	0.01	0.02	0.03
MnO	0.13	0.35	0.45	0.34	0.24	0.19	0.19	1.35	0.46	0.18
Total	99.98	100.45	100.01	99.61	100.03	99.93	99.96	99.83	100.47	99.57
Sp.Gr.	3.303	3.384	3.385	3.382	3.358	3.364	3.332	3.420	3.364	3.324

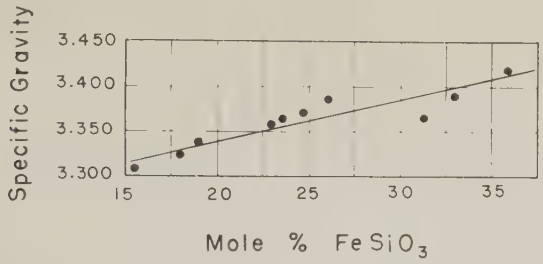

FIG. 1. Relation between specific gravity and mole per cent ferrous silicate.

X and Y ions are Ca^{+2}, Mg^{+2}, and Fe^{+2} respectively, but limited substitution usually takes place. In general:

$$W = Ca^{+2}, Na^{+1}$$
$$X = Mg^{+2}, Fe^{+2}, Mn^{+2}, Ni^{+2}$$
$$Y = Al^{+3}, Fe^{+3}, Cr^{+3}, Ti^{+4}$$
$$Z = Si^{+4}, Al^{+3}$$

In some of the possible substitutions listed (Na^{+1} for Ca^{+2}, Ti^{+4} for Al^{+3}, Al^{+3} for Si^{+4}, and elements of the Y group for X) electrical neutrality will not be maintained unless there is a distribution of substituting ions so that their charges will balance one another. The number of ions going into each group must satisfy (*a*) the electrical requirement that the -12 charge of the six O^{-2} ions is neutralized by the sum of the ionic charges in the W, X, Y, Z groups, and (*b*) the structural requirement that each of the (W) and (X, Y) groups, which have coordinations of 8 and 6 respectively, must contain two ions.

Steps for determining the correct proportion of ions in each group given by Hess (1949) were followed. Each of these steps corresponds to a column in Tables 5–14.

1. Na and Cr ions are combined (1:1) to make $NaCrSi_2O_6$. If K ions are present, they are united with Na ions.
   a. If Na is in excess of Cr, see steps 2 and 3.
   b. If Cr is in excess of Na, see step 5.
2. If some Na ions are left over, they are combined with Fe^{+3} ions (1:1) to make $NaFeSi_2O_6$.
   a. If Na is in excess of Fe^{+3}, see step 3.
   b. If Fe^{+3} is in excess of Na, see step 6.
3. If there are still some Na ions left, they are combined (1:1) with Al ions to make $NaAlSi_2O_6$.
4. Ti ions are combined with Al ions (1:2).
5. Cr ions are combined with Al ions (1:1).

6. Fe^{+3} ions are combined with Al ions (1:1).
7. Of the remaining Al ions, one-half is allotted to each of the Y and Z groups.

From the theoretical formula it can be seen that the ratio of cations to oxygen is 2:2:6. Hence if the chemical analysis is accurate and the sample pure, (a) the total number of ions in the Z group will theoretically equal the total number of ions in the W and (X, Y) groups, and (b) the ratio of (W, X, Y) and Z to the total number of O^{-2} ions will be 2:2:6. This is tested by first dividing the total number of oxygens by six, and then dividing the resulting figure into the total number of ions in Z and (W, X, Y) respectively. If the analysis is satisfactory,* the result of these divisions will equal $2.00 \pm .02$. The columns entitled "Cations to Six O" in Tables 5–14 show the results of this test. It can be seen that all the analyses are quite satisfactory with the possible exception of 35-32N. Although this sample is the purest, 99.8%, it appears to have the greatest deviation, +.07. The large deviation of +.06 in the case of 35-6N is explained by the fact that this sample is least pure, 96.6%.

Ca:Mg:Fe ratios have been calculated and are given in Tables 5–14. The procedure of Hess is again followed, so that in this calculation Fe^{+2} and Mn are added to Fe^{+3}, and Ni is added to Mg. The amount of Al replacing Si in the chains is given below the Ca:Mg:Fe ratios.

X-Ray Diffraction Data

X-ray diffractometer curves for each sample were obtained using a wide range Philips geiger counter *x*-ray diffractometer with filtered copper K radiation.† Samples were scanned at the rate of 1° per minute, and for all runs the scaler was set at 2×, the multiplier at 0.6, and the time constant at 8. Table 3 is a representative example of the *d*-spacings and relative intensities of peaks calculated from these curves.

Indices were determined by comparing observed $\sin^2 \theta$ values with $\sin^2 \theta$ values calculated from the theoretical formula for a monoclinic unit cell using the cell dimensions and axial angle determined by Warren and Bragg (1928) for diopside.

The calculation of $\sin^2 \theta$ values for planes satisfying the space group conditions (C_{2h}^6) was performed on an IBM 602A computer. The indices of reflections for the clinopyroxenes were obtained by comparison of calculated $\sin^2 \theta$ values with $\sin^2 \theta$ values obtained from 2θ readings taken from the spectrometer curves. Where good agreement was found, the indices used to determine the calculated $\sin^2 \theta$ values were assigned to the observed reflection.

* A satisfactory silicate analysis is accurate to 2%.

† 40 KV at 17 MA.

TABLE 3. EXAMPLE OF d-SPACINGS AND SPECIFIC GRAVITIES
Sample 35-1N

d (Å)	I/I_0	d (Å)	I/I_0
3.332	5	1.589	5
3.229	95	1.550	10
3.115	5	1.525	5
2.991	100	1.503	5
2.949	85	1.485	5
2.891	30	1.422	10
2.568	10	1.408	5
2.518	40	1.386	5
2.302	10	1.374	5
2.206	5	1.328	10
2.149	20	1.282	5
2.132	25	1.265	5
2.108	15	1.248	5
2.036	10	1.212	5
2.014	5	1.196	5
1.859	5	1.173	5
1.836	10	1.0745	10
1.772	5	1.0718	10
1.754	10	1.0690	10
1.674	5	1.0646	5
1.650	10	1.0418	5
1.624	20	1.0298	5
1.620	20	1.0183	5

Figure 2 shows the actual relationship between twice an angle (2θ) and the sine of the angle squared ($\sin^2\theta$). Figure 3 is based on this relationship, and indicates the amount of deviation of 2θ for various portions of the $2\theta - \sin^2\theta$ curve (Fig. 2) corresponding to a deviation in calculated and observed $\sin^2\theta$ values. Taking into account minor shifts of peaks, the maximum $\Delta 2\theta$ acceptable here for a spectrometer chart running at the rate of 1° per minute is 0.3°. Hence the agreement between calculated and observed $\sin^2\theta$ values may be tested by finding the difference between them ($\Delta\sin^2\theta \times 10^{-4}$) and then using the curves of Fig. 3 to find the corresponding $\Delta 2\theta$. If $\Delta 2\theta$ is less than 0.3°, the reflection is given the indices from which the calculated $\sin^2\theta$ value was derived.

OPTICAL DATA

With few exceptions the methods for determination of the optical properties of clinopyroxenes given by Hess (1949) were used in this investigation. In order to facilitate comparison of the optical and chemical properties of the clinopyroxenes of this study with those of the clino-

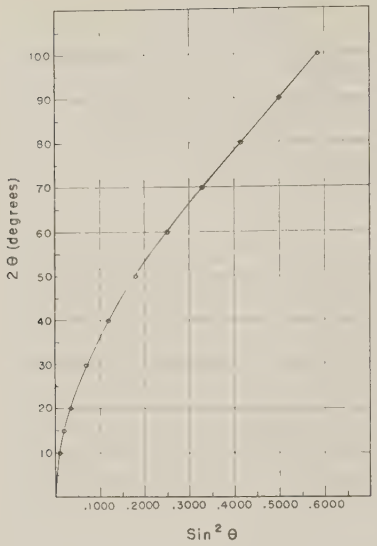

FIG. 2. Relation between twice an angle and the sine of the angle squared.

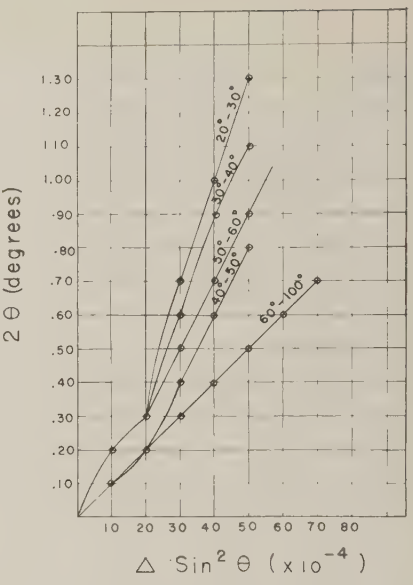

FIG. 3. Relation between 2θ and $\sin^2 \theta$.

pyroxenes studied by Hess, his basic form of reporting these values has been followed (Tables 24–33).

Optic Angle

Optic angle determinations were made using a four-axis universal stage. Grains were selected whose optic plane could be made vertical, and 2V was measured directly by rotation from one "optic eye" to the other. The 2V values were corrected for the refractive index of the hemispheres and for the Y-index of the particular clinoypyroxene being measured.

Refractive Indices

Of the indices given for each clinopyroxene only the Y index actually has been measured, X and Z having been calculated from birefringence and optic angle values. {100} parting tablets were used for the determination of Y. These are recognized by their low birefringence, and, if bounded by cleavage planes, by parallel extinction. In such grains the optic plane is upright and an optic axis emerges about 20° from the vertical, hence an off-center optic axis figure will be obtained in convergent light. When the isogyre is rotated to the E-W position, Y, the optic normal is N-S, and the grain is in the proper orientation to determine the X-index.

All refractive index measurements were made in white light at 25° C. Each clinopyroxene was first bracketed between two liquids whose refractive indices were .001 apart. Liquids at intervals of .0002 within these groups were prepared as needed, using a Pulfrich refractometer with a sodium light and constant temperature (25° C.), thus giving the final Y-index value to $\pm .0001$.

Extinction Angle, $Z \wedge C$

The clinopyroxenes of this study did not show twinning or exsolution lamellae, therefore neither of the methods suggested by Hess (1949) for the determination of $Z \wedge C$ could be used. However, two other methods, both of which give results consistent within $\pm 2°$ were used.

A. *Cleavage Method*

Since the precise measurement of $Z \wedge C$ depends on the exact orientation of the clinopyroxene so that {010} is horizontal, the biggest problem is the recognition of grains in which this condition obtains. Grains which lie in this approximate orientation can be recognized by their high birefringence, the birefringence on {010} being the maximum. If the grain should happen to have the {010} direction exactly horizontal, the {110} cleavages will make an angle of 46.5° with vertical, since for clinopyroxene the cleavage angle facing {010} is 93°. Furthermore, in grains in which two sets of cleavages are developed, these will be seen to dip inward at equal angles in opposite directions. Should the clinopyroxene grain be ground so that the surface which is horizontal lies between the {010} and {110} directions, the angle which one of the {110} cleavages makes with vertical will be less than 46.5°, while the angle which the {110} cleavage makes will be greater than 46.5°, the minimum or maximum respectively being reached when the {110} direction is horizontal.

Hence, if a universal stage is used, it is possible to orient grains of clinopyroxene so that their {010} direction is horizontal. This is done in the following way:

1. A grain is located which lies with {010} approximately horizontal. Such a grain may be recognized by its high birefringence, as mentioned above, and by the fact that the cleavage or cleavages will appear broad. The grain is placed so that its cleavage is parallel to the H or the K axis.
2. The height of the thin section is adjusted so that the plane of a selected cleavage will contain either the H or K axis of rotation of the U-stage. This condition obtains when cross hair (N-S for H, E-W for K) seems to lie in the cleavage plane throughout a rotation about H or K.
3. The angle which the cleavage makes with vertical (θ) is measured by rotating the cleavage plane on either H or K until it stands vertical. When the cleavage plane is vertical, it will appear as a sharp, well-defined line.

4. Since θ represents the angle between a cleavage plane and vertical, it also represents the angle of dip of the cleavage plane when the thin section is horizontal. Hence, if the cleavage plane is counter-rotated by an amount $46.5°-\theta$, the {010} direction will be made horizontal.

Once the {010} direction has been made horizontal, Z∧C is measured in the usual way.

B. [001] *Zone Method*

In some of the clinopyroxenes studied, {110} cleavage was absent or poorly developed. In such cases extinction angles were measured in the zone [C01], the maximum extinction angle being that on {010}. The zone [001] is recognized by the general shape of grains and by the fact that the other two cleavages {100} and {010} also lie in this zone. Grains which have {010} nearly horizontal can be recognized by their high birofringence.

A comparison of the extinction angles obtained by the two methods is given below for 35-1N (Table 4).

Table 4. Comparison of Results from Cleavage and Zone Methods of Extinction Angle Measurements

Cleavage Method	Zone Method
37.3	37.3
38.0	37.3
38.6	37.6
38.7	38.6
	38.8

Birefringence

Since the maximum birefringence in clinopyroxene is seen when {010} is horizontal, one of the procedures outlined above was used to orient grains for birefringence measurements. Determinations were made using a Berek compensator with the aid of special slides which are prepared as follows: A mixture of equal parts of clinopyroxene and quartz (crushed to approximately the same size) is poured into a Buehler mount cylinder to form a layer one grain thick on the cylinder bottom. Next, about 3–4 cc. of Transoptic mounting powder is loaded into the cylinder on top of the clinopyroxene-quartz layer, and the piston introduced. The cylinder thus loaded is placed in a Buehler press and subjected to a pressure of 5000 psi.

The surface of the grain mounts containing the clinopyroxene-quartz layer is semi-polished on a lap until the grains show relief and have flat

surfaces. The semi-polished surface is cemented to a glass slide using liquid balsam, and the mount is ground as thin as possible, using a grinding wheel. Further grinding is accomplished with a fine-grade abrasive paper, and grinding is continued until the clinopyroxene-quartz layer is approximately .04 mm. thick, and until the grains show relief and have flat surfaces. The surface is then semi-polished and covered with a cover glass, using liquid balsam.

The method of slide preparation described above insures as nearly as possible the coplanar distribution of clinopyroxene and quartz grains. In making actual retardation measurements, grains not having flat surfaces should be avoided, as such grains will give a retardation for a thickness which is less than the true thickness of the slide at that particular point.

After the {010} retardation of a clinopyroxene grain has been measured, the thickness at this point is determined by measuring the retardation of several neighboring quartz grains. The quartz grains chosen for this purpose must be capable of having their *c*-axis rotated into a horizontal position so that maximum birefringence is obtained. Since the birefringence of quartz is known, retardation can be directly converted to thickness. This thickness value, of course, must be corrected for the angle of tilt of the universal stage. Since in most cases a double tilt was required to make the *c*-axis horizontal, the thickness was corrected by multiplying by the cosine of the angle between the microscope axis and the perpendicular to the inner stage. This angle is obtained by reference to plate 9 in Emmons (1943). The thickness is further corrected by dividing by the cosine of the angle of tilt necessary to make clinopyroxene {010} planes horizontal. Curves given in Winchell (1929) convert the doubly corrected thickness and the retardation values to birefringences.

Chemical Crystallography

The clinopyroxenes studied here gave a number of reflections whose $\sin^2\theta$ values did not agree well enough with calculated $\sin^2\theta$ values to be assigned indices. A number of unidentified lines were also observed by Kuno and Hess (1935) in their paper on the unit cell dimensions of clinoenstatite and pigeonite. Since they obtained excellent agreement between their *d*-spacings and *d*-spacings calculated from their unit cell dimensions, and since the number of unidentified lines was few and their intensities weak, they concluded that the unidentified reflections were due to sample impurity, and that all clinopyroxenes have the same structure as diopide.

One of the unidentified reflections observed in the present study appeared consistently in all the diffraction patterns with the exception of

TABLE 5. 35-1N

Dionside. Chester 14373.
Upper Bridge. Crum Creek Reservoir.

	Wt. %	Atomic Ratios		1 Cr / Na	2 Fe‴ / Na	3 Al / Na	4 2Al / Ti	5 Al / Cr	6 Al / Fe‴	7 Al / Al	Z / Y / W	Cations to Six O
SiO_2	52.67	Si	876								Z	
Al_2O_3	1.42											
Fe_2O_3	1.23	Al	28				4		½	11½	892	1.98
FeO	4.34									12		
MgO	15.59	Fe‴	15		14½				½			
CaO	23.81	Cr	0									
Na_2O	0.45	Fe	60									
K_2O	0.00	Mn	2								WXY	2.03
H_2O	0.20	Ni	0								917	
TiO_2	0.14	Mg	386½									
Cr_2O_3	0.00	Ca	425									
MnO	0.13	Na	14½		14½							
NiO	0.00	K	0									
		Ti	2				2					
	99.98	O	2702									

Indices of Refraction Pleochroism:
nX 1.6791 Nonpleochroic
nY 1.6843 Colorless
nZ 1.7071

Birefringence, x10^4 aver.: 280
262, 270, 272, 290, 308

2V aver.: 50½°
44½°, 43 3/4°, 50°, 51 3/4°, 52°, 52°, 52 3/4°, 53½°, 55¼°

ZAc aver.: 38°
37°, 37½°, 37½°, 37½°, 37½°, 38°, 38½°, 38½°, 38½°, 38 3/4°, 38 3/4°

Specific Gravity: 3.303

$Ca_{47.8}$ $Mg_{43.5}$ $Fe_{8.7}$
% Al in Z = 1.8

Sample purity: 98.6%

TABLE 6. 35-5N

Augite. West Chester. 92755. Tallyville.

	Wt. %	Atomic Ratios		1 Cr / Na	2 Fe‴ / Na	3 Al / Na	4 2Al / Ti	5 Al / Cr	6 Al / Fe‴	7 Al / Al	Z / Y / W	Cations to Six O
SiO_2	51.03	Si	849								Z	
Al_2O_3	2.40											
Fe_2O_3	1.88	Al	47				7		10	15	881	1.99
FeO	8.97									15		
MgO	13.11	Fe‴	24		14				10			
CaO	21.75	Cr	0									
Na_2O	0.43	Fe	125									
K_2O	0.00	Mn	5								WXY	2.02
H_2O	0.24	Ni	0.1								899½	
TiO_2	0.28	Mg	325									
Cr_2O_3	0.00	Ca	388									
MnO	0.35	Na	14		14							
NiO	0.01	K	0									
		Ti	3½				3½					
	100.45	O	2661									

Indices of Refraction Pleochroism:
nX 1.6868 Faintly pleochroic
nY 1.6908 in green.
nZ 1.7125

Birefringence, x10^4 aver. 257
240, 245, 249, 271, 279

2V aver.: 46½°
44°, 44 3/4°, 45°, 45½°, 45 3/4°, 45 3/4°, 46½°, 48½°, 48 3/4°, 48 3/4°, 50¼°

ZAc aver.: 43°
41°, 42°, 42½°, 42 3/4°, 43½°, 43½°, 44½°, 44 3/4°

Specific Gravity: 3.384

$Ca_{44.7}$ $Mg_{37.5}$ $Fe_{17.8}$
% Al in Z = 3.6

Sample purity: 99.3%

TABLE 7. 35-6N

Augite. Wilmington 31268. Wilmington, Delaware.

			1	2	3	4	5	6	7		
						2Al	Al	Al	Al	Z	Cat-
		Atomic Ratios	Cr	Fe'''	Al	Ti	Cr	Fe'''	Al	Y	ions to
			Na	Na	Na					W	Six O
SiO_2	51.00	Si 835								Z 867½	1.99
Al_2O_3	2.49										
Fe_2O_3	2.03	Al 49				6		10½	16		
FeO	9.31								16½		
MgO	12.53	Fe''' 25½		15				10½			
CaO	21.08	Cr 0									
Na_2O	0.47	Fe 129½									
K_2O	0.00	Mn 6									
H_2O	0.37	Ni 0.1								WXY 898½	2.06
TiO_2	0.27	Mg 311									
Cr_2O_3	00.00	Ca 376									
MnO	0.45	Na 15		15		3					
NiO	0.01	K 0									
		Ti 3									
	100.01	O 2618									

Specific Gravity: 3.385

$Ca_{44.3}$ $Mg_{36.7}$ $Fe_{19.0}$

% Al in Z = 3.7

Indices of Refraction Pleochroism:
nX 1.6918 Faintly pleochroic
nY 1.6959 in green.
nZ 1.7210

Birefringence, x10^4 aver.: 292

269, 296, 299, 304

2V aver.: 43 3/4°

41½°, 43°, 43 3/4°, 44°, 44½°, 44½°, 44½°, 45½°

Zʌc aver.: 40½°

39½°, 39 3/4°, 40°, 40°, 40½°, 41½°, 42 3/4°

Sample purity: 96.6%

TABLE 8. 35-8N

Augite. Wilmington 32237. Wilmington, Delaware.

			1	2	3	4	5	6	7		
						2Al	Al	Al	Al	Z	Cat-
		Atomic Ratios	Cr	Fe'''	Al	Ti	Cr	Fe'''	Al	Y	ions to
			Na	Na	Na					W	Six O
SiO_2	50.17	Si 835								Z 875½	1.99
Al_2O_3	2.38										
Fe_2O_3	3.39	Al 47				7		27	01		
FeO	8.05								01		
MgO	13.22	Fe''' 43		16				27			
CaO	21.10	Cr 0									
Na_2O	0.49	Fe 112									
K_2O	0.00	Mn 5									
H_2O	0.18	Ni 0.1								WXY 900½	2.01
TiO_2	0.28	Mg 328									
Cr_2O_3	0.00	Ca 376½									
MnO	0.34	Na 16		16							
NiO	0.01	K 0									
		Ti 3½				3½					
	99.61	O 2640									

Specific Gravity: 3.382

$Ca_{43.5}$ $Mg_{38.0}$ $Fe_{18.5}$

% Al in Z = 4.6

Indices of Refraction Pleochroism:
nX 1.6865 Nonpleochroic
nY 1.6909 Color: green
nZ 1.7119

Birefringence, x10^4 aver.: 254

244, 254, 264

2V aver.: 50½°

48°, 49½°, 50½°, 50½°, 51½°, 54½°

Zʌc aver.: 42°

40½°, 41 3/4°, 42°, 43½°

Sample purity: 97.9%

TABLE 9. 35-9N

Salite. Wilmington 32237. Wilmington, Delaware.

		1	2	3	4	5	6	7		
					2Al	Al	Al	Al	Z	Cat-
	Atomic Ratios	Cr	Fe'''	Al	Ti	Cr	Fe'''	Al	Y	ions to Six O
		Na	Na	Na					W	
SiO_2 51.55	Si 858								Z 890	1.99
Al_2O_3 2.44	Al 48				8			16		
Fe_2O_3 2.03								16		
FeO 7.28										
MgO 13.65	Fe''' 25		17				8			
CaO 21.73	Cr 0.1									
Na_2O_3 0.52	Fe 101									
K_2O 0.00	Mn 3								WXY 892	2.00
H_2O 0.26	Ni 0.1									
TiO_2 0.31	Mg 338									
Cr_2O_3 0.01	Ca 388									
MnO 0.24	Na 17		17							
NiO 0.01	K 0									
	Ti 4				4					
100.03	O 2673									

Specific Gravity: 3.358

$Ca_{45.4}\ Mg_{39.6}\ Fe_{15.1}$

% Al in Z = 3.6

Indices of Refraction
nX 1.6911
nY 1.6951
nZ 1.7167

Pleochroism:
Nonpleochroic
Color: green

Birefringence, x10^4 aver. 256

233, 266, 269

2V aver.: 46 3/4°

42 3/4°, 44 3/4°, 44 3/4°, 45°, 45 3/4°, 46½°, 47°, 48°, 51 3/4°, 52½°

ZΛc aver.: 39½°

38°, 38 3/4°, 39°, 39½°, 40°, 40°, 40½°, 40 3/4°

Sample purity: 98.4%

TABLE 10. 35-13N

Augite. Norristown 85826. Radnor Quarry.

		1	2	3	4	5	6	7		
					2Al	Al	Al	Al	Z	Cat-
	Atomic Ratios	Cr	Fe'''	Al	Ti	Cr	Fe'''	Al	Y	ions to Six O
		Na	Na	Na					W	
SiO_2 50.95	Si 846							3	Z	
Al_2O_3 3.49				11½	9			24½	891	2.02
Fe_2O_3 1.40	Al 69									
FeO 9.52								25		
MgO 12.22	Fe''' 17½		17½							
CaO 20.55	Cr 3/4	3/4								
Na_2O 0.70	Fe 132½									
K_2O 0.24	Mn 3								WXY	
H_2O 0.24	Ni 0.1									
TiO_2 0.36	Mg 303								3 8804	1.99
Cr_2O_3 0.06	Ca 366½									
MnO 0.19	Na 23	3/4	11½	11¼						
NiO 0.01	K 5		5							
	Ti 4½				4½					
99.93	O 2651									

Specific Gravity: 3.364

$Ca_{44.6}\ Mg_{36.8}\ Fe_{18.6}$

% Al in Z = 5.1

Indices of Refraction
nX 1.6858
nY 1.6905
nZ 1.7139

Pleochroism:
Nonpleochroic
Color: green

Birefringence, x10^4 aver.: 281

265, 280, 281, 298

2V aver.: 48°

43½°, 45½°, 46½°, 48½°, 48 3/4°, 48 3/4°, 48 3/4°, 51½°, 51 3/4°

ZΛc aver.: 41°

40°, 40°, 40½°, 41½°, 41½°, 41½°, 42½°

Sample purity: 98.3%

TABLE 11. 35-19N

Salite. West Chester 96413.

			1	2	3	4	5	6	7		
						2Al	Al	Al	Al	Z	Cat-
		Atomic Ratios	Cr	Fe'''	Al	Ti	Cr	Fe'''	Al	Y	ions to
			Na	Na	Na					W	Six O
SiO_2	51.43	Si 856								Z	
Al_2O_3	2.63										
Fe_2O_3	1.70	Al 52	–	–	–	Z	–	$7\frac{1}{2}$	$18\frac{1}{2}$	889	1.99
FeO	5.92								19		
MgO	14.83	Fe''' 21		$13\frac{1}{2}$				$7\frac{1}{2}$			
CaO	22.18	Cr $\frac{1}{2}$	$\frac{1}{2}$								
Na_2O	0.44	Fe 82									
K_2O	0.00	Mn 3								WXY	
H_2O	0.31	Ni 0.1								907	2.03
TiO_2	0.28	Mg 368									
Cr_2O_3	0.04	Ca 396									
MnO	0.19	Na 14	$\frac{1}{2}$	$13\frac{1}{2}$							
NiO	0.01	K 0									
		Ti $3\frac{1}{2}$				$3\frac{1}{2}$					
	99.96	O 2685									

Specific Gravity: 3.332

$Ca_{45.5}$ $Mg_{42.3}$ $Fe_{12.2}$

% Al in Z = 3.7

Indices of Refraction Pleochroism:

nX 1.6862 Nonpleochroic

nY 1.6908 Color: Faint green

nZ 1.7141

Birefringence x10^4 aver.: 279

265, 269, 274, 284, 305

2V aver.: 48°

44 3/4°, 44 3/4°, 45 3/4°, 47½°, 48°, 48°, 48 3/4°, 50½°, 50 3/4°, 51½°

ZΛc aver.: 39½°

37°, 37 3/4°, 38°, 38 3/4°, 39°, 39 3/4°, 40°, 40°, 40°, 41½°, 41½°

Sample purity: 98.8%

TABLE 12. 35-24N

Salite. Chester 43216. Lima Quarry.

			1	2	3	4	5	6	7		
						2Al	Al	Al	Al	Z	Cat-
		Atomic Ratios	Cr	Fe'''	Al	Ti	Cr	Fe'''	Al	Y	ions to
			Na	Na	Na					W	Six O
SiO_2	50.77	Si 845								Z	
Al_2O_3	1.65										
Fe_2O_3	4.46	Al 32	–	–	–	Z	–	–	$8\frac{1}{2}$	868	2.00
FeO	8.69								0		
MgO	10.14	Fe''' 56		$48\frac{1}{2}$				$7\frac{1}{2}$			
CaO	20.70	Cr 0.1									
Na_2O	1.41	Fe 121									
K_2O	0.14	Mn 19								WXY	
H_2O	0.22	Ni 0.1								877	2.02
TiO_2	0.28	Mg 251									
Cr_2O_3	0.01	Ca 369									
MnO	1.35	Na $45\frac{1}{2}$		$45\frac{1}{2}$							
NiO	0.01	K 3		3							
		Ti $3\frac{1}{2}$				$3\frac{1}{2}$					
	99.83	O 2613									

Specific Gravity: 3.420

$Ca_{45.2}$ $Mg_{30.8}$ $Fe_{24.0}$

% Al in Z = 2.6

Indices of Refraction Pleochroism:

nX 1.6972 Faintly pleochroic

nY 1.7029 Color: Vivid green

nZ 1.7215

Birefringence, x10^4 aver.: 243

237, 237, 239, 258

2V aver.: 57 3/4°

55°, 56½°, 57°, 57°, 57½°, 58°, 58 3/4°, 59°, 59½°, 60°

ZΛc aver.: 42½°

40°, 40°, 42°, 42°, 42°, 44°, 44°, 44°, 44 3/4°

Sample purity: 98.9%

TABLE 13. 35-25N

Salite. Chester 43216. Lima Quarry.

		1	2	3	4	5	6	7		
					2Al	Al	Al	Al	Z	Cat-
	Atomic Ratios	Cr	Fe'''	Al	Ti	Cr	Fe'''	Al	Y	ions to Six O
		Na	Na	Na					W	
SiO_2 52.37	Si 871								Z 887	1.99
Al_2O_3 1.38										
Fe_2O_3 3.32	Al 27			1	4			11		
FeO 7.02								11		
MgO 13.59	Fe''' 41½		41½							
CaO 21.46	Cr ½	½								
Na_2O 1.19	Fe 98									
K_2O 0.24	Mn 6½								WXY 2	2.02
H_2O 0.18	Ni 0.3									
TiO_2 0.19	Mg 312								8974	
Cr_2O_3 0.05	Ca 383									
MnO 0.46	Na 38	½	36½	1						
NiO 0.02	K 5		5							
	Ti 2				2					
100.47	O 2672									

Indices of Refraction Pleochroism:
nX 1.6937 Faintly Pleochroic
nY 1.6983 Color: Vivid green
nZ 1.7157

Birefringence, x10^4 aver.: 220

212, 212, 222, 234

2V aver.: 54½°

51½°, 51½°, 51 3/4°, 52½°, 53½°, 53½°, 54°, 54½°, 54 3/4°, 55°, 56°, 56 3/4°, 61°

ZΛc aver.: 39½°

38½°, 39°, 39½°, 39½°, 39½°

Specific Gravity: 3.364

$Ca_{45.5}$ $Mg_{37.1}$ $Fe_{17.4}$

% Al in Z = 1.8

Sample purity: 99.5%

TABLE 14. 35-32N

Augite. Chester. 22476.

		1	2	3	4	5	6	7		
					2Al	Al	Al	Al	Z	Cat-
	Atomic Ratios	Cr	Fe'''	Al	Ti	Cr	Fe'''	Al	Y	ions to Six O
		Na	Na	Na					W	
SiO_2 50.00	Si 832								Z	
Al_2O_3 3.05										
Fe_2O_3 1.50	Al 60				10		13½	18	873½	1.97
FeO 5.87								18½		
MgO 15.60	Fe''' 19		5½				13½			
CaO 22.42	Cr ½	½								
Na_2O 0.18	Fe 82									
K_2O 0.00	Mn 2½								WXY	2.07
H_2O 0.27	Ni 0.4								921	
TiO_2 0.40	Mg 387									
Cr_2O_3 0.07	Ca 400									
MnO 0.18	Na 6	½	5½							
NiO 0.03	K 0									
	Ti 5				5					
99.57	O 2667									

Indices of Refraction Pleochroism:
nX 1.6860 Nonpleochroic
nY 1.6906 Colorless
nZ 1.7137

Birefringence, x10^4 aver.: 277

256, 275, 286, 290

2V aver.: 48°

45½°, 46°, 46°, 46 3/4°, 47°, 47½°, 48 3/4°, 49½°, 48 3/4°, 51½°, 52½°

ZΛc aver.: 42½°

40 3/4°, 41½°, 41 3/4°, 41 3/4°, 42½°, 42 3/4°, 44 3/4°

Specific Gravity: 3.324

$Ca_{44.9}$ $Mg_{43.5}$ $Fe_{11.6}$

% Al in Z = 4.5

Sample purity: 99.8%

the pattern of 35-9N. Several other unidentified reflections occurred at random in two patterns (35-6N, 35-32N), most of them occurring in 35-6N, the specimen with the lowest purity. While unidentified reflections which occur randomly are due to sample impurity, it is doubtful that this explanation will serve for unidentified lines which persist from specimen to specimen. Line 1, and possibly line 3 of Table 15 fall into this category, hence another explanation must be sought for them.

Modern theories (Fyfe, 1951) propound that bond type as well as ionic radius governs the isomorphous substitution of atoms. In ionic

TABLE 15. UNIDENTIFIED LINES: *d*-SPACINGS AND INTENSITIES

Line	35-1N		35-5N		35-6N		35-8N		35-9N	
	d	I/I_0	*d*	I/I_0	*d*	I/I_0	*d*	I/I_0	*d*	I/I_0
1	3.115	5	3.099	5	3.118	5	3.097	5		
2					1.922	5				
3					1.691	5				
4					1.359	5				

Line	35-13N		35-19N		35-24N		35-25N		35-32N	
	d	I/I_0	*d*	I/I_0	*d*	I/I_0	*d*	I/I_0	*d*	I/I_0
1	3.124	10	3.087	5	3.097	10	3.140	10	3.005	5
2										
3										
4									1.692	5

crystals no restrictions are imposed on the bonds; therefore atoms having similar ionic radii will be able to replace one another, and the resulting coordination can be predicted by the radius ratio rule. In covalent crystals the radius ratio rule does not hold. Here the directional properties of the bonds determine the polyhedral configuration, the acceptance or rejection of possible replacements, and therefore the extent of isomorphous substitution. To complicate the situation is the well-known fact that most bonds are a combination of the two types mentioned above. The partial covalence of ionic bonds shortens the ionic radius sum, thus resulting in a distorted configuration which partially controls the acceptance of atoms available for substitution. The type of bonding between any cation and anion is a function of their electronegativities, and the amount of ionic character of the resulting bond can be predicted from the difference in electronegativity between the two (Pauling, 1939).

In order to obtain a clear picture of clinopyroxene structure, therefore, it is advisable to consider the following mutually related factors (Table 16): ionic radii, radius sum, radius ratio, coordination number, electronegativity, and per cent covalency. Whereas in diopside the total effect of these factors on the structure is constant, a complex situation arises in the case of other clinopyroxenes where variability of total effect, and hence structure, might be suspected because of the extreme variability of clinopyroxene composition. It should be noted at this point that no

Table 16. Factors Affecting Structure of Clinopyroxenes

	Cation	Ionic Radius	Anion	Radius Sum	Radius Ratio	C.N.	Elec-neg.	% Coval.*
W—	Ca^{+2}	.99	O^{-2}	2.39	.707	8	2.5	24
	Na^{+1}	.95	O^{-2}	2.35	.679	8	2.6	21
	K^{+1}	1.33	O^{-2}	2.73	.950	9	2.7	19
X—	Mg^{+2}	.65	O^{-2}	2.05	.464	6	2.3	28
	Fe^{+2}	.75	O^{-2}	2.15	.536	6	1.85	43
	Mn^{+2}	.80	O^{-2}	2.20	.571	6	2.1	35
	Ni^{+2}	.69	O^{-2}	2.09	.493	6	1.8	44
Y—	Al^{+3}	.50	O^{-2}	1.90	.357	4	2.0	37
	Fe^{+3}	.60	O^{-2}	2.00	.429	6	1.7	49
	Cr^{+3}	.64	O^{-2}	2.04	.457	6	1.9	41
	Ti^{+4}	.68	O^{-2}	2.03	.486	6	1.9	40
Z—	Si^{+4}	.41	O^{-2}	1.82	.293	4	1.7	49
	Al^{+3}	.50	O^{-2}	1.90	.357	4	2.0	37

* The per cent covalency values were obtained from the electronegativities by reference to Pauling's curve (1939).

major deviation between clinopyroxene and diopside structures is possible, since the fundamental motif, the manner is which the silica tetrahedra are joined, is the same in both cases. The unidentified lines of Table 15 which persist from specimen to specimen indicate that substructural changes do take place, however, and it will be the purpose of what follows to suggest possible reasons for their occurrence.

A solution to part of the problem lies in the realization that polyhedral configurations found in the diopside structure cannot help being modified in more chemically complex clinopyroxenes. Such a modification is suggested by the absence of several diopside reflections in some of the clinopyroxene diffraction patterns. In the diopside structure Ca has a coordination number of 8, Mg of 6, with respect to surrounding oxygens.

In more complex clinopyroxenes, Ca is replaced by W (Ca^{+2}, Na^{+1}, K^{+1}) and Mg by X, Y (Mg^{+2}, Fe^{+2}, Mn^{+2}, Ni^{+2}; Al^{+3}, Fe^{+3}, Cr^{+3}, Ti^{+4}.) If the crystal is regarded as strictly ionic, some modification of polyhedral distances will result from discrepancies in ionic radii, and in two instances (K in W, Al in Y) a change in coordination can be predicted. This situation is further complicated by the fact that clinopyroxene is not strictly ionic, hence M-O (cation-oxygen) bonds resulting from various substitutions exhibit a range of type, some being more covalent than others. Partial covalence has the effect of shortening inter-atomic distances, imposing directional restrictions, and in some cases producing resonance. All three of these may lead to configuration and/or coordination changes. Furthermore, the introduction of one element into a given position affects the electronegativity of surrounding oxygens, and hence influences the acceptance or rejection of possible neighboring atoms.

Of particular interest is the effect which substitution of Al for Si in the silica tetrahedra has on further substitutions. Al is more electropositive than Si; therefore when it replaces Si the bonds to the neighboring oxygen atoms become more ionic, and as a result the O-M bonds (bonds from non-bridging oxygens to metal ions) become more covalent. It should be expected, therefore, that these more covalent sites (i.e., more covalent than around Si-O bridges) will be attractive to covalent atoms on the verge of substitution. This is verified by the proportional increase of Fe^{+2}/Mg ratio in silicates as more and more Al substitutes for Si (Ramberg, 1952). This neat relationship obtains only when all other factors are constant; i.e., when only Fe^{+2} and Mg have to be considered. Since Fig. 4 fails to show such a simple relationship, it is evident that other substituting elements must be influential in the case of chemically complex clinopyroxenes.

It is a well-known fact (Ramberg, 1952) that the amount of Al in Si positions increases as polymerization of silicate structure is developed to a higher degree (tectosilicates have more Al in Si positions than do nesosilicates). But this does not explain why different amounts of Al enter Si sites in clinopyroxenes where the degree of polymerization is supposedly constant. Nor does it explain increase of Al substitution for Si concomitant with increase of total Al present (Fig. 5). Since such a relationship between total Al and per cent Al in Z does exist, it is tempting to suggest that geochemical conditions which supplied Al were also influential in determining degree of acceptance of Al in Si positions, and that the introduction of Al into Si sites causes partial polymerization of chains giving rise to clinopyroxenes that are transitional between single and double chain inosilicates. Such a condition might arise in the following way. If for the moment the crystal is regarded as ionic, there will be,

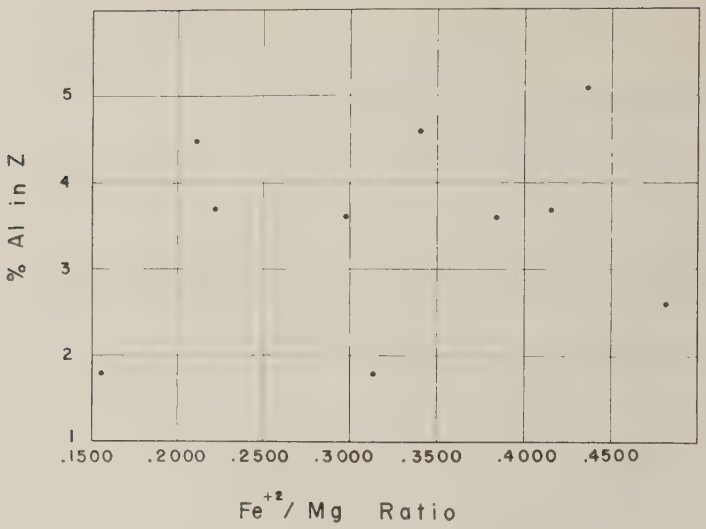

FIG. 4. Relation between % Al in Z and Fe^{+2}/Mg ratio.

as noted before, a drop in coordination number from 6 to 4 when Al substitutes for Si. This means that there are two oxygens "left over." It is not hard to visualize a situation in which these oxygens become shared by tetrahedra in adjacent chains. Such partial polymerizations

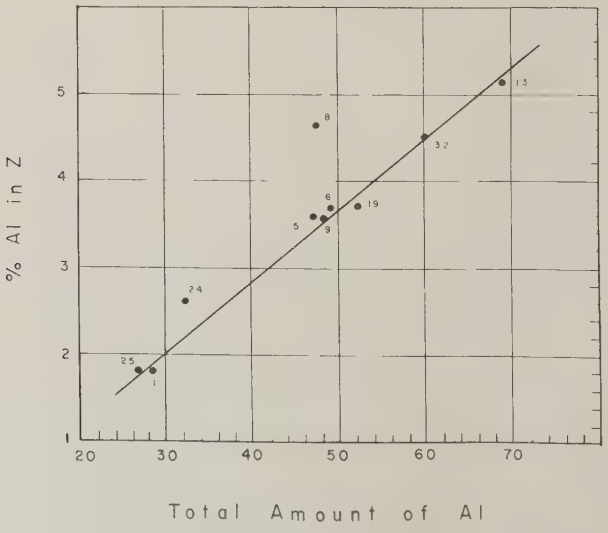

FIG. 5. Relation between % Al in Z and total amount of Al (atomic ratio).

are substructural changes, and when they are developed to a certain degree it is reasonable to expect that they will be detected by x-ray diffraction procedures. When they are developed beyond a certain limit the x-ray beam, which records statistically, will note a structural change, i.e., the change from single to double chains.

The geochemical conditions held responsible above both for supplying Al and controlling its substitution for Si remain unknown. But one clue, the known transition of pyroxene to amphibole in metamorphic rocks, such as phyllite and schist, which have been subjected to direct componental stresses enables us to speculate that conditions other than those prevalent in igneous reaction series, namely the presence of directed stresses, foster the entrance of Al into Si sites causing the partial polymerization of silicate chains.

On the basis of the several lines of evidence presented in this section, (*a*) the presence of strong persistent unidentified reflections on diffraction curves, (*b*) the absence of several diopside reflections in clinopyroxene diffraction patterns, (*c*) theoretical considerations which enable us to visualize numerable adjustments of polyhedral distances, configurations, and coordinations, and (*d*) widely variable and probably highly influential geologic conditions, it is postulated that substructural changes occur in chemically and/or geologically complex clinopyroxenes. It will be the purpose of another paper to study these changes in detail.

Optical Crystallography

It would be difficult to add anything to the excellent optical property curves for clinopyroxenes given by Hess (1949). In constructing these curves it was assumed that the following amounts of minor oxides were present:

	%
Al_2O_3	3.0
Fe_2O_3	1.5
Na_2O	0.4
TiO_2	0.4
MnO	0.3
Cr_2O_3	1.1

Since the actual amounts of minor oxides present in the clinopyroxenes of this study differ from the values given above, some of the optical properties observed (Tables 5-14) differ from those predicted from chemical composition (expressed in terms of Ca:Mg:Fe ratios, Fig. 6) using the optical property curves of Hess. Optical properties which show the greatest deviation from predicted values are 2V and birefringence. In both these cases deviations from predicted values seem to be

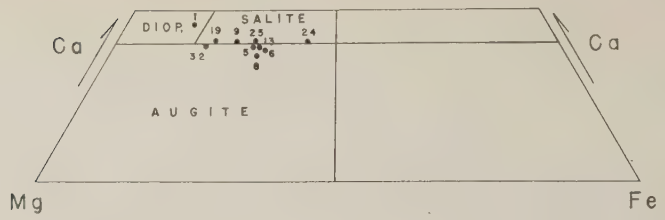

FIG. 6. Partial ternary diagram showing compositions of clinopyroxenes in terms of Ca:Mg:Fe ratios. Ni is added to Mg; Fe^{+3} and Mn are added to Fe^{+2}.

especially related to differences between the assumed amount of Al_2O_3 and the amount actually present in the particular clinopyroxene being studied. Figures 7 and 8 show these relationships. Agreement between the three indices of refraction and their predicted values is good, the maximum discrepancy being $\pm .007$, the average $\pm .003$.

Another type of discrepancy should be mentioned here, namely, the discordance or range of values obtained in the measurement of optical properties both in this and in other studies. While cumulative errors cause some of the discordance, the wide ranges observed in many cases

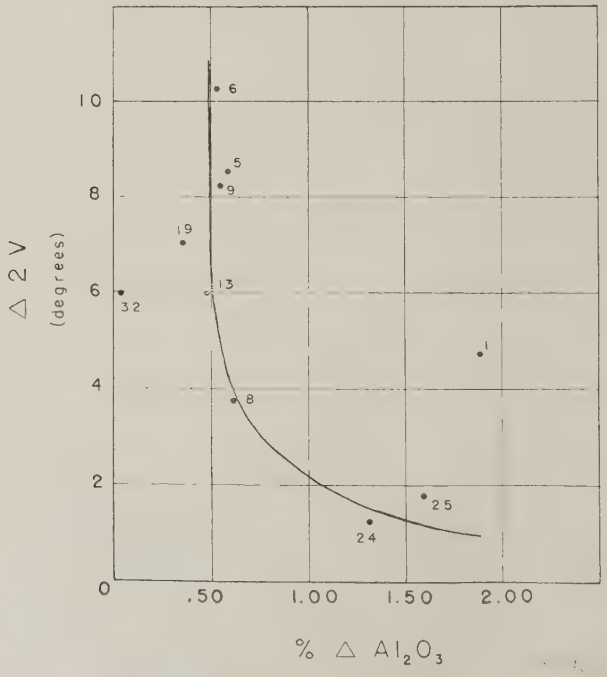

FIG. 7. Relation between 2V and % Al_2O_3.

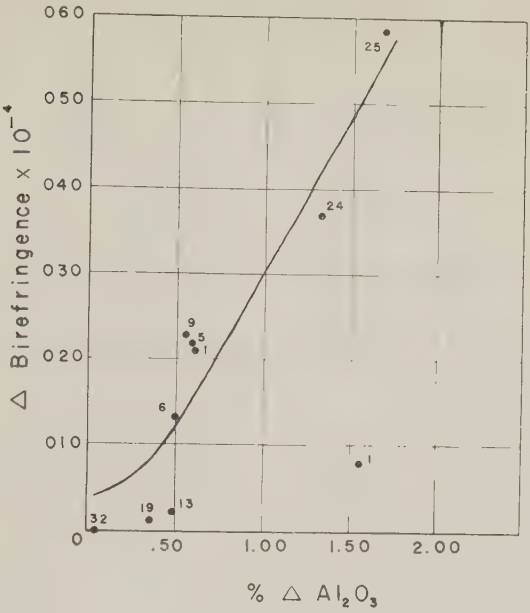

FIG. 8. Relation between birefringence and % Al_2O_3.

demand a more suitable explanation. Perhaps the answer lies in the fact that there is no reason why all grains of a chemically complex mineral should be exactly the same. If the complex history of most rock bodies, and particularly metamorphic ones, is called to mind, situations can indeed be visualized which would vary both the elemental supply and the physical-chemical conditions at various portions of the rock body. Hence inter-grain variation could be due to either different elemental supply or different physical-chemical conditions. Furthermore, wide intra-grain variation should be expected in chemically complex minerals such as clinopyroxene where random distribution of metal cations produces lattice planes in which all directions are singular. Since average optical parameters are generally arrived at from measurements taken from several grains, both these features of complex minerals in complex rocks, inter-grain and intra-grain variation, would lead to the discordance obtained in the measurement of optical properties.

GEOCHEMISTRY

Detailed structural and petrologic studies of the Wilmington gabbroic complex (Ward, 1958) show beyond doubt the metamorphic character of the rocks containing the clinopyroxenes. Although the clinopyroxenes

TABLE 17. Fe^{+2}/Mg RATIOS OF CLINOPYROXENES

Sample	Hypersthene	Clinopyroxene	Δ Fe^{+2}/Mg
35-1	*	.1552	
35-5	.7021	.3846	.3175
35-6	.7413	.4164	.3249
35-8	.6344	.3415	.2929
35-9	.5767	.2988	.2719
35-13	.7755	.4373	.3382
35-19	.4151	.2228	.1923
35-24	†	.4821	
35-25	†	.3141	
35-32	.3712	.2119	.1593

* Hy present but not studied.
† No Hy present.

have had a metamorphic evolution, several lines of geochemical evidence exist which indicate that they were originally of igneous genesis. When dealing with the crystallization of igneous rocks it is to be expected that as the series olivine→orthopyroxene→monoclinic pyroxene→hornblende progresses, both Fe^{+2}/Mg and Mg/Ca ratios will simultaneously decrease (Rankama, 1950). Tables 17 and 18 give the Fe^{+2}/Mg and Mg/Ca ratios of the clinopyroxenes of this paper and their coexisting hypersthenes studied by Clavan (1954). The igneous origin of these coexisting pairs is shown by the fact that both the Fe^{+2}/Mg and Mg/Ca ratios of hypersthene are greater than those of clinopyroxene.

Since igneous orthopyroxenes are more ferrous than their monoclinic

TABLE 18. Mg/Ca RATIOS OF CLINOPYROXENES

Sample	Hypersthene	Clinopyroxene	Mg/Ca
35-1	*	.9094	
35-5	3.9000	.8376	3.0624
35-6	3.0437	.8271	2.2166
35-8	2.8722	.8711	2.0011
35-9	3.8643	.8711	2.9932
35-13	1.3235	.8267	0.4968
35-19	3.1200	.9292	2.1908
35-24	†	.6802	
35-25	†	.8146	
35-32	1.6436	.9675	0.6761

* Hy present but not studied.
† No Hy present.

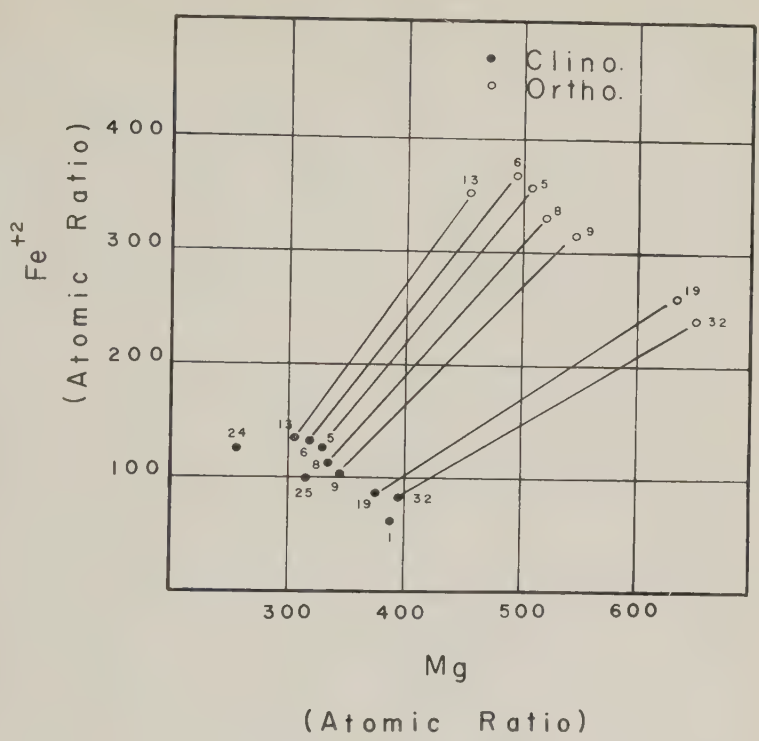

FIG. 9. Clinopyroxene-orthopyroxene partition based on molecular ratios of Fe^{+2} and Mg.

counterparts, further evidence supporting the igneous origin of the pyroxenes studied here is given by Fig. 9. This shows there is a definite partition between hypersthene and its coexisting clinopyroxene, hypersthene being more ferrous and more magnesian than clinopyroxene.

In his paper on the "Pyroxenes of Common Mafic Magmas" Hess (1941) showed that if the compositions of coexisting igneous pyroxenes are plotted on an En:Fs:Wo ternary diagram, the clinopyroxene-orthopyroxene joins converge to $En_{25}Wo_{75}$, and composition of one pyroxene can be predicted if the composition of its counterpart is known. Figure 10 shows the general convergence of clinopyroxene-orthopyroxene joins to $En_{25}Wo_{75}$ for the pyroxenes studied here. This convergence is further indication of their igneous origin. Lack of absolute convergence to $En_{25}Wo_{75}$ is a reflection of the masking effects of metamorphic processes.

Whereas the three lines of evidence mentioned above (*a*) the decrease in Fe^{+2}/Mg and Mg/Ca ratios going from orthopyroxene to clinopyrox-

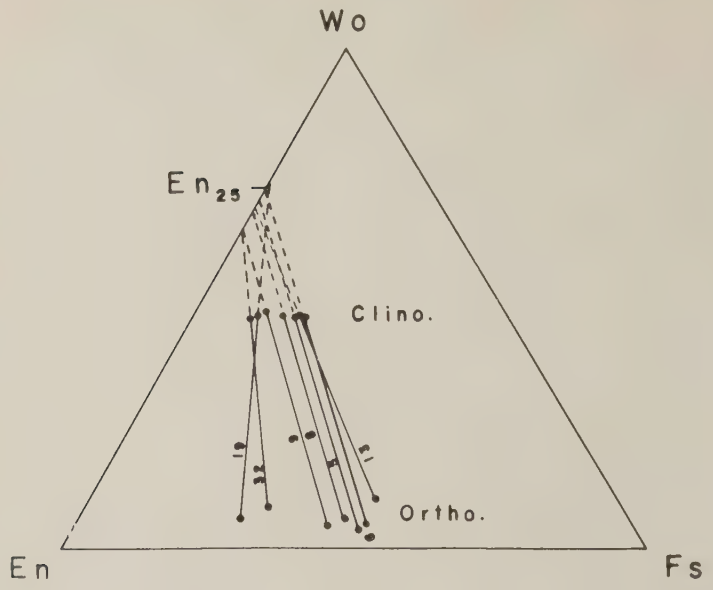

$$Wo = CaO + Na_2O$$
$$En = MgO$$
$$Fs = FeO + MnO + NiO$$

FIG. 10. Convergence of clinopyroxene-orthopyroxene joins.

ene, (*b*) the predominance of ferrous iron in orthopyroxenes rather than in clinopyroxenes, and (*c*) the convergence of clinopyroxene-orthopyroxene pairs to $En_{25}Wo_{75}$, indicate that the rocks studied here are of igneous origin, lack of correspondence between certain expected and observed geochemical relations offers some insight to their complex evolution.

In the normal igneous situation orthopyroxene will be less magnesian than clinopyroxene. From the partition shown in Fig. 9 it is seen that for the pyroxenes studied here the opposite relation holds. This suggests that Mg has been introduced during metamorphism and for some reason has been concentrated in orthopyroxenes rather than clinopyroxenes.

In a truly igneous rock there is no equilibrium between pyroxene counterparts since they are members of one reaction series. According to Ramberg (1952) if equilibrium does exist between orthopyroxene and clinopyroxene in the same rock, the Mg/Fe^{+2} ratio will increase in going

from orthopyroxene to clinopyroxene. Such an increase is shown between pyroxene pairs from rocks of the Piedmont Province indicating that equilibrium has been established, but further evidence must be obtained before accepting this idea.

If equilibrium has been established between pyroxene pairs, it is possible that it was brought about by the introduction of Mg during metamorphism. Figure 11 shows that the change in indices of refraction and specific gravity between ortho- and clinopyroxene is related to the change in Mg/Fe^{+2} ratio suggesting that the optical properties of one or both pyroxenes have been modified by their metamorphic evolution.

Summary of Experimental Observations

1. Specific gravities of clinopyroxenes increase proportionally as mole per cent ferrous silicate increases.
2. Good results are obtained by both the cleavage and zone methods of measuring extinction angles.
3. Diffraction patterns of clinopyroxenes contain persistent unidentified reflections which are believed to be due to substructural differences between complex clinopyroxenes and diopside.
4. A number of diopside lines are omitted on clinopyroxene diffraction patterns.
5. No relationship exists between Fe^{+2}/Mg ratio and amount of Al in Si sites for clinopyroxenes studied here.
6. The per cent of Al in Z is proportional to the total amount of Al present.
7. The difference between optical properties determined in this paper and values predicted from chemical composition using the curves of Hess (1949) are accounted for by the difference between actual and assumed amounts of minor oxides.
8. Differences between the assumed and actual amount of Al_2O_3 particularly seem to explain deviations of 2V and birefringence from predicted values.
9. Good agreement is obtained between the three indices of refraction and their predicted values.
10. Wide ranges were obtained in the measurement of some optical properties.
11. Fe^{+2}/Mg ratios of hypersthenes studied by Clavan (1954) are greater than those of coexisting clinopyroxenes.
12. Hypersthenes (Clavan, 1954) are richer in both Mg and Fe^{+2} than their clinopyroxene counterparts.
13. Clinopyroxene-orthopyroxene joins show a general convergence to $En_{25}Wo_{75}$ on an En:Fs:Wo ternary diagram.

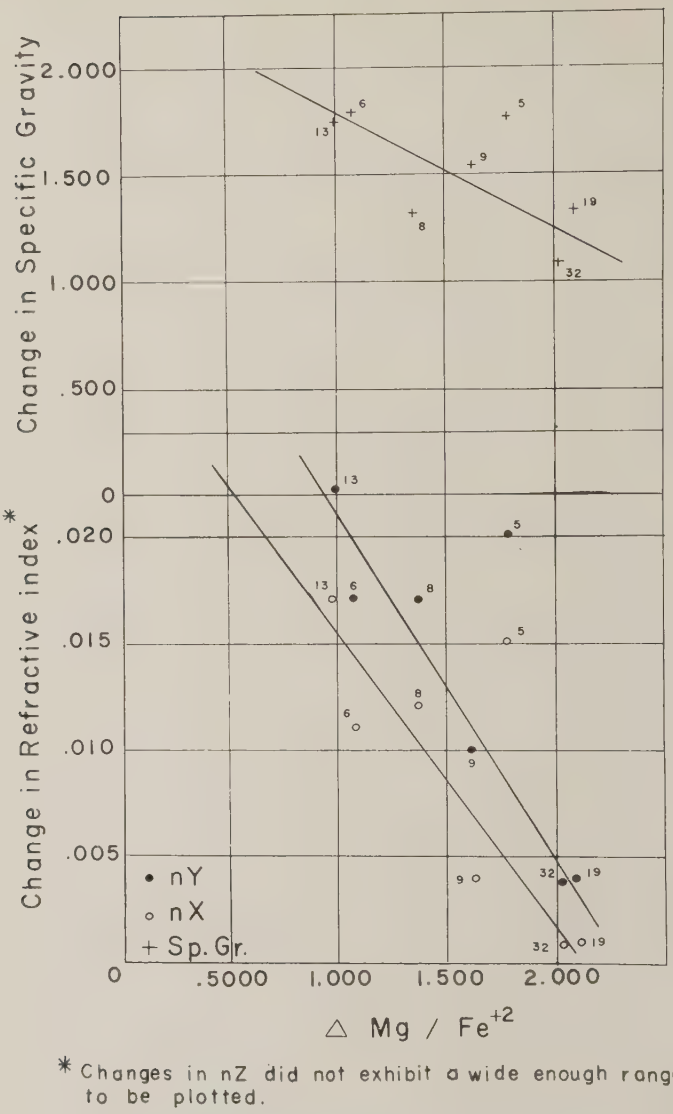

FIG. 11. Relation between change in refractive index and specific gravity and change in Mg/Fe^{+2} ratio.

14. The Mg/Fe^{+2} ratio increases in going from orthopyroxene to clinopyroxene.
15. Changes in indices of refraction and specific gravity between orthopyroxene-clinopyroxene pairs are related to change in their Mg/Fe^{+2} ratio.

Conclusions

The clinopyroxenes studied here are of igneous origin but have undergone subsequent metamorphism. During metamorphism Mg may have been introduced and concentrated in the coexisting orthopyroxene rather than in clinopyroxene. This possibly has produced equilibrium between clinopyroxene and orthopyroxene existing in the same rock. The optical properties of one or both pyroxenes have been modified by their metamorphic evolution. This also produced inter-grain and intra-grain variations which explain the wide ranges obtained in the measurement of some of the optical properties. Physical geologic conditions are also probably influential in determining (*a*) the amount of Al entering Si tetrahedra and (*b*) polyhedral distances, configurations, and coordinations. Considering this and the possible substitutions in clinopyroxenes leads to a picture of variable polyhedral distances, configurations, and coordinations in chemically and/or geologically complex clinopyroxenes, and to the suggestion that they may be substructurally different from diopside. Substructural difference is also suggested by the presence of persistent unidentified lines and by the omission of diopside lines in *x*-ray diffraction patterns of clinopyroxenes.

Acknowledgments

We are grateful to Prof. Edward H. Watson and Prof. Dorothy Wyckoff for suggesting this study and for their unlimited interest and support. We are also indebted to Dr. A. L. Patterson for reading the manuscript and making many helpful suggestions. Diffractometer curves were run in Prof. Paul F. Kerr's mineralogical lab at Columbia University; $\sin^2\theta$ calculations were done by Dr. A. L. Patterson, Dr. Jenny P. Glusker, and Marilyn Dornberg on the IBM 602A computer at the Institute for Cancer Research. Maria L. Busé assisted in the preparation of Berek compensator slides and in the compilation of some of the *x*-ray crystallographic tables, Amy H. Garthly in the preparation of figures and tables, and Sonya P. Montgomery and Judy Walker typed the final paper. To all these people we extend our sincerest thanks.

Bibliography

Berman, H. (1937), Constitution and classification of natural silicates: *Am. Mineral.*, **22**, 343–415.

Clavan, W. S., McNabb, W. M., and Watson, E. H. (1954), Some hypersthenes from S.E. Pennsylvania and Delaware: *Am. Mineral.*, **39**, 566–580.

Emmons, R. C. (1943), The Universal Stage: *G. S. A. Memoir* **8**.

Fyfe, W. S. (1951), Isomorphism and bond type: *Am. Mineral.*, **26**, 50–53.

Hess, H. H. (1941), Pyroxenes of common mafic magmas, Part I: *Am. Mineral.*, **26**, 515–535.

——— (1949), Chemical composition and optical properties of common clinopyroxenes: *Am. Mineral.*, **34,** 621–666.

Kuno, H. and Hess, H. H. (1953), Unit cell dimensions of clinoenstatite and pigeonite in relation to other common clinopyroxenes: *Am. J. Sci.*, **251,** 741–752.

Pauling, L. (1949), The nature of the chemical bond: Cornell Univ. Press.

Ramberg, Hans (1952), Chemical bonds and distribution of cations: *Jour. of Geol.*, **60,** 331–355.

Rosenzweig, A., and Watson, E. H. (1954), Some hornblendes from Southeastern Pennsylvania and Delaware: *Am. Mineral.*, **39,** 581–599.

Ward, R. (1958), Petrology and metamorphism of the Wilmington complex, Delaware and adjacent Pennsylvania, and Maryland: Doctoral Dissertation, Bryn Mawr College, Pa.

Warren, B. E., and Bragg, W. L. (1928), The structure of diopside: *Zeit. Krist.*, **69,** 168–193.

Winchell, N. H., and Winchell, A. N. (1929), Elements of optical mineralogy, Part III, Determinative Tables: John Wiley & Sons, Inc., N. Y.

Manuscript received October 18, 1958.

NOTES AND NEWS

TETRAHEDRAL BORON IN TEEPLEITE AND BANDYLITE

VIRGINIA ROSS AND JOHN O. EDWARDS, *Department of Chemistry, Brown University, Providence, Rhode Island.*

The trivalent boron-oxygen radius ratio is 0.20 (Pauling, 1945) allowing boron either triangular or tetrahedral coordination. In the simple anhydrous borates, triangular coordination is very common; while in hydrous or hydroxy-borates and boro-silicates either tetrahedrally coordinated boron occurs alone or both types of coordination prevail as shown, for example, by Christ and Clark (1957). In the simple hydroxyl borates: teepleite, $Na_2B(OH)_4Cl$ and bandylite, $CuB(OH)_4Cl$, Fornaseri (1949, 1950, 1951) and Collin (1951) cited from *x*-ray analyses the presence of discrete tetrahedral $B(OH)_4^-$ ions.

Natural teepleite was first described by Gale, Foshag and Vonsen (1939) as a mineral component of Borax Lake, California, resulting from the reaction of halite with borate-rich brine. Palache and Foshag (1938) previously had discussed the formation of bandylite as a secondary mineral in altered volcanic rock at Calama, Chile. *X*-ray Weissenberg analysis of teepleite was carried out by Switzer (Gale et al.). From single crystal studies of bandylite, Berman (Palache and Foshag) implied that the two minerals were characterized by the same space group symmetry, $P\ 4/n\ mm$. The correct space group of bandylite has since been shown by Collin to be $P\ 4/n$. Since no *x*-ray powder data have been published to facilitate the identification of these two species, they are given in Tables 1 and 2. The axial ratios of the two minerals differ by as much as 0.24 and their *x*-ray powder patterns are quite dissimilar. From the previous literature this distinction has not been made obvious.

The crystal structures of teepleite and bandylite are nevertheless similar, in that they have been found to consist of discrete $B(OH)_4$ ions and octahedrally coordinated sodium and copper ions having four nearest neighbor oxygen atoms and two chlorine ions. The four sodium ions in teepleite are located at $(\frac{1}{4}, \frac{1}{4}, \frac{1}{2})$ (Fornaseri, 1949); in bandylite the copper ions are at $(0, \frac{1}{2}, 0.639)$ (Collin, 1951). The structure of bandylite proposed by Fornaseri (1950) was based upon the original space group and differed with respect to the orientation of the polyhedra in the basal plane.

The tetrahedral configuration about the boron in teepleite has now been confirmed by infra-red and nuclear quadrupole resonance studies at Brown. The Raman spectrum of the borate ion in aqueous solution was reinvestigated and compared to the vibrational frequencies of the

TABLE 1. *X*-RAY POWDER DIFFRACTION DATA FOR SYNTHETIC TEEPLEITE

CuK_α (Corrected for camera radius and film shrinkage) Tetragonal, *Space Group* $P4/nmm$. $a_0 = 7.26 \pm .01$ Å°, $c_0 = 4.85 \pm .01$ Å°, $c/a = 0.668$ (least squares analysis). $a_0 = 7.27$, $c_0 = 4.84$ Å°, $c/a = 0.666$ (Switzer).

I	*d* (meas)	*d* (calc)	*hkl*	I	*d* (meas)	*d* (calc)	*hkl*
4	5.13	5.13	110	7	1.815	1.815	400
0.5	4.86	4.85	001	5	1.761	1.763	222
6	4.03	4.03	011	7	1.709	1.711	330
2	3.63	3.63	200	8	1.659	1.655	411
5	3.52	3.53	111	5	1.619	1.617	003
8	2.90	2.91	021	3	1.578	1.578	013
10	2.697	2.700	121	7	1.539	1.542	113
5	2.565	2.567	220			1.540	421
0.5	2.425	2.425	002	5	1.476	1.477	023
5	2.295	2.300	102	6	1.446	1.447	213
		2.296	130	0.5	1.425	1.425	412
7	2.264	2.269	221	7	1.396	1.398	332
4	2.195	2.193	112			1.391	051
2	2.162	2.166	301	1	1.365	1.368	223
9	2.015	2.017	022			1.366	511
3	1.941	1.943	122	6	1.348	1.350	422
3	1.858	1.860	231	6	1.299	1.299	521

TABLE 2. *X*-RAY POWDER DIFFRACTION DATA FOR BANDYLITE, MINA QUETANA, CHILE

Film, Harvard Collection No. 5503, Cu-radiation, Ni-filter, (uncorrected for camera radius and film shrinkage). Tetragonal, $P\,4/n$, $a_0 = 6.19$ Å, $c_0 = 5.61$ Å, $c/a = 0.906$ (Collin).

I	*d*	*hkl*	I	*d*	*hkl*
10	5.59	001	4	1.394	
6	4.35	110	3	1.381	
5.5	4.13	101	2.5	1.330	
8	3.08	200	2	1.317	
3	2.80	002	2	1.265	
2	2.69	201	4B	1.137	
8	2.54	102	4B	1.130	
2	2.43	121	1	1.060	
4	2.18	220	0.5	1.030	
7	1.952	122	1	.983	
4	1.858		1	.976	
2	1.764		2	.955	
6	1.655		1	.922	
3	1.544		1	.883	
5	1.457		0.5	.875	

B = broad line.

infrared spectrum of teepleite and theoretical Heath-Linnett values (Edwards, Morrison, Ross and Schultz, 1955). For this purpose large crystals of teepleite were prepared by evaporation of a solution containing equal volumes of sodium borate and sodium chloride. Nuclear magnetic resonance analysis of synthetic teepleite using a field of 5,250 gauss and a Pound-Watkins recording spectrometer yielded a quadrupolar coupling constant, $eqQ = 0.094 \pm 0.001$ Mcps, corresponding to the resonance of tetrahedrally-coordinated B^{11} with an approximately isometric charge distribution.

Acknowledgment

The nuclear magnetic resonance analysis of teepleite was carried out through the courtesy of Professor P. J. Bray and G. O'Keefe of the Department of Physics, Brown University. The authors are grateful to Professor C. Frondel for the preparation and loan of the *x*-ray diffraction powder photograph of bandylite from the Harvard University Collection. This research was supported by the U. S. Army Office of Ordnance Research.

References

Christ, C. L. and Clark, J. R. (1957), Nature of the polyions in some borate Minerals: Abstr., G.S.A. 38th Ann. Meet., *Bull. Geol. Soc. Amer.*, **68,** 1708.

Collin, R. L. (1951), The crystal structure of bandylite, $CuCl_2 \cdot CuB_2O_4 \cdot 4H_2O$: *Acta. Cryst.*, **4,** 204.

Edwards, J. O., Morrison, G. C., Ross, V. F. and Schultz, J. (1955), The structure of the aqueous borate ion: *J. Am. Chem. Soc.*, **77,** 266.

Fornaseri, M. (1949), La struttura cristallina della teepleite: *Period. Min.*, **18,** 103.

——— (1950), La struttura cristallina della bandylite: *Period. Min.*, **19,** 159.

——— (1951), Struttura di metaborati tetragonali e loro relazione cristallochimiche: *La Ricercha Scientifica*, **21,** 3.

Gale, A., Foshag, W. F. and Vonsen, M. (1939), Teepleite, a new mineral from Borax Lake, California: *Am. Mineral.*, **24,** 48.

Palache, C. and Foshag, W. F. (1938), Antofagastite and bandylite, two new copper minerals from Chile: *Am. Mineral.*, **23,** 85.

Pauling, L. (1945), The Nature of the Chemical Bond: Cornell University Press, 382.

THE AMERICAN MINERALOGIST, VOL. 44, JULY–AUGUST, 1959

NOTES ON A SECOND OCCURRENCE OF GROUTITE

Curt G. Segeler, *Brooklyn, New York.*

The talc mines at Talcville, about 8 miles southeast of Gouveneur, New York have long attracted the attention of amateur mineral collectors and others. The prime reason for this interest is the lilac colored variety of tremolite (called hexagonite in some of the older textbooks)

which is found there in abundance. The color has been shown by chemical tests to be due to the presence of divalent manganese. Some parts of the talc itself are similarly colored, presumably for the same reason. The occurrence of groutite at this locality appears to be associated with the availability of soluble manganese.

While collecting at this locality, and specifically at the dumps of the No. Two and One Half Mine, I noticed a few vugs in the talc in which there were small calcites covered with brilliant black acicular crystals. In the sunlight and against the background of the light colored talc, the appearance of these crystals was quite striking. They ranged in size from 1 to 5 mm., forming slender striated prisms. They showed 110 and 010 faces, together with the basal pinacoids. A few were found with dome faces. Many of the crystals were twinned. A few appeared to have been deposited in a radiating pattern but for the most part they were scattered over the surface of the calcite.

This occurrence suggests that the calcite provided the alkaline environment which caused the formation of the groutite. It seems logical that acid waters dissolved some of the Mn from the host rocks—the talc or the hexagonite—and that these solutions were neutralized by contact with the calcite. Conditions were right for the formation of groutite. This theory appears consistent with the general behavior of divalent Mn. Its various lilac colored compounds are generally soluble and $MnCO_3$ is easily precipitated by the alkali carbonates. On long continued boiling the precipitate converts to H_2MnO_3. While this is not groutite, the chemical procedures are not carried out under the same conditions as the geological process. Hence, this has only been offered as a possible analogy.

On account of their small size and, because of the striations, the crystal data obtained on a two circle goniometer (made available thru the courtesy of Dr. Brian Mason of the Museum of Natural History of New York) can not be considered exact. However, approximately the same axial ratios were obtained as those published by Gruner (1). In this connection it may be of interest to compare the axial ratios of the principal members of the goethite group of minerals.

Montroseite	H VO_2	$a:b:c$	.509 :1:.301
Diaspore	H AlO_2	$a:b:c$	.4689:1:.3019
Goethite	H FeO_2	$a:b:c$	.4593:1:.3034
Groutite	H MnO_2	$a:b:c$	.4262:1:.2663

The identification of the groutite specimens from Talcville, N. Y. was confirmed by x-ray powder photographs compared with those of the type material made available by Dr. John Gruner.

Reference

(1) Gruner, J. W. (1945), Groutite, $HMnO_2$, a new mineral of the diaspore-goethite group: *Am. Mineral.*, 30, 169.

THE AMERICAN MINERALOGIST, VOL. 44, JULY–AUGUST, 1959

AN OCCURRENCE OF GEIKIELITE

WILLIAM S. WISE, *Johns Hopkins University, Baltimore, Maryland.*

Geikielite, the magnesium-analog of ilmenite, has been found *in situ* in some highly metamorphosed magnesian-marbles in the Santa Lucia Mountains, Monterey County, California, and this is the fourth *in situ* occurrence of geikielite thus far described. Dick (1893) identified bluish- to brownish-black pebbles in the gem sands of Ceylon as geikielite, which he believed was a magnesium analog of perovskite. Crook and Jones (1906) also described geikielite from a collection of Ceylon gem sands during a general study of such materials.

Kashin (1937) found geikielite associated with chlorites in the chrome-spinel deposits of the southern Ural Mountains, USSR, whereas Murdoch and Fahey (1949) reported an occurrence of this mineral in metamorphosed magnesian-limestones near Riverside, California. In the latter occurrence geikielite is associated with calcite and brucite, although spinel and geikielite are concentrated in certain zones. An analysis of this geikielite showed 1.4% FeO and 31.8% MgO.

Geikielite with 12.30% FeO, 2.8% Fe_2O_3, and 21.75% MgO occurs as rare inclusions in chromian-chlorites in a serpentinized body of dunite (Efremov, 1954) near Mount Jemorakly-Tube, North Caucasus, USSR.

OCCURRENCE

The geology of the Santa Lucia Mountains, California, includes large massifs of metamorphosed rocks of the sillimanite zone. The original rocks were mostly sediments with some limestones and magnesian-limestones in ranging states of purity. During metamorphism of the impure magnesian-limestones, coarse grained marbles have formed with associated phlogopite, clinohumite, forsterite, spinel, and occasionally geikielite.

Geikielite occurs as small (0.01 mm. to 0.10 mm.), black and opaque, irregular to occasionally rounded grains, closely associated with rutile and spinel. If rutile is present, it is always in juxtaposition with geikielite, and powder photographs of apparently pure material show a mixture of the two minerals. Spinel is also closely associated with the geikielite.

In the associated ferro-magnesian minerals the amount of iron is notably small:

The spinel contains 5.2% of $FeAl_2O_4$, which was determined through (1) chemical analysis, in which FeO = 2.4%; (2) comparison of the cell edge ($a_0 = 8.092$ Å) with that of pure artifical spinel ($a_0 = 8.080$ Å, Swanson and Fuyat, 1953); (3) comparison of the refractive index (1.721) with that of pure spinel (1.719, Palache, et al., 1944, p. 690).

The phlogopite contains approximately 19% annite, determined through (1) refractive index, $\gamma = 1.600$, indicating 20% annite (Wones, 1958a or 1958b); (2) $d_{060} = 1.537$ Å, indicating 18% annite (Wones, 1958a or 1958b); (3) the intensity ratio of 004/005 is 0.49, corresponding to 19% of the octahedral positions filled by iron (Gower, 1957).

The clinohumite is practically the pure magnesium end-member, since the refractive indices give a mean refractive index of 1.646 (Sahama, 1953). The olivine contains from 2% to 5% fayalite, which was determined from $2V_x = 97°$ to 94° (Winchell and Winchell, 1951).

Geikielite was also found in a locality in the same marble layer but about 800 yards to the south. Sample #2 is that from the southern locality, while Sample #1 is from the main area studied.

Mineralogy and Paragenesis

The geikielite can best be separated from the associated minerals, especially rutile and spinel, by passing 250-mesh material through a Frantz magnetic separator set at 0.6 amps with $7\frac{1}{2}°$ tilt and 15° slope (spinel is separated at 0.9 amps, leaving the rutile).

Powder photographs of the geikielite from both localities were taken and are compared with the pattern of artificial $MgTiO_3$ (Table I). The cell dimensions, as calculated from the powder patterns, are given in Table II.

The principal point of distinction between geikielite and ilmenite patterns is the appearance of reflections for the planes (003) and (101) in the geikielite patterns. Although the powder patterns appear to be distinctive, geikielite has at times been mistaken for ilmenite.

The *d*-spacings and cell dimensions of Sample #2 are larger than those in Sample #1, and these data suggest that the former has a higher amount of iron. This supposition was borne out by qualitative density determinations. The density of grains from Sample #1 average about 4.2, while most of the grains from Sample #2 would float in Clerici's Solution (density 4.2). Pure geikielite has a density of 4.05 and ilmenite, 4.79 (Palache, et al., 1944, p. 536). Since the material was too scarce and usually too impure for a chemical analysis, the amount of iron can only be estimated from the approximate density, electromagnetic properties, and cell dimensions. The limits may be set at 25% and 40% $FeTiO_3$.

The abundance of magnesium and scarcity of iron in the rock may be the reason for development of geikielite instead of ilmenite, since underlying the marbles a biotite-plagioclase schist contains bands of calcite, pale-green pleonaste, and ilmenite with some rutile and sphene. The formation of spinel results from the low amount of silica in the system, and this fact probably accounts for the formation of geikielite in place of

TABLE I. POWDER-DIFFRACTION DATA FOR THE SANTA LUCIA GEIKIELITE

Radiation CuKα=1.5418 Å and CuKa_1=1.5405 Å. Camera diameter 114.59 mm.

hkl	Sample #1		Sample #2		*d* Å ($MgTiO_3$)
	d (meas) Å	I	*d* (meas) Å	I	
003	4.67	10	4.67	10	4.64
101	4.19	5	4.19	5	4.18
102	3.723	30	3.70	30	3.703
104	2.735	100	2.742	100	2.722
110	2.536	40	2.542	60	2.527
113	2.226	45	2.232	40	2.218
202	2.0	d*			2.090
204	1.859	45	1.861	30	1.852
116	1.714	65	1.718	60	1.708
108			1.627	10	1.6148
214	1.4993	10	1.502	30	1.4938
030	1.4650	10	1.466	30	1.4592
208	1.3628	5			1.3606
1·0·10	1.3280	5	1.334	15	1.3247
220			1.2695	5	1.2634
128			1.204	d	1.1978
2·0·10			1.180	5	1.1735
134			1.1525	5	1.1462
226			1.1155	5	1.1093
2·1·10			1.0715	5	1.0642
324			0.970	d	0.9646
140			0.958	d	0.9552
			0.920	d	
			0.889	d	

* Diffuse line.

sphene in such a calcium-rich environment. Sphene was formed in less magnesian layers of the marble associated with minor amounts of quartz and diopside. The existence of rutile as excess TiO_2, may (but not

TABLE II. CELL DIMENSIONS FOR $MgTiO_3$, SANTA LUCIA GEIKIELITE, AND ILMENITE (BASED ON THE HEXAGONAL CELL)

	a_0 Å	c_0 Å
$MgTiO_3$ (Swanson, *et al.* 1955)	5.054	13.898
Sample #1	5.072 ± .005	13.950 ± .005
Sample #2	5.080 ± .005	13.895 ± .005
Ilmenite (United Steel Co., Sheffield)	5.079	14.135

necessarily) result from a deficiency of magnesia at the time of the formation of geikielite.

I am indebted to Dr. C. O. Hutton for his willing assistance and helpful criticism.

References

Crook, T. and Jones, B. M. (1906), Geikielite and the ferromagnesium titanites: *Min. Mag.*, **14,** 160–166.

Dick, A. (1893), On geikielite, a new mineral from Ceylon: *Min. Mag.*, **10,** 145–147.

Efremov, N. (1954), Geikielite from Mount Jemorakly-Tube, North Caucasus, USSR: *Am. Mineral.*, **39,** 395–397.

Gower, J. A. (1957), *X*-ray measurement of the iron magnesium ratio in biotites: *Am. J. Sci.*, **255,** 142–156.

Kashin, S. A. (1937), Metamorphism of chromspinelids in the Camel Mountains (Southern Urals): Chromites of the USSR: Acad. Sci. USSR.

Murdoch, J. and Fahey, J. J. (1949), Geikielite, a new find from California: *Am. Mineral.* **34,** 835–838.

Palache, C., Berman, H., and Frondel, C. (1944), *The System of Mineralogy,* Wiley, New York.

Sahama, Th. G. (1953), Mineralogy of the humite group: *Annales Acad. Scient. Fenn.* Ser. A II, No. 31, 50 pp.

Swanson, H. E., and Fuyat. R. K. (1953), Standard X-ray diffraction powder patterns: *U. S. Nat. Bur. Stand., Circ. 539,* **2,** 35.

Swanson, H. E., Gilfrich, N. T. and Ugrinic, G. M. (1955), Standard *X*-ray diffraction powder patterns: *U. S. Nat. Bur. Stand., Circ. 539,* **5,** 43.

Wones, D. R. (1958a), The Phlogopite-annite join: *Carn. Inst. of Wash. Yearbook* **57,** 194–195.

Wones, D. R. (1958b), Phase relations of biotites on the join phlogopite-annite: *Bull. G.S.A.*, **69,** 1665.

THE AMERICAN MINERALOGIST, VOL. 44, JULY–AUGUST, 1959

CERIANITE, CeO_2, FROM POÇOS DE CALDAS, BRAZIL

Clifford Frondel and Ursula B. Marvin, *Harvard University, and Union Carbide Ore Company, New York.*

Cerianite has been identified as a secondary mineral from Morro do Ferro on the Poços de Caldas plateau, Minas Gerais, Brazil. The cerianite occurs in soft, weathered materials lying within a radioactive zone on the southeastern slope of Morro do Ferro. Samples of these materials were collected in July, 1956, by T. C. Marvin, Geologist for the Union Carbide Ore Co., during a visit to the locality in company with Helmuth Wedow, of the U. S. Geological Survey, who had made a detailed study of the geology of the mountain. The samples containing cerianite were taken from a small, irregular zone, a few inches in width, of especially high

radioactivity, at a depth of 3 to 4 feet in the wall of a prospecting trench. Freshly broken masses are weakly coherent to friable, with a greenish yellow to buff color, and, on drying, these break down surficially to a buff colored powder of flour-like consistency composed chiefly of cerianite. Small amounts of very fine-grained hydromica and kaolinite are admixed, and the masses are cut by tiny veinlets of limonite.

Morro do Ferro is a hill composed of deeply weathered phonolite and nepheline syenite cut by massive dikes of magnetite. Bastnaesite, thorogummite, and allanite have been reported from this locality (1). The cerianite is a weathering product and may have been derived from these minerals. Cerium is the only rare-earth that has a tetravalent, as well as a trivalent, state that is stable under geologic conditions. The dioxide is formed by the hydrolysis of soluble cerium salts under oxidizing conditions. Cerous hydroxide is a strong reducing agent, particularly in alkaline solution, and oxidizes to hydrous ceric oxide. The other rare-earths are not known to form oxides or compounds, other than the basic carbonates, under weathering conditions. In any case, the other rare-earth oxides are not isostructural with CeO_2. During weathering, cerium may, in this way, become separated mineralogically from rare-earths with which it was directly associated in primary minerals such as bastnaesite, $(Ce, La)(CO_3)F$. Cerium dioxide is formed also by the thermal decomposition in air of cerium compounds.

The cerianite was identified by its *x*-ray diffraction pattern which checks with that of synthetic CeO_2, and with the ASTM file. The unit cell dimension is a_0 5.411 ± 0.004 Å, comparing closely with the values, 5.397 Å to 5.416 Å, reported (2) for synthetic CeO_2. A sample from which most of the admixed hydromica and kaolinite had been removed by separation in methylene iodide was found, by *x*-ray fluorescence analysis, to contain Ce as the only major constituent together with minor Fe and very small amounts of Y, Th, Zr, and U. The Fe probably is due to admixed limonite, and the other elements may be present either in solid solution or as finely divided admixed thorogummite or other minerals. In synthetic materials, CeO_2 forms a complete series with UO_2 and ThO_2 in the fluorite structure-type (2). Under an oil immersion lens, the irregular grains of cerianite are isotropic with an index of refraction above 2.0. The mineral does not fluoresce in ultraviolet radiation, but a sample of synthetic CeO_2, prepared by igniting ceric sulfate in air, fluoresced a bright salmon pink in long-wave, and dull salmon pink in short-wave, ultraviolet.

Cerianite was first described by Graham (3) in 1955 from Lachner Township, Sudbury district, Ontario. It occurs very sparingly as minute crystals in partly absorbed inclusions of wall-rock in a dike-like zone of

carbonate rock cutting a nepheline syenite. The Ontario mineral contains roughly 5 weight per cent of ThO_2 in solid solution

References

(1) Oliveira, A. I. Reservas Brasileiras de Tório: *Engenharia, Mineração e Metal.*, **24,** 164, Sept. 1956.
(2) See literature cited by Frondel, C., Systematic Mineralogy of Uranium and Thorium; *U. S. Geol. Survey Bull.*, **1064,** 53 (1958)
(3) Graham, A. R. Cerianite, CeO_2, a new rare earth oxide mineral: *Am. Mineral.*, **40,** 560–564, 1955.

THE AMERICAN MINERALOGIST, VOL. 44, JULY–AUGUST, 1959

A NEW DILUENT FOR BROMOFORM IN HEAVY LIQUID SEPARATION OF MINERALS*

Robert Meyrowitz, Frank Cuttitta, and Nelson Hickling,
U. S. Geological Survey, Washington 25, D. C.

Dimethyl sulfoxide, $(CH_3)_2SO$, has been tested and is recommended as a diluent for bromoform in place of acetone. Its vapor pressure and flammability is much less than that of acetone. It is a colorless, odorless liquid.

Carbon tetrachloride, CCl_4, benzene, C_6H_6, ethyl alcohol, C_2H_5OH, and acetone, $(CH_3)_2CO$, have been used as diluents in the preparation of heavy liquids for the separation of minerals (Krumbein and Pettijohn, 1938, p. 321). The mixture most commonly used is acetone-bromoform. The disadvantages of acetone as a diluent are its high vapor pressure and its flammability.

The vapor pressures of dimethyl sulfoxide and bromoform are relatively low and of the same order of magnitude (Table 1). Changes in composition of mixtures of these compounds due to differential evaporation are small. These mixtures maintain relatively constant specific gravities during use and in storage as compared to the acetone-bromoform mixtures. A mixture having a specific gravity 2.58 did not change measurably in the second decimal place after 30 mineral separations, including filtering. There is a slight darkening in the color of the mixture after use.

Table 1 compares the salient properties of dimethyl sulfoxide, acetone, and bromoform.

The combining volumes of bromoform-dimethyl sulfoxide mixtures are additive and a straight-line mixing curve (volume+volume) can be

* Publication authorized by the Director, U. S. Geological Survey.

Table 1. Some Physical Properties of Dimethyl Sulfoxide, Acetone, and Bromoform

	Melting point ° C.	Boiling point ° C.	Vapor pressure mm Hg at 20° C.	Vapor pressure mm Hg at 30° C.	Specific gravity	Index of refraction	Flash point ° F.	Viscosity 25° C. cp
Dimethyl sulfoxide[1]	18.4	189	0.37	0.79	1.100 (20° C.)	1.48	203	1.98
Acetone	−95[2]	56.5[2]	185[3]	283[3]	.79 (20° C.)[2]	1.36[2]	15[2]	.32[2]
Bromoform	6–7[2]	149.5[2]	5 (22° C.)[4]	9.4 (25° C.)[3]	2.89[2]	1.60[2]	None	1.89[2]

[1] Stepan Chemical Co., Technical Bulletin, Dimethyl sulfoxide, December 29, 1954.
[2] Hodgman, 1957.
[3] National Research Council, 1928.
[4] Perry, 1950

used to prepare a liquid of desired specific gravity. Acetone, dimethyl sulfoxide, and water are miscible in all proportions. The separated minerals can be washed free of a bromoform-dimethyl sulfoxide liquid using acetone, and the bromoform can be recovered from the washings by the same procedure commonly used for its recovery from bromoform-acetone mixtures, that is, mixing the washings with large volumes of water (Krumbein and Pettijohn, 1938, p. 322).

The price of technical grade dimethyl sulfoxide is similar to that of N.F. grade acetone.

Information supplied by the manufacturer of dimethyl sulfoxide states that "limited tests carried out on rats, guinea pigs, and rabbits indicate that no damage to lung tissue, no allergenicity nor skin irritation is caused by dimethyl sulfoxide." However, "due care should be exercised in its handling and application."

References

Hodgman, C. D., 1957, Handbook of chemistry and physics: 39th ed., Cleveland, Chemical Rubber Publishing Co.

Krumbein, W. C., and Pettijohn, F. J., 1938, Manual of sedimentary petrography: New York, Appleton-Century-Crofts, Inc.

Perry, J. H., ed., 1950, Chemical engineers handbook: 3d ed., New York, McGraw-Hill Book Co., Inc.

National Research Council, 1928, International critical tables of numerical data, physics, chemistry and technology: 1st ed., v. 3, New York, McGraw-Hill Book Co., Inc.

THE AMERICAN MINERALOGIST, VOL. 44, JULY-AUGUST, 1959

AN ELUTRIATING TUBE FOR THE SPECIFIC GRAVITY SEPARATION OF MINERALS*

I. C. Frost, *U. S. Geological Survey, Denver, Colorado.*

Introduction

Studies of the isotopic composition of lead in nature require the isolation of relatively pure galena from associated host minerals. Separation techniques based on the use of heavy liquids, sulfide flotation, water superpanning, electromagnetic separations, hand-picking and elutriation have all been utilized on various samples, depending on the properties of the associated minerals. Some of these techniques are time-consuming and require expensive reagents or apparatus, and the use of heavy liquids and sulfide flotation techniques require reagents which may be toxic or chemically corrosive to some metal sulfides. Water elutriation, therefore, seemed particularly attractive and a study was made to adapt or develop suitable apparatus and techniques for ore mineral separations.

Taggart (1945) describes several elutriators which employ rising liquid for size classification of a mineral. Gross, Zimmerley and Probert (1929), of the Bureau of Mines describes a method for sizing ore by elutriation, and Cooke (1937) also of the U. S. Bureau of Mines, reports on a short column hydraulic elutriator for size classification of subsieve sizes. These methods are based on Stokes' law which relates the settling rate of spherical particles of known radius and density through a medium of known viscosity and density. By causing the medium to flow upward, the grains can be given a positive, zero, or negative rate of settling relative to the apparatus. By adjusting this flow closely, sized mineral grains can be fractionated according to their specific gravities.

Description of Elutriation Apparatus

An all-glass elutriating tube modified and adapted from models described by H. L. Gibbs (written communication, 1958) and by Taggart (1947) was constructed. The tube assembly with constant-head water supply and receiver flasks for recovery of sinks and floats is shown as figure 1. The elutriator tube may be constructed inexpensively by any glass blower. The increasing cross-sectional areas of the tube were so chosen that the velocity of rising water is reduced approximately 50 per cent with its entry into each larger section. The volume of the tube below

* Publication authorized by the Director, U. S. Geological Survey.

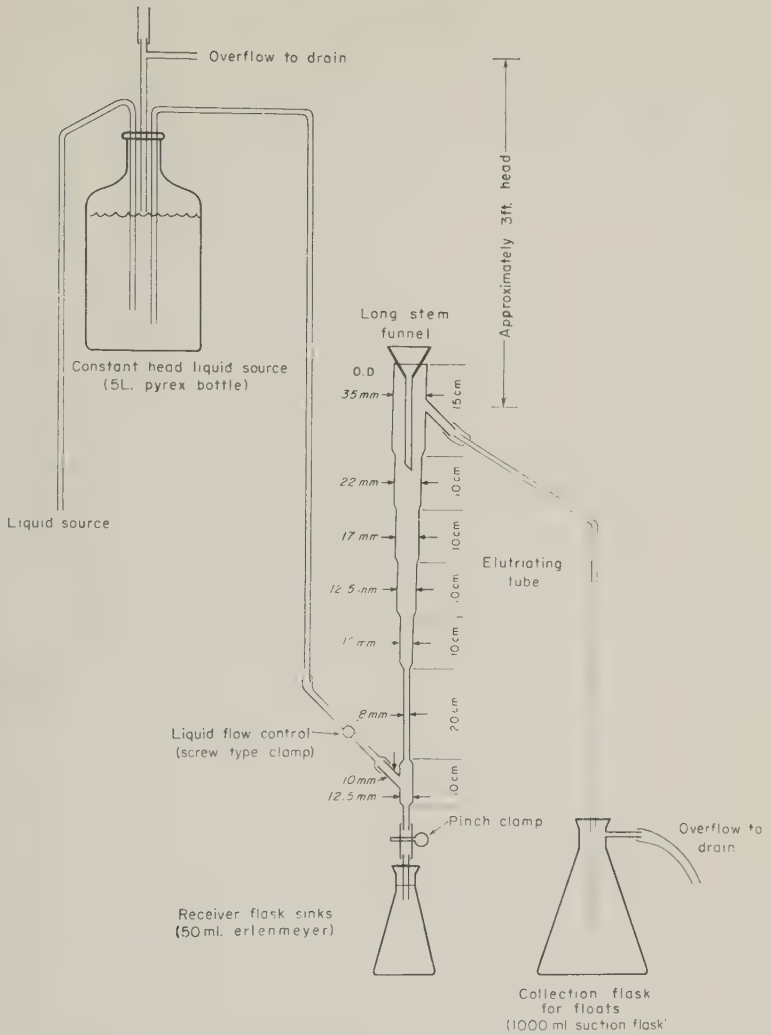

FIG. 1. Schematic diagram of elutriating apparatus.

the overflow outlet is approximately 125 ml. This capacity is designed for a sample load of not more than 10 grams at any one time. The inlet at an enlarged portion near the bottom of the tube was designed to minimize eddy currents in the small-diameter fractionating section. It is essential that the tube be mounted exactly vertical for efficient elutriation. The elutriating water in storage at the start of any mineral separa-

tion is treated with a commercial wetting agent to insure complete wetting of all mineral particles. The amount of wetting agent added is not too critical and may be determined from dilution directions supplied with the reagent used. The long-stem funnel placed in the top of the elutriating tube permits the sample slurry to be introduced below the overflow at a point least subject to lift from rising water.

Operation of the Apparatus

Not more than 10 grams of crushed sample, which has carefully been sieved to uniform particle size, is mixed into a slurry with water containing a wetting agent. The slurried sample is quickly transferred to the elutriating tube by means of a small stream of water from a wash bottle. The upward flow of water is adjusted so that those minerals having the highest specific gravities are suspended above the bottom fractionating section. After 2 or 3 minutes of fractionation the rate of flow is decreased so that those mineral grains having the highest specific gravities slowly drop from the bottom fractionating section into the receiver flask. Visual observations are used to determine the desired fraction of the sample. The receiver flask can be removed at any time by applying a pinch clamp to the rubber connection used to attach the receiver flask to the elutriating tube. A new receiver flask, filled with water, may then be attached to the elutriating tube. This permits small fractions of mineral separates to be removed at will and observed by a hand lens or binocular microscope. Adjustment of the water flow by the screw clamp gives decreasingly slower water velocities and thereby separation by sinking of minerals of decreasing specific gravity.

In our work most minerals have been separated as described above, but it is also possible to collect the minerals from the top overflow by increasing the velocity of flow. Those minerals of lowest specific gravity and such other minerals as micas which may have large surface areas in relation to their diameters may be more easily collected as floats. Biotite has been satisfactorily separated from samples both as floats and as residue after removal of all minerals which sank prior to the biotite.

A short time spent with the elutriator will permit one to determine the best procedure to follow for the specific separations being made. Sometimes a few mineral particles having lower specific gravities than the mineral being separated may be mechanically carried down with the sinks. An additional pass of this mineral concentrate through the column will remove these minerals with lower specific gravity. Maximum recovery of a desired mineral may also be best obtained by means of an initial separation for removal of the bulk of the impurities and followed

by a second elutriation to recover the concentrated mineral. Should the initial elutriating conditions not prove satisfactory, no part of the sample need be lost as both the sinks and floats are easily recovered.

Satisfactory mineral separations have been accomplished on a wide range of particle sizes, providing that each closely sized fraction is elutriated separately, and that the grains are not mineralogically composite. Galena separates of better than 95 per cent purity were obtained easily from seven different size fractions, between 40 and 200 mesh, from a specimen containing galena, gahnite, biotite, and quartz.

By using sized one-gram samples each of quartz, pyrite, and galena, it was possible to keep essentially all of a given mineral in any two adjacent sections of the elutriating tube. No differences in this respect were observed between samples sized to -40 $+60$, -60 $+80$, or -80 $+100$ mesh.

Qualitative comparisons between water elutriation and other mineral separations techniques are difficult to evaluate. Not only the purity of the separate but also its percentage recovery must be considered. Separations of galena from pyrite, difficult and time consuming by sulfide flotation and water super panning, were readily made by elutriation. A synthetic mixture containing equal amounts of pyrite and galena sized to -100 $+120$ mesh yielded 81 per cent of the galena with a purity visually estimated at better than 95 per cent, and almost complete recovery of pyrite, of similar purity, was made from an ore composed primarily of quartz and pyrite. Free gold also was easily separated from host material.

Extension and Adaptations

An elutriating tube similar in design to the one described but proportionally larger, should prove advantageous for mineral separations of larger samples. The larger tube would also be especially suited for fine-grained materials which settle slowly and therefore require only a minimum flow of rising water. Although water has much to recommend it, other liquids or gases might be adapted as the elutriating medium. Gaudin and others (1930) proposed the use of acetone as an elutriating medium; this was investigated and found satisfactory. Its lower specific gravity and viscosity together with its wetting properties would recommend it for some specific mineral separations.

Sizing by elutriation is common practice, and the elutriating tube described permits easy particle sizing of material of uniform density and shape. Water elutriation also makes field separations possible as a field reconnaissance tool in heavy minerals exploration.

The author wishes to acknowledge the helpful suggestions of R. S.

Cannon, Jr., under whose immediate supervision this work was carried out.

References

Cooke, S. R. B., 1937, Short column hydraulic elutriator for subsieve sizes: U. S. Bur. Mines Rep. Inv. 3333.

Gaudin, A. M., Groh. J. O., and Henderson, H. B., 1930, Sizing by elutriating of fine ore-dressing products: Indus. and Eng. Chemistry, v. **22** p. 1363.

Gross, John, Zimmerley, S. R., and Probert, Alan, 1929, A method for sizing of ore by elutriation: U. S. Bur. Mines, Rep. Inv. 2951.

Taggart, A. E., 1945, Handbook of mineral dressing: New York, John Wiley and Sons, Inc.

THE AMERICAN MINERALOGIST, VOL. 44, JULY–AUGUST, 1959

USING THE MICROSCOPE FOR SPECIFIC GRAVITY DETERMINATION OF MINUTE MINERAL GRAINS

B. M. Shaub, *Northampton, Massachusetts.*

The determination of the specific gravity of the larger pieces of solid materials is comparatively easy and is accurately performed by means of the various balances now in common use. The system of comparing the specific gravity of an unknown solid with that of calibrated heavy liquids is also very useful for quick determinations of their relative specific gravities. The approximation to the actual specific gravity of the unknown by this method depends upon the variation in the specific gravities between the individual liquids in the set. The actual specific gravity of a solid can, of course, be determined by adjusting the density of the liquid to equal that of the solid. This state is obtained when the latter merely swims about in the liquid for its movement is then determined by convection currents rather than by any differences in specific gravities.

The application of the heavy liquid technique for specific gravity determination can be done with considerable facility by means of a petrographic microscope or any microscope which permits tilting the stage and tube to 60 degrees or preferably more. A sample of the material is prepared by crushing a fragment of the specimen, allowing some of the pieces to be several times larger than the majority of the smaller ones. A microscope slide is made from the crushed material in the same manner as in preparing a specimen for the index of refraction determination. After covering the grains with a cover glass a liquid of known specific gravity is placed between the slide and the cover glass. The slide is then placed on the microscope stage and the stage is then tilted to 60 degrees or more. Upon rotation of the stage one will observe that the smaller

particles will either rise or sink in the liquid between the glass slide and the cover glass, depending upon the relative densities of the mineral fragments and the liquid. Surface tension will hold the cover glass in place if the separation is not too great. The movement of the particles in the liquid is, of course, slowed up when the viscosity of the specific gravity liquid is appreciable. As petrographic microscopes invert the image, a grain heavier than the liquid will appear to rise in the medium; however, one soon becomes accustomed to this reversal.

The fine-grained material, which must have a specific gravity within the range of the liquids used, can be most effectively handled by mixing it with a small amount of coarser material to provide and maintain a relatively larger space between the slide and the cover glass. Two advantages are that only a very small amount of material is required and with smallness of the pieces one also obtains a maximum of purity and freedom from associated minerals.

The specific gravities of the rock-forming minerals come within the range of the common heavy liquids, hence the microscopic method of determining the specific gravity of such minerals may readily and quickly be carried out. One can easily pick out individual clean grains from a mixture by using the optical features of the microscope as he is proceeding with the manipulations for determining the specific gravity. The specific gravity of detrital material too fine-grained for handling by conventional methods or in too small amounts can readily be determined by this method.

The accuracy of the method will depend largely on the differences between the specific gravities of the adjacent individual liquids in the set and upon their viscosities, also on the angle to which the microscope is tilted. The optimum position is when the tube is horizontal. For small particles in the more viscous liquids the movement may be slight when the gravities are approximately the same, hence the operator must pay strict attention to the relative motion between the free and stationary particles in the preparation.

In making a more precise determination of the specific gravity of a solid the density of the liquid in use can be adjusted to match the material after which the density of the final liquid can be determined by any one of the several usual methods.

The transfer of a limited amount of sample material from one slide to another will depend upon the degree of skill that the researcher possesses. The transfer is performed in the same manner as transferring scarce material from slide to slide during the determination of the indices of refraction.

THE AMERICAN MINERALOGIST, VOL. 44, JULY–AUGUST, 1959

THE EFFECT OF HEAT TREATMENT ON THE SUPERSTRUCTURE IN THE PLAGIOCLASES IN RELATION TO CHANGES IN LATTICE ANGLES

WILLIAM L. BROWN,* *Eidgenössische Technische Hochschule, Zürich, Switzerland.*

A baffling feature in the structure of the low-temperature plagioclases of intermediate composition is the presence of a superstructure of complex nature. Subsidiary reflections occurring in pairs in non-Bragg positions were first found by Chao and Taylor (1940) on rotation photographs. The study of the position of these reflections as a function of composition and thermal state was begun by Cole, Sörum and Taylor (1951) and continued systematically by Gay (1956). The effect of heat treatment was investigated by Gay and Bown (1956), but attention was focussed on the mode and rate of disappearance of these reflections and not on the changes in the lattice constants evidenced by the main reflections. The pairs of subsidiary reflections approximate to type-(*b*) reflections (Laves and Goldsmith, 1951; Gay, 1953) and normally merge to form such in the compositional range An_{70-75}. Various theories (Chao and Taylor; Megaw, 1957; Chayes, 1958) have been advanced to account for these "split" reflections, but, at present, none seems to be satisfactory, though it is possible that the work of Chayes may lead to a solution of the problem.

Two crystals containing respectively 35 and 50% anorthite by weight were selected for the study of the relation of the changes in the split type-(*b*) reflections and in the lattice angles on heat treatment. Split type-(*b*) reflections were present in the unheated materials; those for the labradorite with 50% anorthite were sharp and almost as strong as type-(*a*) reflections, whereas those for the andesine with 35% anorthite were slightly diffuse and weaker. The crystals were then heated at 1140° C., removed from the oven after given periods of time and *x*-rayed at room temperature. The results are given in Table 1. A rapid but small change occurs in the angles γ^* and $(010)/(\bar{1}01)$ in the first 1-2 days; no further change occurs even on heating for 70 days at this high temperature. The final value of γ^* for both specimens corresponds to that of high albite, i.e. to the point B in figure 6 in Brown (1959).

The split type-(*b*) reflections gradually disappear with increase in heating time. Those for the andesine were no longer visible on *a*-axis pre-

* Present address; Mineralogy Department, The Pennsylvania State University, University Park, Pennsylvania.

TABLE 1. RECIPROCAL LATTICE ANGLES OF HEATED SPECIMENS
Temperature—1140° C.

Andesine, An_{36}, S349[1]				Labrodorite, An_{50}, S113[1]			
Number of days	α^*	γ^*	(010)/($\bar{1}$01)	Number of days	α^*	γ^*	(010)/($\bar{1}$01)
0	86°04′	88°29′	87°20′	0	86°06′	88°18′	87°30′
0.25	86°00′	88°26′	87°22′	0.25	86°05′	88°18′	87°36′
2.25	86°03′	88°02′	87°44′	2.25	86°02′	88°03′	87°50′
5	86°07′	88°05′	87°40′	5	86°02′	87°54′	87°51′
15	86°13′	88°07′	87°49′	15	86°07′	87°49′	87°53′
20	86°03′	88°05′	87°46′	20	86°04′	87°50′	87°51′
25	86°08′	88°02′	87°44′	25	86°02′	87°50′	87°53′
50	86°10′	88°03′	87°51′	50	86°07′	87°54′	87°54′
70	86°12′	88°08′	87°56′	70	86°09′	88°00′	87°58′

[1] The angles were measured on the Buerger precession camera and are accurate to ±5′. The S numbers are the specimen numbers in Brown (1959).

cession photographs of very long exposure after only 5 days at 1140° C. The labradorite required much more time, since the type-(*b*) reflections disappeared only after heating for 70 days at 1140° C. This time is much greater than those found by Gay and Bown. With progressive heating the pairs of spots became progressively weaker relative to the type-(*a*) reflections. The relative intensities of spots in the pairs did not change, but they became gradually more diffuse and finally merged to form a dumbbell-shaped area of blackening on *a*-axis precession photographs, before becoming too weak to detect. The sequence of stages with time on heating is very similar to the sequence found with decreasing anorthite content in plagioclases of low-temperature origin in the range An_{50-25}. The very diffuse type-(*b*) reflections in low-temperature plagioclases in the range An_{27-30} disappear in a few hours at high temperature, so the rate was not studied. Though no plagioclase more basic than An_{50} was studied, it is probable that the time required to effect the disappearance of the split type-(*b*) reflections would be greater in such plagioclases. Prolonged heating results in the disappearance of the single type-(*b*) reflections in bytownites (Gay, 1953, 1954).

There appears to be no connection between the changes in the lattice angles and the disappearance of the type-(*b*) reflections on heat treatment in the plagioclases. On the other hand, there is a connection between the anorthite content and the time required to produce the disappearance of the split type-(*b*) reflections. It is probable that the lattice constants of the plagioclases are determined by the short-range Si/Al order, whereas

the split type-(*b*) reflections are probably connected with longer-range Si/Al and Ca/Na order with the resultant presence of domains. Reference is made here to the electron-microscope photograph published by Baier and Pense (1957) of a replica of a face ground on labradorite in which evenly spaced linear traces of separation 0.3 μ (about 250 unit cells) are seen. The nature of these lamellae and the effect of heat treatment on them is being studied.

References

Baier, E. and Pense, J. (1957), Elektronenmikroskopische Untersuchungen an Labradoren: *Naturwiss.*, **44,** 110–111.

Brown, W. L. (1959), Lattice changes in heat-treated plagioclases—the existence of monalbite at room temperature: *Z. Krist.*, in press.

Chao, S. H. and Taylor, W. H. (1940), Isomorphous replacement and superlattice structures in the plagioclase feldspars: *Proc. Roy. Soc.* (*London*), **176A,** 76–87.

Chayes, F. (1958), A possible explanation of the δ_c separations in intermediate plagioclases: *Acta Cryst.*, **11,** 323–324.

Cole, W. F., Sörum, H. and Taylor, W. H. (1951), The structures of the plagioclase felspars: *Acta Cryst.*, **4,** 20–29.

Gay, P. (1953), The structure of the plagioclase felspars: III An X-ray study of anorthites and bytownites: *Min. Mag.*, **30,** 169–177.

——— (1954), The structure of the plagioclase felspars: V The heat treatment of lime-rich plagioclases: *Min. Mag.*, **30,** 428–438.

——— (1956), The structure of the plagioclase felspars: VI Natural intermediate plagioclases: *Min. Mag.*, **31,** 21–40.

Gay, P. and Bown, M. G. (1956) The structure of the plagioclase felspars: VII The heat treatment of the intermediate plagioclases: *Min. Mag.*, **31,** 306–313.

Laves, F. and Goldsmith, J. R. (1951), Short-range order in anorthite: A.C.A. Meeting, Chicago, October 1951. (Abstract p. 10). Compare *Acta Crysts.*, (1954), **7,** 131–132.

Megaw, H. (1957), Structure and disorder in plagioclase felspars: *Acta Cryst.* **10,** 761.

THE AMERICAN MINERALOGIST, VOL. 44, JULY–AUGUST, 1959

DIFFERENCES IN THE MONTMORILLONITE SOLVATING ABILITY OF POLAR LIQUIDS

W. D. Johns, *Washington University, St. Louis, Missouri,*

AND

R. T. Tettenhorst, *University of Illinois, Urbana, Illinois.*

The polar organic liquids which are most commonly employed to demonstrate the expandable nature of montmorillonite units are ethylene glycol and glycerol (Bradley, 1945; MacEwan, 1948). Heretofore, it has been generally assumed that these two organic liquids exhibit nearly the

same ability to solvate materials which have an expandable nature. That this supposition is incorrect has recently been revealed during the course of a study of montmorillonites (Tettenhorst, 1957).

A series of pure, dioctahedral montmorillonite samples have been analyzed in an attempt to explain the nature of the variations in properties from sample to sample. As a part of this study, three separate portions of 8 samples were made homoionic with Li^+, Zn^{++}, and K^+. Upon heating to 200°–300° C, some of the montmorillonite layers of each sample collapsed to mica-like or pyrophyllite-like dimensions. It is significant that the extent of the irreversibility of the collapse depends on the solvating agent which was employed to demonstrate the reexpandability.

In order to demonstrate the expandable character of those units not affected by the above treatments, parallel investigations involving solvation with water, glycerol and ethylene glycol were employed. In every instance, ethylene glycol reexpanded more layers than glycerol, and glycerol reexpanded more layers than water, after lithium, zinc, or potassium saturation and heat treatment. This was true whether or not these solvating agents were applied to the oriented clay slides as a liquid at room temperature or by the vapor pressure method (Brunton, 1955). This difference in behavior leads to the conclusion that these polar substances actually differ in their ability to reexpand montmorillonite layers which have been artificially modified. Estimates of the percentage of the reexpandable units following cation saturation, heat treatment, and solvation are tabulated in Table 1 for 8 different montmorillonites.

Prior to cation saturation, all of the montmorillonite layers of each sample expanded with water, glycerol, and ethylene glycol. It is apparent

Table 1. Reexpansion of Montmorillonites Following Cation Saturation and Heat Treatment to 200–300° C.

Sample No.	Li			Zn			K		
	Water	Glycerol	Glycol	Water	Glycerol	Glycol	Water	Glycerol	Glycol
1	0	10	65	0	70	100	0	55	90
2	0	10	70	0	80	100	0	50	85
3	0	5	45	0	70	100	0	50	75
4	0	5	40	0	70	100	0	55	85
5	0	45	75	0	80	100	0	80	100
6	0	25	75	nd	nd	nd	0	35	50
7	0	5	20	nd	nd	nd	0	85	100
8	0	5	25	nd	nd	nd	0	50	65

Numbers represent % units expanded. nd = not determined.

from Table 1 that differences in the effect of lithium, zinc, and potassium treatments on the individual units within a montmorillonite are least apparent after solvation with ethylene glycol. For example, consider montmorillonite number 5 which has been potassium saturated and heated to 300° C. Solvation with water following treatment indicates that the montmorillonite has been modified in some manner, since, unlike the natural material, it does not reexpand in water. On the other hand, ethylene glycol solvation would have suggested that treatment had not affected the expandability, since all of the layers expanded completely like the natural material. Glycerol treatment, however, is more revealing, and indicates the presence of two kinds of layers (with respect to reexpandability) following treatment.

It is not our intention to discuss the manner in which certain montmorillonite layers have been differentially modified. Greene-Kelly (1953) and others have dealt with this matter. We only wish to emphasize that glycerol appears in these instances to be a better agent than ethylene glycol in revealing differences between silicate layers in a montmorillonite. This is particularly important in light of recently adopted practice (Weaver, 1958) in which glycol is used following potassium treatment to reveal differences in expanding characteristics and therefore, to distinguish between stripped micas and montmorillonites. It is likely that other polar organic liquids may be found which are even more selective than glycerol. The interpretation of the significance of the expandability of clays may be meaningless unless the character of the solvating agent is also taken into consideration.

It is apparent that further study of the mechanism of clay-organic complex formation is necessary. The fact that certain solvating agents are preferentially adsorbed by montmorillonite layers must be related to the structure of the organic molecule and its configuration when in contact with the clay surface.

References

Bradley, W. F. (1945), Molecular associations between montmorillonite and some polyfunctional organic liquids: *Jour. Amer. Chem. Soc.*, **67**, 975–981.

Brunton, G. (1955), Vapor pressure glycolation of oriented clay minerals: *Amer. Mineral.*, **40**, 124–126.

Greene-Kelly, R. (1953), Irreversible dehydration in montmorillonite, Part II: *Clay Minerals Bulletin*, **2**, 52–56.

MacEwan, D. M. C. (1948), Complexes of clays with organic compounds, I: *Trans. Faraday Soc.*, **44**, 349–367.

Tettenhorst, R. (1957), Unpublished M.A. thesis, Washington Univ., St. Louis, Mo.

Weaver, C. E. (1958), The effects and geologic significance of K "fixation" by expandable clay minerals derived from muscovite, biotite, chlorite and volcanic material: *Am. Mineral.*, **43**, 839–861.

THE AMERICAN MINERALOGIST, VOL. 44, NOS. 7 AND 8, 1959

A NATURAL COBALT ANALOGUE OF PENTLANDITE

OLAVI KOUVO, MAIJA HUHMA, AND YRJÖ VUORELAINEN,
Outokumpu Co., Finland.

Much pertinent information regarding the synthetic (Fe, Co, Ni)$_9$S$_8$ pentlandites is to be found in the literature of inorganic chemistry. This information is well summarized in the work of Ibrahim (1959). The homogeneous π-phase, (Fe,Ni)$_9$S$_8$, with the atomic ratio Ni:Fe close to one, is isostructural with Co$_9$S$_8$(Lindqvist *et al.*, 1936). Cobalt, however, has been shown to be present in natural pentlandites in amounts ranging from nil to about 2.9 wt.-% (Ibrahim, 1959).

Further evidence for the existence of natural solid solution along the nickel pentlandite—cobalt pentlandite join is obtained by observing the change in chemical composition in some pentlandites of Northern Karelia in Finland. Pentlandites rich in cobalt have been recognized at several localities in Northern Karelia, associated with copper and iron sulfides. In the following, the pentlandite of Varislahti and Savonranta pyrrhotite deposits as well as of the Outokumpu mine (Vähätalo, 1953) will be described. The name cobalt pentlandite is here adopted for the natural pentlandite rich in cobalt. The mineral was first noticed in 1957 as a minor constituent of the Varislahti sulfide deposit. Of the several cobalt minerals (linnaeite-siegenite, cobaltite, safflorite), cobalt pentlandite is the most abundant and has the widest geographical distribution. It is found associated with other sulfides, notably pyrrhotite. It occurs as exsolved lamellae as well as separate crystals rarely exceeding 4 mm. in diameter. Crystals have cubic cleavage. The color is more lustrous than that of nickel pentlandite.

The results of the chemical analyses are shown in Table 1. By comparing the analyses 4 and 5, it will be seen that the pentlandite in the lamellae shows the higher nickel content. The nickel pentlandite associated with pyrrhotite (analysis no. 7) is found in the Outokumpu ore as an especially rare accessory mineral in the parts of the contact zones of ore and serpentine (Vähätalo, 1953).

In Fig. 1 the cobalt and nickel pentlandites are plotted according to atomic percentages of the three cations.

X-ray powder diffraction patterns were made of some concentrates using a 114.6 mm. diameter camera and *x*-ray diffractometer technique. The results obtained were corrected by using silicon as a standard. The powder data of cobalt pentlandite (analysis no. 3) are shown in Table 2 together with those of nickel pentlandite (ASTM 8–90).

Table 1. Chemical Composition of Some Pentlandites

	1	2	3	4	5	6	7
Co	49.33	46.52	42.73	30.94	22.77	18.84	1.92
Ni	9.06	9.11	9.78	21.10	23.52	26.98	31.82
Fe	10.32	11.57	13.22	15.62	20.46	21.10	32.30
S	31.29	32.80	34.25	32.34	33.25	33.07	33.96

1–2. Pyrrhotite-cubanite-chalcopyrite ore. Vrl-15, Varislahti, Kuusjärvi parish.
3. Pyrrhotite-chalcopyrite-pyrite ore. 285 Mpl 2, Outokumpu mine.
4–5. Pyrrhotite-chalcopyrite-pyrite ore. X area, Outokumpu mine.
6. Pyrrhotite ore. Sr-Sä 35, Säimen, Savonranta parish.
7. Lenticular body of pyrrhotite in skarn rock. 320 Mp 3, Outokumpu mine.

As may be expected from the variability in chemical composition, the lattice constants also vary slightly. The following results show that there is a general increase in lattice constants of pentlandites with decrease in Co:(Fe,Ni) ratio:

	a_0
Outokumpu, analysis No. 7	$10.067_5 \pm .001$ Å
Outokumpu, analysis No. 4	$9.999_8 \pm .001$ Å
Varislahti, analysis No. 2	$9.969_7 \pm .001$ Å
Co_9S_8, synthetic (Ibrahim, 1959)	$9.929 \pm .002$ Å

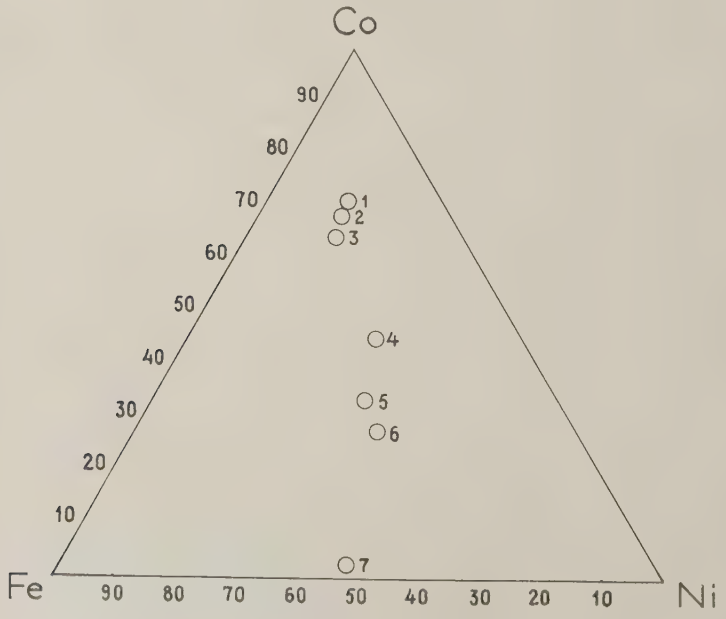

Fig. 1. Atomic per cent diagram of pentlandites, analyses 1–7.

TABLE 2. *X*-RAY POWDER SPACING DATA FOR NATURAL COBALT PENTLANDITE AND NICKEL PENTLANDITE

hkl	Cobalt Pentlandite (analysis No. 3)		Nickel Pentlandite (ASTM 8–90)	
	d (Å)	I	*d* (Å)	I
111	5.75	m	5.78	30
002	4.97	vw	5.01	5
022	3.52	vw	3.55	5
113	3.008	vs	3.03	80
222	2.878	m	2.90	40
004	2.496	vvw	2.51	5
133	2.288	mw	2.30	30
024	2.237	vvw	2.25	5
115, 333	1.918	s	1.931	50
044	1.763	vs	1.775	100
135	1.686	vw	1.697	5
335	1.522	w	1.530	10
226	1.505	w	1.514	10
355, 731	1.298	mw	1.307	20
008	1.246	mw	1.255	20
157, 555	1.151	w	1.160	5
119, 357	1.097	vvw	1.105	5
139	1.045	w	1.052	$5a_1$
448	1.018	m	1.025	$20a_1$
159, 377			0.9704	$5a_1$
088			0.8878	$5a_1$
579			0.8068	$5a_1$
0·4·12			0.7941	$10a_1$

Optical properties of the cobalt pentlandites are similar to the optical properties of nickel pentlandite. Under microscope the color is slightly lighter than that of nickel pentlandite.

As can be seen from the measurements kindly made by Mr. Lauri Hyvärinen of the Geological Survey of Finland, the Vickers-hardness (M_{H50}) falls off slightly with decreasing cobalt content:

Varislahti, analysis No. 1	310 kg./mm.^{2}
Outokumpu, analysis No. 4	280 kg./mm.^{2}
Kotalahti, nickel pentlandite	260 kg./mm.^{2}
Savonranta, analysis No. 6	245 kg./mm.^{2}

Grinding hardness of cobalt pentlandite is slightly lower than that of pyrrhotite.

The etch reactions are similar to those obtained with the nickel pentlandite: negative with KOH, $HgCl_2$, KCN, HCl, and $FeCl_3$. A reaction

occurs with HNO_3: a bright blue stain with cobalt pentlandite but a brown stain with nickel pentlandite.

Some qualitative studies of *x*-ray powder patterns showed a loss of intensity of pentlandite lines during heating at about 350° C. (20 times for 2 minutes in air). Spinel (M_3S_4) pattern appeared, increased in intensity, and the siegenite member of the M_3S_4 group was the final product, when the pentlandite structure disappeared.

This work is part of a program being conducted by the Outokumpu Company. Acknowledgement is made gratefully to Mrssrs. Jorma Kinnunen, M.A., and Lasse Kosomaa, M.A., for providing the chemical data obtained, and to Mr. P. Westerlund, Min.Eng., for his help in flotation of some samples for final purification.

The authors wish to express their appreciation to the Outokumpu Company for permission to publish this paper.

References

Ibrahim, M. A. (1959), Ternary Phase in the M_9S_8 Section of the System Fe-Co-Ni-S. A thesis for the Degree of Master of Engineering: Nova Scotia Technical College, Halifax, N. S., Canada.

Lindqvist, M., Lundqvist, D. and Westgren, A. (1936), The Crystal Structure of Co_9S_8 and of Pentlandite (Ni, Fe)$_9S_8$: *Svensk Kem. Tidskr.* **48,** 156.

Vähätalo, Veikko O. (1953), On the geology of the Outokumpu ore deposit in Finland: *Bull. Comm. géol. Finlande* **164.**

PEACOCK MEMORIAL PRIZE

The Walker Mineralogical Club announces that it has awarded its Peacock Memorial Prize (1958) of two hundred dollars "for the best scientific paper on pure or applied mineralogy, including crystallography, mineralogy, petrology, ore genesis, and geochemistry," submitted by a graduate student, to

Mr. R. L. Moxham,
1395 Birch Avenue,
Burlington, Ontario.

a graduate student in the Department of Geology, Hamilton College, McMaster University. The subject of Mr. Moxham's paper was "Minor Element Distribution in Some Pyroxenes of Metamorphic Origin." He did his work under Professor Denis M. Shaw, Chairman of the Department of Geology, Hamilton College, McMaster University.

The Walker Mineralogical Club announces at this time that it is offering the Peacock Memorial Prize again in 1959. A copy of the announcement and conditions follows.

Peacock Memorial Prize for 1959

TWO HUNDRED DOLLARS—$200.00

For the best scientific paper on pure or applied mineralogy, including crystallography, mineralogy, petrology, ore genesis and geochemistry.

Conditions

1. The author of the paper shall be any graduate student enrolled in a Canadian university, a Canadian graduate student enrolled in any university, or any graduate student on a Canadian subject.

2. The paper, written in French or English, will be accepted for competition up to two years after completion of the work, even though the author may be enrolled no longer as a graduate student.

3. The paper may be in the form of: (a) a thesis,
(b) a paper ready for publication,
(c) a printed publication.

4. The paper may offer new or refined observations; or a significant synthesis and interpretation of existing data; or some new or improved application of mineralogy to useful ends; or the results of other work of sufficient interest and value.

5. Each paper must be accompanied by a letter from the candidate's supervisor stating the nature and extent of the assistance he may have given to the work submitted.

6. The paper is to be addressed to:
The Secretary, Walker Mineralogical Club,
100 Queen's Park, Toronto 5, Ontario.

7. CLOSING DATE OF THIS COMPETITION—December 31, 1959.

If no paper of sufficient merit is received, the prize will not be given. All papers submitted will be returned to their authors as soon as the judging is completed. Announcement of the award will be made in the appropriate publications.

Eighth National Clay Conference

On October 12, 13, and 14, 1959, the Eighth National Clay Conference will be held on the University of Oklahoma campus at Norman, Oklahoma under the auspices of the Clay Minerals Committee of the National Academy of Sciences-National Research Council.

A field trip will be arranged for either Sunday, October 11 or Thursday, October 15, probably to the Wichita Mountains in southwest Oklahoma to visit clay occurrences of geological interest.

Two symposia of invited papers will be held on the subjects of "Clay-Water Systems" and "Clay Mineral-Geochemical Prospecting Methods." In addition to these special symposia there will be general sessions of contributed papers. All those having contributions should contact Professor C. G. Dodd, Chairman, Eighth National Clay Conference, University of Oklahoma, Norman, Oklahoma. The title and a letter of intent should be sent in by June 1, and a 250 word abstract by July 1.

Further information and a preliminary announcement of the Conference may be obtained by writing Professor Dodd.

Bequest to Columbia University

Columbia University has announced what is believed to be one of the largest single bequests in Columbia's 205-year history. This bequest, from the late Henry Krumb, is expected to total nearly $6 million immediately, and eventually may amount to about $10 million. About one-half is directed to be applied toward the cost of a proposed Engineering Center on the Morningside campus. A similar amount is to be used for improving and building up the School of Mines.

Organic Geochemistry Section of the Geochemical Society

A group of organic and petroleum geochemists plan to organize an Organic Geochemistry Section within The Geochemical Society. The purpose of this section is to offer a common forum for research workers who are active in the various fields of organic and petroleum geochemistry. Recent advances in these fields indicate the desirability of the exchange of ideas and of their coordination with modern concepts of inorganic geochemistry and geology. The interest shown by earth scientists in The General Petroleum Geochemistry Symposium, which was held recently at Fordham University, supports this view.

Plans are being made to organize the Organic Geochemistry Section at the 1959 annual meetings of the Geological Society of America and The Geochemical Society in Pittsburgh, Pennsylvania, November 2–4. Information regarding this section may be obtained from the members of the Interim Executive Committee, who are listed below. The members of this committee invite suggestions and comments regarding this matter. It would be helpful if interested individuals could, in advance of the annual meeting, signify their intention to affiliate with the Section, whether or not they plan to attend the meeting.

The only requirements for affiliation with the Section are membership in the Geochemical Society and an interest in organic geochemistry. Membership in the society is open to individuals who have a bachelor's degree or its equivalent in a natural science and an interest in applying that science to geologic problems. Dues are $2.00 per year. Application blanks can be obtained from the Secretary, Professor Konrad B. Krauskopf, Department of Geology, Stanford University, California.

Edward G. Baker
Esso Research and Engineering Co.
P. O. Box 51
Linden, New Jersey

Bartholomew Nagy, Chairman
Department of Chemistry
Fordham University
New York 58, New York

Earl Ingerson
Department of Geology
The University of Texas
Austin 12, Texas

Paul A. Witherspoon
Department of Petroleum Engineering
University of California
Berkeley 4, California

Soviet Physics-Solid State

The American Institute of Physics is now publishing an English translation of a new *USSR Academy of Sciences* journal—Soviet Physics-Solid State.

It offers results of theoretical and experimental investigations in the physics of semiconductors and dielectrics, and on applied physics associated with these fields.

Regular subscriptions: U. S. and Canada	$55.00
Elsewhere	59.00
Libraries of non-profit	25.00
Degree granting institutions	29.00

American Institute of Physics,
Circulation Department
335 East 45th St., New York 17, N. Y.

BOOK REVIEWS

DETERMINATION MICROSCOPIQUE DES MINÉRAUX DES SABLES, by Solange Duplaix. 2nd Edition. 96 pages, 75 illustrations. Librairie Polytechnique Ch. Béranger, Paris and Liège. 1958. Price in France not known but 26 shillings in England.

This book commences with a short, superficial treatment of the methods of preparation of sediments of different types for heavy liquid fractionation, and a discussion of separatory techniques. In dealing with heavy media the diluents or wash liquids suggested for use with bromoform do not seem to be the most convenient ones since mixtures of bromoform and diiodomethane are often employed. The short section that follows immediately thereafter briefly touches upon the Becke bright line test, refractive index liquids, procedure for examining mineral fractions, and grain counting.

The major portion of the book is taken up with listings and discussion of the properties of minerals commonly found in sediments; 59 of them are arranged in alphabetical order. On turning to actinolite, the first mineral to be discussed, one is surprised to find the composition of this amphibole expressed as $Ca\ (Mg, Fe, Mn)_3\ Si_2O_{12}$, and after having read through the mineral descriptions that follow, one realizes that the chemical compositions listed by the author for crossite, glaucophane, riebeckite, and tremolite are, in every instance, completely inaccurate. The reviewer has excluded green hornblende from this observation since the composition is given in the broadest terms only, but it would have been helpful not to have labelled green hornblende a metasilicate. There are so many inaccuracies in the formulae of the amphiboles named that it is pointless to discuss them, except in one particular case, viz. the author's omission of hydroxyl. The rôle of water in tremolite and other amphiboles was carefully studied by Allen and Clement in 1908, and later W. T. Schaller pointed out the need to consider amphiboles as hydrous minerals. Then in 1929–30 Warren, Kunitz, and others should have left us in no doubts about this question. How long are we to wait before some notice is to be taken of these data?

For each mineral an outline of the main physical properties is provided but often the data provided are misleading, since they tend to suggest that a particular mineral may be recognized by a set of rather precise constants. For instance, the refractive indices listed for allanite may be correct in so far as one particular specimen is concerned, but they do not reflect the very wide range of values that are commonly found. Furthermore, the data also suggest that allanite and zircon are always anisotropic; very often this is not so. In the same way we find the refractive indices of tourmaline given to four significant figures as $N_g = 1.6435$ and $N_p = 1.6222$; this is quite misleading. Similarly it would have been more helpful if the empirical formulae had been expressed in such a way that some recognition were given to the accepted silicon-oxygen ratios in the different silicate groups; the formula for biotite is a case in point. Then, on the other hand, a number of inaccuracies are present. For example, since the vibration direction $Z = b$, and it is the acute bisectrix for light of all wavelengths in brookite, an optic axial plane cannot be parallel to (010) under any set of circumstances, and again the elongation of crossite may also be parallel to Y.

The formal descriptions of each mineral are complemented by short statements that deal with frequency of occurrence in sediments, diagnostic properties, and suggestions for ease of recognition. In the author's treatment of xenotime, an often quoted statement is repeated viz. that it is necessary to employ spectroscopic methods in order to distinguish between xenotime and colored (presumably yellow) zircon. This is, of course, unnecessarily misleading, since distinction between these minerals on the basis of refractive index is so simple, and yet so completely unambiguous. Furthermore, the reviewer may add that similar means will permit one to distinguish quickly between monazite and zircon. If sulphur-saturated diiodomethane is employed as immersion liquid, then one will find that α for

xenotime is always much less than the liquid; α for monazite is about equal to it, whereas the same vibration direction for zircon has a refractive index that is very much greater.

Seventy-five nicely executed figures, not sixty-nine as stated on the title page, have been provided to illustrate the characteristic form and general appearance of twenty-six of the fifty-nine minerals listed.

Tables in which minerals are listed according to density, refractive index, birefringence, and color are provided together with an inadequate bibliography and an index.

C. Osborne Hutton
School of Mineral Sciences,
Stanford University, California

DONNÉS DES PRINCIPALES ESPÈCES MINÉRALES. By Raymond Fischesser. J. and R. Sennac, 54 rue du Faubourg Montmartre, Paris 9e, France, 1955. 660 pp. 5200 fr.

Although this book was published in 1955, it unfortunately has not received any notice in the *American Mineralogist*. It is a compilation of determinative data on the principal mineral species, brought together by Raymond Fischesser, who is the chief Engineer of Mines and Assistant Director of the National School of Mines, Paris. The book consists of a series of abbreviated descriptions of most of the important rock-forming minerals, as well as of many of the less common ore and gangue species.

The arrangement of the descriptions departs radically from those in most descriptive mineralogical texts. The minerals are arranged into three major groups, 1) the silicates, 2) elements of mineral deposits, and 3) mineralizers and metallic minerals. These three major subdivisions are further broken down into 13 subgroups, the first four of which fall under the silicates (Group I). These are: Division 1) Essential rock silicates, 2) Metamorphic silicates, 3) Accessory rock silicates, 4) Alteration silicates and secondary silicates. In Part II, Division 5 describes the minerals of gangue assemblages and 6) the minerals of evaporite deposits (odd bedfellows indeed). In Part III there appear the following divisions: 7) Mineralizers and minerals of the acid-forming metals, 8) Sulfides, 9) Oxides, 10) Alteration minerals of sulfides and oxides, 11) Rare earth and uranium minerals, 12) Copper minerals, and 13) Minerals of the precious elements. Obviously this sort of arrangement, while attempting to be primarily genetic in character, contains categories of non-genetic aspect. Thus the classification, which attempts to ground itself on paragenesis, fails in certain respects.

Part IV consists of the synoptic tables, of which there are seven: Table 1, Classification by crystal system and specific gravity; Table 2, by habit and form; Table 3, by occurrence in hydrothermal deposits, using the subdivisions hypothermal, mesothermal, leptothermal, and epithermal; Table 4, by color; Table 5, by various physical properties including a) streak, b) feel, c) sectility; Table 6, by fluorescence; Table 7, by index of refraction; Table 8, by blowpipe tests, including those in closed tube, in open tube, on the charcoal block, bead tests, various reactions, and finally, chemical characteristics of the principal elements. The book concludes with a species index and with a bibliography.

Each of the species is described under the following headings: varieties, associated minerals, occurrence and deposits, crystal structure, form, physical properties, chemical properties, and alteration. For most species there are included drawings of crystals or aggregates. On these drawings faces are designated by letter symbols, but these are not identified in terms of Miller indices, although angles between certain faces are listed. One of the chief omissions is the absence of any x-ray data whatsoever.

The book is sectioned by means of a series of heavier sheets which form divider pages for the various groups, and to these are attached index tabs which permit easy access to

any of the groups or subgroups and thus to the various species, provided the reader can remember into which of the various "genetic" categories the author has placed a particular species; otherwise it is still necessary to refer to the species index. The book is incomplete with respect to mineral identification at the advanced level, particularly in its almost total disregard of major chemical variations in species and series and in the relation of this variation to variations in optical and physical properties. To the absence of basic data on this phenomenon in even "elementary" mineralogical reference works this review is a threnody. If indeed, as the author suggests, the work is to be considered as a "Mineralogical dictionary," then it must be reported that several aspects of its "definitions" are sterile.

E. Wm. Heinrich
Department of Mineralogy
The University of Michigan

PRÉCIS DE PÉTROGRAPHIE, Roches Sédimentaires, Métamorphiques et Éruptives. By Jean Jung. Masson et Cie, 120 Blvd. St. Germain, Paris 6e, France, 1958. 314 pages, with 160 figures, 20 plates, $24\frac{1}{2} \times 18\frac{1}{2}$ cm. 3600 fr.; bound, 4600 fr.

This is a good general presentation of the fundamental petrography of the major rock types. It is based on a series of lectures to students and consists of four parts. The initial section (48 pages), which deals with the rock-forming minerals, has its first part (the silicates) subdivided on the basis of the linkage of silica tetrahedra. This part is followed by descriptions of minerals other than silicates. Part one concludes with a table giving, in highly abbreviated form, some of the optical characteristics of the significant rock-forming minerals. The table is too generalized to be of much value in mineral determination, and the section contains but two charts (for the plagioclases) relating optical to compositional variation.

Part two (90 pages) deals with sedimentary rocks and is graced with some excellent photographs, both of hand-specimens and of these rocks in thin section, as well as a few electron micrographs of some of the clay minerals. In addition, there are numerous clear and carefully delineated drawings of various rock thin sections. In fact, these drawings constitute one of the major attractive features of the book. Part three, dealing with metamorphic rocks, consists of 51 pages and, like its counterpart on the sediments, is prefaced by a very brief and general discussion of genetic principles. Again both photographs of hand specimens and drawings of the rocks in thin section serve admirably to illustrate the major varieties. The last section, on igneous rocks (eruptive rocks) consists of 104 pages and has a slightly more extensive section dealing with the origin of these rocks and with their structures and textures.

For English workers the book is well designed to serve as a reference work, especially to outline adequately the French presentation of systematic microscopic petrography. The book is aptly titled; it is indeed a précis of microscopic petrography. Unfortunately, the price seems to be inordinately high for students and, as is apparently customary for most French books, the table of contents is last, an arrangement which, to the reviewer, seems as useful as concluding a scientific article with its abstract.

E. Wm. Heinrich
Department of Mineralogy
The University of Michigan

NEW MINERAL NAMES

Gallite

H. Strunz, B. H. Geier, and E. Seeliger. Gallit, $CuGaS_2$, das erste selbstandige Galliummineral, und seine Verbreitung in den Erzen der Tsumeb- und Kipushi-Mine. *Neues Jahrb. Mineral., Monatsh.* **1958,** No. 11–12, 241–264.

Galium has long been known to be present in amounts up to 1.85% in germanite from Tsumeb and various unidentified minerals have been thought to be gallium minerals. This is now proved to be the case.

Analyses by W. Reiner gave Cu 23.52, 35.52; Pb 14.25, 3.00; Zn 3.36, 2.76; Fe 3.41, 4.93; Ge 0.66, 0.45; Ga 23.06, 17.11; As 1.00, 0.90; S 24.16, 27.90; SiO_2 4.05, 4.92, sum 97.47, 97.49%. Recalculation, deducting (based on microscopic counts) quartz 4.0, 4.9; renierite 13.4, 8.0; tennantite 1.0, 0.4; galena 14.0, 1.7; bornite ———, 5.6; chalcocite ———, 5.3; digenite ———, 0.5; pyrite ———, 0.8; and "arsenate" ———, 2.0 give for the gallite Cu 26.9, 30.8; Pb 3.0, 2.3; Zn 4.6, 4.4; Fe 2.7, 4.9; Ga 35.4, 29.2; S 27.4, 28.4%, corresponding to $CuGaS_2$, with some substitution of Cu or Ga by Fe and Zn. The mineral was also synthesized by passing H_2S over an equimolar mixture of Ga_2O_3 and Cu_2O at 400°; the product gave an *x*-ray pattern identical with that of the mineral.

X-ray study by single crystal and powder photographs showed gallite to be tetragonal, structure like that of chalcopyrite, space group probably D_{2d}^{12}-$I\bar{4}2d$. The unit cell has a_0 5.35, c_0 10.48 Å, Z = 4. Hahn *et al.* (*Z. anorg. allgem. Chem.* **271,** 153–170 (1953)) found a_0 5.34_9, c_0 10.47 Å for synthetic $CuGaS_2$. Twinning on {112} was observed. Indexed *x*-ray powder data are given; the strongest lines are 3.064 (10), 1.876 (7), 1.611 (6), 1.088 (6), 1.214 (5).

The mineral is gray, luster metallic, streak gray-black, hardness 3–3½, G. 4.40 (calcd.), the mineral sinks slowly in Clerici solution with G.4.2. The mineral polishes well; reflecting power 26% in air, 13% in oil, internal reflections not observed, anisotropy low. Twenty photomicrographs are given.

The mineral occurs in renierite and germanite and as exsolution lamellae along (100) and (111) of sphalerite; when the latter is replaced by germanite, galena, or tennantite these lamellae or gallite may remain. Gallite contains exsolution lamellae of sphalerite oriented on (001).

The mineral occurs at Tsumeb, S. W. Africa, also observed by Uytenbogaardt from the Prince Leopold Mine, Kipushi, Belgian Congo, in a similar mineral assemblage.

The name is for gallium, of which this is the first mineral.

Michael Fleischer

Lusungite

L. Van Wambeke. Une nouvelle espece minerale: la lusungite en provenance de la pegmatite de Kobokobo (Kivu-Congo Belge). *Soc. belge geol, paleontol, et hydrol., Bull.* **67,** 162–169 (1958).

The mineral occurs in the phosphate zone of the Kobokobo pegmatite. It is dark brown and is associated with goethite (limonite) and quartz. *X*-ray study showed it to be hexagonal rhombohedral, space group D_{3d}^5—$R\bar{3}m$, a_0 7.04 ± 0.007, c_0 16.80 ± 0.01 Å, c_0/a_0 = 2.836; rhombohedral cell a 6.92A, α 61°12′. An indexed *x*-ray powder pattern is given; the strongest lines with intensities and (*hkl*) are: 2.98 (100), (201); 5.77 (90), (101), (003); 3.53 (61), (110); 2.477 (40), (024). The pattern is very close to those of hidalgoite, svanbergite, and plumbogummite.

Analysis on 1 mg. was made by the *x*-ray fluorescence method with a helium chamber. It showed Fe, Pb, Sr, P major; Ba, Ca minor (less than 3%), Al, As, less than 1%; S absent.

The weight ratio PbO/SrO was determined to be 1.40, hence Sr predominates over Pb. The formula, by analogy to those of other members of the plumbogummite group, is (Sr, Pb)$Fe_3(PO_4)_2(OH)_5 \cdot H_2O$.

In thin section the mineral is yellow-brown, very slightly pleochroic, uniaxial, probably positive, birefringence 0.03–0.04; the indices could not be measured accurately because of admixed limonite, but were variable, 1.77 1.855, much higher than those of goyazite, the analogous Sr-Al, and plumbogummite, the analogous Pb-Al compounds.

The name is for the Lusungu River.

M. F.

Birunite

S. T. Badalov and I. M. Golovanov. Birunite a new mineral of the thaumasite group. *Doklady Akad. Nauk Uzbekistan S.S.R.* **1957,** 12, 17–21 (in Russian).

The mineral occurs as dull white fibrous incrustations 2–3 mm. thick bordering veinlets of thaumasite that fills fractures in enstatitic rock in one part of the Kurgashinkan deposit, Almalyk ore field. Analysis gave CaO 41.46, MgO 0.61, SiO_2 26.70, CO_2 15.51, SO_3 3.33, H_2O 12.17, sum 99.78%. This corresponds, after deduction of about 5% opal (seen under the microscope as very fine isotropic disseminations) to 8.5 $CaSiO_3 \cdot 8.5\ CaCO_3 \cdot CaSO_4 \cdot 15H_2O$. Analysis of the associated thaumasite gave the usual formula $CaSiO_3 \cdot CaCO_3 \cdot CaSO_4 \cdot 15H_2O$. Birunite dissolves in 10% HCl much more slowly, leaves scarcely any residue, and forms a silica gel immediately, whereas thaumasite gives a precipitate of gypsum and gives a silica gel slowly.

The DTA curve shows a small endothermal break at 120–200°, another broad endothermal break at 550–720°, and an exothermal peak at 770–870° C. A heating curve shows a loss of about 12% H_2O to 200° and further gradual losses from 300 to 800°.

Birunite has hardness 2, G. 2.36. It has one perfect cleavage. It is optically biaxial, positive, (orthorhombic?) with *n*s, α1.527, γ1.531.

Un-indexed *x*-ray powder data are distinct from those of thaumasite, xonotlite, gypsum, calcite, and quartz. The strongest lines are 2.595 (10), 1.781 (10), 1.939 (8) (Given as 1.339, but between 2.037 and 1.841, hence probably a misprint. M.F.), 1.712 (4), 1.292 (3).

The name is "in honor of the great scientist of the Middle Ages in Uzbekistan—Abu-r-Raikhana al-Biruni."

M. F.

Imanite, Baikovite

A. V. Rudneva. New minerals of titaniferous slags. *Akad. Nauk S.S.S.R., Inst. geol. rudnykh mestorozhd., petrog., mineral., geokhim., Inst. khimii silikatov* **1958,** 285–298 in Russian).

These are not mineral names. Descriptions with analyses, optics, and *x*-ray data are given of the synthetic compounds. Imanite, $3CaO \cdot Ti_2O_3 \cdot 3SiO_2$, is isotropic, $n1.905 \pm 0.02$. The name is from the initials of Institut Metallurgii, Akad. Nauk. Baikovite, for Academician A. A. Baikov, is a spinel, $MgTi_2O_4$. Weakly birefringent, n 1.807 ± 0.002.

M. F.

Freboldite

Hugo Strunz. Mineralogische Tabellen, 3rd Ed. **1957,** p. 98.

The name freboldite, for Professor Georg Frebold, Hannover, is given to the unnamed cobalt selenide, probably CoSe, of Ramdohr and Schmitt, see *Am. Mineral.*, **41,** 164–165 (1956).

M. F.

Wyartite

C. Guillemin and J. Protas. Ianthinite et wyartite *Bull. soc. franc. mineral crist.*, **82,** 80–86 (1959).

The material referred to ianthinite by Bignand (1955) (see *Am. Mineral.* **40,** 943–944 (1955) and Frondel, U. S. Geol. Survey Bull. **1064,** 128–130 (1958)), is distinct from ianthinite and is named wyartite for Professor J. Wyart, professor of mineralogy at the Sorbonne.

Wyartite occurs in small crystals with (001) predominant, striated, and (110) (?) Color black to violet-black, greenish or alteration. Streak brownish-violet. Luster dull, on cleavage vitreous to sub-metallic. Opaque to translucent. Orthorhombic with a_0 11.25±0.03, b_0 7.08±0.02, c_0 20.98±0.05Å., Z=2 (Bignand). Cleavage (001) perfect, also (010). Hardness 3–4. G. (by hydrostatic method) 4.69±0.05; Bignand's value 4.94 was obtained on partly dehydrated material. Optically biaxial, neg., β 1.89±0.02, γ 1.91±0.02, 2V 48°, elongation negative. Strongly pleochroic, X (=*c*) gray, Y (=*b*) violet, Z (=*a*) (lavender blue).

Analysis gave UO_3 70.7, UO_2 10.1, CaO 6.3, CO_2 3.4, H_2O 9.7, sum 100.2%, corresponding to $3CaO \cdot UO_2 \cdot 6UO_3 \cdot 2CO_2 \cdot 12$–$14\ H_2O$. Spectrographic analysis showed also traces of Mg.

A dehydration curve shows loss of weight occurring from 20° to 260°, constant weight to about 600°, and then a further loss, but the weight losses are not given. A D.T.A. curve shows endothermic breaks at 80° and 160° (dehydration), a small exothermic break at 280° (oxidation of UO_2 ?), a small endothermic break at about 960° and an endothermic break at about 1020°.

Unindexed *x*-ray powder patterns are given; the strongest lines are at 10.39, 10.375 (vs), 3.27 (s-vs), 5.18, 5.205 (s), 3.53, 3.55 (m-ms), 3.46, 3.47 (m-ms), 3.35 (m-ms), 2.93, 2.99 (m-ms). Patterns (different) are given for samples heated at 60°, 150°, and 400°.

Wyartite occurs at Sbinkolobwé, Katanga, as an alteration product of a red alteration product of uraninite (wölsendorfite?). Wyartite alters much less readily than ianthinite.

M. F.

Laitakarite

Atso Vorma. Laitakarite, a new Bi-Se mineral in Orijarvi (in Finnish). *Geologi* **11,** No. 2, 11 (1959) and private communication from A. Vorma.

The mineral was found as thin veinlets (<2 mm.) in quartz-anthophyllite-cordierite rock at Orijarvi mine, S. W. Finland, associated with native Bi, chalcopyrite, sphalerite, molybdenite, native Ag, pyrite, and galena. Weissenberg and powder photographs show it to have space group $R\ 3m$; the unit cell has a_0 4.225, c_0 39.93Å. (hexagonal setting), A_{rh} 13.53Å., γ 17°58′ (rhombohedral setting). It is isostructural with joseite. The formula is Bi (Se,S) with S:Se about 1:2. G. 7.93. The mineral is named for Aarne Laitakari, director of the Geological Survey of Finland.

M. F.

Unnamed ($FeCl_3 \cdot 6H_2O$)

Carlo Garavelli. Presenza di cloruro ferrico esaidrato fra i minerali di neoformazione del giacimento elbano di Rio Marina. *Periodico mineral (Roma)*, **27,** 211–214 (1958).

Sea water, driven by storms into pyritic deposits of Rio Marina, Elba, caused alteration of pyrite to copiapite and other sulfates and the formation of orange-red incrustations containing gypsum, NaCl, and birefringent crystals with indices above that of methylene iodide. Chemical analysis of the mixture (Fe_2O_3 10.2%) corresponded to $FeCl_3 \cdot 6H_2O$ after deduction of gypsum, NaCl, $CaCl_2$, and $MgCl_2$. The *x*-ray powder pattern (not given) is said to agree closely with the A.S.T.M. data for $FeCl_3 \cdot 6H_2O$, especially the lines at 6.00, 4.00, 3.16, and 1.95.

M. F.

Unnamed

M. D. Dorfman. New data on minerals of Yukspor in the Khibina Tundra. Voprosy Geol. i Mineral Kol'skogo Poluostrova (Problems of geology and mineralogy of the Kola Peninsula), *Akad. Nauk S.S.R., Kola Filial*, **1**, 146–164 (1958) (in Russian).

In 1951 a railroad tunnel through Yukspor Mt. was begun. It cut a series of ijolite-urtite rocks and 3 nepheline-aegirine-feldspar pegmatites were cut in which several apparently new minerals were found.

Mineral No. 2

This mineral occurs as grayish-yellow pseudomorphs after eudialyte in masses up to 2.5 cm. in diameter. Cleavage indistinct. Hardness 3–3½. Luster greasy or silky. G. 2.89. Optically uniaxial, neg., ω 1.625, ϵ 1.622.

Analysis by Z. I. Goroshchenko and E. E. Kostyleva gave SiO_2 45.98, TiO_2 0.28, ZrO_2 11.94, Al_2O_3 0.28, Fe_2O_3 0.07, FeO 2.68, MnO 3.49, MgO 0.18, CaO 10.62, SrO 0.44, TR_2O_3 3.83, Na_2O 11.16, K_2O 1.36, $(Nb,Ta)_2O_5$ 2.40, CO_2 2.51, P_2O_5 none, S 0.08, Cl_2 0.42, H_2O^- 0.16, H_2O^+ 1.37, sum 99.25—$(O{=}Cl_2)$ 0.09 = 99.16%. A little catapleite was present, filling fractures. *X*-ray spectrographic determinations of the individual rare earths are given. The formula is $(Na, Ca, TR, etc)_6ZrSi_6O_{18}(OH, Cl)$. An analysis of the eudialyte gives the same formula, but shows somewhat more Si, Na, and Ca and less Mn, Nb, and rare earths. The mineral is easily fusible to a yellow vesicular glass. Soluble in acids with gelatinization.

X-ray powder data by A. P. Denison are given for Mineral No. 2 (47 lines) and for eudialyte (17 lines); these are stated to show that the minerals are different. The strongest lines of mineral no. 2 are 3.196 (10), 2.862 (10), 1.783 (10, broad), 2.153 (9, broad), 1.986 (8), 2.980 (7).

Discussion.—The *x*-ray pattern for mineral no. 2 agrees very closely (except that all lines above 4.78 are missing) with the pattern given for eudialyte by Claringbull in the A.S.T.M. file. The mineral is therefore simply eudialyte.

Mineral No. 3

The mineral is gray to greenish-gray (if aegirine is present), finely foliated. Luster vitreous, pearly on the perfect cleavage. Brittle. Hardness about 4. G. 2.578. Orthorhombic, extinction parallel, biaxial, positive, *ns* α 1.5285, β 1.5313, γ 1.5323, 2V 29°, elongation with respect to the perfect cleavage negative. Pectolite replaces the mineral along cleavages.

Analysis by L. D. Nikitina of material containing some inclusions of pectolite, aegirine, and stilpnomelane (?) gave SiO_2 46.36, TiO_2 0.07, Al_2O_3 6.48, Fe_2O_3 0.67, FeO n.d., MgO 0.14, MnO 0.08, BeO 0.17, CaO 14.55, SrO 0.12, TR_2O_3 0.11, Na_2O 6.88, K_2O 17.94, F 2.81, Cl 3.47, S 0.66, H_2O^+ 1.23, H_2O^- 1.06, sum 102.80 (given as 102.20% M.F.). From this is deducted $O{=}F_2$ 1.18, $O{=}Cl_2$ 0.78, O=S 0.33 (given as 0.03 M.F.), total 100.51% (given as 100.21% M.F.). Spectrographic analysis showed also Y, Ba, and Cu. The formula is $(K,Na)_4Ca_2(Al,Fe)(Si_{5.9}Al_{0.1})(O,OH,F)_{18} \cdot 0.6NaCl$. The mineral fuses easily, even in the alcohol flame (m.p. 850–900°), to a glass with *n* 1.534. Dissolves in acids with the separation of gelatinous silica. The D.T.A. curve shows no breaks.

X-ray powder data by A. P. Denisov are given (52 lines). More than half of these match lines of pectolite, given for comparison. The strongest lines and those of pectolite are 3.077-10 (3.08-9), 2.904-9 (2.89-10), 3.474-8 broad (———), 2.477-7 (2.42-5), 1.928-7 (1.933-2), 1.864-7 (1.869-5), 1.769-7 (1.77-7), 1.532-6 (1.539-7).

Mineral No. 4

Mineral 4 occurs in perthite-like intergrowths with pectolite; individual grains are 0.01–0.05 mm. Water-clear, luster vitreous. Optically biaxial, α 1.481, γ 1.490, 2V 60–66°; not orthorhombic.

Analysis by A. V. Mokretsova of such intergrowths gave SiO_2 56.90, TiO_2 0.04, Al_2O_3 10.26, Fe_2O_3 0.27, FeO 0.22, MnO 0.44, MgO 0.15, CaO 16.70, Na_2O 6.14, K_2O 6.16, H_2O^- 0.22, H_2O^+ 2.63, F 0.31, sum 100.44 − (O=F_2) 0.13 = 100.31%. Deducting pectolite (all the CaO, Na_2O, MnO, and corresponding amounts of SiO_2 and H_2O), this is said to give the formula $2K_2O \cdot 3Al_2O_3 \cdot 7SiO_2 \cdot 3(H_2O,F)$. (The SiO_2 is half the correct value; the calculation gives nearly $K_2Al_3Si_7O_{18}(OH,F)_3$ M.F.). The mineral dissolves in HCl. In the closed tube it gives off no water.

A D.T.A. curve of the intergrowth gave endothermal breaks at 339–425° and 747–770°; the latter is characteristic of pectolite.

An *x*-ray powder diagram by A. P. Denison (61 lines) gave the following considered to be characteristic of Mineral No. 4 and not pectolite 3.249-10, 1.765-7, 3.491-5, 1.456-6, diffuse, and many weaker lines.

Mineral No. 5, Mineral No. 6

These are listed as being associated with Mineral No. 3. No data are given except that Mineral No. 5 is rose-colored, Mineral No. 6 coppery-yellow.

M. F.

Cousinite

J. F. Vaes. Cousiniet, een nieuw uraanmineral. *Geologie en Mijnbouw*, **20,** 12, 449 (1958)

The mineral occurs at the Shinkolobwe Mine, Katanga, as an alteration product of ore containing uraninite and molybdenite. It is in thin black blades with high vitreous luster. Analysis on 270 mg. gave UO_2 55.25, MoO_3 28.35, PbO 4.60, MgO 4.10, loss on ignition 6.64, insoluble 2.43, sum 101.37%. After deducting the lead and a corresponding amount of MoO_3 as wulfenite, identified as present, and assuming that the loss in weight on ignition is low because of a gain in weight of 3.27% due to oxidation of UO_2 to UO_3, this gives the formula $MgO \cdot 2MoO_3 \cdot 2UO_2 \cdot 6H_2O$. If the loss in weight is used in the calculation, the formula has $4H_2O$.

No physical properties or *x*-ray data are given, nor is the origin of the name stated.

Discussion.—Insufficient data. Compare with moluranite, Am. Mineral. 43, 380 (1958). M. F.

DISCREDITED MINERALS

Amphitalite (=mixture, mostly augelite)

Ake Henriques. Amphitalite, a mixture. *Arkiv. Mineral. Geol.* **2,** 369 (1958).

Optical and *x*-ray examination of the type material (Dana's System, 7th Ed., v. II, p. 873) shows it to be a mixture of augelite with apatite, lazulite, rutile, kyanite, quartz, and mica.

M. F.

Tetragophosphite (=Laculite)
Rhodophosphite (=manganoan Apatite)

Ake Henriques, Tetragophosphite discredited. *Arkiv. Mineral. Geol.*, **2,** 371–372 (1958).

Optical and *x*-ray study of the type material described by Igelstrom in 1896 shows that tetragophosphite is lazulite and that rhodophosphite is a manganoan apatite.

M. F.

CORRECTION

Mrs. Daphne D. Ross has kindly called my attention to an error in the abstract on seidozerite, *Am. Mineral.* **44,** 468 (1959). The strongest *x*-ray lines there listed are actually for låvenite. The strongest lines for seidozerite are 2.97 (10), 2.87 (7), 1.830 (7), 2.58 (4), 1.633 (4). I regret the error.

M. F.

MINERAL SPECIMENS *For Sale or Exchange*
MICROSCOPES BOOKS · GEOLOGICAL SUPPLIES
Catalog on request
SCOTT J. WILLIAMS
Mineralogist
2346 S. SCOTTSDALE ROAD · SCOTTSDALE, ARIZONA, U.S.A.

d. m. organist
PETROGRAPHIC
LABORATORY
BOX 176 • NEWARK, DELAWARE

THIN SECTIONS OF
ROCKS, MINERALS, ORES, CERAMICS
PREPARED ROCK SECTIONS FOR
STUDENT USE
GRAIN COUNTS • PETROGRAPHIC ANALYSIS

MINERALOGICAL SOCIETY OF AMERICA
MEMBERSHIP INFORMATION

Membership: Membership in The Mineralogical Society of America is open to persons interested in the fields of mineralogy, petrography, crystallography and allied sciences. Prospective members should obtain an application blank from the Treasurer. Upon the return of the blank to the Treasurer, properly filled out and accompanied by a remittance of $4.00 for annual dues, his name will be added to the mailing and membership list. Membership includes receipt of the Society's journal, *The American Mineralogist.* Membership is effective as of January of each year and members receive all numbers of the journal for the year. Dues may be remitted directly to the Treasurer or through an agent, payable to The Mineralogical Society of America. No discount is allowed agents on membership dues. Memberships are personal and may not be held in order to obtain the lower rate for the journal for organization use.

MINERALOGICAL SOCIETY OF AMERICA
Marjorie Hooker, Treasurer
c/o U. S. Geological Survey, Washington 25, D.C.

RECENT ACQUISITIONS IN BULK MINERALS AND ROCKS

These are just a few of the many new items that we have acquired in recent months in order to better serve the growing demand for the best in bulk minerals and rocks for teaching, laboratory instruction or research work. (For the complete listing to supplement catalog 583, write for "Ward's Mineral Department Specimen Specials"—Spring 1959)

	Price per lb.
Analcime. Calif. Small xls in rock	$1.50
Ancylite. Montana. Crystalline	4.20
Atacamite. Australia. Crystalline	4.20
Cancrinite. Ontario. Crystalline pink	1.50
Cancrinite. Maine. Yellow in syenite	3.00
Cassiterite. Wash. Massive in andalusite	1.20
Corundum. Transvaal. Massive, nearly pure	1.00
Cryolite. Greenland. Pure white masses	1.80
Dumortierite. Nevada. Lilac colored masses	.60
Gadolinite. Norway. Black massive in feldspar	8.50
Garnet. (Andradite). Ariz. Greenish crystallized	2.50
Helvite. N.M. Yellow-brown in rock	3.50
Hemimorphite. Penna. Brown xline	3.50
Idocrase. (Vesuvianite). Me. Brown xline	1.50
Illite. N.Y. Shale containing 85% illite	1.00
Petalite. Rhodesia. White cleavable	1.00
Pyroxene. (Hedenbergite). Mont. Green xline	1.20
Rutile. Norway or Mexico. Nearly pure, red brown	7.00
Basalt. Lintz, Germany. Dense, black, some olivine aggregates	.70
Chert breccia. Okla. Gray chert in dark matrix	.70
Graywacke. Ontario. Dark colored	.70

REFERENCE CLAY MINERALS

An excellent suite of reference samples of important clays which can serve for purposes of comparison in the general field of clay mineralogy. Included in the suite are: halloysite, kaolinite, dickite, montmorillonite, metabentonite, illite and pyrophyllite.

Write for GN 15.

All prices are list at Rochester, N.Y.

WARD'S *NATURAL SCIENCE ESTABLISHMENT, INC.*
P.O. BOX 1712 ROCHESTER 3, N.Y.

GEORGE BANTA COMPANY, INC., MENASHA, WISCONSIN, U.S.A.